Published by Saint Petersburg
Mining University

SINCE 1907

E-ISSN 2541-9404
ISSN 2411-3336

JOURNAL OF MINING INSTITUTE

ZAPISKI GORNOGO INSTITUTA

SCIENTIFIC JOURNAL

Volume 260

№ 2 • 2023

INDEXING IN
SCOPUS (Q1)
WEB OF SCIENCE (ESCI)

WWW.PMI.SPMI.RU

Journal of Mining Institute

Saint Petersburg
Mining University

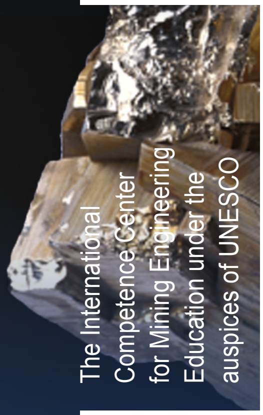

The International
Competence Center
for Mining Engineering
Education under the
auspices of UNESCO

The scientific periodical “Journal of Mining Institute” is published since 1907 by Saint Petersburg Mining University – the first higher technical educational institution in Russia, founded in 1773 by the decree of Catherine II as the embodiment of the ideas of Peter I and M.V. Lomonosov on the training of engineers for the development of mining business.

The International Competence Center for Mining Engineering Education under the auspices of UNESCO operates on the basis of Saint Petersburg Mining University and contributes to active interaction of the Journal with the international scientific community.

The purpose of the Journal is to create an information space in which Russian and foreign scientists can present results of their theoretical and empirical research on the problems of the mining sector.

Published articles cover the issues of geology, geotechnical engineering and engineering geology, mining and petroleum engineering, mineral processing, energy, geoecology and life safety, economics of raw materials industries.

The Journal is indexed by Scopus (Q1), Web of Science Core Collection (ESCI), DOAJ Seal, RSCI, GeoRef, Google Scholar, RSCI. It is included in the White list of the Ministry of Education and Science of the Russian Federation.

The Journal is published six times a year. The average first decision time is one month.

Articles are published free of charge. Translation is provided by the author.

Photo on the cover is an exhibit of the Mining Museum – pyrite, a druse of large cubic crystals on coarse-grained pyrite (Berezovskoe deposit, Sverdlovsk Region, Urals, Russia). Pyrite was used for the extraction of fire, as a raw material for sulfuric acid, sulfur, iron sulfate, and for the production of expanded clay, cement, concrete, and for pit smelting. Pyrite is one of the most abundant sulfides in the Earth’s crust.

The Mining Museum is the world’s third largest natural-science exposition, it contains more than 230 thousand exhibits, including precious metals and stones, unique collections of minerals, ores, rocks, paleontological remains, meteorites, a collection of models and prototypes of mining equipment, pieces of stone-cutting and jewelry art.

JOURNAL OF MINING INSTITUTE

ZAPISKI GORNOGO INSTITUTA

PEER-REVIEWED SCIENTIFIC JOURNAL

Published since 1907

ISSN 2411-3336
e-ISSN 2541-9404

Volume 260

ST. PETERSBURG • 2023

Journal founder: Saint Petersburg Mining University

CHIEF EDITOR
V.S.Litvinenko, Doctor of Engineering Sciences, Professor, Member of the International Academy of Higher Education, RANS, RAHS, MANEB, Rector (Saint Petersburg Mining University, Saint Petersburg, Russia)

DEPUTY CHIEF EDITOR
S.G.Skublov, Doctor of Geological and Mineralogical Sciences, Associate Professor, Member of the Russian Mineralogical Society, Expert of the RSF and RAS (Saint Petersburg Mining University, Saint Petersburg, Russia)

EXECUTIVE SECRETARY
S.V.Kupavykh, Candidate of Engineering Sciences, Director of the Publishing House “Journal of Mining Institute” (Saint Petersburg Mining University, Saint Petersburg, Russia)

EDITORIAL TEAM

O.Ye.Aksyutin, Doctor of Engineering Sciences, Corresponding Member of the RAS, Board Member, Head of Department (PAO Gazprom, Moscow, Russia)

A.A.Baryakh, Doctor of Engineering Sciences, Professor, Member of the RAS, Director (Perm Federal Research Center Ural Branch RAS, Perm, Russia)

V.N.Brichkin, Doctor of Engineering Sciences, Vice Rector for Scientific Personnel Training (Saint Petersburg Mining University, Saint Petersburg, Russia)

S.G.Gendler, Doctor of Engineering Sciences, Professor, Member of the RANS, Head of Department of Occupational Safety (Saint Petersburg Mining University, Saint Petersburg, Russia)

O.M.Ermilov, Doctor of Engineering Sciences, Professor, Member of the RAS, RAHS, Deputy Engineer-in-Chief of Science Programmes (OOO Gazprom Development Nadym, Nadym, Russia)

V.P.Zubov, Doctor of Engineering Sciences, Professor, Head of Department of Underground Mining (Saint Petersburg Mining University, Saint Petersburg, Russia)

G.B.Kleiner, Doctor of Economics, Professor, Corresponding Member of the RAS, Deputy Director (Central Research Institute of Economics and Mathematics of the RAS, Moscow, Russia)

A.V.Kozlov, Doctor of Geological and Mineralogical Sciences, Member of the Russian Mineralogical Society, Associate Professor (Saint Petersburg Mining University, Saint Petersburg, Russia)

Y.B.Marin, Doctor of Geological and Mineralogical Sciences, Professor, Corresponding Member of the RAS, President (Russian Mineralogical Society, Saint Petersburg, Russia)

V.A.Morenov, Candidate of Engineering Sciences, Associate Professor (Saint Petersburg Mining University, Saint Petersburg, Russia)

M.A.Pashkevich, Doctor of Engineering Sciences, Professor, Head of Department of Geoecology (Saint Petersburg Mining University, Saint Petersburg, Russia)

T.V.Ponomarenko, Doctor of Economics, Professor (Saint Petersburg Mining University, Saint Petersburg, Russia)

O.M.Prishchepa, Doctor of Geological and Mineralogical Sciences, Member of the RANS, Head of Department of Geology of Oil and Gas (Saint Petersburg Mining University, Saint Petersburg, Russia)

A.G.Protosenya, Doctor of Engineering Sciences, Professor, Head of Department of Construction of Mining Enterprises and Underground Structures (Saint Petersburg Mining University, Saint Petersburg, Russia)

V.E.Somov, Doctor of Economics, Candidate of Engineering Sciences, Member of the RANS, Director (OOO Kinef, Kirishi, Russia)

A.A.Tronin, Doctor of Geological and Mineralogical Sciences, Acting Director (Saint Petersburg Scientific-Research Centre for Ecological Safety RAS, Saint Petersburg, Russia)

V.L.Trushko, Doctor of Engineering Sciences, Professor, Member of the International Higher Education Academy of Sciences, RANS, RAHS, MANEB, Head of Department of Mechanics (Saint Petersburg Mining University, Saint Petersburg, Russia)

P.S.Tsvetkov, Candidate of Economics, Associate Professor (Saint Petersburg Mining University, Saint Petersburg, Russia)

A.E.Cherepovitsyn, Doctor of Economics, Professor, Head of Department of Economics, Organization and Management (Saint Petersburg Mining University, Saint Petersburg, Russia)

Ya.E.Shklyarskiy, Doctor of Engineering Sciences, Professor, Head of the Department of General Electric Engineering (Saint Petersburg Mining University, Saint Petersburg, Russia)

V.A.Shpenst, Doctor of Engineering Sciences, Professor, Dean of Energy Faculty (Saint Petersburg Mining University, Saint Petersburg, Russia)

Oleg Antzutkin, Professor (University of Technology, Luleo, Sweden)

Gabriel Weiss, Doctor of Sciences, Professor, Pro-Rector for Science and Research (Technical University, Kosice, Slovakia)

Hal Gurgenci, Professor (School of Mining Machine-Building in University of Queensland, Brisbane, Australia)

Edwin Kroke, Doctor of Sciences, Professor (Institute of Inorganic Chemistry in Freiberg Mining Academy, Freiberg, Germany)

Zhou Fubao, Doctor of Sciences, Professor, Vice President (China University of Mining and Technology, Beijing, PR China)

Zhao Yuemin, Doctor of Sciences, Professor, Director of Academic Committee (China University of Mining and Technology, Beijing, PR China)

Responsible editors of the volume: Doctor of Engineering Sciences **Mariya A. Pashkevich**, Candidate of Engineering Sciences **Aleksandr S. Danilov** (Saint Petersburg Mining University)

Sections

• Geology • Geotechnical Engineering and Engineering Geology • Economic Geology • Energy

Registration Certificate PI No. FS77-70453 dated 20.07.2017

PH License No. 06517 dated 09.01.02

Editorial staff: Head of the Editorial Center V.L.Lebedev; Editors: E.S.Dribinskaya, M.G.Khachirova, V.E.Filippova, L.V.Nabieva
Computer Design: V.I.Kashirina, N.N.Sedykh

© Saint Petersburg Mining University, 2023

Passed for printing 25.04.2023. Format 60 × 84/8. Academic Publishing Division 40.
Circulation: 300 copies. Order 316. Printed by RIC of Saint Petersburg Mining University. Free sale price.

Mailing address of the Journal Founder and the Editorial Board
21st Linia V.O., No. 2, St. Petersburg, Russia, 199106
Phone: +7 (812) 328-8416; Fax +7 (812) 327-7359;
E-mail: pmi@spmi.ru Journal website: pmi.spmi.ru

CONTENTS

Journal of Mining Institute. 2023. Vol. 260. P. 153-154
© Mariya A. Pashkevich, Aleksandr S. Danilov, 2023

Editorial

ECOLOGICAL SECURITY AND SUSTAINABILITY

In 2015, UN Member States adopted the 2030 Agenda for Sustainable Development, aimed at balancing initiatives by the world community and individual countries in the environmental, social, and economic spheres. The global sustainable development goals are to promote the well-being of the world population, preserve the planet's resources, and maintain ecological security, which is vital in the age of the rapid industrial growth and ever-increasing anthropogenic pressure on the environment. For the successful achievement of sustainability goals in the manufacturing sector, integrated measures should be undertaken for monitoring and assessing the technogenic impact of industrial facilities. Additionally, it is necessary to develop environmentally-friendly technologies in the fields of gas and water treatment, land reclamation, and waste disposal. Therefore, fundamental and applied research in these related spheres is of particular importance.

Currently, environmental monitoring of all components of the environment, along with anthropogenic objects and processes, receives considerable attention, which is determined by the vector of development in science and technology. In this regard, the latest innovations in green technology in this area are becoming increasingly significant.

Scientists from the Saint Petersburg Mining University study the impact of the mining industry on the biosphere. The paper by Mariya A. Pashkevich et al. (DOI: 10.31897/PMI.2023.32) comprehensively considers the formation of an ecological catastrophe in the area of long-term development, enrichment and metallurgical processing of copper sulfide ores.

In the article by Aleksandr I. Semyachkov and colleagues (DOI: 10.31897/PMI.2023.24), waste disposal sites (dumps and sludge storages) are considered to be sources of environmental and economic damage to the aquatic environment. The authors have studied one of the largest tailings in the Middle Urals that poses a potential environmental and man-made threat, as it creates specific hydrogeoecological conditions on the territory.

A team of authors from the Perm State National Research University, led by Sergei A. Buzmakov (DOI: 10.31897/PMI.2023.22) considered the need to expand the range of observations of the technogenic processes development in oilfields using unmanned aerial photography to determine interpretation signs that register the consequences of technogenic transformation of the natural environment.

Studies of the distribution of natural and technogenic radionuclides in groundwater of the industrial zone in Sosnovy Bor town were carried out by Valentina A. Erzova, Corresponding Member of the RAS Vyacheslav G. Rumynin et al. (DOI: 10.31897/PMI.2022.27). Based on the results of the analysis, isotope contamination of the first two aquifers from the surface was revealed. A 3D geological model and hydrodynamic and geomigration models of the industrial zone of the nuclear power plant were constructed. Modeling has shown that during the time of the operation of the Leningrad Nuclear Power Plant there was no intake of contaminated water by the drainage system of the new power plant.

According to the results of monitoring the soil cover of the Nakyn kimberlite field in the Yakutia diamond province, Yana B. Legostaeva and colleagues (DOI: 10.31897/PMI.2023.35) revealed a technogenic impact of objects of mining and processing of mineral raw materials, which is of multielement nature, in local areas with high and very high contamination levels.

Iskhak M. Farkhutdinov and colleagues (DOI: 10.31897/PMI.2023.4) described the results of the analysis of the uranium content in man-made carbonates (scale crusts) on the territory of Ufa, depending on specific subsurface geology of the territory (gypsum, limestone), types of water supply, and water treatment processes for centralized type of water supply.

The elaboration of analytical methods for qualitative and quantitative analysis of various ecotoxicants faces a number of challenges, such as a lack of information on isomers and homologues of compounds that have already been studied. This problem was considered in the paper by Vladimir G. Povarov and Ignatyi I. Efimov (DOI:10.31897/PMI.2023.41), who explored the capabilities of the UNIFAC model for solving existing problems using the example of calculating the properties of real ecotoxicants.

Ensuring the sustainable development of regions and the rational use of natural resources becomes possible through the development of eco-technologies and the use of innovative methods of environmental protection in manufacturing.

Various methods for producing biodiesel fuel were considered in the work of Natalia K. Kondrasheva and Anzhelika M. Eremeeva (DOI: 10.31897/PMI.2022.15). Based on the analysis of the physical and chemical characteristics of biodiesel fuel, it has been determined that the best way to produce it is through transesterification of vegetable oils.

The problem of pollution of surface and ground waters with heavy metals, as well as methods for treatment of industrial wastewater containing ions, were considered by Natalya Yu. Antoninova and colleagues (DOI: 10.31897/PMI.2023.34). Studies were conducted on the redistribution of heavy metals in the “wastewater – waste” system using iron-magnesium production waste.

The effectiveness of soil reclamation by agrochemical and geochemical methods at the site of acid mine water discharge in the Kizel Coal Basin was studied by Natalya V. Mitrakova and colleagues (DOI: 10.31897/PMI.2023.31).

In the work of Svetlana V. Sverguzova et al. (DOI: 10.31897/PMI.2023.23), innovative approaches to the disposal of the dust from electric arc furnaces were considered. Based on the results of the analysis of physical and chemical properties, along with chemical and disperse compositions of dust and surface microstructure, it was concluded that this type of waste can be used as a raw material for coagulant production, resulting in a high efficiency (95 %) of water treatment from heavy metal ions.

Igor V. Sokolov and colleagues (DOI: 10.31897/PMI.2023.21) considered the topical issue of disposing the maximum possible volume of waste from the mining and processing of low-grade iron ores by placing them in the formed gob.

The development of more environmentally friendly, cost-effective, and less labor-intensive biological methods of remediation was considered in the work of Irina D. Sozina and Aleksandr S. Danilov (DOI: 10.31897/PMI.2023.8). As a result of their research, various bio-based products with proven efficacy, based on strains and consortia of microorganisms, have been developed to restore oil-contaminated soil.

The paper by Andrei M. Gerasimov and colleagues (DOI: 10.31897/PMI.2023.33) explores the possibility of recycling wastes from the processing of various ores by using them, after preliminary thermochemical treatment, as pozzolanic additives to cements and concretes, including concrete mixtures.

Responsible scientific editors of the volume Doctor of Engineering Sciences Mariya A. Pashkevich,
Candidate of Engineering Sciences Aleksandr S. Danilov

ISSN 2411-3336; e-ISSN 2541-9404

JOURNAL OF MINING INSTITUTE

Zapiski Gornogo instituta

Journal homepage: pmi.spmi.ru

Research article

Environmental damage from the storage of sulfide ore tailings

Mariya A. PASHKEVICH[1], **Alexey V. ALEKSEENKO**[2], **Ruslan R. NUREEV**[1]✉
[1] *Saint Petersburg Mining University, Saint Petersburg, Russia*
[2] *United Nations University, Institute for Integrated Management of Material Fluxes and of Resources, Dresden, Germany*

***How to cite this article*:** Pashkevich M.A., Alekseenko A.V., Nureev R.R. Environmental damage from the storage of sulfide ore tailings. Journal of Mining Institute. 2023. Vol. 260, p. 155-167. DOI: 10.31897/PMI.2023.32

***Abstract*.** The mining industry is one of the most challenging in ensuring environmental safety. During the last century, the Karabash Copper Smelting Plant was processing sulfide ores and depositing the tailings into storage facilities that now occupy an area of more than 50 hectares. To date, abandoned tailings are a significant source of natural water, air, and soil pollution in the Karabash city district. The article comprehensively examines the environmental impact of the Karabashmed copper smelter, one of the oldest metallurgical enterprises in Russia. The effects of seepage from the two Karabashmed tailings facilities on water resources were assessed. We revealed that even outside the area of the direct impact of processing waste, the pH of natural water decreases to values 4-5. Further downstream, the infiltration water from the tailings pond N 4 reduces the pH of river water to 3.0-3.5. The presented results of environmental engineering surveys are derived from sampling water and bottom sediments of the Ryzhiy Stream and the Sak-Elga River, sample preparation, and quantitative chemical analysis. The study revealed significant exceedances of the maximum permissible concentrations for a number of chemical elements in the impact zone of the copper ore processing tailings.

***Keywords*:** river pollution; bottom deposits; metals; technogenic sediments; pyrite oxidation; tailings storage facilities

Received: 02.11.2022 ***Accepted: 02.03.2023*** ***Online: 13.04.2023*** ***Published: 25.04.2023***

Introduction. Waste from mining and processing of minerals poses a severe threat to the environment and human health, especially in spent mines where conservation and reclamation works have not been carried out [1-4], which is comparable to the impact of the most dangerous industries [5, 6]. The natural oxidation of sulfide minerals under the combined action of water and oxygen forms acidic effluents with a high content of sulfates and metal ions in the solution, which can pollute both underground and surface waters [7, 8]. Most often, such effluents are formed during the oxidation of iron sulfides under supergene conditions: pyrite and, less frequently, pyrrhotite [9]. Acid runoff is a significant source of pollution in many mining provinces, and the methods used to reduce environmental impacts are usually expensive and time-consuming. In some cases, work to minimize ecological damage may lead to secondary pollution [10].

Man-made environmental disasters during the extraction and processing of sulfide ores, such as on the tributary of the Guadalquivir River in Spain [11] with a decrease in pH from 8.5 to 4.5 and water pollution with sludge waste containing 0.6 % As, 1.2 % Pb and 0.8 % Zn, or an outflow of 280000 m^3 of acid mine waters in the Sichuan Basin in China [12] have been registered and studied in detail in many regions. The long-term anthropogenic load on the natural media in the vicinity of Karabash has led to pollution and degradation of adjacent landscapes. As a result of the activity of the Karabashmed enterprise, an adverse environmental situation has developed in the area of its impact. Since the enterprise was commissioned in 1910, it has been significantly affecting all natural resources due to the insufficient purification of industrial waste gases and the lack of processing of copper ore tailings.

By 1989, the state of the environment in the impact zone of the Karabash copper smelter reached the level of an environmental catastrophe. A significant release of sulfur dioxide into the atmospheric air (about 90 % of the total mass of pollutants) provoked acid rain, damaging the soil cover. Because of the oppression of biocenosis and pollution of soils and water bodies with metals, the Regional Committee for Nature Protection and the Minister of Metallurgy of the USSR decided to stop the copper smelting in Karabash in 1989.

This measure stopped emissions of pollutants into the atmospheric air from the territory of the enterprise and, as a result, improved the environmental situation [13]. For the first time in a long while, the restoration of a phytocenosis began on the western slope of Zolotaya Mountain. In 1998, it was decided to resume the reorganized Karabashmed copper smelting plant operation. The restarted production raised the anthropogenic load and negatively affected the environment. Without modern gas cleaning equipment, emissions of pollutants into the atmospheric air led to a significant excess of the Maximum Permissible Concentrations (MPC), and the lack of a waste recycling system provoked secondary pollution of the atmosphere and hydrosphere. The composition of emissions into the atmospheric air is shown in Fig.1.

Since 2004, the reorganized enterprise has been intensively attempting to reduce the negative impact on the environment, primarily on atmospheric air. Among other environmental measures, copper smelting furnaces were modernized. In 2006, Ausmelt melting units (Australia) were introduced into the production cycle. The commissioning of new equipment took three years, but the first results in reducing the negative environmental impact became noticeable from the moment the new furnaces were installed. The dynamics of the atmospheric emission volumes by various pollutants during the period of copper smelting in 1907-2013 are shown in Fig.2.

Analyzing Fig.2, it can be noted that because of the long-term activity of the enterprise, a significant mass of pollutants was released into the atmospheric air: more than 14.5 million tons, of which the bulk is sulfur dioxide, inorganic dust, and zinc oxide. In the period from 2007 to 2013, which coincides with the introduction of environmental protection measures at the industrial site, there has been a significant reduction in emissions of sulfur dioxide (a six-fold decrease), dust (300 times), and zinc oxide (100 times).

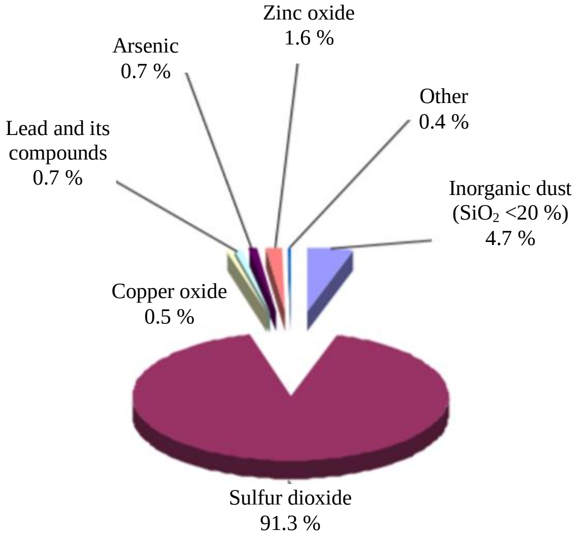

Fig.1. The composition of the main pollutants emitted into the atmospheric air from 1907 to 2006

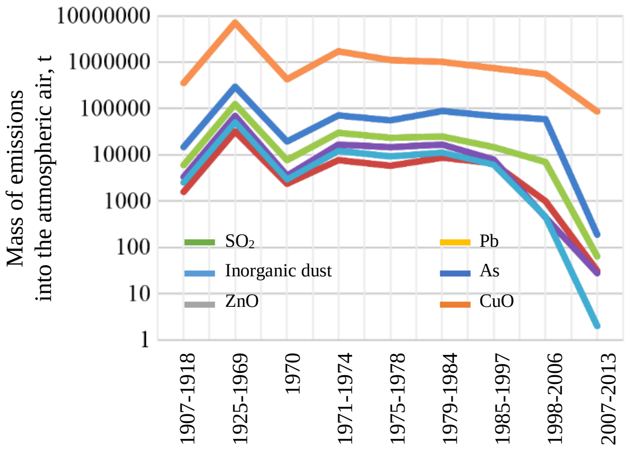

Fig.2. Emissions of pollutants into the atmosphere for the entire period of operation of the copper smelter in the Karabash urban district of Chelyabinsk Oblast (as of 01.01.2014)

The negative impact of copper smelting on the environment is complex [14]. Industrial pollutants released into the atmospheric air accumulate in surface watercourses, bottom sediments, and soils.

The soil cover in the impact zone has been significantly transformed, and because of acid precipitation, the phytocenosis has been suppressed, up to the formation of man-made wastelands. Metals in mobile and immobile modes of occurrence accumulate in the upper layers of the soil cover. The mobile metals are available for absorption by plants, so their contents are significantly heightened in root systems, particularly in copper, zinc, and lead cases. Except for the element accumulation by vegetation, there is a low infiltration rate into the soil with atmospheric precipitation [15, 16].

Depending on climatic conditions, potentially dangerous immobile metals can turn into mobile ones and vice versa. Mobile modes of occurrence of metals pose the greatest danger since they are most accessible to living organisms. As a result, the accumulated environmental damage can affect the vegetation cover in the impact zone of the enterprise for a long time.

Numerous investigators have studied and analyzed the impact of Karabashmed on the quality of the soil cover in the affected area. The results of these analyses are presented in Table 1.

Table 1

Studies of the negative impact of the copper smelter on the soil cover

Source	Bulk content of elements, mg/kg							
	Cu	Zn	As	Cd	Pb	Cr	Ni	Fe
[17]	12200	–	–	–	–	–	–	196700
[18]	4383.2	–	–	27.3	2260.3	–	–	–
[19]	1066	10953.2	235.8	–	1233.6	700.9	991.5	46.5
[20]	4031.9	1882.4	724.7	19.1	1168.7	–	–	–
[21]	2569	2655.4	–	11.4	586.6	–	–	–
[22]	–	–	293.7	7.6	–	398.1	246.9	–
[23]	10720	3388	–	25	–	–	–	48750
[24]	4340	1877	493	12.7	900	313	280	4750
[25]	30	50	–	6	5	–	10	220
[26]	3100	–	–	–	1300	900	1200	–
[27]	637.5	3380	–	25.6	117.5	–	618	–
[28]	16416.4	6851.8	825.5	15.2	2146.3	1191.1	944.4	257288
Background concentration	20.56	17.2	–	1.1	6.3	–	7.8	–
MPC*	3	23	2	2	6	6	4	–

---

* Maximum Permissible Concentrations are taken from the Russian Sanitary Rules and Norms, 1.2.3685-21 “Hygienic standards and requirements for ensuring the safety and (or) harmlessness of environmental factors for humans”.

Based on the presented results, we conclude that in the area affected by copper smelting, there are many-fold exceedances of the maximum permissible concentrations in the soil cover for several elements: copper, zinc, arsenic, lead, iron, etc. The specific association of the elements indicates that Karabashmed is the source of contamination.

In addition to the negative impact on atmospheric air and soil, pollution of the water basin is observed in the impact zone of Karabashmed and around the tailings storage facilities. The main pollutants of surface watercourses – primarily of the Sak-Elga River and the Argazinskiy Reservoir – are the drainage waters from tailings, stormwater, and industrial effluents of the enterprise, the collapse zone of the spent Stalinskiy (Tisovskiy) mine, the Ryzhiy Stream, sulfide-silicate deposits in the river floodplain (Fig.3).

When infiltrating through the tailings, rain and meltwater are enriched with potentially toxic elements which and later discharge into water bodies. The Ryzhiy Stream is one of the most well-known pollution sources in the study area (Fig.4, *a*). Its waters are characterized by extremely high metal content.

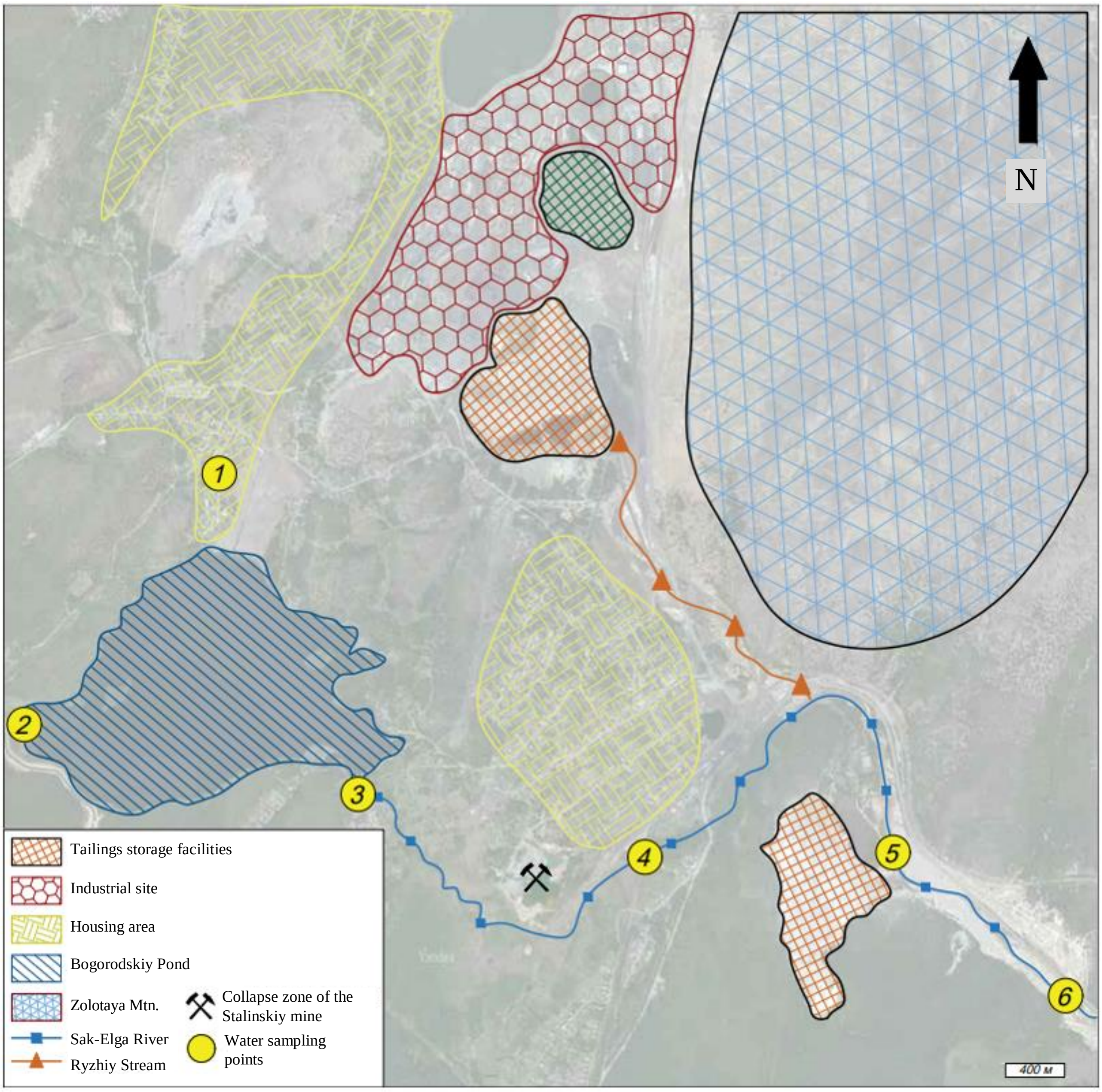

Fig.3. Sketch map of the study area

The stream flows into the Sak-Elga River. Due to the difference in debits (the ratio is from 1:12 to 1:30 depending on the season), the metal content in the water decreases by two orders of magnitude.

Many authors have analyzed the negative impact of tailings and industrial wastewater in various studies. During the field campaign, we investigated the Ryzhiy Stream, its confluence with the Sak-Elga River, mine waters, and certain lakes and reservoirs of Chelyabinsk Oblast. As a result of the dilution of the acidic polluted waters of the Ryzhiy Stream with the water of the Sak-Elga River, which has an average pH of 7.5, an alkaline hydrolytic geochemical barrier is formed. Metals precipitate there as hydroxides accumulated in the bottom sediments. Metal concentrations in bottom sediments are many-fold higher than the MPC, and these deposits can be secondary pollutants of water resources. The results of the analysis of water pollution by various authors are presented in Table 2.

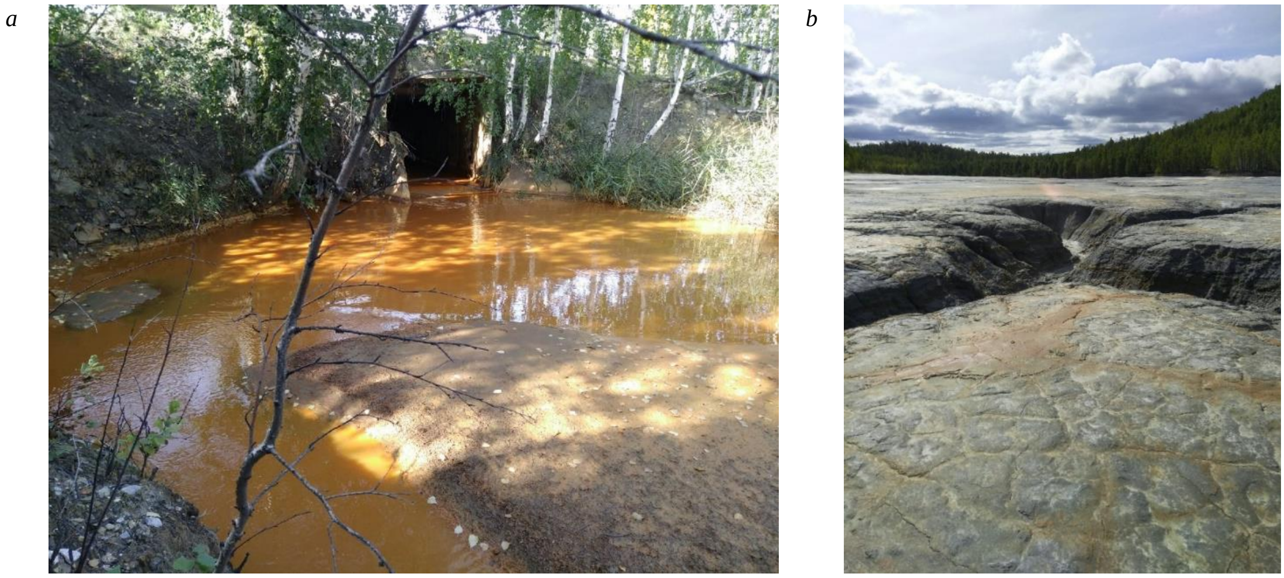

Fig.4. Sources of pollution: the Ryzhiy Stream (*a*), the tailings storage facility N 4 (“Novoye”) (*b*)

Table 2

Studies on the negative impact of the copper smelter on water resources

Source	pH	Bulk content of elements, mg/l							
		Cu	Zn	Cd	Pb	Fe	Ni	As	SO_4
[29] (the Ryzhiy Stream)	1.58	132.5	420.8	2.49	3.72	382.4	4.63	–	–
[29] (mine drainage, 1994)	2.1	24	350	–	–	70	–	0	3900
[29] (mine drainage, 1997)	2.5	35	100	–	–	170	–	0	6500
[29] (mine drainage, 1998)	2.7	13	0	–	–	0	–	–	2000
[29] (mine drainage, 2000)	6.6	0	0	–	–	0	–	–	500
[29] (mine drainage, 2014, 70 m)	–	0.02	0.2	–	–	0.05	–	–	230
[30] (the Ryzhiy Stream, 2008)	2	55	96	0.43	0.012	390	–	0.015	–
[31] (lakes, 2001)	7.1	9.3	107	0.2	1.5	334	3.6	–	1557
[32] (Sak-Elga River, 2014)	3.8	0.85	–	–	–	72.1	–	–	–
[33] (the Ryzhiy Stream, 2014)	5.25	30	65	–	–	180	–	–	–
[34] (lake Uvildy, 2005)	–	12.4	12	–	–	–	–	–	–
[35] (the Ryzhiy Stream, 2016)	2.7	51.34	167.39	1.1	1.38	629.15	3.42	0.62	–
[36] (the Ryzhiy Stream, 2011)	–	75	100	0.8	0.1	700	-	0.01	–
[37] (the Ryzhiy Stream, 2017)	–	45	40	1.3	1.2	42	0.9	-	–
[38] (drainage water, 2017)	–	87	47	–	–	1200	–	1.8	–
[24] (Sak-Elga River, 2011)	2.4-2.7	58	87	–	1.5	375	–	–	–
[39] (drainage water, 2018)	2.03	458	543	–	–	5674	–	–	–
[40] (the Ryzhiy Stream, 2014)	3	50	2	–	0.5	200	–	–	90
Background concentration	6.82	3.2	11.2	0.02	0.27	7.68	4.25	–	–
MPC*	–	0.001	0.01	0.005	0.006	0.1	0.01	0.05	100

---

[*] Maximum Permissible Concentrations are taken from the Order of the Ministry of Agriculture of the Russian Federation of December 13, 2016, N 552.

In addition to the direct atmospheric air pollution, Karabashmed negatively impacts the hydro- and lithosphere through the accumulated waste of copper ore processing. The industrial cycle includes flotation, which produces vast volumes of tailings, i.e., a finely dispersed mass of aluminosilicate and sulfide composition [41]. Residuals of this type should be stored in specially equipped facilities. Tailings are a constant source of secondary environmental pollution: dusting surfaces increase the load on atmospheric air and promote the migration of pollutants, and the absence or violation of the integrity of hydrofiltration screens contributes to the infiltration of pollutants with storm drains into soils and water bodies.

In the vicinity of Karabash, two tailings storage facilities (TSF) affect the environment most significantly: the TSF N 3 with 4.5 million tons of accumulated waste and the TSF N 4 (“Novoye”) with 5.9 million tons (Fig.4, *b*).

The range of studies on tailings’ chemical and phase composition is minimal. In this regard, the question of studying the composition of tailings at different depths and the dynamics and nature of the wastewater infiltration process remains open. Table 3 presents the results of various authors’ chemical analyses of the tailings.

Table 3

Studies of the chemical composition of accumulated processing tailings

Source	Bulk content of elements, mg/kg					
	Cu	Zn	Fe	As	Pb	Mn
[30]	370	330	77000	170	230	–
[36]	500	500	100000	100	250	–
[40]	2000	800	124000	–	–	–
[29]	1540	1572	337421	–	4116	435
[42]	1066.9	10953	–	235.8	1233	3374.8
[43]	370	390	–	–	–	–
[33]	6	10.4	220	–	1	–
MPC[*]	3	23	–	2	6	60

---

[*] Maximum Permissible Concentrations are taken from the Russian Sanitary Rules and Norms, 1.2.3685-21 “Hygienic standards and requirements for ensuring the safety and (or) harmlessness of environmental factors for humans”.

To reduce the negative impact of accumulated copper processing waste, it is necessary to develop comprehensive environmental protection solutions, including a project for the reclamation of tailings bodies and wastewater treatment [44].

The main objectives of the work are (i) to monitor the zone of the negative environmental impact of tailings; (ii) to identify distribution patterns of pollutants from the TSF; (iii) to assess the possibility of recycling accumulated copper processing waste; (iv) to examine the correlation between concentrations of valuable elements and the depth of the tailings; and (v) to forecast the feasibility of developing a comprehensive environmental protection system in contaminated areas.

Methods. The technogenic sediments of the Karabash copper smelting plant are a typical example of accumulated environmental harm. The TSF N 3 and N 4 are of particular interest. The considered tailings are the residuals of the processing of sulfide copper-pyrite ores. Their composition is determined by the mineral composition of the ore entering the processing plant. Pyritic deposits, as a rule, are characterized by a variety of forms and types of occurrence of minerals in host rocks. Copper-pyrite deposits of the Southern Urals are represented by iron, copper, and zinc sulfides: 60-90 % pyrite, 0.2-25 % sphalerite, and 0.1-10 % chalcopyrite. Tennantite, galena, magnetite, hematite, bornite, etc., are minor minerals. Quartz, sericite, chlorite, barite, and calcite are the most common non-metallic minerals.

The studied TSF N 3 and 4 were formed from 1958 to 1990 with multi-tiered protecting dams of ca. 10 m in height. To assess the potential danger of sulfide-containing waste, monitoring studies were conducted in the area adjacent to the tailings of the Karabash copper smelter. The TSF N 3 covers an area of 39.5 hectares and accommodates, according to various estimates, from 3.0 to 4.5 million tons of tailings. The TSF N 4 occupies an area of 27.7 hectares and holds from 4.0 to 5.9 million tons of tailings. In the vertical section of the TSF N 4, three contrasting zones are distinguished: an oxidation zone up to 1.7 m deep from the daylight surface; a cementation zone with a thickness of up to 1.5 m; and a cementation zone with signs of secondary sulfide accumulation.

Below a depth of 3 m, conspicuous layers of black color appear with a characteristic smell of organic matter, which indicates the reducing environment with little or no free oxygen.

The conducted studies allowed us to assess the level of transformation of artificial deposits, the possibility of their recycling to extract potential mineral raw materials, and the level of their impact on natural resources.

The monitoring included visual assessment of the tailings; sampling of the section from the surface and up to a depth of 4 m at the TSF N 3 and 4; and sampling of water and bottom sediments of the Sak-Elga River.

To assess the vertical migration of pollutants and the degree of preservation of valuable components in the TSF N 3 and 4, we drilled 12 wells to different depths. Sampling was carried out in the summer (August 2020) following GOST 12071-2014 "Soils. Sampling, packing, transportation and keeping of samples". We took 46 samples using a manual drill sampler with a rotary handle. The description of the sampling conditions is shown in Fig.5.

The samples from the tailings were placed in sealed polyethylene bags for further transportation in a cooled state. Sample preparation was carried out in the laboratory of the Research and Educational Center for the Collective Use of High-Tech Equipment at Saint Petersburg Mining University

The qualitative and quantitative composition of the tailings was determined using the Shimadzu XRF-1800 X-ray fluorescence spectrometer. The analysis was carried out following GOST R 56157-2014 "Soil. Procedures (methods) of analysis of composition and properties of soil samples. General requirements for development". The samples were dehumidified in a drying cabinet at a temperature

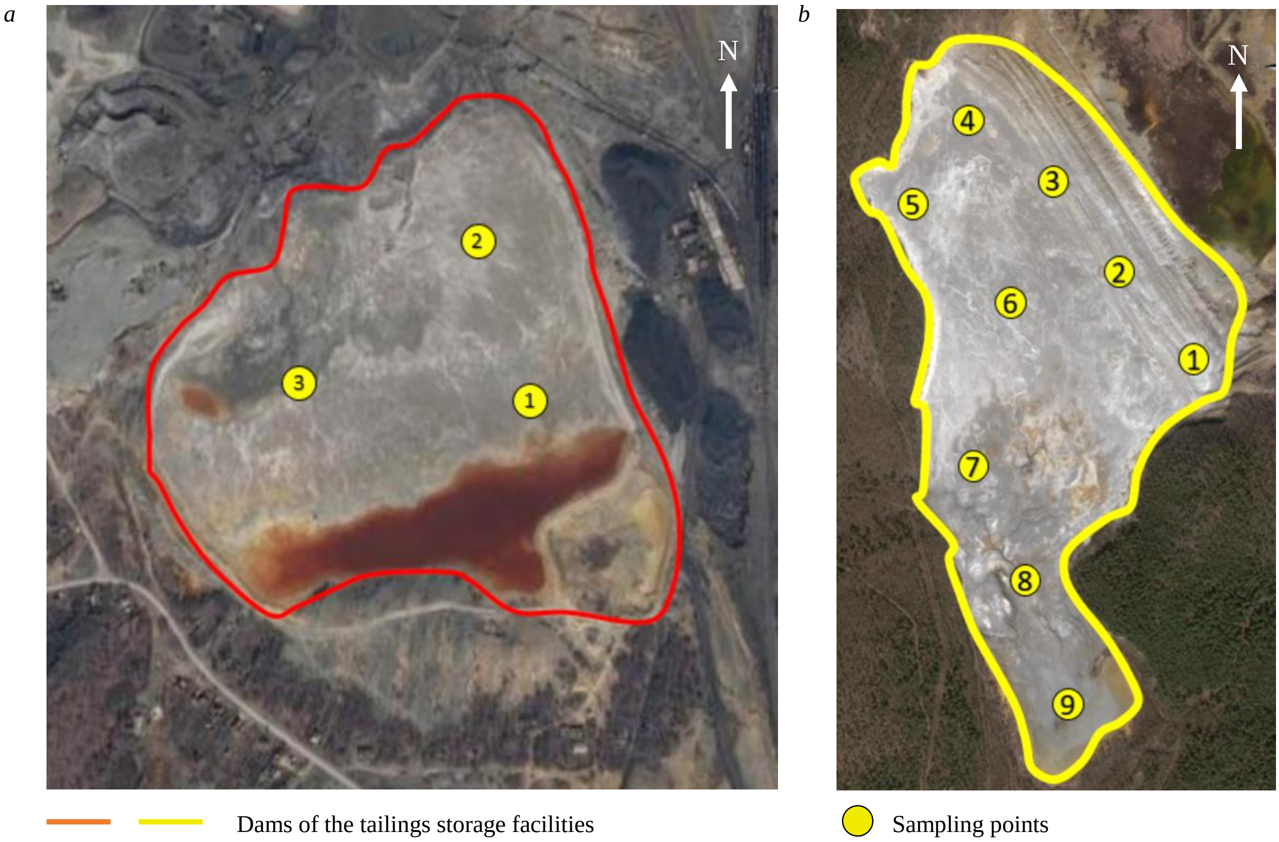

Fig.5. Characteristics of sampling conditions in the territories of the storage facilities N 3 (*a*) and N 4 (*b*)

N 1: 3 samples from the depth of 0; 0.5; and 1 m; N 2: 2 samples from 0 and 0.5 m; N 3: 4 samples from 0; 0.5; 1; and 2 m (*a*);

N 1: 4 samples from the depth of 0; 0.5; 1; and 2 m; N 2: 6 samples from 0; 0.5; 1; 2; 3; and 4 m; N 3: 5 samples from 0; 0.5; 1; 2; and 3 m; N 4: 4 samples from 0; 0.5; 1; and 2 m; N 5: 5 samples from 0; 0.5; 1; 2; and 2.5 m; N 6: 4 samples from 0; 0.5; 1; and 2 m; N 7: 4 samples from 0; 0.5; 1; and 1.5 m; N 8: 1 superficial sample; N 9: 4 samples from 0; 0.5; 1; and 2 m (*b*) of 40 °C for several days until the mass stabilized. A ball mill was used to grind the samples. The samples were crushed until a dispersion of 0.35 mm was reached. The powdered samples were mixed with a binder (cellulose) and pressed into tablets using the Spex manual hydraulic press.

The gross content of copper, gold, and silver in the studied tailings was determined using an ICPE-9000 optical emission spectrometer.

The decomposition of samples to determine the gross content of elements was carried out according to the MVI-80-2008 method, “Methodology for measuring the mass fraction of elements in soil and bottom sediment samples by atomic emission and atomic absorption spectrometry”.

To assess the migration ability of potentially toxic impurities washed out by precipitation, we examined the Sak-Elga River upstream and downstream from the influx into the Bogorodskiy Pond; upstream and downstream from the confluence with the Ryzhiy Stream; and in the area of unloading acidic effluents from the TSF N 4.

The determination of potentially toxic elements in the waters was carried out using the method of atomic absorption spectrometry and induction-coupled plasma spectrometry. Analytical work was carried out on the Shimadzu ICPE-9000 device and the Shimadzu atomic absorption spectrometer AA6300 (Japan).

Determination of the content of elements in sediment samples was carried out according to RD 52.18.289-2022 “Mass fraction of mobile forms of metals in soil. Measurement technique by atomic absorption spectrometry”.

Results and discussion. The conducted studies allowed us to establish that acid drainage runoff is formed during the infiltration of atmospheric precipitation through the body of the TSF. The physico-chemical composition of the solution directly depends on the minerals composing the body of the tailings through which it passes.

The analysis of tailings sampled from different horizons makes it possible to identify a direct dependence of the concentration of pollutants on the depth of a layer. Thus, the water accumulates the maximum mass of pollutants in an acidic environment while passing from the surface of the TSF to its base. The sulfide minerals that make up the bulk of the TSF react with the sediments of a neutral medium and produce a highly acidic solution. The resulting acidic runoff mobilizes non-ferrous metals and provokes their migration into the deeper horizons with the subsequent increase in their concentration therein.

Drainage sub-basement waters reach aquifers and the nearest surface watercourses. In this case, the main receiver of such waters is the Ryzhiy Stream, which flows into the Sak-Elga River, a tributary of the Miass River.

The Ryzhiy Stream has exceptionally high concentrations of metals in its waters. At its confluence with the Sak-Elga River, a complete transformation of river waters occurs, characterized by a drop in pH to 3.0, and water quality deteriorates significantly at the point of mixing of watercourses. During the summer low streamflow period, the qualitative elemental composition of river waters becomes close to the composition of sub-basement waters. The excess concentrations of copper, zinc, iron, and manganese over the natural background values reach a 1000-fold level. After the confluence of the Ryzhiy Stream into the Sak-Elga River, the concentrations of pollutants gradually decrease downstream due to the difference in the flow rates; however, the waters are still characterized by a high pollution level.

The analysis of the content of mobile forms of metals in absolutely dry samples of bottom sediments confirms the negative anthropogenic impact of infiltration wastewater from the accumulated processing waste on the qualitative composition of the Sak-Elga River. The maximum concentration of mobile forms of metals is observed at point 5 in cases of copper, 1990.0 mg/kg (Enrichment Factor, EF = 663.3); zinc, 5750.0 mg/kg (EF = 250.0); arsenic – 172.8 mg/kg (EF = 86.4); nickel, 128.0 mg/kg

(EF = 32.0); iron, 21,266.0 mg/kg. At point 6, the content of mobile forms of metals decreases, but their concentrations also significantly exceed the MPC: copper, 613.0 mg/kg (EF = 204.3); zinc, 4900.0 (EF = 213.0); arsenic, 68.0 (EF = 34.0); nickel, 116.0 (EF = 29.0); iron, 19,080.0.

In addition, dry tailings are exposed to wind erosion that creates man-made dust deposits on the soil and vegetation cover over an area of more than 40 km^2, high-contrast in metal content with a total EF of more than 400, which corresponds to an environmental disaster zone. The geochemical association of metals in technogenic sediments is as follows: Hg_{148}-Cu_{87}-Sb_{43}-Ag_{40}-Pb_{37}-As_{20}-Bi_{19}-Zn_{13}-$Ni_{1.7}$.

The combination of these factors indicates the need to significantly reduce the environmental load by eliminating the impact of the accumulated waste. There is a need to assess the possible recycling of accumulated waste. For this purpose we analyzed the tailings from the storage facilities N 3 and 4 (Table 4).

Table 4

Composition of the samples from the processing tailings, g/t

Compound	Tailings Storage Facility N 3			Tailings Storage Facility N 4		
Depth, m	0.5	1	2	1	2	4
SO_3	441.9	407.2	440.3	252.1	331.3	366.9
Fe_2O_3	263.3	265.1	271.2	166.6	207.9	195.9
SiO_2	194.2	201.5	167.5	388.7	300.1	265.9
Al_2O_3	52.6	56.8	57.8	12.4	83.9	108.8
CaO	21.4	30.9	25.8	36.6	26.3	19.1
K_2O	10.1	10.0	8.2	17.3	12.6	15.1
BaO	5.9	5.1	5.1	5.3	8.3	4.5
TiO_2	1.5	2.2	1.3	3.3	2.6	1.8
ZnO	1.4	1.8	1.5	0.9	0.9	0.5
As_2O_3	0.3	0.5	0.6	0.6	035	0.2
PbO	0.3	0.3	0.3	0.1	031	0.2
ZrO_2	0.1	0.1	0.06	0.1	0.1	0.08
SrO	0.07	007	0.06	0.08	0.1	0.06
MgO	2.8	9.9	9.2	16.2	16.9	12.6
Cu	884.8	3732.4	5526.6	1916.5	2459.2	4464
Au	0.77	0.82	0.87	0.19	1.17	0.49
Ag	9.76	11.33	14.59	1.83	2.01	7.42

The results of the analysis of TSF N 3 and 4 show (Fig.6) that iron, sulfur, aluminum, and silicon are the major elements, while gold and silver are significant impurities.

Pyrite (FeS_2) is the tailings' main mineral, forming iron sulfate and sulfuric acid when interacting with atmospheric precipitation and oxygen. With the decomposition of residual pyrite, drainage waters containing sulfuric acid and trivalent iron sulfate are formed, which leads to significant pollution of aquifers and surface watercourses.

A layer-by-layer sampling of tailings from different depths revealed the regularity of the accumulation of non-ferrous metals and the growth of their content with increasing depth. The gold content in the tailings (0.83-3.48 g/t) is comparable to its levels in pyrite ores, so the waste can be regarded as a potential technogenic mineral raw material suitable for recycling to extract valuable components. We carried out an experiment simulating the process of recycling the accumulated tailings. The Albion acid leaching method was taken as a basis. An installation for process simulation in laboratory conditions has been designed. The lab-scale plant consists of a 2000 ml glass cup, a turbine agitator, a Memmert water bath, an oxygen tank, and a 150MI pH meter with a Hanna electrode.

During the experiment, the leaching of copper and zinc from low-grade finely ground rocks was stimulated for 48 hours at an elevated temperature of ca. 95 °C with further filtration through

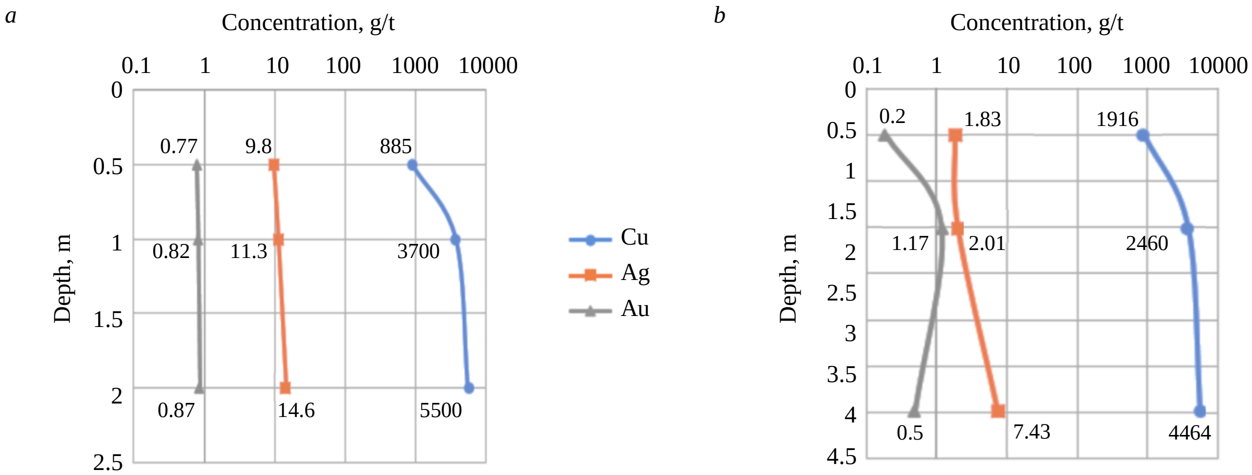

Fig.7. Distribution of elements along the vertical sections of tailings N 3 (*a*) and N 4 (*b*)

a Bunsen flask. Due to the limited mass of material, the experiment was carried out on the tailings from the facility N 3 (point 3, 2 m depth) with average contents of 0.72 % Cu and 0.92 % Zn.

The resulting green color of the solution indicates an intensive transition of zinc into the solution, which was confirmed by analyses. The results of the experiment are shown in Table 5.

Secondary waste processing using the Albion method aims to extract at least 98 % of copper and zinc. The production of copper, as the main valuable component, at the level of 43-44 % does not correspond to the degree of extraction at the current smelting plant, 98.5 %. It can be concluded that recycling the tailings by acid leaching is economically impractical.

Table 5

Changes in the content of Cu and Zn during the simulation of the Albion process

Element	Initial content in tailings, %	Initial content in 1 liter of solution, mg/l	End content in 1 liter of solution, mg/l	Experimental extraction, %	Extraction at the processing plant, %
Cu	0.72	3456	1510.4	43.7	98.5
Zn	0.92	4416	3888.1	88.0	99.0

It is necessary to develop environmental protection measures to reduce the negative impact of accumulated waste by combining methods of step-by-step land rehabilitation and the treatment of sub-basement wastewater. The approach includes the phased implementation of the engineering reclamation and biological restoration on the entire surface of TSF N 3 and 4 with a solution for the neutralization of infiltrating acid effluents. One such solution may be the creation of a geochemical barrier with an alkaline and/or sorption filter loading for neutralization and sorption of acidic wastewater in the area of their discharge along the perimeter of tailings.

It is also possible to preserve man-made deposits by shielding the surface with compacted natural clays or insulating the walls and surface of tailings with polymer sheets (geomembranes) with further revegetation. These conservation options will prevent the discharge of acid effluents from tailings dumps into surface watercourses, as well as preserve a potential technogenic deposit for further extraction of useful components.

Conclusion. A review of the published data allows us to conclude that the enterprise and the accumulated waste from the processing of copper ores have a negative environmental impact. In the period from 1907 to 2006, the atmospheric air was affected eminently, as over 14 million tons of pollutants were emitted. To date, the volume of pollutant emissions into the air has been reduced down to the maximum permissible concentrations thanks to the new gas cleaning equipment. Accumulated waste from the processing of copper ores continues to pollute the environment. The drainage runoff of tailings dumps is discharged into groundwater and surface watercourses, polluting them with dissolved metals; due to prolonged pollution, bottom sediments with high concentrations of metals are formed in the Sak-Elga River.

The analysis of the water samples and tailings revealed that: 1) the water of the Ryzhiy Stream contains high concentrations of metals – Cu (more than 5000-fold exceedance over the MPC), Zn (10,000-fold), Fe (more than 3900-fold), etc., and pollutes the Sak-Elga River; 2) the levels of non-ferrous metals in the tailings increases with the depth. At a depth of more than 2 m from the surface of the tailings, the concentrations of non-ferrous metals are Cu 5500 g/t; Au 0.87 g/t; and Ag 14.6 g/t. This fact allows us to consider tailings storage facilities N 3 and 4 as secondary sources of mineral resources.

The experiment on the secondary processing of accumulated waste showed that acid leaching is impractical. The extraction ratio was 43.7 % for copper and 88 % for zinc. At the same time, the extraction of copper and zinc from the prepared ore with a similar metal content at the processing plant reaches 99 %. It is necessary to develop a comprehensive solution to reduce the negative impact of accumulated waste by reclamation of the tailings storage facilities.

REFERENCES

1. Sudarikov S.M., Yungmeister D.A., Korolev R.I., Petrov V.A. On the possibility of reducing man-made burden on benthic biotic communities when mining solid minerals using technical means of various designs. *Journal of Mining Institute*. 2022. Vol. 253, p. 82-96. DOI: 10.31897/PMI.2022.14

2. Cánovas C.R., Macías F., Basallote M.D. et al. Metal (loid) release from sulfide-rich wastes to the environment: The case of the Iberian Pyrite Belt (SW Spain). *Current Opinion in Environmental Science and Health*. 2021. Vol. 20. N 100240. DOI: 10.1016/j.coesh.2021.100240

3. Danilov A.S., Smirnov Y.D., Korelskiy D.S. Effective methods for reclamation of area sources of dust emission. *Journal of Ecological Engineering*. 2017. Vol. 18. Iss. 5, p. 1-7. DOI: 10.12911/22998993/74947

4. Plokhov A.S., Kharko P.A., Pashkevich M.A. Effect of tailings storage facility on surface water at copper-pyrite deposit. *Mining Informational and Analytical Bulletin*. 2021. N 4, p. 57-68 (in Russian). DOI: 10.25018/0236_1493_2021_4_0_57

5. Erzova V.A., Rumynin V.G., Sudarikov S.M. et al. Influence of North-West Nuclear Complexfacilities on Groundwater Contamination (Leningrad Region). *Bulletin of the Tomsk Polytechnic University. Geo Assets Engineering*. 2021. Vol. 332. N 9, p. 30-42 (in Russian). DOI: 10.18799/24131830/2021/9/3351

6. Rumynin V.G., Nikulenkov A.M., Rozov K.B. et al. The status and trends in radioactive contamination of groundwater at a LLW-ILW storage facility site near Sosnovy Bor (Leningrad region, Russia). *Journal of Environmental Radioactivity*. 2021. Vol. 237. N 106707. DOI: 10.1016/j.jenvrad.2021.106707

7. Pozo-Antonio S., Puente-Luna I., Lagüela-López S., Veiga-Ríos M. Techniques to correct and prevent acid mine drainage: A review. *DYNA*. 2014. Vol. 81, p. 73-80. DOI: 10.15446/dyna.v81n186.38436

8. Kharko P.A., Matveeva V.A. Bottom Sediments in a River under Acid and Alkaline Wastewater Discharge. *Ecological Engineering & Environmental Technology*. 2021. Vol. 22. N 3, p. 35-41. DOI: 10.12912/27197050/134870

9. Kasimov N.S. Landscape Ecogeochemistry. Moscow: Publisher Filimonov M.V., 2013, p. 208 (in Russian).

10. Zhihong Tu, Qi Wu, Hongping He et al. Reduction of acid mine drainage by passivation of pyrite surfaces: A review. *Science of the Total Environment*. 2022. Vol. 832. N 155116. DOI: 10.1016/j.scitotenv.2022.155116

11. Pain D.J., Sánchez A., Meharg A.A. The Donana ecological disaster: Contamination of a world heritage estuarine marsh ecosystem with acidified pyrite mine waste. *Science of the Total Environment*. 1998. Vol. 222, p. 45-54. DOI: 10.1016/S0048-9697(98)00290-3

12. Bo Li, Guo Liu, Yuhan Nie, Zhong Ye. Causes and Effects of a Water Spill from the Underground Pit of the Dashu Pyrite Mine, Southern Sichuan Basin, Southwest China. *Mine Water and the Environment*. 2021. Vol. 40. Iss. 4, p. 864-876. DOI: 10.1007/s10230-021-00825-8

13. Bachurina A.V., Zalesov S.V., Tolkach O.V. The Effectiveness of Disturbed Lands Forest Reclamation in the Zone of Copper-melting Works. *Ecology and Industry of Russia*. Vol. 24. N 6, p. 67-71 (in Russian). DOI: 10.18412/1816-0395-2020-6-67-71

14. Argimbaev K.R., Kornev A.V., Kholodnyakov G.A. Substantiation of the Possibility of Involvement in Processing of the Iron-Containing Tails with the Subsequent Clotting of the Obtained Concentrates. *Journal of Mining Institute*. 2013. Vol. 206, p. 120-124 (in Russian).

15. Matveeva V.A., Lytaeva T., Danilov A.S. Application of Steel-Smelting Slags as Material for Reclamation of Disturbed Lands. *Journal of Ecological Engineering*. 2018. Vol. 19. Iss. 6, p. 97-103. DOI: 10.12911/22998993/93511

16. Petrov G.V., Kalashnikova M.I., Fokina S.B. Regularities of selenium and chromium behavior in redox processes during hydrometallurgic treatment of solid phase products of rhenium extraction. *Journal of Mining Institute*. 2016. Vol. 220, p. 601. DOI: 10.18454/PMI.2016.4.601

17. Vodyanitskii Y.N., Minkina T.M., Kubrin S.V. et al. Iron sulphides and their effect on the XRF measurement of the bulk chemical composition of badland soils near the Karabash copper smelter, Southern Urals, Russia. *Geochemistry: Exploration, Environment, Analysis*. 2018. Vol. 19. Iss. 2, p. 176-183. DOI: 10.1144/geochem2017-081

18. Smorkalov I.A., Vorobeichik E.L. Soil respiration of forest ecosystems in gradients of environmental pollution by emissions from copper smelters. *Russian Journal of Ecology*. 2011. Vol. 42. N 6, p. 464-470 (in Russian). DOI: 10.1134/S1067413611060166

19. Minkina T.M., Linnik V.G., Nevidomskaya D.G. et al. Forms of Cu (II), Zn (II), and Pb (II) compounds in technogenically transformed soils adjacent to the Karabashmed copper smelter. *Journal of Soils and Sediments*. 2018. Vol. 18. Iss. 6, p. 2229-2230. DOI: 10.1007/s11368-017-1777-2

20. Kumar A.T., Maleva M., Kiseleva I. et al. Toxic metal(loid)s contamination and potential human health risk assessment in the vicinity of century-old copper smelter, Karabash, Russia. *Environmental Geochemistry and Health*. 2020. Vol. 42. Iss. 12, p. 4113-4124. DOI: 10.1007/s10653-019-00414-3

21. Shimalina N.S., Pozolotina V.N., Orekhova N.A., Antonova E.V. Assessment of biological effects in Plantago major L. Seed progeny in the zone of impact from a Copper Smelter. *Russian Journal of Ecology*. 2017. Vol. 48. N 6, p. 513-523 (in Russian). DOI: 10.1134/S1067413617060108

22. Lezhnin V.L., Kazantsev V.S., Polzik E.V. A Multifactor Assessment of Effects of Technogenic Pollution on the Occurrence of Lung Cancer in the Population of an Industrial Town. *Hygiene and Sanitation*. 2014. Vol. 93, p. 26-30 (in Russian).

23. Elizareva E.N., Yanbaev Y.A., Redkina N.N. et al. Assessment of Soil Pollution in the Zone of Influence of Metallurgical Enterprises. *Vestnik of Orenburg State Pedagogical University*. 2017. N 9, p. 8-13 (in Russian).

24. Tatsy Y.G. Assessment of the Distribution of Heavy Metals around a Cu Smelter Town, Karabash, South Urals, Russia. *E3S Web of Conferences*. 2013. Vol. 1. N 19010. DOI: 10.1051/e3sconf/20130119010

25. Ulrikh D.V., Timofeeva S.S. Phytoremediation of Polluted Soil and Industrially Affected Subsoil of Waste Storage in the Copper Mining Areas in the South Ural. *Mining Informational and Analytical Bulletin*. 2016. N. 3, p. 341-349 (in Russian).

26. Tatsii Y.G., Udachin V.N., Aminov P.G. Environmental geochemistry of mercury in the area of emissions of the Karabashmed copper smelter. *Geochemistry International*. 2017. Vol. 55. N 10, p. 935-945. DOI: 10.1134/S0016702917100093

27. Shabanov M.V., Strekulev G.B. Geochemical Processes of Accumulation of Heavy Metals in the Landscapes of the Southern Urals. *Bulletin of the Tomsk Polytechnic University. Geo Assets Engineering*. 2021. Vol. 332. N 1, p. 184-192 (in Russian). DOI: 10.18799/24131830/2021/1/3011

28. Mikhailov G.G., Lonzinger T.M., Morozova A.G. et al. Evaluation of Effectiveness of Composite Sorbent For Rehabilitation of Contaminated Sites of Karabash Industrial Area. *Bulletin of the South Ural State University. Series* “*Metallurgy*”. 2014. Vol. 14. N 3, p. 12-18 (in Russian).

29. Ulrikh D.V. Scientific substantiation and development of technologies for the integrated restoration of technogenically disturbed territories in the areas of mining and processing of copper ores: Avtoref. dis. … d-ra tekhn. nauk. Chelyabinsk: Yuzhno-Uralskii gosudarstvennyi universitet, 2020, p. 44 (in Russian).

30. Yurkevich N.V., Saeva O.P., Pal’chik N.A. Arsenic mobility in two mine tailings drainage systems and its removal from solution by natural geochemical barriers. *Applied Geochemistry*. 2012. Vol. 27. Iss. 11, p. 2260-2270. DOI: 10.1016/j.apgeochem.2012.05.012

31. Brooks S.J., Udachin V., Williamson B.J. Impact of copper smelting on lakes in the southern Ural Mountains, Russia, inferred from chironomids. *Journal of Paleolimnology*. 2005. Vol. 33. Iss. 2, p. 229-241. DOI: 10.1007/s10933-004-3936-x

32. Denisov S.E., Ulrikh D.V., Zhbankov G.O. Formation of Hydrochemical River Regime under Extreme Contamination by Waste Water (the Sak-Elga River in the Chelyabinsk Region). *IOP Conference Series: Materials Science and Engineering*. 2017. Vol. 262. N 012186. DOI: 10.1088/1757-899X/262/1/012186

33. Korneeva T.V., Kucher D.O. Complex of Geochemical and Geophysical Approaches Using for Investigation of the Vertical and Lateral Distribution of Highly Toxic Solutions (Karabash District). *Interexpo GEO-Siberia*. 2014. Vol. 2, p. 116-121 (in Russian).

34. Rogozin A.G., Gavrilkina S.V. Causes for high concentration of copper and zinc in the water of some lakes in the Southern Urals. *Water Resources*. 2008. Vol. 35. Iss. 6, p. 701-707. DOI: 10.1134/S0097807808060092

35. Mikhailov G.G., Morozova A.G., Lonzinger T.M. Research of Surface Phase Formation in Interaction of Granular Composite Sorbent with Technological Multicomponent Saline Solutions. *Solid State Phenomena*. 2017. Vol. 265, p. 845-850. DOI: 10.4028/www.scientific.net/SSP.265.845

36. Yurkevich N.V., Saeva O.P., Karin Y.G. Geochemical anomalies in two sulfide-bearing waste disposal areas: Fe, Cu, Zn, Cd, Pb, and As in contaminated waters and snow, Kemerovo and Chelyabinsk regions, Russia. *Toxicological & Environmental Chemistry*. 2015. Vol. 97. Iss. 1, p. 76-89. DOI: 10.1080/02772248.2015.1041955

37. Maleva M.G., Borisova G.G., Shiryaev G.I. et al. Adaptive potential of *Typha latifolia* L. under extreme technogenic pollution. *AIP Conference Proceedings*. 2019. Vol. 2063. N 030013. DOI: 10.1063/1.5087321

38. Abrosimova N., Bortnikova S. The Role of Anionogenic Elements (As, Sb, Mo, Se, S, P, N, Cl, F, C) in the Formation of Technogenic Geochemical Anomalies. *IOP Conference Series: Earth and Environmental Science*. 2017. Vol. 95. Iss. 4. N 042024. DOI: 10.1088/1755-1315/95/4/042024

39. Zhbankov G.O., Denisov S.E., Ulrikh D.V. Efficiency analysis and justification of waste water purification methods for the water protection system against pollution. *IOP Conference Series: Materials Science and Engineering*. 2018. Vol. 451. N 012236. DOI: 10.1088/1757-899X/451/1/012236

40. Ulrikh D.V., Bryukhov M.N., Timofeeva S.S. Rationale for technique of operational sampling apatite-staffelite ores of kovdorsky deposit. *Mining Informational and Analytical Bulletin*. 2015. Vol. 4, p. 139-143 (in Russian).

41. Pashkevich M.A., Kharko P.A. The use of a composite mix to remove metals from acidic drainage waters at tailings facilities. *Obogashchenie rud*. 2022. N 4, p. 40-47 (in Russian). DOI: 10.17580/or.2022.04.07

42. Minkina T.M., Linnik V.G., Nevidomskaya D.G. et al. Heavy Metals Compounds in Soils in the Zone of Karabash Copper Smelter. Current Problems of Status and Evolution of Taxons of the Biosphere. Moscow: Vernadsky Institute of Geochemistry and Analytical Chemistry of the Russian Academy of Sciences (GEOKHI RAS), 2017. Vol. 26, p. 294-300 (in Russian).

43. Ryzhova L.P., Nosova E.V. To the Question of the Effectiveness of Technogenous ore Mineral Deposits Mining. *Mining Informational and Analytical Bulletin*. 2015. N 8, p. 49-55.

44. Altushkin I.A., Levin V.V., Sizikov A.V., Korol Y.A. Experience of development of porphyry copper type deposits in the Urals. *Journal of Mining Institute*. 2017. Vol. 228, p. 641-648. DOI: 10.25515/PMI.2017.6.641

Authors**:** **Mariya A. Pashkevich,** *Doctor of Engineering Sciences*, *Head of the Department*, *https://orcid.org/0000-0001-7020-8219* (*Saint Petersburg Mining University*, *Saint Petersburg*, *Russia*), **Alexey V. Alekseenko,** *Candidate of Engineering Sciences*, *Adjunct Professor*, *https://orcid.org/0000-0002-9785-7662* (*United Nations University*, *Institute for Integrated Management of Material Fluxes and of Resources*, *Dresden*, *Germany*), **Ruslan R. Nureev,** *Postgraduate Student*, *nureev_rr@mail.ru*, *https://orcid.org/0000-0002-1647-7095* (*Saint Petersburg Mining University*, *Saint Petersburg*, *Russia*).

The authors declare no conflict of interests.

ISSN 2411-3336; e-ISSN 2541-9404

JOURNAL OF MINING INSTITUTE

Zapiski Gornogo instituta

Journal homepage: pmi.spmi.ru

Research article

Hydrogeoecological conditions of technogenic groundwater in waste disposal sites

Aleksandr I. SEMYACHKOV, Viktoria A. POCHECHUN ✉, **Konstantin A. SEMYACHKOV**
Institute of Economics, Ural Branch of the RAS, Yekaterinburg, Russia

How to cite this article: Semyachkov A.I., Pochechun V.A., Semyachkov K.A. Hydrogeoecological conditions of technogenic groundwater in waste disposal sites. Journal of Mining Institute. 2023. Vol. 260, p. 168-179. DOI: 10.31897/PMI.2023.24

Abstract. The specific hydrogeoecological conditions of aquifers of some technogenic formations, mainly iron ore skarn-magnetite and titanium-magnetite formations, are considered. The resulting wastes, which are stored in waste disposal sites during development of deposits, due to the impact of a number of factors (natural and technogenic) form technogenic waters. Waste disposal facilities are complex engineering structures (dumps and sludge storages), which in turn create their own hydrogeoecological conditions, which must be investigated in order to prevent and minimize environmental and economic damage caused by these objects to the aquatic environment. The paper presents long-term field and laboratory studies of the aquatic environment under the influence of a waste disposal facility in the Middle Urals – one of the largest tailings, representing a potential environmental and man-made hazard. This tailing dump contains tens of tons of waste – enrichment tailings and creates specific hydrogeoecological conditions on the territory. Based on many years of monitoring studies, an analysis of these conditions was carried out – the quality of groundwater affected by the tailings was assessed. It is shown that groundwater is of technogenic nature, i.e. are man-made waters that have a significant impact on the surface and underground hydrospheres of the territory.

Keywords: hydrogeoecological conditions; waste disposal facilities; dumps and tailings; groundwater; surface water

Received: 30.09.2022 ***Accepted: 13.02.2023*** ***Online: 13.03.2023*** ***Published: 25.04.2023***

Introduction. During the development of deposits, waste, that must be stored in waste disposal sites (WDS) and which represent technically complex structures, is generated. They can be divided into “dry” storage facilities (various dumps) and “wet” storage facilities (tailing dumps). As a result of natural and technogenic processes impact (precipitation, condensation, discharge of technical water), groundwater is formed in WDS in the form of technogenic aquifers.

The purpose of the study is to research the conditions for the formation and discharge of groundwater in WDS. At the same time, it is necessary to assess the factors of groundwater volume and quality formation in WDS, as well as their impact on the surface and underground hydrosphere.

The studies were carried out in the Middle Urals, where more than 10 billion tons of waste are located. WDS are placed in specific hydrological and hydrogeological conditions in the open structure of the mountain-folded Urals and, in turn, create specific hydrogeoecological conditions. All this determines the need to study the hydrogeoecological conditions of waste disposal sites, the impact of which on the aquatic environment is often assessed as catastrophic [1-3].

Methods. The work used hydrogeoecological analysis, geochemical and retrospective methods. The work is based on a large number of field observations that the authors have been conducting for more than 20 years at waste disposal sites from the enterprises of mining and industrial complex of the Middle Urals. The paper analyzes the results of the own monitoring studies of environmental components – surface and ground waters, as well as geological materials.

As an example, the sludge storage of the Kachkanarsky Mining and Processing Plant (MPP) was studied, the chemical composition of its waste, mg/dm^2: Sc – 0.013; TiO_2 – 0.7; Y – 0.01; CaO – 19.2; ZnO_2 – 0.1; SiO_2 – 47.5; Fe – 6.3; MgO – 13.4. To control the groundwater quality in the area of tailing dump impact, a regime network of observation wells was created, including 12 wells of the same type, which are located on the first aquifer of groundwater from the surface. The depth of the wells was 21-47 m, the diameter was 112-132 mm, with 127 mm casing of the upper zone of clay-grus formations and isolation of the annular space from the ingress of surface melt and rain water into the aquifer of fractured-pore groundwater to be opened for prevention of distortion of the results of hydrochemical testing of groundwater. The wells are located at the foot of the sludge storage dams outside the outlets of the sludge water filtrate.

The main principles of well placement relative to the tailings boundaries are accessibility of the approach to the places of laying, uniformity of distribution along the tailings perimeter and compliance with the direction of groundwater flows movement.

The impact of discharge from the tailing dump on the underground hydrosphere is reflected by three wells. Ground and surface water samples were taken quarterly according to established methods and analyzed in accredited chemical laboratories. In total, more than 200 samples were analyzed.

Discussion of the results. The mountainous and folded Urals (Sverdlovsk, Chelyabinsk, Orenburg regions and Bashkiria) are assigned to the groundwater basin of fracture zones in the rocks of the Middle and Lower Paleozoic [4-6]. The geological structure of the basin is extremely complex. Long-term continental development led to formation of a relatively low-mountain relief with a preserved weathering crust that plays a dual role. First, the residual crust slows down the infiltration of precipitation; secondly, it helps to equalize infiltration. In areas of clayey crusts development, colmatation of cracks in the weathering zone is noted. Therefore, great importance is attached to linear zones of increased fracturing, which formed in the post-Hercynian and especially in recent times.

With the end of the Hercynian era of folding, geological development of the region did not stop, it continued in the form of physical, chemical weathering and arch-block uplifts with erosion processes. As a result, a vertically regular system of cracks of varying intensity forming fracture zones was formed. The zones were formed at different times, but the basis for the emergence of each subsequent one, according to the principle of inherited development, was the previous one. Although the filtration and storage properties, chemical composition of waters, speed of movement and unloading of fractured zones differ, they form one aquifer.

Thus, two taxonomic units or two aquifer complexes can be distinguished. One of the complexes is composed of loose Mesozoic and Cenozoic deposits, and the second is a single aquifer complex of rock fracture zones from Cambrian to Devonian (Fig.1).

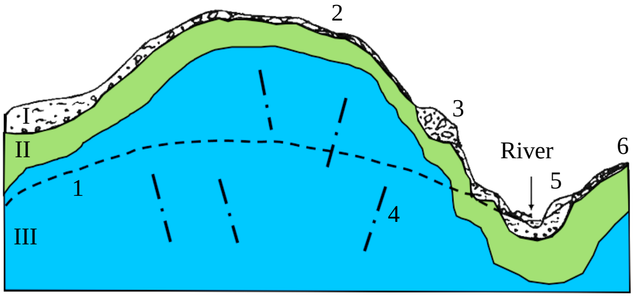

Fig.1. Groundwater layout
in the hydrogeological massifs of the Urals

Aquifer systems: I – loose Mesozoic and Cenozoic deposits;
II – zones of regional fracturing; III – zones of tectonic faults
1 – groundwater level; 2 – zone of aeration and seasonal fluctuations in the level of groundwater; 3 – groundwater of WDS;
4 – tectonic disturbances; 5 – groundwater of alluvial deposits

Mesozoic and Cenozoic formations of alluvial, eluvial-deluvial and technogenic genesis contain pore water. All of them form separate aquifers that differ in filtration and storage properties, thickness, sediment composition and occurrence conditions.

The WDS aquifer was formed in connection with the development of numerous deposits of solid minerals in the Urals, inevitably accompanied by excavation of ores and waste rocks from the bowels, which are stored in dumps. They are supplemented by sludge from processing plants and ash from thermal power plants, tailings from dredges in river valleys.

Dumps and sludge storages have a local distribution, but play a significant role in changing the natural situation in the area of mines, forming a technogenic landscape. Large volumes and areas of dumps contribute to the accumulation of atmospheric precipitation, melted snow water, and condensation of vapors from the air [7-9].

Estimation of the factors of groundwater volume and quality formation in WDS. There are dry (for example, dumps of off-balance ores) and wet (tailing and sludge dumps) types of waste storage [10-12]. During dry storage, technogenic waters are formed mainly under the influence of atmospheric precipitation. In wet storage, the main role during the operation of the facility is played by production water, and after the termination of its operation, atmospheric precipitation [13-15]. There are three most characteristic options for the WDS location on the relief [16-18]:

- on the watershed – during dry storage, technogenic waters are formed only under the influence of atmospheric precipitation, and during wet storage – industrial waters (Saldinskoye sludge storage);
- on the slope – formation of the chemical composition of technogenic waters involves flat runoff flowing along the relief into the dump (Tonsky dump of the Vysokogorsky Mining and Processing Plant);
- in the channel part of temporary or permanent watercourses, surface waters are involved in the formation of technogenic waters (Cheremshanskoye sludge storage, open-hearth slag dump of OAO NTMK).

The most important hydrometeorological factors are the amount of precipitation, their average intensity, duration, chemical composition and pH. The morphometric parameters of the WDS can have a great influence on groundwater discharge. Therefore, in dry storage, the determining factor is the capacity of the WDS – the larger it is, the longer the contact of atmospheric water with the dump and the higher the volume of groundwater. In this case, the length and width of the WDS can be significant characteristics [19].

At the Goroblagodatsky deposit, groundwater of technogenic deposits has a wide area development around existing mines and the open pit mine. A certain role in changing the natural environment of the deposit area is played by waste rock dumps and sludge storages, which occupy huge areas (dump 6 – 1120000 m^2, dumps 13, 14, 15 – 2250000 m^2, Polovinkinsky sludge storage – 2.3 million m^2). Large areas of dumps and their height contribute to the accumulation of liquid atmospheric precipitation, melted snow water, condensation of air moisture and their gradual consumption, which manifests itself in the form of hollows, permanent and temporary sources, in feeding small reservoirs.

Infiltration of atmospheric precipitation, snowmelt, replenishment due to surface runoff, and condensation of air moisture leads to accumulation of water under dump N 6 and their sudden breakthrough to the surface. Directly in the area of the breakthrough, the catchment area of dump N 6 is 524 thousand m^2, the volume is 17.5 million m^3. Depending on the amount of precipitation and condensation of air moisture, breakthroughs can occur both annually and with a break of up to two years. Breakthroughs in the summer (starting from the second half of summer) are characterized by suddenness, and in the case of their annual manifestations, the flow rate reaches 60-70 m^3/h, the duration of the outflow 15-20 days. The total reserves of waters pouring out during this time are 21-25 thousand m^3. In cases of water accumulation for two years, breakthroughs also occur suddenly, but the flow rate increases significantly, amounting to approximately 300 m^3/h with a total outflow duration of up to 95 days.

In winter, the flow of water occurs at the initial moment slowly with the formation of ice, which, as it grows, moves towards the village of Blagodat. The gradual movement of water leads to flooding of the basements of houses, road to the crushing and processing plant N 3 is blocked by icing. The height of the icing reaches 0.5-3.0 m, the area is approximately 70 thousand m^2. Only with an increase in the flow rate of the breakthrough, the water makes its way, and the comparatively fast unloading of the water accumulated under the dump takes place along the ditch. The total volume of water, subject to accumulation for several years, is significant – up to 500-600 thousand m^3 (Fig.2).

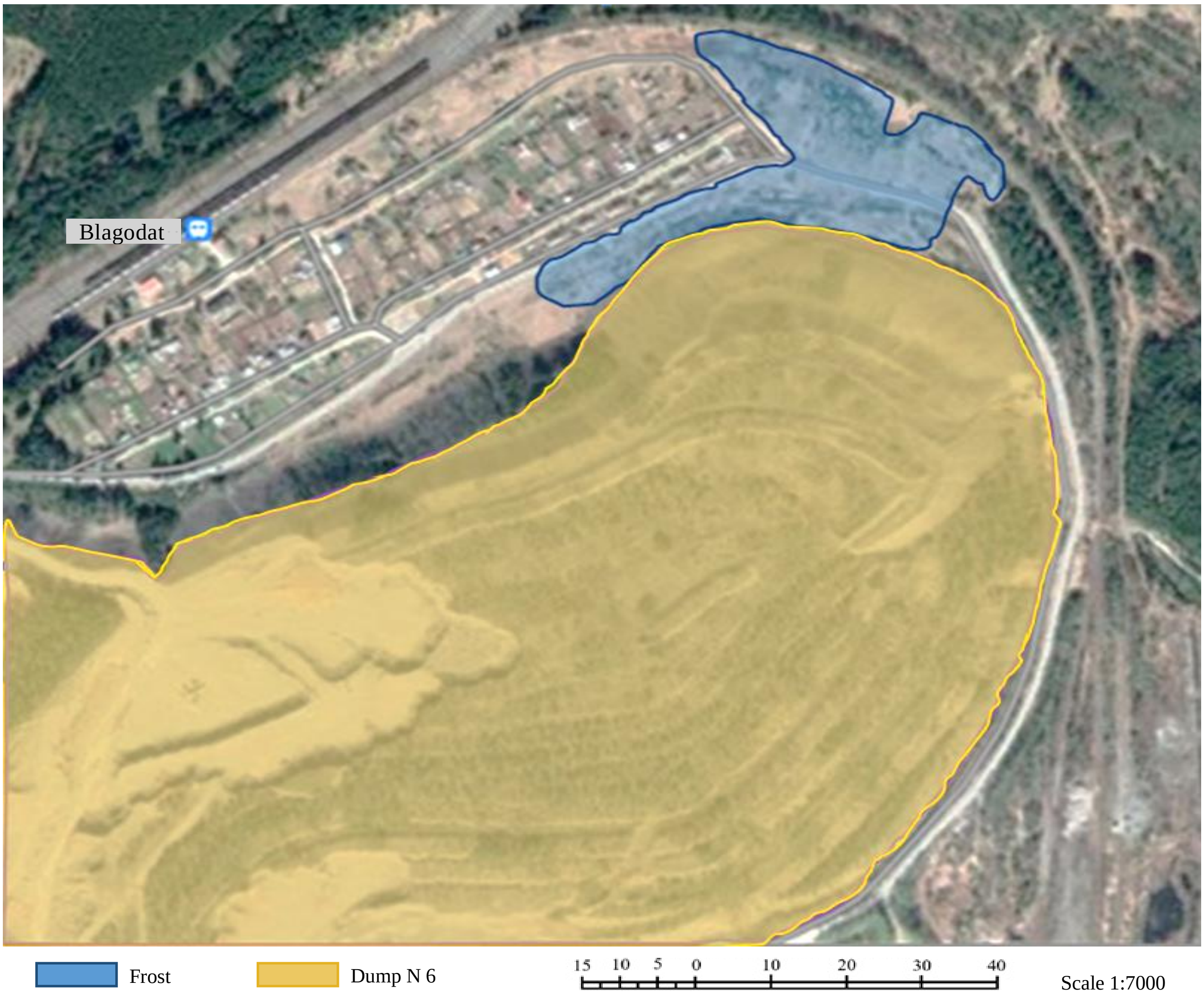

Fig.2. Scheme of the location of ice from groundwater from the WDS at the Goroblagodatsky field

The accumulation of a large mass of water and a sudden breakthrough are explained by the fact that the dump is composed of particles of inhomogeneous size – clay, wood, rubble and blocks. Cold air in winter, warm air in summer ventilates the dump, bringing heat or cold according to the season. In winter, the dump is frozen in the edge parts, the inner parts remain unfrozen due to the high power. Condensation of air moisture occurs both in warm and cold periods with the formation of a rock-ice lens at the border of the thawed and frozen parts of the dump. The accumulation of water occurs both in the form of ice and in liquid form. It is retained as a dam, by a rock-ice lens, and in its marginal parts by layers of clays that create conditions for accumulation. With the accumulation of water to a critical level, the lens thaws and a sudden breakthrough occurs, usually in November-December. Breakthroughs have been occurring continuously for 50 years.

At the Estyuninskoye deposit, a permanent spring was recorded at the foot of the northern dump. At the same time, there was a hidden discharge of water from technogenic deposits into underground workings, which became apparent after the occurrence of a landslide cirque in the area of rock fall. Dumps are located on the surface of relatively flat areas of the terrain, adjacent to the slopes of the mountains and are always above the groundwater level. The thickness and area of the underlying clay deposits are such that they allow water to be retained all year round, so such aquifers can be considered permanent.

Sludge storages occupy low relief areas, for example, in river valleys, in depleted quarries, where, in addition to water involved in the transport of sludge, groundwater is recharged [20-23]. Similar aquifers were formed at the Gusevogorskoye deposit of titanomagnetites (tailing dump), at the Cheremshanskoye sludge dump of the Vysokogorskoye deposit, at the Polovinkinsky and Saldinsky sludge storages of the Goroblagodatsky ore field. Under the sludge reservoirs, groundwater level rose by 15-20 m with formation of spreading domes, springs formed at the base of the dams.

Geological and technical section along the observation network well: technogenic deposits tQ (depth of occurrence 0-3 m, layer thickness 3 m); deluvial loam Q (depth of occurrence 3-3.9 m, layer thickness 0.9 m); eluvial light yellow dense loam Q (depth of occurrence 3.9-8 m, layer thickness 4.1 m); gabbro S_1I_{1-2} (depth of occurrence 8-27 m, layer thickness 19 m); drilling diameter 127-132 mm, casing depth 110 mm; drilling depth 6.7 m; water level – appearance 12 m, steady 12 m.

Assessment of groundwater quality formation in WDS. Formation of groundwater composition during their interaction with the solid phases of WDS occurs as a result of leaching [24], i.e., selective dissolution of one or several components of solid phase by liquid. Dissolution occurs until the chemical potentials of dissolving component in the liquid and solid phases are equal. The limiting concentration of the component C_n achieved in this case corresponds to the state of a saturated solution and is called solubility, the value of which depends on many factors. Therefore, when studying the patterns of interaction in the water-rock system, natural modeling methods are of great importance.

To predict the removal of components from the solid phase of WDS into the liquid one, it is necessary to determine the following parameters: leaching rate constant, day^{-1}; initial specific volume of the substance, units; filtration or infiltration rate, dm/day; substance density, g/dm^3; concentration of saturated solution, g/dm^3.

To determine the leaching rate constant, a filtration experiment is carried out on a special stand. A 500 ml test sample is placed in a filtration column, and distilled water is filtered through it with a pH corresponding to the pH of the sediments or filtration waters of the area. Filtration rate should be close to the real situation. From the moment the filtrate arrives, the countdown begins and sampling is carried out.

The study of the removal of pollutants from slimes and slags showed that slags with a higher metal content, a more coarsely dispersed composition and, as a result, a smaller area of contact between the solid and liquid phases, have a lower leaching capacity [25-27]. The authors calculated the time of complete leaching of metals in the considered waste. This period takes into account the contact time of water and solid phases. For dry-storage waste with an average rainfall of about eight hours and an average rainless period of 40 days, the total duration of contact between sediments and solid phase will be about one day per year. With this in mind, the time for complete leaching of metals from sludge by atmospheric precipitation will be hundreds, and from slag – thousands of years [28-30].

When examining the territory of the tailing dump in Kachkanar, carried out in different seasons, seven sources of formation of groundwater discharge were identified (Table 1). Thus, the total permitted wastewater discharge as a result of groundwater discharge from the tailings is 30,796.0 thousand m^3/year. With sewage, suspended solids, sulfates, nitrogen compounds, iron, vanadium, copper, and oil products enter water bodies. The main environmentally hazardous component in the sludge water cycle is the nitrate ion supplied by quarry waters [31].

Assessment of groundwater impact in WDS on the surface and underground hydrosphere. Let us analyze the impact on surface and ground waters of one of the largest tailings in the Middle Urals, which is the object of waste disposal – tailings for the enrichment of titanomagnetite ores of the Gusevogorskoye deposit. The area of the tailing dump is 19.75 km^2. The structure of the tailing dump includes dams: N 1 (filled with a maximum height of 82.5 m), N 2 (filled with a maximum dam height of 61.5 m) and eastern (filled with a height of 79 m). The filtration waters of the dams form three wastewater outfalls that enter the river Vyya. Table 2 compares the volumes of actual wastewater discharge from tailing dump into the river with permitted values in the dynamics of recent years.

As can be seen from Table 2, for all issues over the considered period of time, there are sharp fluctuations in volumes with periodic excesses of the allowable discharge. The increase in the volume of wastewater is due to the growth of the dam body due to its alluvium, the decrease in volume is due to the increase in the dam body due to the loading of downstream slopes with rock.

Table 1

Groundwater discharge indicators of the tailings in Kachkanar

Source of emission of pollutants		Pollutant	Wastewater discharge volume		
			thousand m^3/year	mg/dm^3	t/year
Rogalevsky compartment	Filtration through dam N 3 (dam outlet N 4)	Suspended solids	1361.0	4.0	5.444
		Dry residue		387.0	526.707
		BOD$_{20}$		2.5	3.403
		BOD$_5$		1.9	2.586
		Sulfates		54.0	73.494
		Nitrate ion		45.0	61.245
		Nitrite ion		0.18	0.245
		Ammonia nitrogen		0.1	0.136
		Iron		0.34	0.463
		Vanadium		0.01	0.014
		Copper		0.0126	0.017
		Oil products		0.11	0.150
	Filtration through dam N 4 (dam outlet N 10)	Suspended solids	1499.0	3.75	5.621
		Dry residue		385.0	577.115
		BOD$_{20}$		5.3	7.945
		BOD$_5$		3.5	5.247
		Sulfates		53.0	79.447
		Nitrate ion		45.0	67.455
		Nitrate ion		0.19	0.285
		Ammonia nitrogen		0.1	0.150
		Iron		0.3	0.450
		Vanadium		0.003	0.004
		Copper		0.0089	0.013
		Oil products		0.11	0.165
	Total for the Rogalevsky compartment 2860.0 thousand m^3/year				
Intermediate compartment	Filtration through dam N 1 (dam outlet N 2)	Suspended solids	521.0	4.0	2.084
		Dry residue		393.0	204.753
		BOD$_{20}$		3.0	1.563
		BOD$_5$		2.0	1.042
		Sulfates		56.0	29.176
		Nitrate ion		40.0	20.840
		Nitrite ion		0.08	0.042
		Ammonia nitrogen		0.39	0.203
		Iron		0.21	0.109
		Vanadium		0.002	0.001
		Copper		0.001	0.001
		Oil products		0.05	0.026
	Filtration through dam N 2 (dam outlet N 3)	Suspended solids	3632.0	2.75	9.988
		Dry residue		384.0	1394.688
		BOD$_{20}$		2.9	10.533
		BOD$_5$		2.0	7.264
		Sulfates		51.0	185.232
		Nitrate ion		45.0	163.440
		Nitrite ion		0.13	0.472
		Ammonia nitrogen		0.1	0.363
		Iron		0.34	1.235
		Vanadium		0.01	0.036
		Copper		0.0126	0.046
		Oil products		0.19	0.690
	Filtration through the eastern dam (dam outlet N 9)	Suspended solids	3095.0	2.78	8.604
		Dry residue		388.0	1200.860
		BOD$_{20}$		2.7	8.357
		BOD$_5$		1.8	5.571
		Sulfates		53.0	164.035
		Nitrate ion		45.0	139.275
		Nitrite ion		0.2	0.619
		Ammonia nitrogen		0.1	0.310
		Iron		0.34	1.052
		Vanadium		0.003	0.009
		Copper		0.0094	0.029
		Oil products		0.11	0.340
	Total for the Intermediate compartment 7248.0 thousand m^3/year				

End of Table 1

Source of emission of pollutants		Pollutant	Wastewater discharge volume		
			thousand m^3/year	mg/dm^3	t/year
Vyisky compartment	Siphon outlet from the tailing dump in the river Vyya (dam outlet N 1)	Suspended solids Dry residue BOD_{20} BOD_5 Sulfates Nitrate ion Nitrite ion Ammonia nitrogen Iron Vanadium Copper Oil products	20688.0	9.0 304.0 3.0 2.0 56.0 40.0 0.08 0.39 0.21 0.002 0.001 0.05	186.192 6289.152 62.064 41.376 1158.528 827.520 1.655 8.068 4.344 0.041 0.021 1.034
	Total for the Vyisky compartment 20,688.0 thousand m^3/year				

Table 2

Dynamics of volumes of actual wastewater discharge from tailings into the river Vyya Findings and their comparison with allowed values

Name of wastewater outlet	Wastewater discharge, thousand m^3		Multiplicity of exceeding the actual discharge of normatively permissible discharge value
	Actual	Permissible discharge standard	
2018			
Dam N 1	60	132	–
Dam N 2	3940	3750	1.1
Eastern dam	1130	1910	–
2019			
Dam N 1	521.0	120.0	4.3
Dam N 2	3632.0	5100.0	–
Eastern dam	2090.0	2890.0	–
2020			
Dam N 1	429.7	521.0	–
Dam N 2	4049.6	3632.0	1.1
Eastern dam	3201.5	2090.0	1.5

The concentrations of chemical elements and substances in the outlets show that there are excesses over the permitted discharge for a number of indicators:

- In dam release N 1: dry residue – up to 1.1 times (1 year out of 5); BOD_{20} – up to 1.2 times (1 out of 5); sulfates – up to 1.1 times (1 out of 5); nitrate ion – up to 2.1 times (5 out of 5); nitrite ion – up to 2.5 times (1 out of 5); iron – up to 2.1 times (2 out of 5); vanadium – up to 1.7 times (1 out of 5); copper – up to 3.0 times (2 out of 5).
- In dam release N 2: dry residue – up to 1.1 times (1 year out of 5); sulfates – up to 1.3 times (1 out of 5); nitrate ion – up to 1.8 times (4 out of 5); nitrite ion – up to 2.6 times (2 out of 5); iron – up to 1.3 times (1 out of 5); vanadium – up to 1.4 times (1 out of 5); copper – up to 2.0 times (1 out of 5); oil products – up to 2.2 times (3 out of 5).
- Filtration through the eastern dam: dry residue – up to 1.1 times (1 year out of 5); sulfates – up to 1.4 times (1 out of 5); nitrate ion – up to 1.8 times (5 out of 5); nitrite ion – up to 4.0 times (3 out of 5); iron – up to 1.4 times (1 out of 5); copper – up to 3.0 times (1 out of 5); oil products – up to 2.2 times (2 out of 5).

When conducting mining operations, explosives, containing high concentrations of nitrates, are used, which are also a characteristic pollutant and have significant excesses. For explosions, ammonium nitrate with a nitrogen content of up to 30 % is used. Every year, the enterprise uses thousands of tons of explosives, and, accordingly, thousands of tons of nitrogen enter the environment.

Table 3

The results of natural waters control at the river Vyya

Composition indicators	MPC$_f$[*] for water bodies, mg/dm^3	Background concentrations, mg/dm^3	The content of pollutants in the control section (after all outlets), mg/dm^3
Suspended solids	+0.75 to the background	3.0	3.0
Dry residue	–	67.7	315.0
BOD$_{20}$	3.0	5.0	4.98
Sulfates	100	4.90	45.0
Nitrate nitrogen (nitrate ion)	9.1	0.99	94.0
Nitrite ion	0.02	0.03	0.055
Vanadium	0.001	0.0015	0.0037
Copper	0.001	0.002	0.0029

---

[*] As a criterion for the groundwater pollution degree, the value of the maximum permissible concentration for fishery water bodies (MPC$_f$) is taken, due to the fact that groundwater in the tailings area is involved in feeding surface water bodies and watercourses of fishery value.

Table 4

Results of groundwater sampling in the area of the tailings

Name of indicator	MPC$_f$, mg/dm^3	2018		2019		2020	
		Content of components, mg/m^3	MPC ratio	Content of components, mg/m^3	MPC ratio	Content of components, mg/m^3	MPC ratio
Well 9							
Sulfates	100	49.3	–	33.4	–	37.9	–
Chlorides	300	26.0	–	4.86	–	10.2	–
Nitrates	40	3.03	–	2.77	–	0.43	–
Manganese	0.01	1.27	127	0.096	9.6	0.154	15.4
Copper	0.01	0.009	–	0.014	1.4	0.003	–
Iron	0.1	0.466	4.66	0.3	3	3.18	31.8
Zinc	0.01	0.012	1.2	0.014	1.4	0.031	3.1
Vanadium	0.001	0.0664	66.4	0.027	27	0.009	9
Dry residue	1000	232.0	–	53.0	–	172.3	–
Suspended solids	3.25	0.3	–	581.6	179	812.3	250
Well 10							
Sulfates	100	98.1	–	–	–	–	–
Chlorides	300	5.2	–	–	–	–	–
Nitrates	40	3.4	–	–	–	–	–
Manganese	0.01	4.0	400	–	–	–	–
Copper	0.01	0.031	3.1	–	–	–	–
Iron	0.1	0.326	3.26	–	–	–	–
Zinc	0.01	0.034	3.4	–	–	–	–
Vanadium	0.001	0.0328	32.8	–	–	–	–
Dry residue	1000	348.0	–	–	–	–	–
Suspended solids	3.25	2.58	–	–	–	–	–
Well 11							
Sulfates	100	71.3	–	79.3	–	96.6	–
Chlorides	300	3.47	–	8.1	–	12.2	–
Nitrates	40	1.6	–	2.34	–	1.17	–
Manganese	0.01	0.126	12.6	0.058	5.8	0.116	11.6
Copper	0.01	0.022	2.2	0.007	–	0.003	–
Iron	0.1	0.217	2.17	2.83	28.3	1.13	11.3
Zinc	0.01	0.006	–	0.034	3.4	0.009	–
Vanadium	0.001	0.0177	17.7	0.015	15	0.036	36
Dry residue	1000	176.0	–	101.0	–	302.0	–
Suspended solids	3.25	18.98	5.8	545.6	168	812.3	250

Note. As a criterion for the degree of groundwater pollution, it is proposed to take the background well 4-n, due to the fact that some pollutants (for example, copper, manganese, vanadium, iron) are typical for the area, which is associated with numerous ore deposits in the area under consideration and a large number of operating and decommissioned mine workings of various depths and areas, as well as waste storage facilities, wastewater outlets of industrial enterprises.

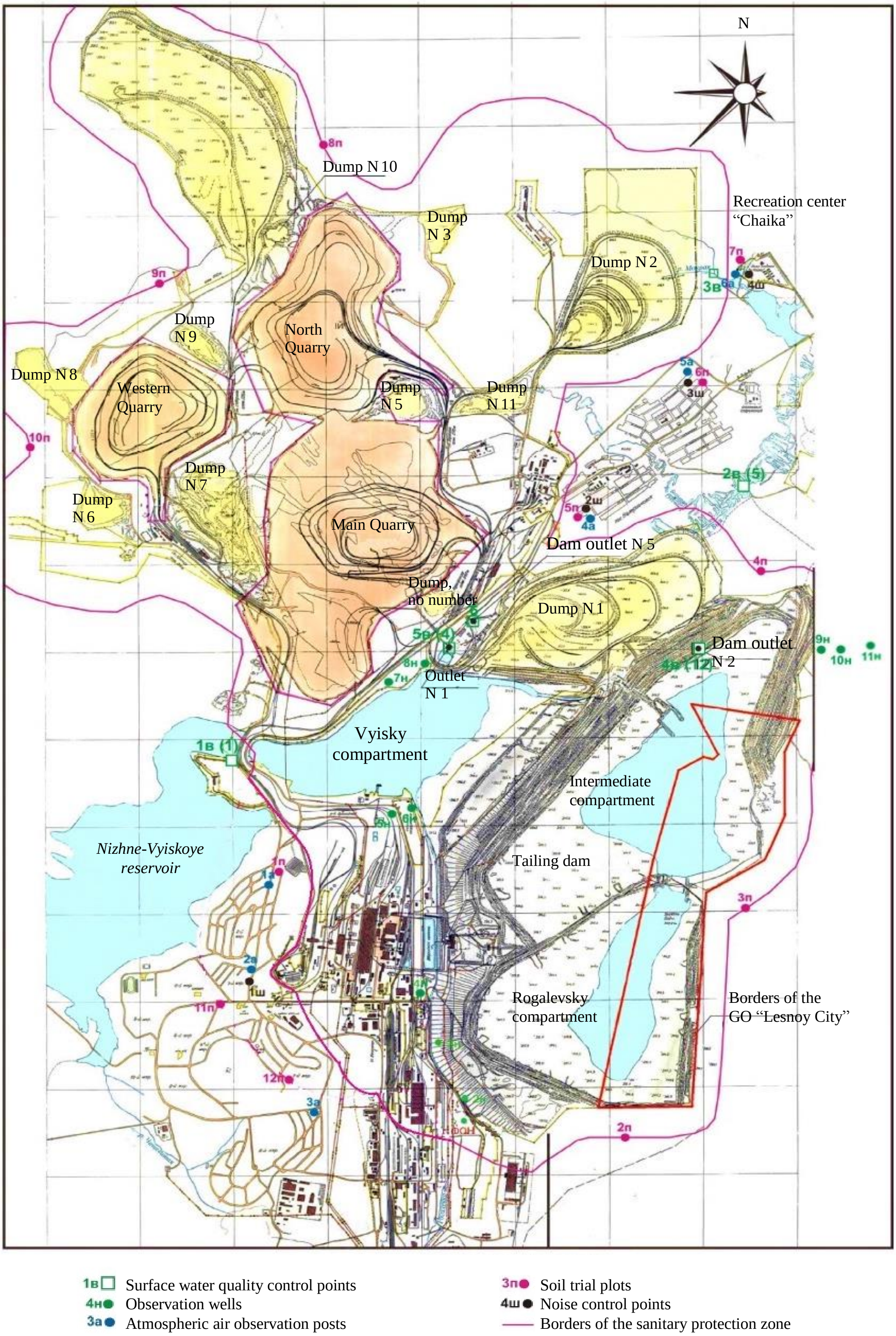

Fig.3. Location of observation points in the monitoring network

Objective indicators of the level of negative impact of a technogenic object on a watercourse are the background values of pollutants controlled in effluents and the results of analyzes in the control section after all outlets [32-34]. To determine the background concentrations of substances in the rivers, a target located above the outlets of wastewater was taken. Control over the state of the river Vyya after discharges of wastewater from all outlets is made by the enterprise that carries out a survey at a control site located below the outlets. The average annual results of monitoring the natural waters of the river are given in Table 3.

Analysis of Table 3 shows that, compared with the background values of chemicals concentrations in the river Vyya, concentration of the following pollutants in the control section increases: dry residue – by 246.4 mg/l (4.7 times, without exceeding the $\mathrm{MPC_f}$ value); sulfates – by 40.13 mg/l (by 9.2 times, without exceeding $\mathrm{MPC_f}$); nitrate nitrogen – by 92.5 mg/l (by 93.5 times); nitrite ion – by 0.05 mg/l (2.5 times); vanadium – by 0.0022 mg/l (2.57 times); copper – by 0.0008 mg/l (1.4 times).

The mechanism of tailings impact on the state of groundwater is the leakage of sludge water through the dam N 1 (outlet of sewage N 2), dam N 2 and the eastern dam (outlets N 3 and 9) in the valley of the river Vyya, where zone of technogenic impact on the state of underground hydrosphere is planned.

The study of groundwater in the area of the tailings is carried out on a network of observation wells specially created for this purpose (Fig.3) [35]. The impact of the tailing dump on groundwater is characterized by the content of pollutants in wells 9, 10 and 11 of the observation network [35]. Testing of these wells was carried out quarterly. The results of testing are presented in Table 4.

The results of studies of groundwater of the regional fracture aquifer, taken in the area of the tailing dump, indicate significant groundwater pollution in terms of the following indicators: manganese (up to 400 MPC), iron (up to 67 MPC), zinc (up to 4 MPC), vanadium (up to 67 MPC), suspended solids (up to 250 MPC).

Conclusion. In hydrogeology, as one of the branches of the Earth sciences, a lot of material has been accumulated for the formation of a new scientific direction on groundwater in waste disposal sites. It has been established that the hydrogeological conditions of groundwater in waste disposal sites are often difficult in terms of the conditions for the costs formation and groundwater quality. The factors of groundwater formation in the WDS, which are associated with the conditions of placement and morphometric parameters, granulometric and chemical composition of the waste, are determined.

Using the example of one of the WDS in the Middle Urals, it is shown that groundwater from waste disposal facilities has a significant negative impact on the surface and underground hydrosphere. Therefore, it is necessary to systematically study hydrogeological conditions of the underground waters of the WDS both at the stage of operation and during the period of waste conservation.

REFERENCES

1. Konovalov V.E. Rehabilitation of mining landscapes. Ekologicheskaya i tekhnosfernaya bezopasnost gornopromyshlennykh regionov: Trudy VI Mezhdunarodnoi nauchno-prakticheskoi konferentsii 10 aprelya 2018 / Ed by A.I.Semyachkov. Ekaterinburg: Institut ekonomiki UrO RAN, Uralskii gosudarstvennyi gornyi universitet, 2018, p. 89-95 (in Russian).

2. Semyachkov A.I., Pochechun V.A., Konovalov V.E., Ganin E.V. Ecological concept of mining landscapes rehabilitation. Ekaterinburg: Institut ekonomiki UrO RAN, 2020, p. 190 (in Russian).

3. Maksimovich N.G., Pyankov S.V. Kizelovsky coal basin: environmental problems and solutions. Perm: Permskii gosudarstvennyi natsionalnyi issledovatelskii universitet, 2018, p. 288 (in Russian).

4. Danilov A., Smirnov Y., Korelskiy D. Effective methods for reclamation of area sources of dust emission. *Journal of Ecological Engineering*. 2017. Vol. 18. Iss. 5, p. 1-7. DOI: 10.12911/22998993/74947

5. Strizhenok A.V., Korelskiy D.S. Improvement of the system of industrial environmental monitoring of atmospheric air in the area of anthropogenic arrays impact. *Journal of Physics: Conference Series*. 2019. Vol. 1384 (1). N 012052. DOI: 10.1088/1742-6596/1384/1/012052

6. Semyachkov A., Slawikowskaja Yu., Pochechun V. Methodological Features of the Assessment of Economic Damage from Adverse Environmental Consequences in Conditions of Territories with a Developed Mining Complex. *Ecology and Industry of Russia*. 2018. Vol. 22. N 4, p. 46-51 (in Russian). DOI: 10.18412/1816-0395-2018-4-46-51

7. Strategic directions and priorities of regional development in the face of global challenges. Under total ed. of Doctor of Economics Yu.G.Lavrikova, Doctor of Economics E.L. Andreeva. Ekaterinburg: UrO RAN, 2019, p. 504 (in Russian). DOI: 10.17059/1_2019

8. Antoninova N.Yu., Rybnikova L.S., Slavikovskaya Yu.O., Shubina L.A. Environmental and economic aspects of selecting reclamation directions for industrial mining and metallurgical waste disposal sites. *Russian Mining Industry*. 2022. N S1, p. 71-77 (in Russian). DOI: 10.30686/1609-9192-2022-1S-71-77

9. Lyashenko V.I., Vorobiev A.E., Khomenko O.E., Dudar T.V. Development of Technologies and Technical Facilities to Reduce the Environmental Impact in the Area of Influence of the Tailings Dam. *Vestnik Magnitogorskogo gosudarstvennogo tekhnicheskogo universiteta im. G.I.Nosova*. 2022. Vol. 20. N 1, p. 25-41 (in Russian). DOI: 10.18503/1995-2732-2022-20-1-25-41

10. Plokhov A.S., Kharko P.A., Pashkevich M.A. Effect of tailings storage facility on surface water at copper-pyrite deposit. *Mining Informational and Analytical Bulletin*. 2021. N 4, p. 57-68 (in Russian). DOI: 10.25018/0236_1493_2021_4_0_57

11. Khansivarova N.M. Assessment of the mechanical stability and protection of groundwater in the territories of the distribution of dispersed subsidence soils. *Natural and Technical Sciences*. 2021. N 10 (161), p. 120-125. DOI: 10.25633/ETN.2021.10.06

12. Kovrigin A.A., Slesarev M.Yu. A change model of the hydraulic characteristics of the territory occupied by the landfill of solid industrial and domestic waste. *Vestnik MGSU*. 2021. Vol. 16. N 6, p. 770-780 (in Russian). DOI: 10.22227/1997-0935.2021.6.770-780

13. Lyamin I.A., Ruzmanov R.Yu. Estimation of ground water protection on the waste disposal site of a mining enterprise. *Bulletin of Perm University. Geology*. 2020. Vol. 19. N 3, p. 241-246 (in Russian). DOI: 10.17072/psu.geol.19.3.241

14. Baev O.A., Silchenko V.F. Impact analysis of waste ponds on surface and underground water (Review). *Ecology and water management*. 2020. N 4 (7), p. 100-113 (in Russian). DOI: 10.31774/2658-7890-2020-4-100-113

15. Rybnikova L.S., Rybnikov P.A. Physico-chemical model of groundwater formation in the areas of flooded copper-pyrite mines of the Urals. *Mining Informational and Analytical Bulletin*. 2019. N S37, p. 584-595 (in Russian). DOI: 10.25018/0236-1493-2019-11- 37-584-595

16. Saburov H.M., Muradov B.Z., Mukhamedgaliev B.A. Environmental pollution industrial waste. *Bulatovskiye chteniya*. 2019. Vol. 4, p. 110-111 (in Russian).

17. Konovalov V.E., Germanovich Iu.G. Substance migration at minerals production and primary processing. *Izvestiya vysshikh uchebnykh zavedeniy. Gornyy zhurnal*. 2018. N 2, p. 30-39 (in Russian). DOI: 10.21440/0536-1028-2018-2-30-39

18. Khayrulina E.A. Influence of slurry storage facility with salt-bearing wastes onthesurface and groundwaters. *Geographical bulletin*. 2018. N 2 (45), p. 145-155 (in Russian). DOI: 10.17072/2079-7877-2018-2-145-155

19. Gyulmammadov Ch.D. Impact of human technogenic activity on hydrogeological conditions. *Science and world*. 2020. N 2-1 (78), p. 15-19 (in Russian).

20. Kuznetsov Yu.S., Chaplia B.Yu., Khafizov A.R., Shulgina A.P. Environmental aspects of large-tonnage production liquid waste storage into the underground storage. *Petroleum Engineering*. 2019. Vol. 17. N 3, p. 56-61 (in Russian). DOI: 10.17122/ngdelo-2019-3-56-61

21. Kletskina O.V., Oschepkova A.Z. About methodical approach to substantiation of criteria of admissible impact of the subject of landfill on underground waters with use of hydrogeological modeling. *Geologiya i poleznyye iskopayemyye Zapadnogo Urala*. 2019. N 2 (39), p. 337-342 (in Russian).

22. Pichura V.I., Skok S.V. Influence of urban systems on hydrogeological and hydrochemical conditions of aquifers**.** *Visnik Natsionalnogo universitetu bioresursiv i prirodokoristuvannya Ukraini*. 2019. N 6 (82), p. 1-16. DOI: 10.31548/dopovidi2019.06.001

23. Simion A.F., Drebenstedt C., Lazar M. The Influence of Tailings Storage Facilities in the Eastern Part of Jiu Valley on the Water Quality. *Gornaya nauka i tekhnika*. 2019. Vol. 4. N 4, p. 292-301. DOI: 10.17073/2500-0632-2019-4-292-301

24. Kharlyamov D.A., Smirnova N.N., Sharafutdinov R.N., Mavrin G.V. An assessment of groundwater quality in territories with various anthropogenic influence. *International Research Journal*. 2022. N 2-2 (116), p. 28-33 (in Russian). DOI: 10.23670/IRJ.2022.116.2.036

25. Trofimova Yu.V., Rastorguev A.V. Assessment of the solid industrial and municipal waste landfill as a source of groundwater pollution. *Inzhenernyye izyskaniya*. 2019. Vol. 13. N 3, p. 28-39 (in Russian). DOI: 10.25296/1997-8650-2019-13-3-28-38

26. Degtyar M., Galkina O. Ecological monitoring of the environmental state of waste concrete objects. *Naukovi notatky*. 2019. N 65, p. 55-60 (in Russian).

27. Fisun N.V. Ecologic potential of the environmental and hydrogeological systems in the area of kuchinsky municipal solid waste landfill (Moscow region). *Proceedings of higher educational establishments. Geology and Exploration*. 2018. N 3, p. 58-64.

28. Ponamarev Yu., Khazipova V. Monitoring underground and surface waters in the area of polygon effect of industrial waste. *Pozharnaya i tekhnosfernaya bezopasnost: problemy i puti sovershenstvovaniya*. 2018. N 1 (1), p. 143-146. (in Russian)

29. Kolesnikova L.A., Kovalchuk T.V. Problems and prospects of environmental safety of mining regions. *Mining Informational and Analytical Bulletin*. 2021. N 2-1, p. 275-286 (in Russian). DOI: 10.25018/0236- 1493-2021-21-0-275-286

30. Shepelev I.I., Eskova E.N., Pilyaeva O.V. Maintaining ecological stability of the operated natural – technical system under the impact of anthropogenic factors. *Problemy regionalnoy ekologii*. 2021. N 1, p. 76-82. DOI: 10.24412/1728-323X-2021-1-76-82

31. Musikhina T.A., Iurlov A.A., Zemtsova E.A., Filatov V.Yu. Comprehensive assessment of the toxicity of river and waste waters, formed on the territory contaminated by industrial waste. *Theoretical and Applied Ecology*. 2021. N 4, p. 133-139. DOI: 10.25750/1995-4301-2021-4-133-139

32. Lyashenko V.I., Golik V.I., Dyatchin V.Z. Increasing environmental safety by reducing technogenic loadin mining regions. *Izvestiya vysshikh uchebnykh zavedeniy. Chernaya metallurgiya*. 2020. Vol. 63. N 7, p. 529-538. DOI: 10.17073/0368-0797-2020-7-529-538

33. Akhmadiyev A. K., Ekzaryan V. N. Rehabilitation of the natural environment as the structural element of ecological security. *Mining Informational and Analytical Bulletin*. 2020. N 2, p. 112-120 (in Russian). DOI: 10.25018/0236-1493-2020-2-0-112-120

34. Glukhov V.V., Movchan K.S. Economic assessment of technology for waste processing taking into account impact on environment. *St. Petersburg State Polytechnical University Journal. Economics*. 2019. Vol. 12. N 1, p. 159-167. DOI: 10.18721/JE.12113

35. Tagilcev S.N., Cherednichenko A.V., Melnik V.V. Aggregation methods hydrogeomechanical, electrical and dowsing to select areas of hydrogeological wells. *Mining Informational and Analytical Bulletin*. 2020. N 3-1, p. 236-246 (in Russian). DOI: 10.25018/0236-1493-2020-31-0-236-246

***Authors*: Aleksandr I. Semyachkov,** *Doctor of Geological and Mineral Sciences, Head of Center, https://orcid.org/0000-0002-3352-2863* (*Institute of Economics, Ural Branch of the RAS, Yekaterinburg, Russia*), **Viktoria A. Pochechun,** *Doctor of Geographical Sciences, Head of Laboratory, viktoriyapochechun@mail.ru, https://orcid.org/0000-0002-2838-1162* (*Institute of Economics, Ural Branch of the RAS, Yekaterinburg, Russia*), **Konstantin A. Semyachkov,** *Candidate of Economics, Senior Researcher, https://orcid.org/0000-0003-0998-0183* (*Institute of Economics, Ural Branch of the RAS, Yekaterinburg, Russia*).

The authors declare no conflict of interests.

ISSN 2411-3336; e-ISSN 2541-9404

JOURNAL OF MINING INSTITUTE

Zapiski Gornogo instituta

Journal homepage: pmi.spmi.ru

Research article

The use of unmanned aerial photography for interpreting the technogenic transformation of the natural environment during the oilfield operation

Sergei A. BUZMAKOV✉, **Pavel Yu. SANNIKOV**, **Leonid S. KUCHIN**, **Ekaterina A. IGOSCHEVA**, **Irina F. ABDULMANOVA**
Perm State National Research University, Perm, Russia

How to cite this article: Buzmakov S.A., Sannikov P.Yu., Kuchin L.S., Igosheva E.A., Abdulmanova I.F. The use of unmanned aerial photography for interpreting the technogenic transformation of the natural environment during the oilfield operation. Journal of Mining Institute. 2023. Vol. 260, p. 180-193. DOI: 10.31897/PMI.2023.22

Abstract. The traditional approach to monitoring observations of the technogenic processes development in oilfields, which consists in determining the concentration of marker pollutants in various natural environments, does not provide the necessary completeness of information and the efficiency of its receipt. The paper considers an example of expanding the range of observations due to unmanned aerial photography and a number of other methods. Interpretation signs (for panchromatic survey) were determined that register such consequences of technogenic transformation of the natural environment as mechanogenesis, bitumization, and halogenesis. Technogenic mechanogenesis is understood as a physical violation of the integrity of ecosystems, the movement of soils and grounds. Bitumization is expressed in the migration of petroleum hydrocarbons through soils, ground, surface, subsurface, and underground waters, and their destruction. Salt migration in these media is defined as halogenesis. The most reliable indicators are linearly elongated areas of dead forests, dark red spots in drying microdepressions and reservoirs. It was found out that the oilfield impact on the raised bog leads to anthropogenic eutrophication, the introduction of plant species, uncharacteristic coenotic groups, the replacement of subshrubs with grasses, and morphometric changes in forest pine. In the peat deposits of the disturbed area, an unusual interlayer of whitish, undecomposed moss was recorded. The moment of the beginning of a pronounced technogenic transformation was registered in the course of work with the archive of multispectral space images. Continuous remote sensing with the help of unmanned aerial photography and interpretation by sedimentological, geobotanical methods significantly expand the possibilities of studying the technogenic transformation of the natural environment. To ensure environmental safety, it is advisable to develop remote methods and technologies to include them in the environmental monitoring system.

Keywords: technogenic transformation; mechanogenesis; bitumization; halogenesis; unmanned aerial vehicle; panchromatic shooting; multispectral survey; sediment; anthropogenic eutrophication; NDVI

Acknowledgment. The study was carried out with the financial support of the Russian Foundation for Basic Research and the Perm Territory under the scientific project N 20-45-596018.

Received: 29.10.2022 ***Accepted: 13.02.2023*** ***Online: 23.03.2023*** ***Published: 25.04.2023***

Introduction. The sustainable development of regions such as the Perm Territory is associated with the protection of the natural environment during the extraction of minerals. Ensuring environmental safety in oil production is largely determined by the level of environmental monitoring. Mechanical disturbances and pollution cause technogenic transformation of the natural environment during the construction and operation of oil production facilities. A pronounced effect occurs through thermal effects [1] and air pollution by ingredients [2] when associated gas is burned. Zonal features of local ecosystems (soil type, climate) significantly affect the nature of the transformation processes manifestation [3].

The generally accepted methods for observing the oilfield impact are based on sampling the main natural media (soil, water, air) [4] and identifying the concentration of marker pollutants:

hydrocarbons, chlorides, phenols, trace elements and polycyclic aromatic hydrocarbons (PAHs) [5]. The resulting estimates are important, but do not enable to unambiguously interpret the direction of technogenic processes and determine their speed in space and time. The use of a set of remote (unmanned aerial photography), geoinformation, geochemical, geobotanical methods significantly improves the spatial and dynamic possibilities of studying technogenic processes [6].

Currently, it is possible to assess the environmental state using the unmanned aerial vehicles (UAVs) [7]. They enable to monitor areal, point, and linear sources of environmental pollution, which allows to determine the levels of pollution quickly and accurately [8]. The expediency and prospects of the development of metrological and methodological support for this type of observations are shown [9].

Space imaging with panchromatic and multispectral cameras makes it possible to identify oilfield infrastructure facilities [10], wood cutting areas [11], soil subsidence areas [12], relatively large oil spills [13-15], and to evaluate vegetation dynamics using the available long-term image archives [16]. Aerial photography in panchromatic mode also makes it possible to record facilities of the oilfield infrastructure, spills, cuttings [17], and monitor the integrity of pipelines [18]. In this case, the accuracy increases, and the areal detection threshold decreases. With the help of multispectral imaging, the dynamics of the restoration of disturbed lands [19] and oil spills [20] is monitored. Lidar (laser) survey is used to assess the state of the forest stand [21]. Thermal imaging aerial photography is widely used to identify oil spills [22, 23], including those on water bodies [24], to determine soil moisture parameters [25], and to identify oil and gas leaks from pipelines [26].

Significant experience in the sedimentological study of peat cores to identify oilfield technogenesis is known from publications based on material from Western Siberia [27, 28]. The most obvious direction is the analysis of microelements distribution along the profile [29-31], and their radial migration over time [32, 33]. The geochemical composition of the peat stratum is affected not only by oil hydrocarbons, but also by the accompanying mineral salt components contained in drilling fluids [34, 35]. This area of research is interested in the experience of using UAVs for environmental monitoring of polymetallic sulphide ore deposits [36].

When studying vegetation in technogenic areas of oilfields, researchers pay attention to changes in the share of ecological groups in the composition of the phytocenosis structure, the introduction and increase in the abundance of individual groups of grasses [37], and morphological changes in tree stand [38]. There is experience in the use of UAVs for the restoration of the natural environment by bioremediation methods [39].

The purpose of the work is to test the use of unmanned aerial photography for interpreting the technogenic transformation of the natural environment during the oilfield operation.

The work was carried out on the example of an oilfield in the north of the Perm Territory in the bog complex of the middle taiga.

Methodology. The general pattern illustrating the stages of the natural environment study during the oilfield operation is shown in Fig.1.

Aerial photography in the optical part of the spectrum was carried out on 22 August 2021, together with employees of OOO Finko, Unmanned Systems Group of Companies (Izhevsk) at an altitude of 400 m above the Earth’s surface. The overlap of images is 55 %, the shooting was made every 70 m of the flight. A Russian-made Supercam S350F unmanned aerial vehicle was used. As a result of processing aerial photography materials, an orthophotomap was created, which for the convenience of work is divided into 71 tiles, with a total volume of 14.6 GB. The resolution of the resulting image is about 8.5 cm/pixel.

The orthophotomaps were interpreted in the ArcGIS (ESRI) software, based on visual features of targets that are univocally identified in images of a given resolution.

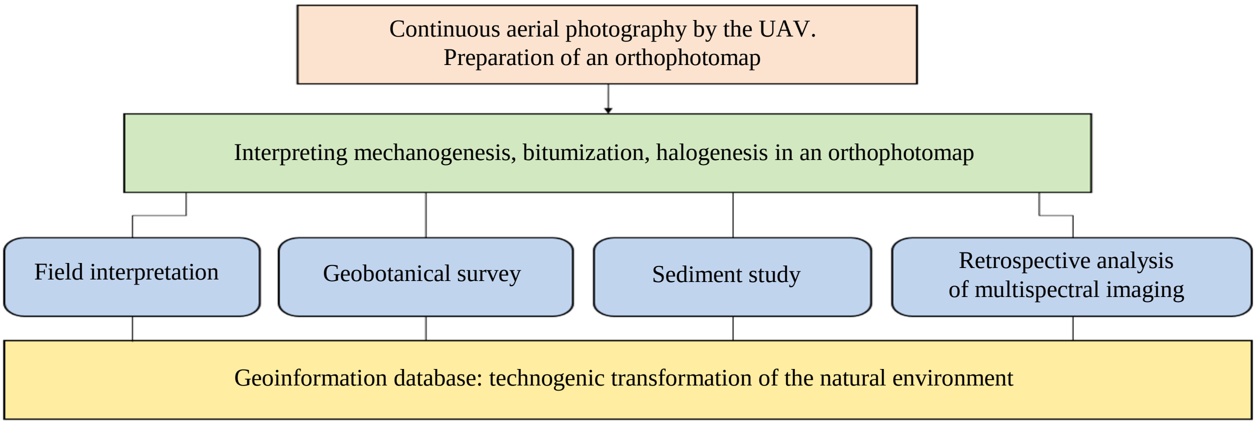

Fig.1. Research stages

Oilfield technogenesis is caused by arrangement, accidents, leaks, and process emissions during the development of oilfields. It is usually divided into three main types: mechanogenesis, bitumization, halogenesis. Mechanogenesis is the movement of grounds, the physical violation of the integrity of natural complexes, soil, and vegetation cover. The most active mechanogenesis is manifested at the stages of construction and arrangement of oilfield facilities. Bitumization is the pollution of the natural environment and its components by oil hydrocarbons. The technogenic halogenesis develops under the influence of highly mineralized flows with bottom waters, in which the most significant are water-soluble chlorides, as well as sulphates and carbonates. The main reasons for the occurrence of bitumization and halogenesis are violations of the tightness of equipment caused by imperfection of technology and violation of process regulations. Interpretation of each type of technogenesis has its own characteristics.

Interpreting the mechanogenesis consequences. Throughout the study area, 10 types of anthropogenic targets were identified, the appearance of which is directly or indirectly due to the development of an oilfield (Fig.2). Oilfield facilities: well sites, pipelines, power lines, roads, quarry, artificial water bodies, other technical facilities; targets of mixed origin: cutting areas, forest roads, and recreation sites. Cutting areas may be caused either by the exploitation of forest resources or by the needs of oil production; forest roads spontaneously arise due to the maintenance of technical facilities; people working near water bodies tend to create recreation sites.

For the identification of mechanogenesis, direct interpretation signs were sufficient: target shape, colour, special signs of oilfield facilities (square outline of the embankment around the wells). Identification of some targets was more difficult. In this case, indirect signs were additionally used: a shadow of a characteristic shape cast by power transmission towers; long straight sections with destroyed forest vegetation were a sign of the right-of-way of oil, gas, water pipelines, power lines; cutting areas (in contrast to windblows and windbreaks) were marked by traces of the movement of heavy logging equipment. Data on annual forest losses [40] were used to refine the identified cuttings. Information about the location and names of individual pipeline strings was taken from the Internet resource “Public Cadastral Map” (Rosreestr).

Interpreting the bitumization consequences. The manifestations of bituminization were determined by the presence of contrasting dark (black) spots on the surface of the ground or water bodies (Fig.3, *a*), which presumably corresponded to oil spills in open areas. Dark red spots in drying microdepressions, presumably associated with the intensive development of certain groups of aquatic organisms, also indicated hydrocarbon pollution. Linearly elongated deadwood strips (dead stands) were considered as sites subjected to bitumization or halogenesis (Fig.3, *b*).

Oilfield facilities Pipelines Power lines

Roads Cutting areas Sand quarry

Artificial water features Technical facilities Recreation site

Fig.2. Fragments of an orthophotomap with examples of interpretable consequences of mechanogenesis

Fig.3. Fragments of the orthophotomap with areas showing signs of bitumization – black and dark red spots (*a*) and linearly elongated stripes of a drying up forest stand (*b*), halogenesis – a change in the reservoir colour to bluish-whitish in the right side of the picture (*c*)

Interpreting the halogenesis consequences. Based on the existing experience from a similar study [41], which the team of authors carried out in the southern part of the Perm Territory on a karst area, three types of interpretation signs were used to search for the sites with technogenic halogenesis manifestation:

- turbidity of the water and change of the reservoir colour to bluish-whitish (Fig.3, *c*), due to a large number of nanometre dispersed particles of hydrogenated sulphates (dissolution of gypsum) in water [42];
- change of the reservoir colour to green-yellow (presumably due to the intensive growth of halophilic aquatic vegetation, algae in saline reservoirs);
- accumulation of white manifestations (spots) on the ground surface.

Preparation of a geoinformation database for the study. To process information in the ArcGIS (ESRI) software, a geoinformation database was created. The oilfield area fully belongs to the drainage basin of the lake with an area of 3419.8 ha. In addition to the initial data (orthophotomaps, lake catchment boundaries, oilfield facilities), the database includes the interpretation results, two polygonal layers for mechanogenesis (117 sites), halogenesis and bitumization (35 sites) targets. Additionally, all sites with the consequences of mechanogenesis were divided into three categories in relation to oilfield activities: not related to oilfields; probably due to oil production; directly related to oil production and related processes.

Field interpretation. During the stage of direct field work (field interpretation), all selected sites were surveyed. In places where the fact of spills was confirmed, characteristic traces of technogenesis were photofixed, geobotanical descriptions were made. At one of the sites, two peat cores were taken to identify the features of petroleum hydrocarbons distribution in the peat profile. Work records were kept in the field observation log.

Study of peat deposits. Drilling of the peat bog and taking of the peat core were carried out using a peat (Russian) drill, according to GOST 17644-83. All extracted deposits were photographed. After the description, half-metre cores were packed in a polyethylene film and placed in PVC plastic pipes to prevent deformation during transportation and storage.

Geobotanical survey. To determine the nature of changes in the vegetation cover as a result of oil pollution, route studies were carried out, and three test sites (TS) were made for geobotanical descriptions: two in the key area and one in the undisturbed (background) area of the bog. Geobotanical descriptions were made according to generally accepted methods. Coenotic analysis of the flora of communities formed on a peat bog was carried out according to the characteristics of the species presented in the database “Flora of vascular plants of Central Russia” of the Institute of Mathematical Problems of Biology of the Russian Academy of Sciences[1]. Analysis of the composition of communities in terms of nutrition and moisture conditions was performed according to the species descriptions of the Plantarium project[2]. To evaluate ecotopes by environmental scales, floristic lists were processed using the EcoScaleWin software[3]. The phytoindication analysis of the communities was carried out according to the generally accepted scales of Ellenberg and Landolt.

Analysis of multispectral satellite imagery of past years. Satellite images were taken from the open USGS EarthExplorer archive. The analysis was performed using Landsat – 5, 7, 8 images for 1999-2022. A total of 27 images were analysed in two modes: in natural colours and by the NDVI index, which was calculated as an average value for the pixels corresponding to the studied areas.

---

[1] Khanina L.G., Zaugolnova L.B., Smirnova O.V. et al. Database “Flora of vascular plants of Central Russia”. URL: https://www.impb.ru/eco/ (accessed 29.10.2022).

[2] Plantarium. Plants and lichens of Russia and neighbouring countries: an open online atlas and guide to plants. URL: https://www.plantarium.ru/ (accessed 29.10.2022).

[3] Zubkova E.V., Khanina L.G., Grokhlina T.I., Dorogova Yu.A. Computer processing of geobotanical descriptions on environmental scales using the EcoScaleWin software. Yoshkar-Ola: Mari State University, Pushchino State University, 2008, p. 96.

Discussion of the results. *Interpretation of aerial photography materials in the optical part of the spectrum*. As a result of the orthophotomap interpretation, 117 sites subjected to mechanogenesis were identified in the study area (Fig.4), with a total area of 358 ha, which corresponds to 9.0 % of the catchment area.

Mechanogenesis, directly caused by oil production, is slightly more than half (51.3 %) of the area of all sites subjected to mechanical impact. Most of these sites are roads, commercial water and oil pipelines, oilfield facilities and a sand pit; 48 % of all sites of mechanogenesis are not associated with oil production, these are cutting areas, to a lesser extent forest roads and recreation sites.

The share of linear infrastructure facilities of the field was 81.1 %, and areal 18.9 %, which is comparable with the results obtained [43] for the Middle Ob region (corresponding to the subzones of the middle and northern taiga), where the average (for 25 deposits) share of linear targets was 84.97 %, and areal 15.11 %. Similar values were noted on the example of 17 fields in the Tyumen Region [44]: the share of linear targets is 18.9 %, areal 21.1 %.

In the surveyed area, the share of lands disturbed during the laying of roads was 1.7 %, 1/3 of which is a spontaneously developing network of forest roads. It was established [45] that for the southern steppe zone these indicators are 4.2 %, for the forest-steppe zone 2.5 %. The markedly lower proportion of areas occupied by road right-of-ways correlates well with the prevalence of natural geographic barriers. In this case, the main barrier to the wide development of the road network is the high swampiness of the area.

Orthophotomaps interpreting revealed 35 sites that had signs of bituminization and halogenesis. Their total area was 7.78 ha. Most of the sites (24) were identified by the presence of black contrasting spots, six sites were identified by the change in the colour of the reservoir to bluish-whitish, three linear sections of deadwood, two dark red depressions were noted. Such interpretation signs of halogenesis as a change in the colour of the reservoir to yellow-green and white salt manifestations on the soil surface were not identified.

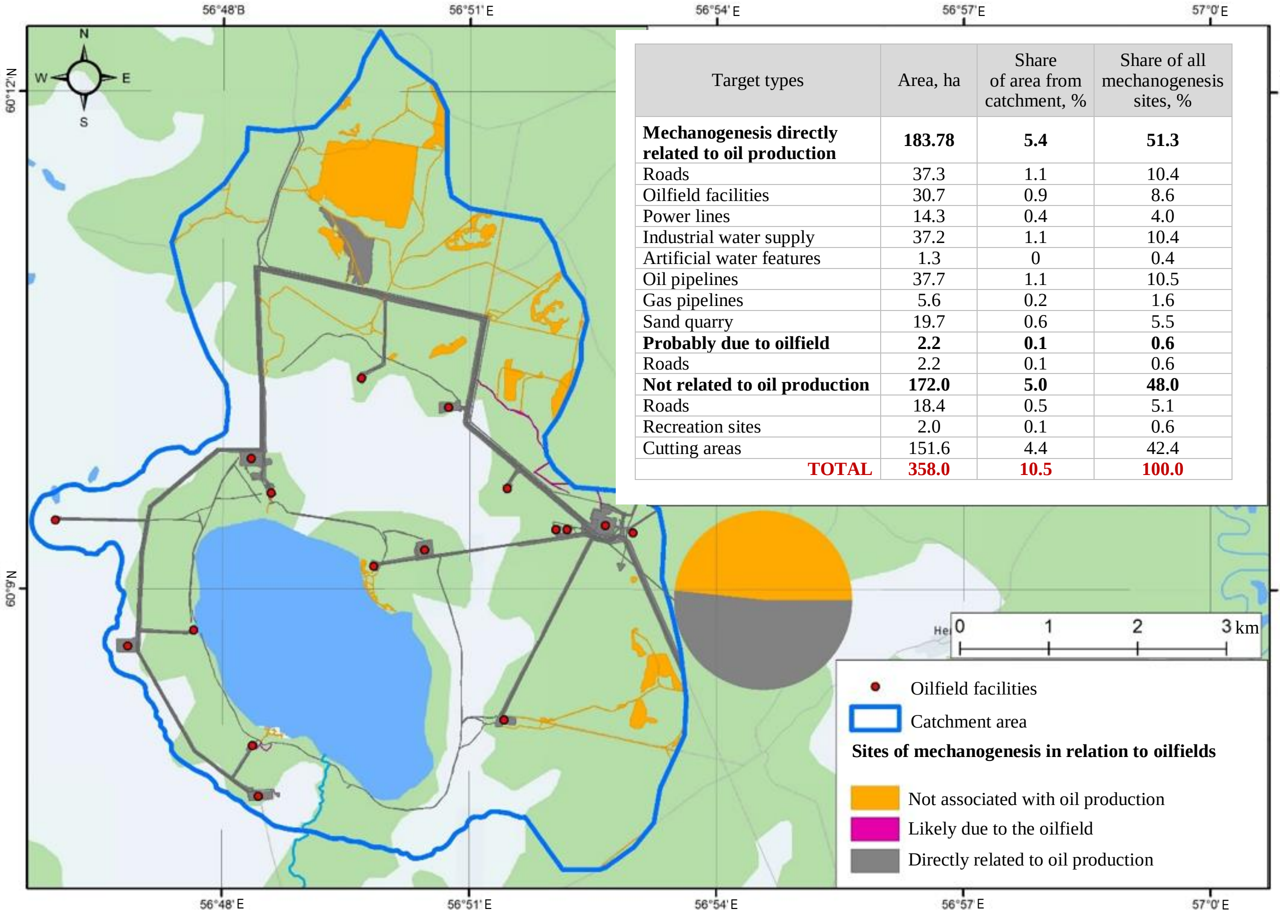

Target types	Area, ha	Share of area from catchment, %	Share of all mechanogenesis sites, %
Mechanogenesis directly related to oil production	**183.78**	**5.4**	**51.3**
Roads	37.3	1.1	10.4
Oilfield facilities	30.7	0.9	8.6
Power lines	14.3	0.4	4.0
Industrial water supply	37.2	1.1	10.4
Artificial water features	1.3	0	0.4
Oil pipelines	37.7	1.1	10.5
Gas pipelines	5.6	0.2	1.6
Sand quarry	19.7	0.6	5.5
Probably due to oilfield	**2.2**	**0.1**	**0.6**
Roads	2.2	0.1	0.6
Not related to oil production	**172.0**	**5.0**	**48.0**
Roads	18.4	0.5	5.1
Recreation sites	2.0	0.1	0.6
Cutting areas	151.6	4.4	42.4
TOTAL	**358.0**	**10.5**	**100.0**

Fig.4. Consequences of mechanogenesis in the study area

Field interpretation. A direct field survey found clear signs of bituminization and halogenesis in 10 of the 35 previously interpreted sites. Of these, six sites identified by the bluish-whitish colour of the water surface (a sign of halogenesis), upon direct examination, turned out to be a series of bog microdepressions, on the surface of which a dense oily film was noted (a manifestation of bitumization). The presumable source of hydrocarbons is an infield oil pipeline running along the nearest road. Only two of the 24 sites previously marked by the presence of black spots showed clear signs of bituminization: oil films on the water surface, an intense smell of hydrocarbons, and extensive areas of destroyed or significantly suppressed vegetation.

In both sites noticed during the interpretation by the presence of dark red spots, during the field survey, signs of oilfield technogenesis were found: abundant red-brown sediment on the surface of the soil, ground vegetation, bottom of a drying reservoir, as well as intensive degradation of the grass-subshrub layer and damage to the needles of the lower tiers of the branches of young pines in the raised bog. The source of impact is probably the oilfield facilities adjacent to these areas. However, the processes that caused such changes are still unclear, which requires additional research.

In two sites of a linearly elongated deadwood strip, the results obtained do not yet allow us to draw an unambiguous conclusion. Their appearance may be associated both with a disturbance of the natural flow of groundwater due to the construction of a road or pipeline, and with an oil and/or bottom water spill (salt pollution).

In 23 sites, the field survey did not reveal any obvious signs of bituminization and halogenesis. In one case, such a site was a strip of dead wood, where the forest stand died as a result of flooding along the industrial site outline. The remaining 22 sites, where preliminary interpretation was not confirmed by field data, were distinguished in the orthophotomap by the presence of black spots on the surface of water or soil. The most typical example (17 sites) of this kind are depressions tens of metres long, formed along roads, pipelines, and well sites. Three more much longer (to 0.2-0.5 km) sites, distinguished by dark colour, were natural flow formations, slightly lowered relative to the general surface of the raised bog and distinguished from the neighbouring ones by a different composition of vegetation. In two small lake-like reservoirs, previously marked by dark colour, signs of bitumization and halogenesis were also not found. The pronounced dark colour of the reservoir is due to peat particles suspended in the water.

It was determined that in the conditions of high swampiness and the widespread distribution of peat soils, the dark colour of natural and technogenic waterlogged depressions is the norm. The efficiency of such a sign is extremely low, in this case it was only 8 %. Thus, for wetlands, a dark colour may not be a sufficient interpretation sign of bituminization. Such areas require additional verification. Promising directions for the research development should be considered the multispectral, thermal imaging, lidar surveys, and their further analysis.

On the contrary, other interpretation signs (dark red colour of water bodies and drying depressions, bluish-whitish colour of water bodies) turned out to be noticeably more effective. If for the karst area in the zone of mixed coniferous and broad-leaved forests, the bluish-whitish colour indicated the halogenesis [42], then in the studied wetland area of the middle taiga, this colour may indicate hydrocarbon pollution.

Studies using airborne spectral photography obtained from UAVs make it possible to calculate the depth and chemical composition of watercourses [46]. Multispectral aerial photography also enables to compile maps of vegetation and other indices (primarily NDVI). The indices show well the current functional state of vegetation and may indicate the restoration of disturbed areas [19]. Aerial photography with a thermal imager, especially in combination with other types of surveys, can provide additional useful information. Thus, oil pollution on the surface of water and soil is detected by a noticeable temperature difference between the contaminated and background areas [24].

In conditions of high swampiness and evenness of the topography, the difference in elevation marks, which determines the flow direction, can be minimal. Neither large-scale topographic maps nor global digital elevation models can provide the required accuracy of slope estimation. Aerial photography with a laser sensor enables to create a high-precision digital topography model. Such data make it possible to unambiguously determine the directions of substances migration and establish the source of pollution. In addition, lidar survey makes it possible to determine the thickness of the hydrocarbon film on the surface of water bodies [23].

Sedimentological study. In the area near the well cluster N 4, during the field survey, the most pronounced manifestations of oilfield technogenesis were found. The site is on a raised bog and has a tongue-like elongated shape with a total length of more than 300 m. Within its limits there are extensive areas of complete or partial degradation of vegetation, spots of open peat, a sharp smell of hydrocarbons, pronounced oil films, damage to the needles of the lower tiers of branches of young pines. The probable causes of the transformation are as follows: oil spill, drill cuttings spill, bottom water spill or mixtures of these substances.

Two peat cores were taken at the site: in the undisturbed background area and within the transformed area. During a visual inspection of the stratigraphic column from the disturbed area, an unusual layer (21-34 cm) of light, undecomposed sphagnum was found. There was no such layer in the background area.

We associate the presence of such an unusual interlayer with the effect of sphagnum "preservation" in anaerobic and highly humid conditions that form during an oil spill. Thus, during oil spills, the upper layers of oligotrophic soils adsorb high-molecular fractions: resins and asphaltenes [26], which have an enveloping effect that prevents aerobic conditions for the sphagnum cushion of the raised bog. As a result, oil hinders the oxidative destruction of organic matter, which is necessary for decomposition processes in the upper layer of the peat bog [31].

The further prospect of studying the obtained sediment is associated with the analysis of the concentration of a number of elements and compounds. The distribution of heavy metals in the peat core is different during bitumization and halogenesis. It was found out [29] that in case of oil pollution, the concentrations of marker elements and compounds along the peat bog profile are distributed as follows: pollutant metals (Ti, V, Cr, Ni, Zr, Ba, and lanthanides) accumulate in the upper layer, labile Cl, Ca, Mn, Zn, Cu, Sr with light fractions of hydrocarbons over time migrate from the upper layers into the depth of the profile.

The ratio of the total content of Ni:Br in the ash of contaminated peat serves as an indicator of the predominant nature of (oil or salt) pollution [32]. It was established that the ratio $Ni:Br > 1.5$ is a sign of oil pollution, the ratio $Ni:Br < 0.7$ is salt, and at $0.7 < Ni:Br < 1.4$ it is mixed.

Comparative microbiological analysis also seems promising. Thus, it was determined that under the influence of oil technogenesis, transformations of microbiota and microbiological activity occur in peat soil. Under conditions of oil pollution, the number and ratio of trophic groups of soil microorganisms change [47].

Analysis of flora and vegetation. In the area near the well cluster N 4 with the most pronounced manifestations of oilfield technogenesis, three geobotanical test sites 20×20 m were made.

Test site N 1 was made at the base of the transformed area. A completely dead tree layer of 19 *Pinus sylvestris* L. is up to eight m high, the diameter of the trunks reaches 22 cm. Closer to the limits of the pollution spot, there is an undergrowth of *Pinus sylvestris*, *Betula pendula* Roth, *Populus tremula* L. about 10 years old. The vitality of young trees is good, the current year increment of pine trunks reaches 25 cm. There are no shrubs. Herbs and shrubs grow in patches, within which the total plant cover is 30 %. Such herbaceous-shrub spots cover about 40 % of the test site surface, the rest of the area is bare. The predominant species is *Calamagrostis epigeios* (L.) Roth, few specimens of

Typha latifolia L. and *Tussi-lago farfara* L., small spots of *Oxycoccus palustris* Pers., *Juncus alpinus* Vill were also found. *Eriophorum polystachyon* L., *Carex canescens* L., *Carex rostrata* Stokes grow closer to the test site edges. There is no living moss cover.

Test site N 2 was made 150 m from the limit of the degraded area. Single trees of *Pinus sylvestris* grow only closer to the limits of the polluted spot and have a height of up to seven metres, a trunk diameter of up to 18 cm. Trees are very weakened, dying. Closer to the spot limits, undergrowth of *Pinus sylvestris*, *Betula pendula*, *Populus tremula* is also common. The undergrowth vitality is good. The current year increment of forest pine undergrowth reaches 30 cm, but the needles on the lower tiers of the branches in some young trees are reddish, but do not crumble. Probably necrosis occurred in the current or last year. Of the shrubs closer to the spot limits, there are single specimens of *Betula nana* L. Subshrubs are absent. Grasses in the central part of the TS grow less frequently (total plant cover 20 %) than on its outskirts (total plant cover 40 %). *Juncus alpinus* and *Carex canescens* predominate in the spot centre. They are mixed with *Eleocharis palustris* (L.) Roem. et Schult. and *Carex limosa* L. Farther from the spot centre, a ring of *Calamagrostis epigeios*, *Eriophorum vaginatum* L. appears. Here, there are more *Carex canescens* and *Carex limosa*. *Carex rostrata* and *Carex juncella* (Fries) Th. Fries grow on the western side of the spot. Closer to the edge there is *Alopecurus aequalis* Sobol. There is no living moss cover.

The background test site was made in a pine-cotton grass-subshrub-sphagnum bog. An extremely sparse stand of *Pinus sylvestris* is to 3 m high, the trunk diameter reaches 11 cm. Single trees above three metres are dry. The diameter of their trunks reaches 19 cm. The tallest tree is 5.5 m high. Two old dry aspens with traces of fire on the trunks are noted. The current year increment of young specimens of forest pine does not exceed 10 cm, the plants are twisted, but are in satisfactory condition, there is no reddening of the needles. *Betula nana* forms an extremely sparse but evenly distributed shrub layer with an average height of 0.7 m. The grass-subshrub layer is formed by *Eriophorum vaginatum* and marsh subshrubs *Chamaedaphne calyculata* (L.) Moench, *Ledum palustre* L., *Andromeda polifolia* L., *Oxycoccus palustris*, with a total plant coverage of 50 %. A continuous moss cover is formed by sphagnum mosses.

On the sites made in the disturbed area, the diversity of plant species is higher than in the background one. A significantly greater current annual increment of forest pine and the appearance in the undergrowth of *Betula pendula* and *Populus tremula*, which are uncharacteristic for oligotrophic bogs, were noted. Tree undergrowth is formed closer to the spot periphery; it is absent in the axial part of the tongue-like spot. Shrubs are almost absent. The open surfaces of the peat bog are overgrown with herbs, sedges, cotton grasses, spike rushes, rushes, graminaceous plants. Moss cover is absent.

The obtained conclusions confirm the study of the anthropogenic dynamics of plant communities in oligotrophic bogs at oilfields in the forest zone of Western Siberia, where the following signs were also noted in the contaminated areas: the appearance in the tree-shrub layer of species atypical for raised bogs, rushes and young plants [37]; morphometric changes in young wood pine specimens [38]; the appearance of graminaceous plants in the herbaceous-shrub layer; active development of mesotrophic and eutrophic species, mainly from the *Cyperaceae* family [37], as well as suppression and decrease in the abundance of oligotrophic shrubs.

A comparative analysis of the represented flora groups identified according to various indicators, coenotic, attitude towards moisture, towards nutritional conditions (trophicity), demonstrated the complex composition of communities in the degraded area and the relatively simple one in the background area (Fig.5), which is due to a mosaic change in the trophicity and humidity of the habitat after the influx of oil organic matter. The former groupings of raised bog vegetation preserved, and pioneer species characteristic of disturbed, meadow, and zonal forest communities added.

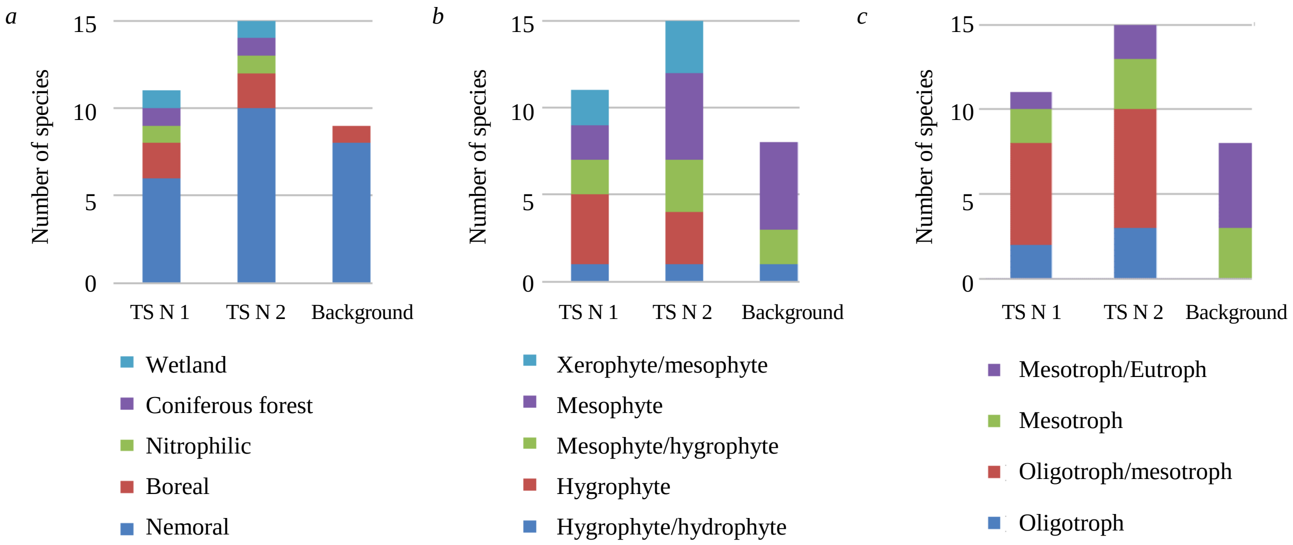

Fig.5. Comparative analysis of the represented flora groups (species) identified according to the following indicators: *a* – coenotic; *b* – attitude towards moisture; *c* – nutritional conditions (trophicity)

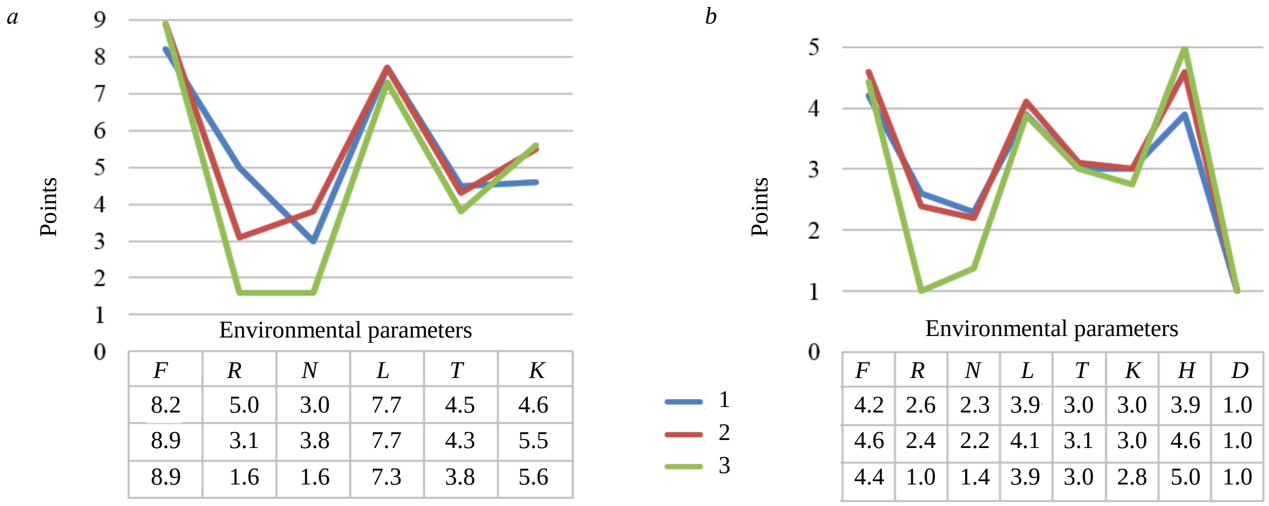

F	*R*	*N*	*L*	*T*	*K*
8.2	5.0	3.0	7.7	4.5	4.6
8.9	3.1	3.8	7.7	4.3	5.5
8.9	1.6	1.6	7.3	3.8	5.6

F	*R*	*N*	*L*	*T*	*K*	*H*	*D*
4.2	2.6	2.3	3.9	3.0	3.0	3.9	1.0
4.6	2.4	2.2	4.1	3.1	3.0	4.6	1.0
4.4	1.0	1.4	3.9	3.0	2.8	5.0	1.0

Fig.6. Environmental parameters of habitats according to the Ellenberg (*a*) and Landolt (*b*) scales
F – soil moisture; *R* – soil acidity; *N* – soil richness with mineral nutrition elements; *L* – photophily; *T* – temperature; *K* – continentality; *H* – humus content in the soil; D – particle size distribution in the soil (aeration deficiency); 1 – TS N 1; 2 – TS N 2; 3 – background

Restorative succession after the influx of petroleum hydrocarbons occurs with the participation of species of various coenotic groups, while the undisturbed community consists only of species of the wetland group and *Pinus sylvestris* (coniferous forest group). Regarding the degree of moisture, the difference between the background and disturbed areas is the appearance of species that prefer both less (mesophytes) and more (hygrophytes/hydrophytes) humidified habitats. The analysis (Fig.5) also demonstrated an increase in the degree of trophicity in contaminated areas, which was previously recorded by studies conducted in Western Siberia [37, 38].

When assessing the environmental parameters of habitats on the Ellenberg scale (Fig.6, *a*), the test sites of the background and transformed areas clearly differ in soil acidity and richness in mineral nutrition elements. If the background area is characterized by plants that grow only on acidic soils, then for both sites in the disturbed area, plants are noted that can grow on both strongly acidic and neutral soils. Indicators of soil richness in mineral nutrition elements are much higher in the disturbed area.

The analysis of environmental parameters on the Landolt scale (Fig.6, *b*) demonstrates similar results: noticeable differences are observed in the degree of acidity and nutritional conditions. The disturbed area is characterized by secondary anthropogenic eutrophication, which is manifested by an increase in the role of mesotrophic and eutrophic species, a weakening of the positions of oligotrophs and oxylophytes, the appearance in the community of species with different requirements for moisture conditions and representatives of coenotic groups uncharacteristic of it, the replacement of subshrubs with herbs, changes in the morphometric characteristics of forest pine undergrowth.

Effective identification and monitoring of oilfield technogenesis are possible on the basis of phytoindication at various levels, organismal, population, coenotic. The prospect of geobotanical research lies in the determination of regional phytoindicators of various types of pollution (salt, oil, mixed) similarly to studies conducted in Western Siberia and the Kaliningrad Region [37] and determining the history of restorative succession in ecosystems of various types.

Reconstruction of the technogenic transformation history. For the site near well cluster N 4 with the most pronounced manifestations of oilfield technogenesis, the history of technogenic transformation was reconstructed using satellite imagery for 1999-2022.

An analysis of the dynamics of plants photosynthetic activity (Fig.7) in the disturbed and background areas showed that until 2010, the NDVI index values in both areas coincided or were very close, the average difference was about 0.006. Since 2010, there is a noticeable (relative to the background) decrease in NDVI in the disturbed area. In 2010-2016, the average difference in the indices is 0.1. In 2017-2022, the average difference between the NDVI of the background and the disturbed area increases to 0.2, and in some years reaches 0.3-0.4.

It is noteworthy that the analysis of the same images in natural colours gives different results. Thus, a noticeable difference between the background and disturbed areas begins to appear only from 2012, i.e., two years later than in plant photosynthetic activity (NDVI). Such a discrepancy indicates that the first reaction of vegetation to the oilfield impact is a drop in photosynthetic activity, and only then a change in the species composition and changes in the structure of the phytocenosis occur.

The main threshold parameter that determines the possibility of using satellite imagery should be considered the area and configuration of the site limits with signs of oilfield technogenesis. For reliable identification, it is necessary that the damaged area occupies at least five to six pixels. For sensors installed on Landsat vehicles, this corresponds to an area of at least 4,500 m^2, and for Sentinel-2, at least 900 m^2.

Fig.7. Dynamics of NDVI in the disturbed and background areas

1 – background; 2 – disturbed

It may be more informative to use an improved version, the Enhanced Normalized Difference Vegetation Index (ENVI), which, in addition to the near infrared, also uses green and blue channels. This is evidenced by the experience of identifying sites subject to hydrocarbon pollution in Indonesia [13].

Conclusion. A continuous survey of the study area of the operated oilfield using aerial photography by an unmanned aerial vehicle made it possible to identify such technogenic processes in the natural environment as mechanogenesis, bitumization, and halogenesis.

Interpreting aerial photography in the visible part of the spectrum makes it possible to unambiguously determine all the main manifestations of mechanogenesis. Directly caused by the oilfield operations, mechanical disturbances of the natural environment amounted to no more than half (51.3 %) of the area of all such sites in the field. The second part of the changes is related to forest management, spontaneous network of forest roads, and recreation.

Sites subject to bitumization and halogenesis are interpreted less reliably. The least reliable interpretation sign was contrasting black spots on the surface of water or soil, which in most cases were due to a natural cause, the ubiquitous distribution of peat soils in the study area. More reliable signs of the oilfield technogenesis development were extensive continuous strips of deadwood, as well as red and dark red spots in drying microdepressions and reservoirs. A direct field examination is necessary for an unambiguous interpretation of the results. It will also be promising to identify regional phytoindicators for various types of technogenesis.

A retrospective analysis of the multispectral space imagery (NDVI dynamics) makes it possible to determine the moment of the technogenic impact beginning. Due to the influx of petroleum hydrocarbons into the natural complex, technogenic bitumization begins, the water and air conditions of peat soils for the background phytocenosis worsen, and plants reduce their photosynthetic activity, which reflects the NDVI index. To apply this method, only relatively large disturbed areas are suitable, at least 0.45 ha (when using Landsat – 5, 7, 8). To identify smaller ones, it is promising to use specially equipped unmanned aerial vehicles.

A comparative analysis of the stratigraphy of peat cores in the background area of the raised bog and the area transformed during bitumization revealed a layer (more than 10 cm) of light undecomposed sphagnum in the transformed area. Presumably, this is due to the effect of sphagnum “preservation” in anaerobic and highly humid conditions, which are formed when oil inflows.

Changes in the vegetation of the raised bog under the influence of oilfield technogenesis are caused by a change in the air-water regime of peat, which leads to a decrease in the role of oligotrophs and increases the importance of mesotrophs and eutrophs in the plant communities structure. The disturbed habitats partially preserved the former groups of raised bog vegetation and pioneer species, characteristic of disturbed meadow and zonal forest communities, added. The changes in the vegetation cover of the raised bog recorded in the region of the middle taiga fir-spruce forests are similar to the data on the raised bogs of Western Siberia.

Thermal imaging, multispectral and lidar surveys in key areas and their analysis, as well as geochemical and microbiological studies of peat in various layers of collected peat cores should be considered promising areas of research.

The use of continuous remote sensing based on unmanned aerial photography and interpretation using sedimentological, geobotanical methods significantly expand the possibilities for studying the technogenic transformation of the natural environment. To ensure environmental safety, it is advisable to develop remote methods and technologies in order to include them in the environmental monitoring system.

REFERENCES

1. Porozova A., Sannikov P. Assessment of the impact of associated gas flaring on the radial growth of Pinus Sylvestris (Ozernoe oil field, Perm region, Russia). *Anthropogenic Transformation of Nature*. 2021. Vol. 7. N 2, p. 58-74 (in Russian). DOI: 10.17072/2410-8553-2021-2-58-74

2. Baktybaeva Z.B., Suleymanov R.A., Valeev T.K. et al. Environmental and Hygienic Assessment of Ambient Air Pollution in Oil-Producing and Oil-Refining Areas of the Republic of Bashkortostan and Population Health Status. *Public Health and Life Environment*. 2020. N 2, p. 26-32 (in Russian). DOI: 10.35627/2219-5238/2020-323-2-26-32

3. Bykova M.V., Pashkevich M.A. Assessment of oil pollution of soils of production facilities of different soil and climatic zones of the Russian Federation. *Izvestiya Tula State University. Sciences of Earth*. 2020. N 1, p. 46-59 (in Russian).

4. Chizhova M.A., Khairullina L.I., Tuchkova O.A. Development principles and structure of environmental monitoring at oil production facilities. *Vestnik Kazanskogo tekhnologicheskogo universiteta*. 2015. Vol. 18. N 16, p. 290-292 (in Russian).

5. Bachurin B.A. Ecology-geochemical estimation of oil degradation products under the hypergenesis condition. *Anthropogenic Transformation of Nature*. 2019. N 5, p. 8-14 (in Russian).

6. Buzmakov S., Sannikov P., Sivkov D. et al. Development of geoinformation systems for environmental management and environmental safety in the areas of exploited oil deposits. *Anthropogenic Transformation of Nature*. 2021. Vol. 7. N 1, p. 102-127 (in Russian). DOI: 10.17072/2410-8553-2021-1-102-127

7. Pashkevich M.A., Smirnov Y.D., Danilov A.S. Estimation of quality of environment with the use of small pilotless aircrafts. *Journal of Mining Institute*. 2013. Vol. 204, p. 269-271 (in Russian).

8. Danilov A.S., Smirnov U.D., Pashkevich M.A. The system of the ecological monitoring of environment which is based on the usage of UAV. *Russian Journal of Ecology*. 2015. Vol. 46. N 1, p. 14-19. DOI: 10.1134/S1067413615010038

9. Kremcheev E.A., Danilov A.S., Smirnov Yu.D. Metrological Support of Monitoring Systems Based on Unmanned Aerial Vehicles. *Journal of Mining Institute*. 2019. Vol. 235, p. 96-105 (in Russian). DOI:10.31897/PMI.2019.1.96

10. Ferrarese F., Pappalardo S., Codato D. et al. High resolution satellite images for environmental monitoring of oil production in Western Amazon: the case of Yasuní National Park. AGILE 2017, 9-12 May 2017, Wageningen.

11. Singh A., Kushwaha S.K.P. Forest Degradation Assessment Using UAV Optical Photogrammetry and SAR Data. *Journal of the Indian Society of Remote Sensing*. 2020. Vol. 49. N 3, p. 559-567. DOI: 10.1007/s12524-020-01232-2

12. Mirzaii Z., Hasanlou M., Samieie-Esfahany S., Ajourlou P. Land Subsidence Monitoring in Azar Oil Field Based on Time Series Analysis. Proceedings of the 3rd International Electronic Conference on Remote Sensing, 22 May – 5 June 2019, Basel, Switzerland. MDPI, 2019. DOI: 10.3390/ECRS-3-06190

13. Susantoro M.T., Wikantika K., Saepuloh A., Harsolumakso A. Utilization of Vegetation Indices to Interpret the Possibility of Oil and Gas Microseepages at Ground Surface. IOP Conference Series: Earth and Environmental Science. The 1st UPI International Geography Seminar 2017, 8 August 2017, Indonesia. 2018. Vol. 145. N 012012. DOI: 10.1088/1755-1315/145/1/012012

14. Novokhatin V.V., Osipova N.G. Space monitoring of emergency oil spills within license areas in Western Siberia. *Moscow Economic Journal*. 2021. N 3, p. 57-63 (in Russian). DOI: 10.24412/2413-046X-2021-10167

15. Löw F., Stieglitz K., Diemar O. Terrestrial oil spill mapping using satellite earth observation and machine learning: A case study in South Sudan. *Journal of Environmental Management*. 2021. Vol. 298. N 113424. DOI: 10.1016/j.jenvman.2021.113424

16. Soromotin A.V., Brodt L.V. Monitoring of Vegetation Cover during the Development of Oil and Gas Fields According to the Landsat Multispectral Survey Data. *Tyumen State University Herald. Natural Resource Use and Ecology*. 2018. Vol. 4. N 1, p. 37-49 (in Russian). DOI: 10.21684/2411-7927-2018-4-1-37-49

17. Wanasinghe T., Gosine R.G., De Silva O. et al. Unmanned Aerial Systems for the Oil and Gas Industry: Overview, Applications, and Challenges. *IEEE Access*. 2020. Vol. 8, p. 166980-166997. DOI: 10.1109/ACCESS.2020.3020593

18. Grib N., Melnikov A., Grib G., Kachaev A. Use of unmanned aerial systems for assessing the dynamics of hazardous engineering and geocryological processes on linear facilities. *E3S Web of Conferences*. 2020. Vol. 192. N 04006. DOI: 10.1051/e3sconf/202019204006

19. Negara T., Jaya I.N.S., Kusmana C. et al. Drone image-based parameters for assessing the vegetation condition the reclamation success in post-mining oil exploration. *Telkomnika* (*Telecommunication Computing Electronics and Control*). 2021. Vol. 19. N 1, p. 105-114. DOI: 10.12928/TELKOMNIKA.V19I1.16663

20. Hassani B., Sahebi M.R., Asiyabi R.M. Oil Spill Four-Class Classification Using UAVSAR Polarimetric Data. *Ocean Science Journal*. 2020. Vol. 55 (3), p. 433-443. DOI: 10.1007/s12601-020-0023-9

21. Vepakomma U., Cormier D. Valuing forest stand at a glance with UAV based LIDAR. ISPRS – International Archives of the Photogrammetry, Remote Sensing and Spatial Information Sciences. 2019. Vol. XLII-2/W13, p. 643-647. DOI: 10.5194/isprs-archives-XLII-2-W13-643-2019

22. Katkovsky L.V. Calculation of objects thermal imaging parameters from unmanned aerial vehicles. *Doklady BGUIR*. 2020. Vol. 18. N 2, p. 53-61 (in Russian). DOI: 10.35596/1729-7648-2020-18-2-53-61

23. Al-Shammari A., Levin E., Shults R. Oil spills detection by means of UAS and low-cost airborne thermal sensors. *ISPRS Annals of Photogrammetry, Remote Sensing and Spatial Information Sciences*. 2018. Vol. IV-5, p. 293-301. DOI: 10.5194/isprs-annals-IV-5-293-2018

24. De Kerf T., Gladines J., Sels S., Vanlanduit S. Oil Spill Detection Using Machine Learning and Infrared Images. *Remote Sensing*. 2020. Vol. 12 (24). N 4090. DOI: 10.3390/rs12244090

25. Yurong Gao, Xugang Lian, Linlin Ge. Inversion model of surface bare soil temperature and water content based on UAV thermal infrared remote sensing. *Infrared Physics & Technology*. 2022. Vol. 125. N 104289. DOI: 10.1016/j.infrared.2022.104289

26. Nooralishahi P., López F., Maldague X. A Drone-Enabled Approach for Gas Leak Detection Using Optical Flow Analysis. *Applied Sciences*. 2020. Vol. 11. N 1412. DOI: 10.3390/app11041412

27. Vodyanitskii Yu.N., Avetov N.A., Savichev A.T. et al. Contents of chemical elements in peat soils salted with drill sewage waters at the oil production site in the Central Ob region. *Agricultural Chemistry*. 2013. N 1, p. 75-84 (in Russian).

28. Kul’kov M.G., Vorob’ev D.S. identification of traces of oil contamination of biogenic sediments by solid-phase extraction combined with thin layer chromatography. *Journal of Analytical Chemistry*. 2017. Vol. 72. N 2, p. 217-225 (in Russian). DOI: 10.7868/S0044450217020074

29. Vodianitsky Yu., Savichev A., Trofimov S., Shishkonakova E. Metals in oiled peat (Western Siberia). *Dokuchaev Soil Bulletin*. 2011. Vol. 67, p. 67-79 (in Russian). DOI: 10.19047/0136-1694-2011-67-67-79

30. Trofimov S.Y., Arzamazova A.V., Kinzhaev R.R. et al. Mineralization of Organic Matter in the Oil-Polluted and Background Soils of the Middle Ob Region under Laboratory Conditions. *Eurasian Soil Science*. 2022. Vol. 55. N 4, p. 533-540. DOI: 10.1134/S1064229322040147

31. Lednev A.V., Skvortsova I.A. Effects of oil pollution and meliorative additives on agrochemical properties of alluvial peat soils. *Agrochemical Herald*. 2017. N 3, p. 49-54(in Russian).

32. Ditts L.Yu., Dudina T.N., Tsuskman E.I., Katunkina E.V. Geoenvironmental issues of oil production areas. *Uspekhi sovremennogo estestvoznaniya*. 2020. N 3, p. 72-77. DOI: 10.17513/use.37348

33. Vodyanitskii Y.N., Avetov N.A., Trofimov S.Y. et al. Influence of oil and stratal water contamination on the ash composition of oligotrophic peat soils in the oil-production area (the Ob region). *Eurasian Soil Science*. 2013. Vol. 46. N 10, p. 1032-1041 (in Russian).

34. Vodyanitskii Yu.N., Avetov N.A., Savichev A.T. et al. Laboratory determination of the solid phase composition of technogenic salted peat bog: possibilities and limitations. *Moscow University Soil Science Bulletin*. 2020. N 3, p. 39-46 (in Russian).

35. Kozlov S.A., Avetov N.A., Savichev A.T. Geochemical features of ombrotrophic bogs and transitional mires under influence of drilling waste pits. *Moscow University Soil Science Bulletin*. 2017. N 4, p. 26-34 (in Russian).

36. Danilov A., Smirnov Y., Petrova T., Pashkevich M. Using drones of preconstruction monitoring conducting in mining enterprise. *International Journal of Ecology & Development*. 2015. Vol. 30. Iss. 1, p. 36-42.

37. Tyurin V.N. Changes in vegetation in contaminated areas of raised bogs (oilfields in Western Siberia). Zapadno-Sibirskie torfyaniki i tsikl ugleroda: proshloe i nastoyashchee: Materialy Pyatogo mezhdunarodnogo polevogo simpoziuma, 19-29 iyunya 2017, Khanty-Mansiisk. Khanty-Mansiisk: Natsionalnyi issledovatelskii Tomskii gosudarstvennyi universitet, 2017, p. 124-126 (in Russian).

38. Avetov N.A., Shishkonakova E.A. A concept of trophy status in connection with anthropogenic eutrophication of raised bogs in the Khanty-Mansy Pre-Ob region. *Dokuchaev Soil Bulletin*. 2013. N 71, p. 36-51 (in Russian).

39. Danilov A.S., Smirnov Yu.D., Pashkevich M.A. Use of biological adhesive for effective dust suppression in mining operations. *Journal of Ecological Engineering*. 2015. Vol. 16 (5), p. 9-14. DOI: 10.12911/22998993/60448

40. Hansen M., Potapov P., Moore R. et al. High-Resolution Global Maps of 21st-Century Forest Cover Change. *Science*. 2013. Vol. 342. Iss. 6160, p. 850-853. DOI: 10.1126/science.1244693

41. Khotyanovskaya Y., Buzmakov S., Sannikov P. Identification of oil mining technogenesis based on aerial photography data. *Journal of Soils and Sediments*. 2022. Vol. 23, p. 973-988. DOI: 10.1007/s11368-022-03357-y

42. Plotnikova M.D., Medvedeva N.A., Bortnik A.A G. About the causes of water turbidity in the river Yasyl. *Anthropogenic Transformation of Nature*. 2019. N 5, p. 45-50 (in Russian).

43. Moskovchenko D.V., Babushkina A.G., Idrisov I.R. Assessment of the technogenic disturbance of oil fields within the Middle Ob river region, Russia, by the use of satellite imagery. *Geoekologiya. Inzhenernaya geologiya, gidrogeologiya, geokriologiya*. 2020. N 5, p. 53-61 (in Russian). DOI: 10.31857/S0869780920050069

44. Soromotin A.V. Ecological Consequences of Different Stages of the Development of Oil and Gas Deposits in the Taiga Zone of the Tyumen Region. *Contemporary Problems of Ecology*. 2011. Vol. 18. N 6, p. 813-822 (in Russian).

45. Myachina K.V. Features of impact of oil-and-gas production objects on subzonal landscapes of the Volga-Ural steppe region. *Byulleten Orenburgskogo nauchnogo tsentra UrO RAN*. 2019. N 4, p. 21-29 (in Russian). DOI: 10.24411/2304-9081-2019-15021

46. Pervukhin D.A., Ilyushin Yu.V. A parallel analysis of hydrolithospheric beds geodata of Narzan mineral water Kislovodsk deposit. *Journal of Mining Institute*. 2016. Vol. 221, p. 706-711. DOI: 10.18454/PMI.2016.5.706

47. Egorova D., Buzmakov S. Bioremediation of Oil-contaminated Dark Gray Soils Using Bacterial and Plant Agents. *Ecology and Industry of Russia*. 2022. Vol. 26. N 3, p. 17-21 (in Russian). DOI: 10.18412/1816-0395-2022-3-17-21

***Authors*: Sergei A. Buzmakov,** *Doctor of Geography*, *Professor*, *lep@psu.ru*, *https://orcid.org/0000-0002-5144-0714* (*Perm State National Research University*, *Perm*, *Russia*), **Pavel Yu. Sannikov,** *Candidate of Geography*, *Associate Professor*, *http://orcid.org/0000-0001-7973-301X* (*Perm State National Research University*, *Perm*, *Russia*), **Leonid S. Kuchin,** *Laboratory Assistant*, *https://orcid.org/0000-0001-5283-5681* (*Perm State National Research University*, *Perm*, *Russia*), **Ekaterina A. Igoscheva,** *Postgraduate Student*, *https://orcid.org/0000-0002-9602-7587* (*Perm State National Research University*, *Perm*, *Russia*), **Irina F. Abdulmanova,** *Laboratory Assistant*, *https://orcid.org/0000-0001-6058-5176* (*Perm State National Research University*, *Perm*, *Russia*).

The authors declare no conflict of interests.

ISSN 2411-3336; e-ISSN 2541-9404

JOURNAL OF MINING INSTITUTE

Zapiski Gornogo instituta

Journal homepage: pmi.spmi.ru

Research article

Forecast of radionuclide migration in groundwater of the zone affected by construction drainage at the Leningrad NPP-2

Valentina A. ERZOVA[1,2]✉, **Vyacheslav G. RUMYNIN**[2,3], **Anton M. NIKULENKOV**[2,3], **Konstantin V. VLADIMIROV**[2], **Sergei M. SUDARIKOV**[1], **Mariia V. VILKINA**[2]

[1] *Saint Petersburg Mining University, Saint Petersburg, Russia*
[2] *Institute of Geoecology named after E.M.Sergeev, RAS, Saint Petersburg Branch, Saint Petersburg, Russia*
[3] *Saint Petersburg State University, Institute of Earth Sciences, Saint Petersburg, Russia*

***How to cite this article*:** Erzova V.A., Rumynin V.G., Nikulenkov A.M., Vladimirov K.V., Sudarikov S.M, Vilkina M.V. Forecast of radionuclide migration in groundwater of the zone affected by construction drainage at the Leningrad NPP-2. Journal of Mining Institute. 2023. Vol. 260, p. 194-211. DOI: 10.31897/PMI.2022.27

***Abstract*.** The distribution of natural (at the level of global background) and technogenic radionuclides in groundwater of the industrial zone in Sosnovy Bor town, where several nuclear power facilities are operating, was analyzed. The main technogenic radionuclides recorded in groundwater samples are cesium (^{137}Cs), strontium (^{90}Sr), and tritium isotopes. The first two aquifers from the surface are subject to contamination: the Quaternary and the upper zone of the Lomonosov aquifer. Based on extensive material on the engineering and geological studies of the work area, a 3D geological model and hydrodynamic and geomigration models of the industrial zone were constructed. By means of modeling, the extent and nature of changes in hydrogeological conditions of area resulting from the construction and operational drainage of the new stage of the Leningrad Nuclear Power Plant (LNPP-2) were determined. The “historical” halo of radioactive contamination of groundwater forming (1970-1990) at the site adjacent to the NPP, where the storage facility of low- and medium-level radioactive waste is located, falls into the zone of influence. Interpretation of monitoring data allowed obtaining the migration parameters for predictive estimates. Modeling has shown that during the time of the LNPP-2 operation there is was no intake of contaminated water by the drainage system of the new power plant.

***Keywords*:** groundwater; radioactive elements; technogenic radionuclides; radioactive contamination halo; sorption; half-life; geomigration modeling

Received: 24.01.2022 ***Accepted: 26.04.2022*** ***Online: 30.05.2022*** ***Published: 25.04.2023***

Introduction. During the NPP construction and operation the geological environment and ecosystems of surface water bodies are subject to various impacts. Traditionally, the following sources of technogenic radionuclides at the NPP site are considered: storage facilities for the plant radioactive waste (RW); spent nuclear fuel storage pools; water leakages from the technological pipelines; reactor plants in emergency conditions (design basis and off-design accidents). Thus, according to the statistical data of the US Nuclear Regulatory Commission [1]), at many of the 55 commercial NPP sites groundwater shows elevated concentrations of tritium, in some cases, ^{14}C carbon and fission products of nuclear materials are present. A characteristic example is tritium contamination of groundwater at the site of the Sequoyah NPP (Tennessee) caused by defects in the pipelines. Large-scale tritium contamination (the activity of tritium in water reaches 500 Bq/l) was recorded at the operating Paks NPP (Hungary) [2], and the zone of potential influence of the tritium halo is near the location site of the new NPP stage (Paks-II). A similar problem is faced during the construction of a new NPP in Lithuania within the industrial area (IA) of the Ignalina NPP decommissioned at the end of 2009 [3]. Many studies have shown that mathematical modeling of groundwater migration is the most reliable tool for predicting changes in its radiological state under conditions of a growing capacity of nuclear power facilities [3]. At the same time, the analysis of the published materials in many cases indicates an insufficient parametric validity of hydrogeological models, in particular, the information obtained in the course of a long-term monitoring of groundwater is not fully used. Monitoring can perform not only control, but also experimental functions helping to specify the filtration and migration parameters of aquifers [4-6].

In Russia, the construction of new power units, including replacement ones, is carried out near the sites of the operating plants or other nuclear facilities (NF), within which there are existing or potential sources of radioactive contamination of groundwater. Thus, the LNPP-2 is in close proximity to the decommissioned LNPP, a regional facility for the management of low and medium level waste (FGUP “FEO”, formerly LSK “Radon”) [7-9] and some other nuclear facilities (NF) in the industrial area (IA) of Sosnovy Bor town. In the immediate vicinity of the Novovoronezh NPP-2 there are also a number of radiation-hazardous facilities (filtration fields contaminated with radionuclides, RW storage facilities), territorially and historically associated with the Novovoronezh NPP first stage site [10]. Since the influence of the new power plants and stages of power units nearing completion extends to the areas with strongly altered (disturbed) natural conditions, the problem of predicting the chemical and radioactive contamination of drainage water extracted during the construction and operational drainage of the NPP, arises. This study focuses on the analysis of this problem in relation to the Sosnovy Bor facility.

Methodology. The analysis is based on the database of groundwater radiation monitoring in the IA (Fig.1) which combines the information collected from local (“departmental”) networks of observational hydrogeological wells at each of the operating NF. Total number of such wells in the industrial area is approaching 200. The collection and generalization of data from object monitoring of the subsoil state at the facilities of the “Rosatom” State Corporation is carried out in a centralized way across the country within the framework of the state program by the experts of the FGBU “Gidrospetsgeologiya”.

Starting in the 1980-1990s, the radiation monitoring services have been monitoring the radiological indicators, level, temperature, and chemical composition of groundwater in the Quaternary and

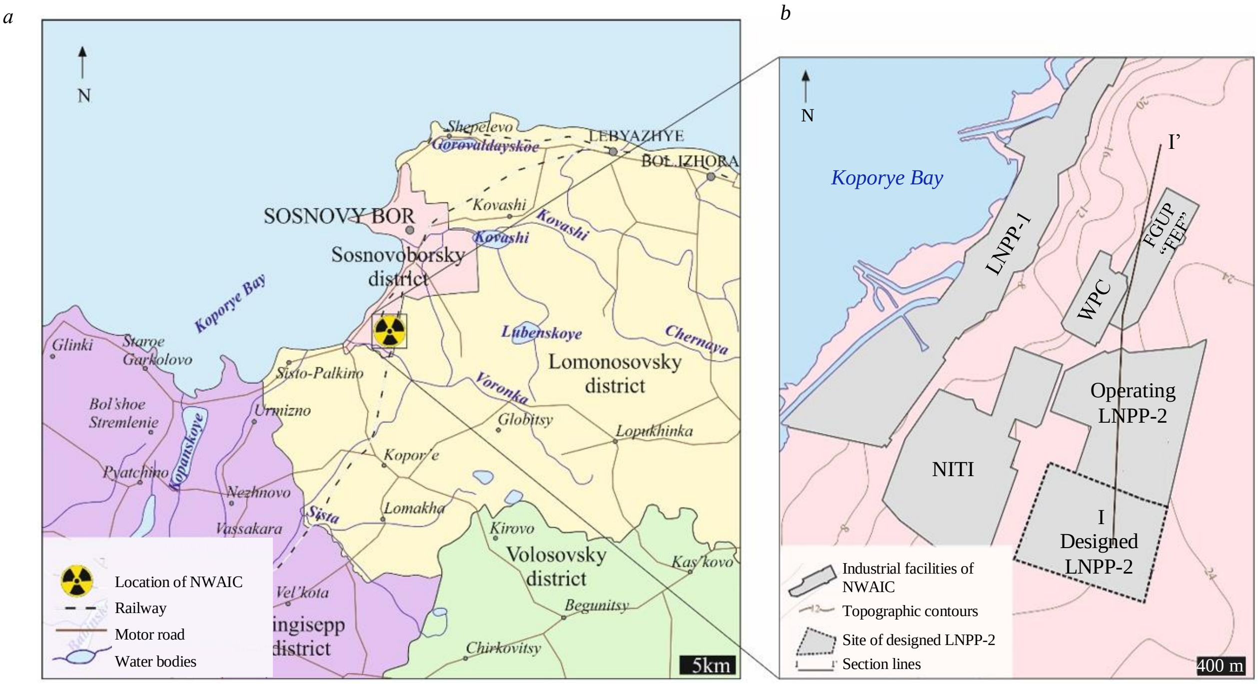

Fig.1. Study area: *a* – regional scheme; *b* – main NF in the industrial zone

upper parts of the Lomonosov aquifers. In accordance with the regulations of a particular facility, radiation monitoring includes the following indicators: total volume α- and β-activity, volume activity of tritium and, selectively, the activities of ^{90}Sr, ^{137}Cs, and actinides. A specific list of monitoring parameters, frequency of sampling and measurements in wells as well as the sampling and analysis methodology, provided there are the national guidance documents, is determined by the regulations of the facilities, often methodologically inconsistent with each other.

Total β-activity is the main indicator controlled by the radiation safety services at the agro-industrial complex (AIC) facilities. Its background values for the European part of the RF are 1-4 Bq/l (excluding tritium activity), of which 50-80 % are due to ^{40}K isotope activity. Owing to the constancy of potassium isotopic composition in groundwater, ^{40}K to stable K^+ ratio is a constant value, and the value of β-activity caused by the presence of ^{40}K isotope Bq/l can be approximately calculated by multiplying the concentration of K^+ ion mg/l by a factor of 0.0276. For K^+ concentration values not exceeding 10-12 mg/l in the Sosnovoborsky district, the calculated value of volume β-activity of groundwater due to the presence of ^{40}K is less than tenths of Bq/l. At background activity of ^{90}Sr not exceeding hundredths of Bq/l, and a priori assumption of an insignificant share of β-activity of ^{137}Cs, total β-activity of groundwater exceeding the value of 0.5-1 Bq/l (taking into account measurement errors) indicates the presence of technogenic radionuclides in it, the main of which, according to the experience of radiation monitoring in the IA, is ^{90}Sr. The same value (1 Bq/kg of specific total β-activity) is regulated by NRB-99/2009 as a criterion of the need for further research into the radionuclide composition of water.

In the first years of operation of local monitoring systems, the accuracy of determining the activity of radionuclides in groundwater in the radiation monitoring laboratories of the facilities was low. For example, at the RW disposal site (LSK “Radon”), the sensitivity threshold for measuring β-activity did not exceed 1 Bq/l; α-activity, 0.2 Bq/l. This made it possible to record the non-exceedance of the maximum permissible values by the radiation indicators.

Groundwater monitoring at the LSK “Radon” started in 1982-1983, when the first 13 wells were drilled into the Quaternary aquifer. Further, the stock of observation wells was increased by 35 wells in 1989-1993 and by 40 in 2007-2011. Many of the first stage wells have already been decommissioned due to poor technical condition. The observations involved 66 control and observation wells (COW) equipped for the Quaternary (depth 2.5-7 m) and Lomonosov (middle and lower zones, depth 7-14 m) aquifers. The measurement time interval is determined by the location of wells relative to the storage buildings and varies from once a week (tritium and β-activity) to single measurements on demand. The level and the number of indicators of the groundwater chemical composition are also selectively controlled.

At the site of NITI named after A.P.Aleksandrov, radiation monitoring of groundwater composition started in the late 1990s. The most complete series of data is available for eight observation wells equipped for the Quaternary and Lomonosov (middle and lower zones) aquifers. The activity of tritium, ^{90}Sr and ^{137}Cs is measured in wells of the operational network with determination accuracy of background values.

The radiation monitoring network of the new LNPP-2 was developed at the stage of its construction (since 2008) and comprises 13 observation wells equipped for the Quaternary and Lomonosov (upper, middle, and lower zones) aquifers. Testing of the COW was carried out as part of the survey work (2010-2015) and included measurements of the activities of tritium, ^{90}Sr and ^{137}Cs.

The first data on the radiological indicators of groundwater between the sites of the facilities were represented by the results of testing carried out by VNIPIET and the NPO “Radium Institute” in 1991 during the period of the maximum leakages of radionuclides at the RW disposal site. The results of analysis of tritium samples showed its irregular distribution across the sampling points, the maximum values ranging from 3,300 to 1,600 Bq/l [7].

In 2009, FGUP "Gidrospetsgeologiya" and SPbO IGE RAS restored and drilled new observation wells between the sites of the LSK "Radon" (FGUP "FEO") and the WPC LNPP, and starting from 2010 to 2015 within the framework of the pre-operational monitoring at the LNPP-2 under construction, radiological monitoring of groundwater was carried out on a grid of 39 wells within the entire IA (Fig.2). Sampling was performed twice a year and included the measurement of α-, β-radioactivity, volume activity of technogenic radionuclides (tritium, ^{137}Cs, ^{90}Sr, $^{238/240}$Pu) and natural radioisotopes (^{222}Rn, ^{224}Ra, ^{226}Ra, ^{228}Ra, ^{210}Pb, ^{210}Po and others) [9].

Measurements of total α- and β-activities were carried out using an UFM-2000 radiometer (NPC "DOZA", Zelenograd). The detection limits for total α- and β-activities are 0.02 and 0.1 Bq/l, respectively. Sample preparation (evaporation of a liquid sample and obtaining dry residue) implies that the measurement of α- and β-activities excludes the influence of tritium. Tritium content was measured with a Tri-Carb 2910TR spectrometric radiometer (Waltham, USA). The detection limit of tritium is 10 Bq/kg; the measurement error is 3-25 %. The activity of ^{90}Sr in groundwater was determined by the daughter ^{90}Y followed by precipitation radiometry using the UMF-2000 radiometer according to the procedure developed at NITI named after A.P.Aleksandrov (Sosnovy Bor) (detection limit 10 Bq/m^3). ^{137}Cs was determined using a DSPEC jr (ORTEC, USA) γ-ray spectrometer (detection limit 10 Bq/m^3).

Notions about the variability of the filtration properties of water-bearing strata within the IA were obtained by analyzing the materials of experimental filtration sampling conducted in 1998-2013. The enclosing medium was characterized by cluster and single pumpings, fillings, and express sampling. To construct a matrix of filtration heterogeneity, data from the database on 137 experimental

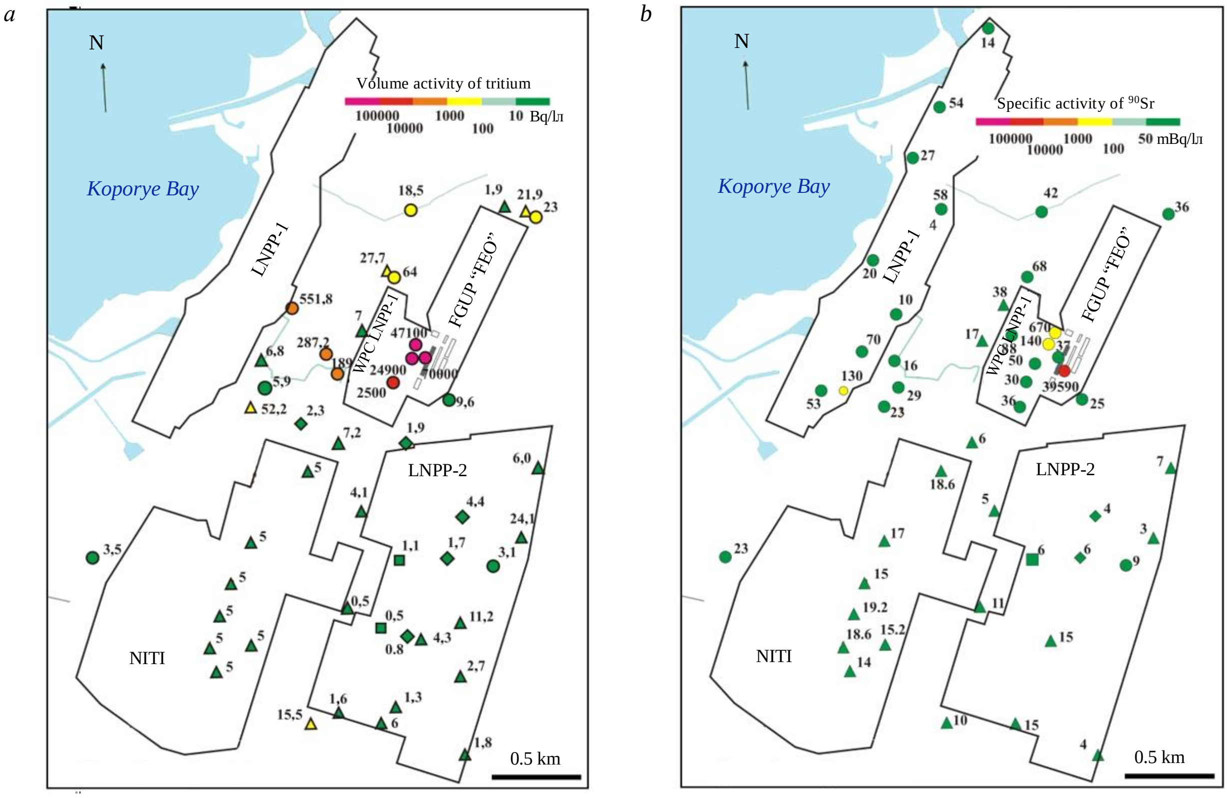

○ 1 △ 2 ◇ 3 □ 4

Рис.2. Distribution of activity in IA based on results of pre-operational monitoring at LNPP-2 (data averaged for 2009-2015): *a* – tritium, Bq/l; *b* – ^{90}Sr, mBq/l

Sampling aquifer: 1 – Quaternary; 2 – Lomonosov (upper zone); 3 – Lomonosov (middle zone); 4 – Lomonosov (lower zone) samples were used: cluster and single pumping and express testing. During processing, the following main calculation schemes were used:

- aquifer complex with overflow from an aquifer with varying pressure (with variable and constant flow);
- pressure aquifer unconfined in plan (with variable and constant flow rate);
- linear source: an imperfect well in a pressure aquifer, confined in section and unconfined in plan (with variable flow rate).

As a result of processing, one or more parameters from the following set were determined:

- piezoconductivity (or water yield) of the main and adjacent aquifer beds (a, m^2/day);
- conductivity of the main and adjacent aquifer beds (T, m^2/day);
- overflow parameter (B, m);
- filtration coefficient (k, m/day).

In processing, basic analytical solutions of such authors as A.F.Moench [11], S.P.Neuman [12], M.S.Hantush [13], Javandel-Witherspoon [14], H.H.Cooper [15] and others were used. All field experiments were reinterpreted using the ANSDIMAT software package [16].

The intensity of radionuclide migration in groundwater is largely controlled by the ability of the porous medium to retain and accumulate radionuclides due to sorption processes. In laboratory experiments, the sorbability of ^{90}Sr and ^{137}Cs radionuclides on the Quaternary sandy-clayey rocks and Cambrian weakly cemented sandstones was studied. The experiments were carried out with artificial solutions imitating the characteristic composition of groundwater. Radioactive labels were introduced into natural water under strict control of the pH constancy inherent in natural waters.

The notion of sorbability of radionuclides is also given by the interpretation of data from long-term radiation monitoring of groundwater within the FGUP “FEO” site [9]. The analysis of the output curves can be performed using the method of statistical time moments [17-23]. For the convenience of calculation, the absolute statistical moments m_j are normalized by the zero moment m_0:

$$\mu'_j = \frac{m_j}{m_0}. \tag{1}$$

The first statistical moment (j = 1) is the center of gravity and allows calculating the average residence time of the component from the source to the measurement point. For subsequent moments, the central moments (or moments relative to the middle) are determined, which characterize the scatter of the points of output curve $c = f(t)$ relative to its center of gravity. The second moment characterizes the hydrodynamic dispersion (scattering degree of a random value relative to the average residence time) and is determined by the dependence:

$$\mu_2 = \mu'_2 - (\mu'_1)^2, \tag{2}$$

The formulas for determining the statistical moments in the case of one-dimensional convective-dispersive transfer of the sorbed components subject to decay, when setting the input step function (Heaviside), have the form [17, 19, 20, 24]:

$$\mu'_1 = \frac{t_s}{2} + \frac{Rx}{a}; \tag{3}$$

$$\mu_2 = \frac{t_s^2}{12} + \frac{2D_L R^2 x}{a^3}, \tag{4}$$

where t_s is the duration of contamination (in this case, continued leakage from storage facilities); D_L pore dispersion coefficient, m^2/day; R sorption delay factor, $R = 1 + K_d\rho_b/n$; K_d sorption distribution coefficient; ρ_b rock density; n porosity; λ radioactive decay constant, $\lambda = 0.693/T_{1/2}$; $T_{1/2}$ half-life of radionuclide; $a = \sqrt{u^2 + 4D_L\lambda}$; u average pore filtration rate.

Equations (3) and (4) can be considered as a system of equations, the solution of which allows determining the velocity u, dispersion coefficient D_L (using non-sorbable component, tritium), and the sorption delay factor R (using data on β-activity). Statistical moments μ'_1 and μ_2 are calculated after approximation of indicator graphs $C(t)$ by step functions.

To predict the migration of radionuclides under changing hydrodynamic conditions of the area, the PMWIN software was used, which comprises the filtration (Modflow) and transport (Modpath) calculation modules [25]. Modflow is based on the differential equation of flow continuity, which is solved by numerical methods [26-28]. The migration problem was solved in a simplified formulation using streamlines on the Modpath module without regard for hydrodispersion [29, 30]. The choice of the Modpath module is due to the fact that at this work stage the following was investigated: movement direction of the contamination halo, its actual rates, and the arrival time of radionuclides to the discharge zones. Since radionuclide concentrations in groundwater were not the subject of consideration, the solution of the complete advective-dispersive problem is redundant and can only lead to additional uncertainties.

As a basis for constructing the surfaces of the top and the base of each model layer, a geological model created in the SGeMS software [31, 32] was used. The filling of the 3D geological model was based on the information on 1,504 wells from the database obtained in the course of engineering geological and hydrogeological surveys in the study area. The average depth of wells was 16 m, a total of about 24,000 m were drilled. In the course of the field and laboratory work, 14 basic engineering geological elements were identified. The interpolation of surfaces between individual wells was carried out using the kriging algorithm (Sequential Gaussian Simulation procedure).

After the filtration model had been produced, it was calibrated in a stationary environment. The data on the average long-term groundwater levels for 110 COW and the volume of actual water inflow into the construction pits at the LNPP-2 were involved. Calibration was carried out until the design and actual values of water levels and the volume of construction drainage began to coincide.

Characteristics of the object of research and modeling. In hydrogeological terms, the Quaternary, the Lower Cambrian aquifers and the Vendian aquifer complex are distinguished in the sedimentary strata (Fig.3). The two first aquifers from the surface, the Quaternary (Q_{IV}) and the Lower Cambrian ($Є_1$), are subject to the greatest technogenic impact in the study area [9].

Water-bearing rocks of the Quaternary aquifer are supra-morainic sands of various genesis, their thickness over most of the area not exceeding 5 m [33, 34]. The aquifer is underlain by weakly permeable loam interbeds to 8 m thick, which are a local aquiclude [35]. Based on the geological section, the aquifer is not protected from surface contamination.

The Lower Cambrian aquifer $Є_1$ underlying the Quaternary aquifer is composed of sands and weakly cemented sandstones which are divided by weakly permeable clay interbeds into separate zones. At the LNPP-2 site, there are three such aquifers in the section, and at the site of the FGUP "FEO" Branch there are only two, whereas beyond the WPC LNPP area, towards the bay, the aquifer completely wedges out. Water is fresh, bicarbonate, of mixed cationic composition.

A characteristic feature of the geological section of the area is the presence of buried riverbeds – paleovalleys filled with sands, sandy loams, loams. On the floors of ancient valleys, total thickness of the Quaternary deposits reaches 40 m; thus, they are cutting through the underlying Lower Cambrian strata. Therefore, paleovalleys create hydrogeological windows, due to which groundwater of the considered aquifers has a good hydraulic connection. Paleovalleys cross the LNPP-2 site and are recorded in the northern and southern parts of the FGUP "FEO" site (Fig.1, 3).

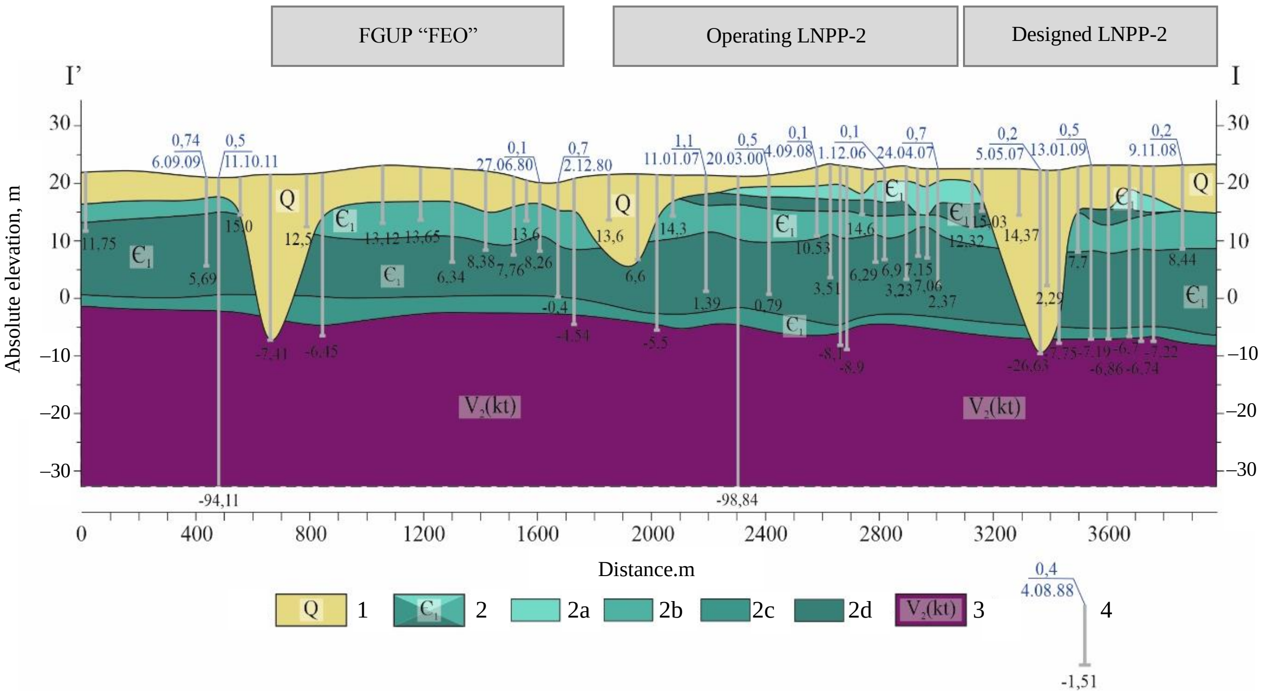

Fig.3. Hydrogeological section along I-I' line (see Fig.1)

1 – Quaternary aquifer; 2 – Lower Cambrian (Lomonosov) aquifer*:* 2a, 2b, 2c – water-bearing layers of the aquifer, 2d – separating aquicludes*;* 3 – Upper Vendian (Kotlin) aquiclude; 4 – well: above – depth to the established groundwater level and measurement date; below – absolute elevation of well bottom

Radiation monitoring carried out during five years in connection with construction of the LNPP-2 allowed establishing the following distribution of radiation indicators in aquifers of the IA (Table 1). The site of the LNPP-2 under construction is completely free from the impact of radioactive contamination: tritium activity values do not exceed 10 Bq/l, and in most wells – 4 Bq/l (Fig.2, *a*). Based on the available data, it is possible to determine the background value of volume activity of tritium in groundwater – 1-4 Bq/l. The volume activity values of other technogenic radionuclides vary within the limits that can be considered as background: ^{90}Sr – 0.004-0.030 Bq/l, ^{137}Cs – 0.004-0.040 Bq/l (Fig.2, *b*). The values of integral radiation indicators are: β-activity – 0.1-1.0 Bq/l, α-activity – 0.01-0.2 Bq/l. The study area in the IA outside the sites of FGUP "FEO", WPC LNPP and LNPP, according to the monitoring results, is characterized by virtually background values of the activity of cesium and strontium isotopes (less than 0.1 Bq/l) and an irregular distribution of tritium. The highest values of tritium are recorded in several wells in close proximity to the contamination sources – near the LNPP site, near the WPC LNPP, and also slightly northwest of the NITI site.

The contents of natural radioactive isotopes (^{222}Rn, ^{228}Ra, ^{210}Pb, ^{232}Th) range from $n \cdot 10^{-3}$ to $n \cdot 10^{-2}$ Bq/l and do not exceed the LI_{dw}. These activities can be regarded as background for the study area. For their statistical confirmation, further monitoring of groundwater is required.

FGUP "FEO" is most important among the operating NF in terms of its impact on groundwater quality (Fig.2). The facility holds over 60,000 m^3 RW with total activity $3.16 \cdot 10^{16}$ Bq [3]. Radionuclides recorded in groundwater at the site are mainly represented by: tritium, ^{90}Sr and ^{137}Cs. ^{239}Pu, ^{238}Pu, ^{241}Am, ^{210}Pb, ^{210}Po, ^{60}Co, ^{226}Ra were determined in water at the level of background activities. Monitoring data allow quantifying the migration process.

Table 1

Statistical data on the content of technogenic radionuclides in groundwater at NWAIC sites

Radionuclide	Number of definitions	Mean, Bq/l	Minimum, Bq/l	Maximum, Bq/l	Level of intervention in drinking water (LI_{dw}) after NRB-99/2009, Bq/l
WPC NPP (2009)					
^{137}Cs	2	1.15	0.1	2.2	11
^{90}Sr	8	0.13	0.01	0.67	4.9
Tritium	3	$1.6\cdot10^{5}$	$2.5\cdot10^{3}$	$4.7\cdot10^{5}$	7,600
LNPP-1 (2009)					
^{137}Cs	3	0.13	0.13	0.14	11
^{90}Sr	9	0.05	0.01	0.13	4.9
^{60}Co	3	0.12	0.1	0.13	40
Between WPC LNPP and LNPP-1 sites (2009-2015)					
^{137}Cs	29	0.17	0.002	4.7	11
^{90}Sr	28	0.02	0.003	0.1	4.9
Tritium	93	59	0.02	1460	7,600
NITI (2009-2010)					
^{137}Cs	7	0.024	0.023	0.027	11
^{90}Sr	8	0.017	0.014	0.022	4.9
Tritium	8	5	5	5	7,600
LNPP-2 (2010-2015) Quaternary aquifer					
$\sum\alpha$	8	0.11	0.03	0.19	0.2
$\sum\beta$	8	0.21	0.1	0.45	1.0
^{137}Cs	8	0.01	0.002	0.037	11
^{90}Sr	7	0.02	0.003	0.11	4.9
Tritium	21	8.74	1.02	56	7,600
Lomonosov aquifer					
$\sum\alpha$	28	0.11	0.02	0.28	0.2
$\sum\beta$	28	0.22	0.03	0.67	1.0
^{137}Cs	26	0.01	0.002	0.03	11
^{90}Sr	29	0.01	0.001	0.03	4.9
Tritium	39	6.14	0.18	99.7	7,600

In groundwater of the LSK “Radon” site in 1987-1991 there was a surge in the activity of technogenic radionuclides caused by the leakage of radioactive solutions from the storage facilities (Table 2). This was caused by an inadequate protection of buildings from atmospheric precipitation and flooding due to the rise in groundwater levels during floods. This led to the RW contact with surface- and groundwater and a subsequent flow of radioactive solutions into aquifers. To eliminate the leakages, the storage facilities were modernized, which reduced the content of technogenic radionuclides.

Table 2

Comparison of volume activity of leachates from storage facilities and groundwater selected from observation wells along the storage perimeter

Characteristic	Tritium	^{137}Cs	^{90}Sr
Leachate at storage bottom			
Maximum values (1998-1999)	$3.7\cdot10^{10}$	$7.4\cdot10^{7}$	$8.5\cdot10^{6}$
Mean values (1998-1999)	$8.1\cdot10^{9}$	$1.1\cdot10^{7}$	$2.2\cdot10^{6}$
Mean values (2009)	$4.9\cdot10^{8}$	$3.2\cdot10^{5}$	$6.7\cdot10^{4}$
Mean values (2014)	$3.5\cdot10^{8}$	$2.3\cdot10^{5}$	$9.4\cdot10^{4}$
Mean values (2017)	$7.6\cdot10^{8}$	$3.6\cdot10^{5}$	$3.6\cdot10^{5}$
Monitoring wells			
Maximum values (1990-1991)	$3.7\cdot10^{10}$	$6.7\cdot10^{5}$	$4.4\cdot10^{6}$
Maximum values (1998-1999)	$1.9\cdot10^{10}$	$8.9\cdot10^{4}$	$9.3\cdot10^{5}$
Intervention level in drinking water (NRB-99/2009)	$7.7\cdot10^{6}$	$11\cdot10^{3}$	$5\cdot10^{3}$

Figure 4 shows that in 1991 the largest area of tritium contamination (activity over $1\cdot10^4$ Bq/l) was recorded in the Quaternary aquifer. The maximum activity was noted in the area of storages N 8 and 9 and in the eastern corner of storage N 4. Observations of groundwater level showed that near the storage, levels in the Quaternary aquifer are higher than in the Lomonosov aquifer. Groundwater level difference between the aquifers reaches about a meter, which can contribute to contamination of the lower aquifer through hydraulic windows (absence of a separating aquiclude, presence of paleovalleys). In 2017, there was a gradual decrease in the activity of groundwater contamination in the Quaternary aquifer and its growth in the Lomonosov aquifer due to the presence of a hydraulic connection between them.

A change in β-activity in aquifers generally corresponds to the patterns revealed in the analysis of tritium contamination: the maximum activity was recorded in the late 1980s in the Quaternary aquifer in the area of storages N 4, 8, 9. Simultaneously with contamination in the upper aquifer, due to hydrogeological conditions of the area, the contamination flows into the lower aquifer. By 2017,

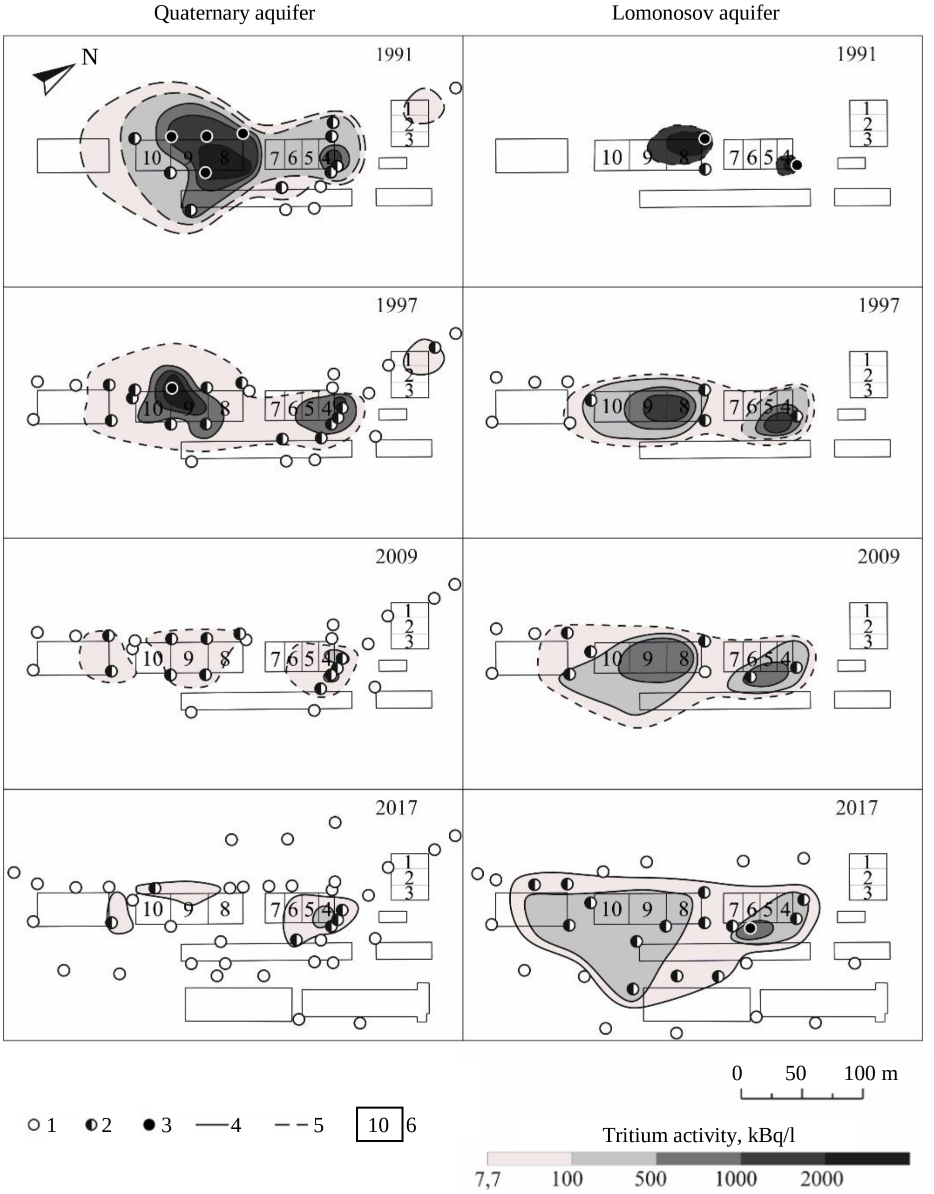

Fig.4. Tritium contamination halo of groundwater in Quaternary and Lomonosov aquifers

1-3 – observation wells (COW): 1 – tritium activity less than 7.7 kBq/l; 2 – tritium activity from 7.7 to $1\cdot10^3$ kBq/l; 3 – tritium activity over $1\cdot10^3$ kBq/l; 4 – confirmed halo contours; 5 – presumed halo contours; 6 – storage facility and its number the values of β-activity in the Quaternary aquifer decreased by several orders of magnitude due to dilution of the halo with clean groundwater and atmospheric precipitation as well as radioactive decay.

Concentration of isotopes of one of the most toxic radioactive components – plutonium (^{238}Pu and ^{239,240}Pu) in groundwater, as shown by the results of α-spectrometric measurements at five observation wells, in almost all samples is hundredths and tenths of a Bq/l. The maximum value 0.013 Bq/l was recorded at one of the COW nearest to the storage facility, which is one order of magnitude lower than the permissible norms after NRB-99/2009 (0.6 Bq/l). In the canyon of the RW storage facility, the content of plutonium isotopes is also approximately two times lower than the LI_{dw} according to NRB-99/09.

Directly beyond the western boundary of the FGUP "FEO" there is another NF – the WPC LNPP site with temporary storage tanks for liquid radioactive waste (Fig.2). In the 1990s there were leakages from them into concrete pallets where the values of radionuclide activity in solutions in the late 1980s reached 2.3·10^4 Bq/l (^{60}Co) – 3·10^4 Bq/l (^{137}Cs) [36]. Due to the aging of pallets and pits, radionuclides got into groundwater. In some wells near the boundary of the WPC with the FGUP "FEO" site, volume β-activity during the measurement period repeatedly exceeded 3.7 Bq/l, which is higher than groundwater activity at the neighboring LNPP site (0.7-1.9 Bq /l). This approximately corresponds to the natural activity of ^{40}K. In the north of the site, local tritium contamination to 170-180 Bq/l was recorded. Elevated levels of ^{90}Sr 0.035-0.57 Bq/l were found along the Koporye Bay line in groundwater within the power plant. In subsequent years, according to the monitoring service of the facility, radiological indicators of groundwater α-, β-activity and tritium do not exceed 7,000 Bq/l [37].

a

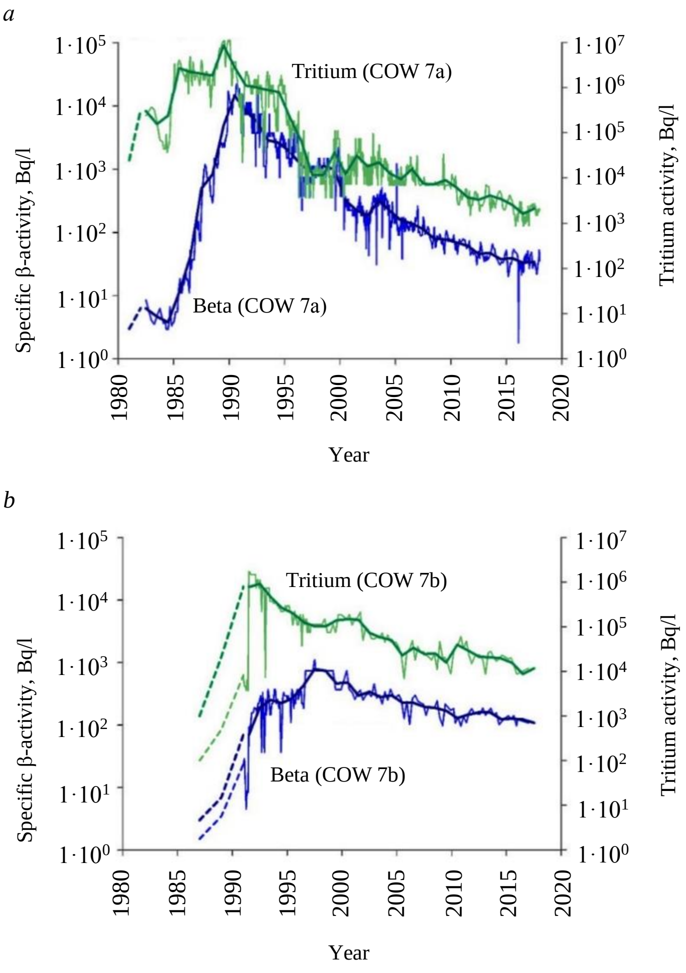

b

Fig.5. Output curves for tritium and β-activity after COW 7a (*a*) and 7b (*b*) (thin lines – quarterly measurements, thick ones – annual average)

Summing up the results of analyzing the radiation state of groundwater, it can be concluded that the most urgent problem is a possible contamination of underground drainage at the LNPP-2 site due to involvement of radionuclides in the water intake as part of the formed contamination halo in the Quaternary and Lomonosov aquifers. The reliability of prediction increases due to detailization of the contamination processes in close proximity of the contamination source for assessing the existing evolution trends of this process. The corresponding prediction estimates also require the use of mathematic modelling techniques.

Monitoring data on wells in the RW storage area (Fig.4) can be used to determine mass transfer parameters. Thus, Fig.5 shows the most typical indicator curves for tritium and β-activity for the COW closest to the storage facility – 7a (Quaternary aquifer) and 7b (Lomonosov aquifer). In the upper aquifer, higher levels of contamination were recorded in wells in 1989-1995; in the lower aquifer, in 1990-2005. In both aquifers, the peaks of β-activity lag behind the tritium peaks by several years, which can be accounted for by a slowdown of sorbing β-emitting radionuclides (primarily ^{90}Sr) with respect to inert tritium.

The interpretation assumed that the leakage of radioactive solutions began in 1979, just a few years after their commissioning, and continued until the end of the 1980s, i.e., t_s is about 10 years. The distance from the contamination source to COW 7a and 7b is 12 and 15 m.

Table 3 presents the calculation results of convective dispersion and sorption indicators. The interpretation of time lags of activity peaks measured at COW 7a and 7b (Fig.5) gave close values of the delay coefficient R, which were used in prediction estimates.

Table 3

Calculation results of transport characteristics of dissolved substances by the method of time moments

Well	Indicator	$t_{\max}^{\text{abs}}$ *, year	μ'_1, year	μ_2, year	u, m/year	D_L, m^2/year	δ_L**, m	R	K_d***, ml/y
7a	Tritium	~1987	10.18	8.7	2.3	0.19	0.08	–	–
	β-activity	~1990	13.64	14.9				1.66	0.09
7b	Tritium	~1991	15.34	24.6	1.4	1.66	1.18	–	–
	β-activity	~1999	22.34	35.2				1.58	0.08

---

* $t_{\max}^{\text{abs}}$ – approximate time of concentration peak; ** $\delta_L = D_L/u$ – microdispersion parameter; *** n = 0.3 and ρ_b = 2.1 g/cm^3 were used in calculation.

The hydrodynamic model comprises the industrial area (6.85×8.05 km). The coast of the Gulf of Finland (type I) served as the outer boundary in the west of the model area. The eastern boundary of the model area was set according to the remote hydroisobath with an absolute elevation of +26 m (type I). The Voronka River was taken as the southern boundary of the model (type III). The northern boundary of the model was set along the streamline of the ground aquifer drawn from the coast of the Gulf of Finland north of the LNPP-1 to the hydroisobath with an absolute elevation of +26 m (type I). The upper limiting surface of the model is the relief surface, and the top of the Kotlin clays, which acts as a regional aquiclude, was taken as the lower boundary. Internal boundaries of the model are channels, creeks, and a developed drainage network of the facilities (type III). In the model there is also the NITI discharge channel and the LNPP channels (Fig.6, *a*). The infiltration recharge was evenly distributed over the model area, with the exception of some local areas associated with location of drainage networks.

Hydrogeological section was approximated by eight model layers: 1 – corresponds to the Quaternary aquifer; 3, 5, 7 – three aquiferous zones of the Lomonosov aquifer; 2, 4, 6 – relative aquicludes separating them; 8 – Upper Vendian aquiclude (Fig.6, *b*).

Lithological structure of the Quaternary sequence in the study area is accompanied by a strong heterogeneity both in plan, and in depth. Lenses of sandy varieties alternate with sandy loams and loams; thickness of the Quaternary deposits is highly variable. In local areas, in places of paleovalleys, a significant increase in thickness to 35 m is recorded. Paleochannel can be filled with both highly permeable gravelly deposits, and low permeable sandy loams and loams. A strong lithological heterogeneity of the Quaternary rocks predetermined a wide range of values for the filtration coefficients of the studied strata (Table 4).

For the upper aquiferous zone of the Lomonosov aquifer, the determination accuracy of parameters is complicated by the limited area of its occurrence within the site as well as a hydraulic association with the Quaternary aquifer. In the middle aquiferous zone, values of the filtration coefficient are similar to those in the upper one. Filtration coefficients of the lower aquiferous zone have lower values than in the upper or middle zones (Table 4).

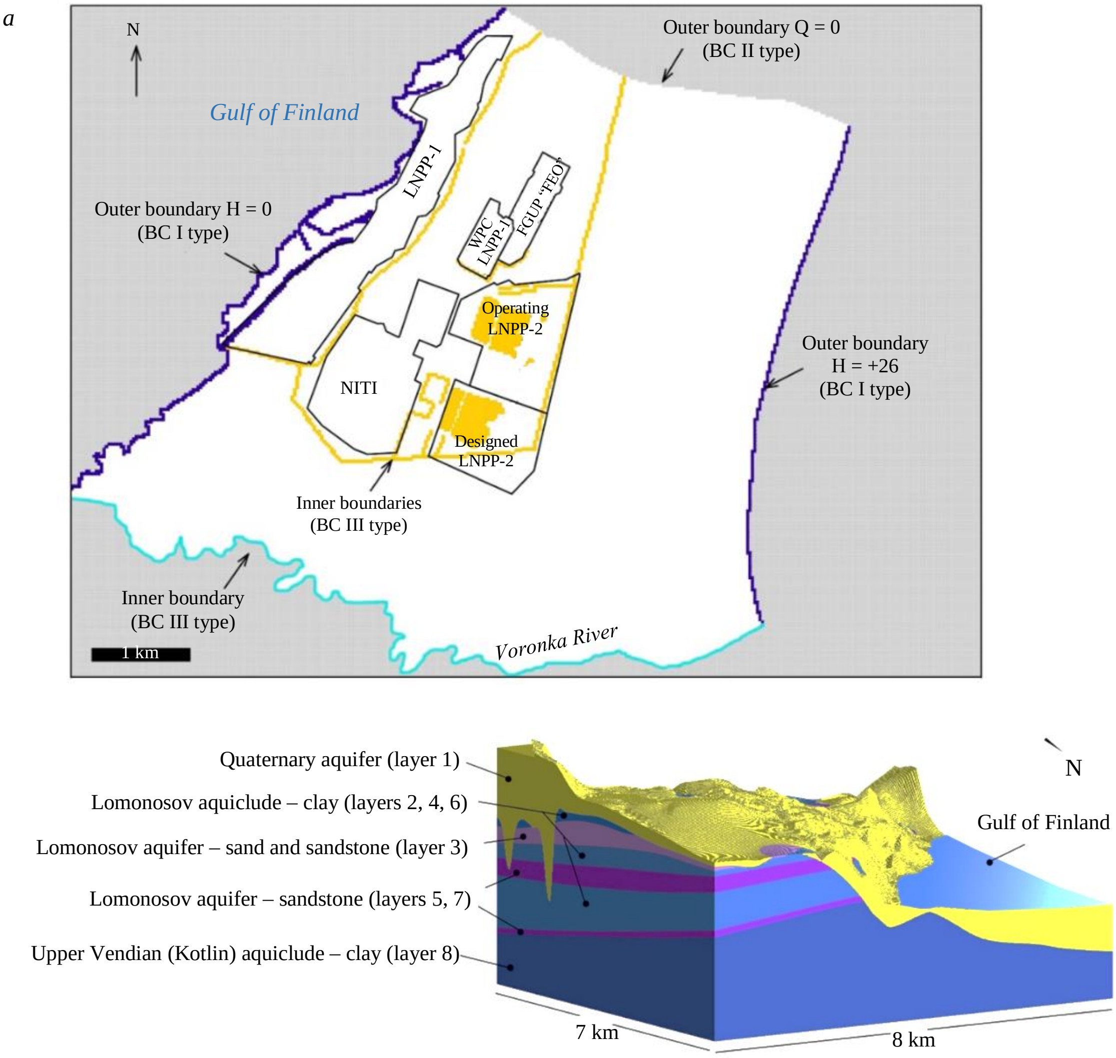

Fig.6. Hydrodynamic type of boundaries of groundwater filtration model (*a*) and its 3D view (*b*)

Table 4

Resulting table of filtration coefficients in the model

Rock type	Filtration coefficient, m/day
Quaternary deposits	
Gravelly sand, gravelly soil	4.1
Medium- and coarse-grained sand	0.24
Fine-grained and dust sand	0.1
Sandy loam	0.05
Cambrian deposits	
Upper aquiferous zone (sand, sandstone)	0.94
Middle aquiferous zone (sandstone)	0.88
Lower aquiferous zone (sandstone)	0.28
Clays	0.0001

The performed correlation between point values of filtration coefficients on individual wells and lithological columns of wells described according to a single lithological scale for the entire array of information, was used to form the matrix of filtration inhomogeneity of model layers. Since a whole number of aquifers wedge out as they approach the Gulf of Finland, a special gridding algorithm was used to imitate their geometry. The layers were wedging out by setting the planned inhomogeneity. Thus, several lithological varieties with markedly different filtration coefficients can be simultaneously present in one model layer. Final values of filtration coefficients were taken from the calibration results of the filtration model (Table 4).

To assess the degree of hydraulic association of the Quaternary aquifer and three zones of the Lomonosov aquifer, the amplitudes of groundwater level fluctuations before the construction of the first stage of the LNPP-2 were analyzed according to regime observation data (Table 5). At a qualitative level, it can be stated (data from wells 2n and 1n) that the hydraulic association of the middle zone of the Lomonosov aquifer and the upper aquifers is quite good. The association proceeds via the hydrogeological windows along the axes of paleovalleys, which are cutting the Cambrian deposits at the LNPP-2 site (Fig.2).

Table 5

Amplitudes of groundwater level fluctuations in aquifers (2007)

Date	Quaternary (well 1n)		Lomonosov					
			Upper zone (well 2n)		Middle zone (well 3n)		Lower zone (well 4n)	
	Absolute elevation, m	Amplitude, m	Absolute elevation, m	Amplitude, m	Absolute elevation, m	Amplitude, m	Absolute elevation, m	Amplitude, m
April	22.98	0.07	20.93	0.15	20.58	0.14	20.89	0.08
	22.92	0.01	20.93	0.15	20.52	0.08	20.92	0.11
May	22.96	0.05	20.95	0.17	20.60	0.16	20.88	0.07
	23.09	0.18	20.95	0.17	20.71	0.27	20.85	0.04
	23.06	0.15	20.96	0.18	20.52	0.08	20.84	0.03
June	22.94	0.03	20.66	–0.12	20.49	0.05	20.82	0.01
	22.90	–0.01	20.73	–0.05	20.33	–0.11	20.73	–0.08
	22.85	–0.06	20.68	–0.10	20.30	–0.14	20.75	–0.06
July	22.79	–0.12	20.63	–0.15	20.26	–0.18	20.72	–0.09
	22.85	–0.06	20.70	–0.08	20.27	–0.17	20.76	–0.05
	22.82	–0.09	20.68	–0.10	20.27	–0.17	20.78	–0.03
August	22.66	–0.25	20.54	–0.24	20.24	–0.20	20.75	–0.06
	22.51	–0.40	20.40	–0.38	20.13	–0.31	20.72	–0.09
	22.84	–0.07	20.74	–0.04	20.26	–0.18	20.78	–0.03
September	22.92	0.01	20.79	0.01	20.48	0.04	20.81	0.00
	23.02	0.11	20.86	0.08	20.51	0.07	20.81	0.00
October	22.77	–0.14	20.81	0.03	20.54	0.10	20.81	0.00
	23.08	0.17	20.91	0.13	20.60	0.16	20.83	0.02
	23.10	0.19	20.95	0.17	20.63	0.19	20.88	0.07
	23.07	0.16	20.89	0.11	20.61	0.17	20.87	0.06
Mean value	22.91	–	20.78	–	20.44	–	20.81	–

The behaviour of groundwater levels in the lower zone of the Lomonosov aquifer differs significantly from other layers (well 4n). Annual amplitudes of water level fluctuations in the lower zone do not exceed 20 cm. Thus, we can state that the lower zone of the Lomonosov aquifer has a weak hydraulic association with the upper aquifers.

Hydraulic relationship of surface and groundwater in the numerical filtration model is controlled by the kinetic constant α, which is controlled by the filtration coefficient k' and thickness m' of the underlying aquiclude:

$$\alpha = \frac{k'}{m'}. \tag{5}$$

Kinetic constant α in the model determines the Q_s flow through the aquiclude:

$$Q = \frac{\mathrm{w}Lk'}{m'}\left(h_s - h\right) = \alpha wL\left(h_s - h\right) = C\left(h_s - h\right), \tag{6}$$

where w is river width inside the block, m; L river length inside the block, m; h_s water level in river, m; h groundwater level, m; $C = \alpha w L$ conductance, m^2/day.

Conductance C was selected on the model in the process of calibration based on general geometry and structure of the groundwater flow as well as other indirect data: for the Voronka River C = 200 m^2/day; for drainage ditches C = 1,000 m^2/day.

Calibration of the model was carried out in a stationary setting for 2013 based on the observation data of groundwater levels in 26 wells and the measurement results of drainage water volume into the construction pit of the first stage of the LNPP-2 (Table 6). Based on the calibration results, each layer is assumed to be isotropic in terms of filtration properties.

Table 6

Results of model calibration

Well number	Absolute elevation of groundwater level, m		
	Actual value	Design value	Difference
1	19.33	18.40	0.93
2	18.46	18.49	0.03
3	16.21	15.46	0.75
4	16.21	15.60	0.61
5	16.21	15.55	0.66
6	19.28	19.91	0.63
7	18.65	18.69	0.04
8	16.75	16.13	2.76
9	19.32	19.71	0.39
10	17.40	16.78	0.62
11	18.57	18.70	0.13
12	18.56	18.01	0.55
13	18.58	18.60	0.02
14	16.28	16.78	0.50
15	20.00	20.42	0.42
16	14.42	14.46	0.04
17	17.26	17.09	0.17
18	17.26	16.90	0.36
19	16.58	16.50	0.08
20	18.77	18.41	0.36
21	5.95	6.16	0.21
22	18.25	17.40	0.85
23	15.28	15.21	0.07
24	15.73	16.47	0.74
25	16.93	16.46	0.47

Drainage water discharge, m^3/day

	Long-run annual averages	Design value
Drain ditch	600-650	577

Discussion of results. Before the start of construction work and commissioning of the first stage of the LNPP-2, piezometric surface of groundwater was characterized by a relatively smooth pressure drop in both aquifers from the recharge area in the east to the water discharge zone in the west into the Gulf of Finland (Fig.7, *a*). Average pressure gradient is about 0.01 m/m including that within the FGUP "FEO" site. Streamlines characterizing the migration trajectories of radionuclides in the area of the RW storage facilities, as follows from the modelling results, have the same prevailing direction – from east to west (Fig.7, *a*). Most of the flow is intercepted by a drainage ditch near the LNPP-1, the other part is intercepted by a ditch running along the perimeter of the FGUP "FEO" and WPC LNPP-1 sites.

Modeling showed that the commissioning of the drainage of the first stage of the LNPP-2 leads to formation of a depression surface in aquifers within the model area (Fig.7, *b*). The maximum decrease in the center of the depression funnel is 10-12 m.

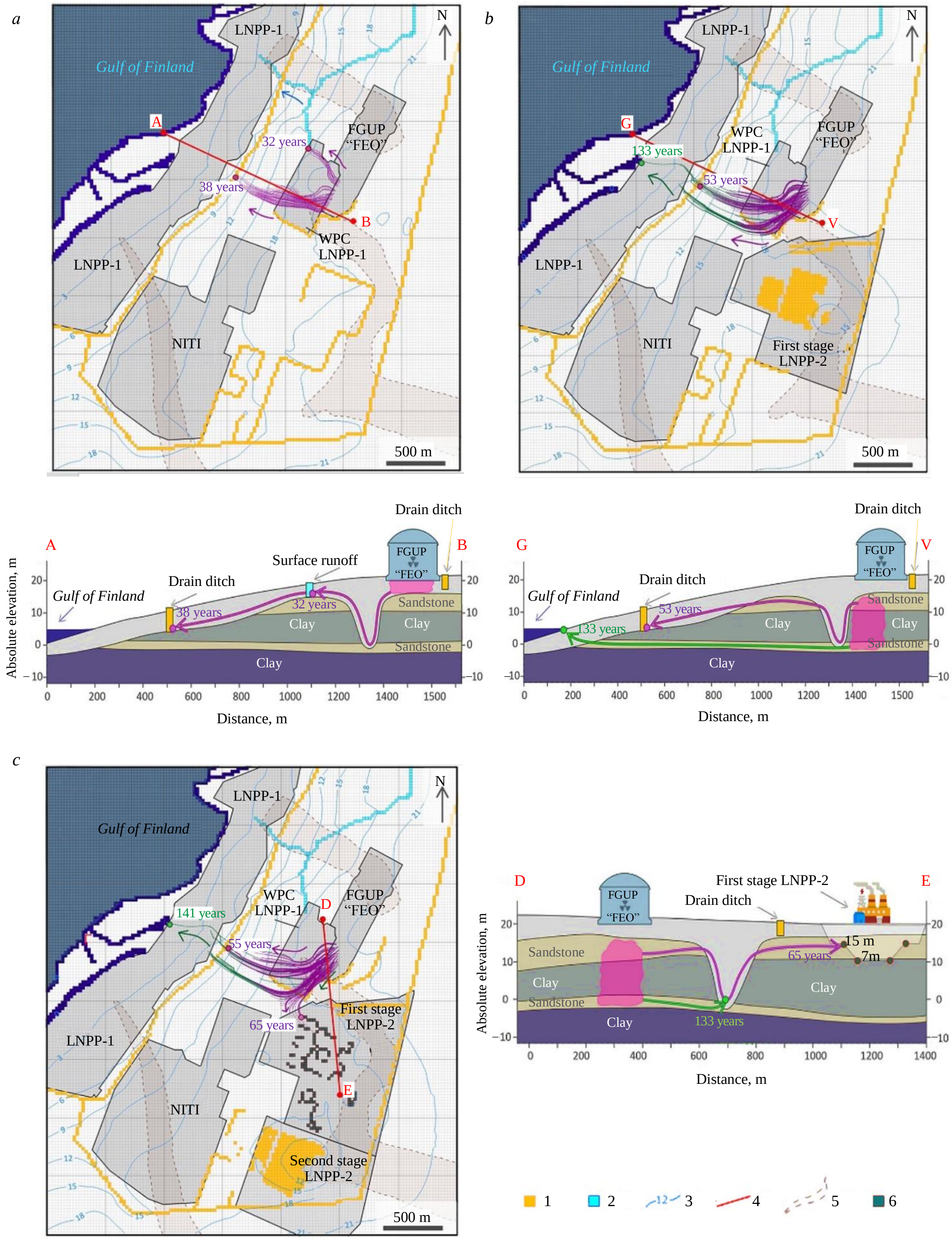

Fig.7. Structure of filtration flow with elements of groundwater flow network in plan and in section:
a – natural regime (prior to the start of the LNPP-2 construction; *b* – after commissioning of the first stage;
c – after commissioning of the second stage)

1 – drains; 2 – surface flow; 3 – hydroisobaths of the first aquifer from the surface; 4 – section line;
5 – projection of paleovalley on to the surface; 6 – drainage system of the first stage of the LNPP-2
Green colour shows migration routes in the lower Lomonosov aquifer, purple colour – in the middle Lomonosov and Quaternary aquifers

There is also a slight (tens of centimeters) decrease in groundwater levels at the southern boundary of the FGUP "FEO" site. Ongoing changes in underground hydrodynamics significantly affect the structure of the flow near the RW storage (Fig.7, *b*). However, there is still a watershed between the two sites, so the main flow direction of the contaminated groundwater remains the north-western one – towards the Gulf of Finland.

Drainage of the second stage of the LNPP-2 leads to additional "deformation" of the groundwater flow network: there is "branching" of a part of the model streamlines from the general north-western direction (Fig.7, *c*). Predictive calculations show that the conditionally neutral component in the contamination halo in this case will reach the LNPP-2 drainage system. This requires approximately 65 years, which is longer than the design working life of the NPP (60 years).

As can be seen in the sections (Fig.7), the structure of the groundwater flow is largely controlled by the presence of paleovalleys, which perform the function of "lithological windows" providing a connection between the aquifers. Radionuclides present in the Quaternary aquifer migrate through one of these "windows" deep into the water-bearing strata, so the Lomonosov aquifer becomes the main transporter of radioactive contamination (section E-F in Fig.7, *c*). Naturally, this effect increases the migration time of the components due to the growing migration path length.

Dissolved ^{90}Sr and ^{137}Cs, in contrast to an inert tracer, are sorbed and retained by soils. If the calculations take into account the sorption delay factor, which was determined from the monitoring data at the FGUP "FOE" site and amounted to R = 1.58-1.66, then it can be stated with confidence that these radionuclides should move one and a half times slower, i.e., for ^{90}Sr and ^{137}Cs, the characteristic residence time in the aquifers will be about 100 years.

Conclusion. To ensure the safe construction and operation of the NPP, it is necessary to assess the impact on the environment. An analysis of radionuclide composition of groundwater and their possible migration routes within the territory of operating and projected NF in the IA under changing hydrodynamic conditions was carried out.

Detailed radiochemical studies of groundwater composition within the existing sites of various NF and between these sites showed the absence of significant radioactive contamination of groundwater. The contents of controlled radionuclides (tritium, ^{90}Sr, ^{137}Cs) are at the level of background activities (with the exception of tritium) or exceed these values no more than 2-3-fold, which is insignificant from the viewpoint of the current quality standards (NRB-99/2009). An exception is the site of groundwater contamination associated with leakages of radioactive solutions from the RW storage facilities of the FGUP "FEO" (1970-1990). Also, the analysis of monitoring data on this site made it possible to estimate the approximate rates of tritium migration with groundwater flow under natural conditions (u = 1.4-2.3 m/year) and the parameters of sorption retention of fission products (R = 1.58-1.66).

To predict a possible impact of the forming contamination halo on the quality of groundwater withdrawn by the drainage system of the projected LNPP-2, a hydrogeological model of the industrial area was developed. Its validation required a generalization of the entire volume of engineering surveys at the facility for more than 50 years. The database underlying the model includes more than 1,500 geological columns of wells, dozens of experimental filtration tests of wells as well as long observation series of the radiation state of groundwater. The constructed model allowed a detailed analysis of the impact of the new facility (LNPP-2) on changes in the hydrogeological environment of the area. Evidence on the decisive role of rock lithology variability in the character of hydrodynamic association of aquifers in local areas has been obtained, which required the involvement of groundwater radiation monitoring data, which is a new element in the development of notions about the hydrogeological conditions of the study area.

Modelling results showed that the depression funnel forming during the operation of the LNPP-2 drainage system reaches the southern boundary of the FGUP "FEO" RW storage site, where a technogenic halo of groundwater contamination is recorded. Thus, the migration direction of dissolved radionuclides changes, which is confirmed by the deformation in the structure of the network of groundwater flow constructed according to the modelling results.

Predictive calculations within the concept of convective transport (taking into account the experimentally determined sorption delay factor) showed that the existing radioactive halo represented by relatively long-lived isotopes of strontium and cesium (^{90}Sr and ^{137}Cs) will migrate towards the LNPP-2 for about 100 years before the radioactively contaminated water becomes a part of water of the power plant drainage system. The risk of radionuclides release into the biosphere over the planned 60-year period of the NPP operation is insignificant.

REFERENCES

1. Groundwater contamination (tritium) at nuclear plants. Report Associated with Events. URL: https://www.nrc.gov/reactors/operating/ops-experience/grndwtr-contam-tritium.html (accessed 20.12.2021).

2. Implementation of new nuclear power plant units, at the Paks site. URL: https://www.paks2.hu/documents/20124/60835/Chapter+1-8.pdf/24ebe701-777f-d79d-47d9-12cf2994a3d0 (accessed 20.12.2021).

3. Jakimavičiūtė-Maselienė V., Cidzikienė V. Modelling of tritium transport in the underground water from hypothetical reactor at the new NPP site in Lithuania. *Progress in Nuclear Energy*. 2015. Vol. 80, p. 1-6. DOI: 10.1016/j.pnucene.2014.11.018

4. Creation of a system for industrial environmental monitoring in hydrocarbon producing and transporting companies of Western Siberia. *Journal of Mining Institute*. 2016. Vol. 221, p. 737-741. DOI: 10.18454/PMI.2016.5.737

5. Golovina E.I., Grebneva A.V. Some Aspects of Groundwater Resources Management in Transboundary Areas. *Journal of Ecological Engineering*. 2021. Vol. 22. N 4, p. 106-118. DOI: 10.12911/22998993/134037

6. Nureev R.R., Pashkevich M.A., Isakov A.E. Assessment of the technogenic impact of the korkinsky coal mine. Proceedings Of the International Forum-Contest of Young Researchers, 18-20 April 2018, St. Petersburg, Russia. Topical Issues of Rational Use of Natural Resources, 2019, p. 371-377.

7. Erzova V.A., Rumynin V.G., Sudarikov S.M. et al. Influence of North-West Nuclear Complex Facilities on Groundwater Contamination (Leningrad Region). *Bulletin of the Tomsk Polytechnic University. Geo Assets Engineering*. Vol. 322. N 9, p. 30-42 (in Russian). DOI: 10.18799/24131830/2021/9/3351

8. Kryshev I.I., Pahomov A.Y., Brykin S.N. et al. Assessment and Prognosis of Radioecological Impact of the Radioactive Wastes Storage Sites of the "North-West Territorial District" Leningrad Branch of Fgup "Rosrao". *Izvestiya vuzov. Yadernaya Energetika*. 2012. N 3, p. 44-52 (in Russian).

9. Rumynin V.G., Vladimirov K.V., Nikulenkov A.M. et al. The status and trends in radioactive contamination of groundwater at a LLW-ILW storage facility site near Sosnovy Bor (Leningrad region, Russia). *Journal of Environmental Radioactivity*. 2021. Vol. 237. N 106707. DOI: 10.1016/j.jenvrad.2021.106707

10. Novovoronezh NPP: experience of using object monitoring data on subsoil condition and mathematical modelling for assessing the impact on ground and surface water. Atomic Energy. URL: http://www.atomic-energy.ru/articles/2014/09/29/51806 (accessed 20.12.2021).

11. Moench A.F. Flow to a well of finite diameter in a homogeneous, anisotropic water table aquifer. *Water Resources Research*. 1997. Vol. 33. Iss. 6, p. 1397-1407. DOI: 10.1029/97WR00651

12. Neuman S.P. Analysis of pumping test data from anisotropic unconfined aquifers considering delayed gravity response. *Water Resources Research*. 1975. Vol. 11. Iss. 2, p. 329-345. DOI: 10.1029/WR011I002P00329

13. Hantush M.S. Flow to wells in aquifers separated by a semipervious layer. *Journal of Geophysical Research*. 1967. Vol. 72. Iss. 6, p. 1709-1720. DOI: 10.1029/JZ072i006p01709

14. Javandel I., Witherspoon P.A. Analytical solution of a partially penetrating well in a two-layer aquifer. *Water Resources Research*. 1983. Vol. 19. Iss. 2, p. 567-578. DOI: 10.1029/WR019I002P00567

15. Cooper H.H., Bredehoeft J.D., Papadopulos I.S. Response of a finite diameter well to an instantaneous charge of water. *Water Resources Research*. 1967. Vol. 3. Iss. 1, p. 263-269. DOI: 10.1029/WR003i001p00263

16. ANSDIMAT – software for analytical modelling of groundwater wells. URL: http://ansdimat.com/ru/ (accessed 20.12.2021).

17. Das B.S., Kluitenberg G.J. Moment analysis to estimate degradation rate constants from leaching experiments. *Soil Science Society of America Journal*. 1996. Vol. 60. Iss. 6, p. 1724-1731. DOI: 10.2136/SSSAJ1996.03615995006000060017X

18. Espinoza C., Valocchi A.J. Temporal moments analysis of transport in chemically heterogeneous porous media. *Journal of Hydrologic Engineering*. 1998. Vol. 3. Iss. 4, p. 276-284. DOI: 10.1061/(ASCE)1084-0699(1998)3:4(276)

19. Goltz M., Huang J. Analytical Modeling of Solute Transport in Groundwater. New Jersey: John Wiley & Sons, 2017, p. 272. DOI: 10.1002/9781119300281

20. Goltz M.N., Roberts P.V. Using the method of moments to analyze three-dimensional diffusion-limited solute transport from temporal and spatial perspectives. *Water Resources Research*. 1987. Vol. 23. Iss. 8, p. 1575-1585. DOI: 10.1029/WR023i008p01575

21. Valocchi A.J. Validity of the local equilibrium assumption for modeling sorbing solute transport through homogenous soils. *Water Resources Research*. 1985. Vol. 21. Iss. 6, p. 808-820. DOI: 10.1029/WR021I006P00808

22. Young D.F., Ball W.P. Column experimental design requirements for estimating model parameters from temporal moments under nonequilibrium conditions. *Advanced Water Resources*. 2000. Vol. 23. Iss. 5, p. 449-460. DOI: 10.1016/S0309-1708(99)00047-0

23. Yu C., Warrick A.W., Conklin M.H. A moment method for analyzing breakthrough curves of step inputs. *Water Resources Research*. 1999. Vol. 35. Iss. 11, p. 3567-3572. DOI: 10.1029/2000WR900322

24. Pang L., Goltz M., Close M. Application of the method of temporal moments to interpret solute transport with sorption and degradation. *Journal of Contaminant Hydrology*. 2003. Vol. 60. Iss. 1-2, p. 123-134. DOI: 10.1016/S0169-7722(02)00061-X

25. Fioreze M., Mancuso M.A. MODFLOW and MODPATH for hydrodynamic simulation of porous media in horizontal subsurface flow constructed wetlands: A tool for design criteria. *Ecological Engineering*. 2019. Vol. 130, p. 45-52. DOI: 10.1016/j.ecoleng.2019.01.012

26. Antonov V.V., Ustyugov D.L. Problems of creating live simulation mathematical models of large regions. *Journal of Mining Institute*. 2003. Vol. 153, p. 115-116 (in Russian).

27. Harbaugh A.W. MODFLOW-2005, the U.S. Geological Survey modular ground-water model – the Ground-Water Flow Process. *Techniques and Methods*. 2005, p. 253. DOI: 10.3133/tm6A16

28. Hughes J.D., Russcher M.J., Langevin Ch.D. et al. The MODFLOW Application Programming Interface for simulation control and software interoperability. *Environmental Modelling & Software*. 2022. Vol. 148. N 105257. DOI: 10.1016/j.envsoft.2021.105257

29. Pollock D.W. User guide for MODPATH version 7 – A particle-tracking model for MODFLOW. Open-File Report: U.S. Geological Survey. 2016, p. 35. DOI: 10.3133/ofr20161086

30. Pietrzak D. Modeling migration of organic pollutants in groundwater – Review of available software. *Environmental Modelling & Software*. 2021. Vol. 144. N 105145. DOI: 10.1016/j.envsoft.2021.105145

31. Li L., Boucher A., Caers J. SGEMS-UQ: An uncertainty quantification toolkit for SGEMS. *Computers & Geosciences*. 2014. Vol. 62, p. 12-24. DOI: 10.1016/j.cageo.2013.09.009

32. Remy N., Boucher A., Wu J. Applied Geostatistics with SGeMS: A User's Guide. Cambridge: Cambridge University Press, 2009, p. 98. DOI: 10.1017/CBO9781139150019

33. Dashko R.E., Lebedeva Y.A. Improving approaches to estimating hydrogeological investigations as a part of engineering survey in megacities: case study of St. Petersburg. *Water Resources*. 2017. Vol. 44. Iss. 7, p. 875-885. DOI: 10.1134/S009780781707003X

34. Protosenya A.G., Lebedev M.O., Karasev M.A., Belyakov N.A. Geomechanics of low-subsidence construction during the development of underground space in large cities and megalopolises. *Journal of Mechanical and Production Engineering Research and Development*. 2019. Vol. 9. Iss. 5, p. 1005-1014. DOI: 10.24247/ijmperdoct201989

35. Dashko R.E., Lokhmatikov G.A. Upper Kotlin clays of Saint Petersburg region as the base and environment of unique structures: engineering geological and geotechnical analysis. *Journal of Mining Institute*. 2022, p. 1-11. (Online first) DOI: 10.31897/PMI.2022.13

36. Rumynin V.G., Pankina E.B., Yakushev M.F. et al. Assessment of nuclear industry complex impact on groundwater and adjacent natural objects (Sosnovy Bor town, Leningrad Region). St. Petersburg: izd-vo Sankt-Peterburgskogo universiteta, 2003, p. 248 (in Russian).

37. EGASMRO. URL: http://egasmro.ru/ru/data (accessed 20.12.2021).

***Authors*: Valentina A. Erzova,** *Postgraduate Student, Junior Researcher, Erzova.spmu@yandex.ru, https://orcid.org/0000-0001-7415-7148 (Saint Petersburg Mining University, Saint Petersburg, Russia; Institute of Geoecology named after E.M.Sergeev, RAS, Saint Petersburg Branch, Saint Petersburg, Russia),* **Vyacheslav G. Rumynin,** *Doctor of Geological and Mineralogical Sciences, Corresponding Member of the RAS; Director, Professor, https://orcid.org/0000-0002-3928-0228 (Institute of Geoecology named after E.M.Sergeev, RAS, Saint Petersburg Branch, Saint Petersburg, Russia; Saint Petersburg State University, Institute of Earth Sciences, Saint Petersburg, Russia),* **Anton M. Nikulenkov,** *Candidate of Geological and Mineralogical Sciences, Leading Researcher, Head of Laboratory, https://orcid.org/0000-0001-5498-076X (Institute of Geoecology named after E.M.Sergeev, RAS, Saint Petersburg Branch, Saint Petersburg, Russia; Saint Petersburg State University, Institute of Earth Sciences, Saint Petersburg, Russia),* **Konstantin V. Vladimirov,** *Junior Researcher, https://orcid.org/0000-0002-9325-8953 (Institute of Geoecology named after E.M.Sergeev, RAS, Saint Petersburg Branch, Saint Petersburg, Russia),* **Sergei M. Sudarikov,** *Doctor of Geological and Mineralogical Sciences, Professor, https://orcid.org/0000-0002-3692-5692 (Saint Petersburg Mining University, Saint Petersburg, Russia),* **Mariia V. Vilkina,** *Junior Researcher, https://orcid.org/0000-0003-3687-7069 (Institute of Geoecology named after E.M.Sergeev, RAS, Saint Petersburg Branch, Saint Petersburg, Russia).*

The authors declare no conflict of interests.

ISSN 2411-3336; e-ISSN 2541-9404

JOURNAL OF MINING INSTITUTE
Zapiski Gornogo instituta
Journal homepage: pmi.spmi.ru

Research article

Geochemical properties and transformation of the microelement composition of soils during the development of primary diamond deposits in Yakutia

Yana B. LEGOSTAEVA[1], **Anna G. GOLOLOBOVA**[1] ✉, **Vladimir F. POPOV**[2], **Victor S. MAKAROV**[3]
[1] *Diamond and Precious Metal Geology Institute, Siberian Branch, RAS, Yakutsk, Russia*
[2] *M.K.Ammosov North-Eastern Federal University, Yakutsk, Russia*
[3] *Institute of Applied Ecology of the North, M.K.Ammosov North-Eastern Federal University, Yakutsk, Russia*

How to cite this article: Legostaeva Ya.B., Gololobova A.G., Popov V.F., Makarov V.S. Geochemical properties and transformation of the microelement composition of soils during the development of primary diamond deposits in Yakutia. Journal of Mining Institute. 2023. Vol. 260, p. 212-225. DOI: 10.31897/PMI.2023.35

Abstract. Extraction of diamonds from primary deposits in Siberia is associated with the development of kimberlite pipes in challenging environmental conditions, accompanied by a complex impact on the environment. The article presents the results of monitoring the soil cover of the Nakyn kimberlite field in the Yakutia diamond province, which is affected by the facilities of the Nyurba Mining and Processing Division. Development of primary diamond deposits has a large-scale impact on the subsoil, topography, and soil cover: creation of the world's largest quarries, formation of dumps more than 100 m high, arrangement of extensive tailings, formation of solid and liquid industrial wastes of various chemical composition. The research is aimed at studying the spatial and temporal patterns of the technogenic impact on the soil cover, identifying the nature and level of transformation of the microelement composition of soils based on the analysis of the intra-profile and lateral distribution of mobile forms of trace elements. The study targets in 2007-2018 were zonal types of permafrost soils of northern taiga landscapes, cryozems, occupying 84 % of the total study area, which are characterized by biogenic accumulation of mobile forms of Ni, Mn, and Cd in the upper AO, A_{cr} horizons, and Cr, Ni, Co, Mn, Cu in the suprapermafrost CR horizon. We found out that the contamination of the soil cover of the industrial site at the Nyurba Mining and Processing Division is of a multielement nature with local highly to very highly contaminated areas. Over a ten-year observation period, areas of stable soil contamination are formed, where the main pollutants are mobile forms of Mn, Zn, Ni. We suggest that against the background of a natural geochemical anomaly associated with trap and kimberlite magmatism, technogenic anomalies are formed in the surface horizons of soils. They are spatially linked to technogenically transformed landscapes. One of the sources of pollutants is the dispersion of the solid phase of dust emissions in the direction of the prevailing winds, which leads to the formation of soils with abnormally high contents of mobile forms of Mn, Zn, Ni.

Keywords: soil contamination; cryozems; trace elements; mobile forms; Yakutia diamond province; kimberlite field

Acknowledgments. Field research, chemical analysis, and mapping were carried out under the project FSRG-2020-0018 “Study of the features of the functioning of the Arctic and subarctic ecosystems of Yakutia in the context of increased technogenic impact and global climate change”. Generalization and interpretation of the material were carried out under the project FUEM-2019-0003 “Geochemical environmental study of technogenic massifs in the Yakutia diamond province”.

Received: 07.04.2022 ***Accepted: 02.03.2023*** ***Online: 10.04.2023*** ***Published: 25.04.2023***

Introduction. Mining enterprises around the world are sources of environmental contamination with heavy metals and trace elements in toxic concentrations at almost all stages of their activities [1, 2], including excavation, drilling, quarrying, and transportation of raw materials, as well as grinding and beneficiation of ores before disposal into tailings. All these operations make a significant contribution to environmental contamination, which is noted in all regions with mining activities – Russia [3], Great Britain [4], Canada [5], Africa [6], China [7], USA [8], and others. Numerous works are devoted to the issues of soil cover contamination, which consider the geochemical specificity of ore occurrence in the areas, soil formation, genesis, formation of technogenic anomalies, spatial and intra-profile distribution of contamination, sorption of pollutants of various genesis, etc. [9, 10]. As a rule, these studies are carried out on the example of regional targets, which sometimes provide an independent view of environmental problems and allow assessing the overall geoenvironmental situation. In addition, regional work is aimed at identifying patterns, for example, for the conditions of the entire Arctic region, and further forecasting that can be interpolated for mining regions, regardless of the nature of the deposit and the method of its development.

Development of mineral deposits is inevitably accompanied by an uncontrolled influx into the soil layer of a considerable number of chemical elements and their compounds brought to the day surface from the Earth’s interior. According to the estimations of scientists from the Institute of Mining, Ural Branch of the Russian Academy of Sciences, more than 100 billion tons of ore, minerals, and building materials are annually extracted from the Earth's interior [11]. As a result, technogenic pressure is exerted both on vast areas and on individual components of the ecosystem during both the exploration and development of deposits, and after the development in the form of dumps, sludge storages and tailings, solid and liquid wastes of various chemical composition [12-14]. Various substances migrating in natural landscapes enter the environment from technogenically conditioned formations [15-17].

The intensity of the long-term technogenic impact and the spatial pattern of the distribution of pollutants in the areas of mining is determined by the chemical composition and geochemical properties of soils, which are a relatively conservative component of the ecosystem [18]. The specificity of any geosystems, including mining regions, is manifested in the fact that the soil cover, as the main depositing natural environment, to the greatest extent reflects the scale and nature of environmental changes in the technogenic period [19-21].

In recent years, quite a lot of research papers have appeared on soil contamination with heavy metals [22-24], including accumulation [25, 26], spatial [27], and intra-profile distribution [28-30]. Soils, being the basic component of the ecosystem, simultaneously play the role of a potential source of secondary contamination for the components of the landscape itself and adjacent areas [31-33]. The most active contamination agents are mobile forms of trace elements that can pass from solid phases into soil solutions and be absorbed by plants [34, 35].

One of the tasks of genetic soil science is to interpret the information recorded in soils, use it to reconstruct the natural conditions of the past, and develop scenarios for future changes in soils and landscapes [36, 37]. Soils reflect natural geochemical anomalies as a result of ore occurrence. At the same time, technogenic geochemical anomalies are formed in soils, which determine technogenic contamination, where pollutant concentrations often reach levels dangerous for living organisms [18]. This study will reveal the nature and level of transformation of the trace element composition of soils based on the analysis of the intra-profile and lateral distribution of mobile forms of trace elements in the permafrost soils of the Nakyn kimberlite field and the industrial site of the Nyurba Mining and Processing Division (NMPD).

Targets and methods of research. The study area is within the Vilyuisko-Markhinskaya denudation plain, located on the border of the Central Siberian plateau and the Central Yakutian lowland of Central Siberia (Russia) with absolute watershed marks from 213 to 269 m [38]. The topography is slightly dissected with relative elevations above the nearest streams from 15 to 35 m.

The study was carried out in the Nakyn kimberlite field within the industrial site of the Nyurba Mining and Processing Division (065°01′31″ N, 117°04′53″ E), which is in the north taiga landscape zone of Western Yakutia (Fig.1).

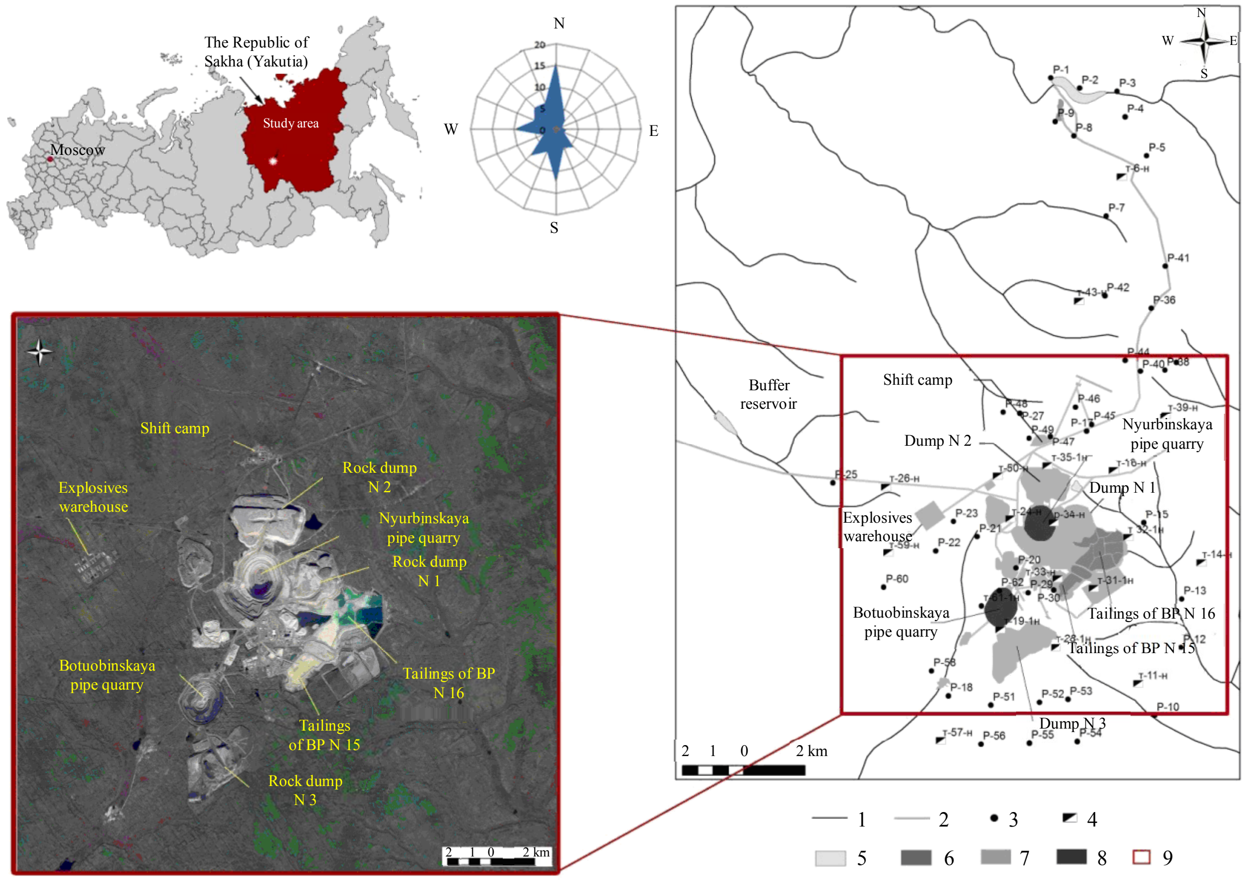

Fig. 1. Study area with observation points

1 – rivers; 2 – roads; 3 – sampling points at a depth of 0-20 cm; 4 – points of sampling soil profiles; 5 – anthropogenically transformed areas; 6 – waste rock dumps; 7 – hydraulic structures, tailings; 8 – kimberlite pipe quarries; 9 – outline of the conditional boundaries of the industrial site

On the Khannya-Nakyn interfluve, comprehensive environmental efforts, including geochemical environmental studies of the soil cover, with the participation of the authors, were carried out since the discovery of the Nakyn kimberlite field in 1994-1995. Since 2007, a network of observation points with a step of 2×2 km was laid on the industrial site of the Nyurba MPD of AK ALROSA (PAO). With a frequency of three to four years, within the framework of production monitoring, surveys of the soil cover and selection were carried out using a single sampling grid. Sampling was carried out in the warm period of time (July-August) by two methods: digging to a depth of 0-20 cm and making soil sections in different biotopes with horizon sampling to the entire depth of seasonal thawing (Table 1). In total, 436 soil samples were taken and analysed.

Table 1

Volumes of soil and soil sampling by years of investigations

Year of investigations	Study target	Number of observation points	Number of samples
2007	Surface layer from a depth of 0-20 cm	50	50
2008	Soil sections	13	34
2011	Monitoring points – from the surface to depths of 0-10 and 10-20 cm	86	172
2014	Monitoring points – from the surface to depths of 0-10 and 10-20 cm	62	124
2018	Soil sections	19	56
Total samples			436

All obtained samples were dried at room temperature and sifted through a sieve < 1.0 mm. Next, the soil samples were ground in a mortar by a pestle until all the particles passed through a sieve with a mesh size of 0.25 mm. Then 10 (±0.1) g of soil material was ground in a mortar to a powder state (GOST ISO 11464-2015).

The pH values of water extracts of soils were determined in the system soil: water suspension (1:2.5) at room temperature by potentiometry on a pH meter (Mettler Toledo, Seven Compact Advanced) according to GOST-26483-85. Soil organic matter (humus) was determined by photoelectric colorimetry on KFK-2 UHL 4.2 according to GOST-26213-91; total nitrogen by spectrophotometry on PE-5300VI according to GOST-26107-84; the content of physical clay by the Kachinsky method (pipette method); the content of mobile forms of elements (Pb, Ni, Mn, Cd, Co, Cr, Zn, Cu, As) on an MGA-915 atomic absorption spectrometer (Lumex Group of Companies, St. Petersburg, Russia) after acid extraction with 1 N HNO_3 (soil and extractant ratio 1:10) according to the M 03-07-2014 procedure. The extractant 1 N HNO_3 extracts the most mobile, acid-soluble, forms of elements that are more strongly bound to the soil, in contrast to H_2O and 1 N HCl [39, 40].

To control the accuracy of measuring the concentration of elements in soils, state standard samples (SSO) of the composition of soils of the following series were used: soddy-podzolic sandy loamy soil (SDPS-1, 2, 3); carbonate serozem (SSK-1, 2, 3) [41].

Analysis of the total multielement load on the soil cover in the Nakyn kimberlite field of the Yakutsk diamond province included the estimation of the following geochemical environmental indicators:

- concentration index

$$\text{K}_c = \frac{C_i}{C_f}, \tag{1}$$

where C_i is the actual content of the pollutant in the soil, mg/kg; C_f is the background content of the pollutant in the soil, mg/kg;

- total contamination index [42]

$$Z_c = \sum_{i=1}^{n} \text{K}_c - (n-1), \tag{2}$$

where K_c is the concentration index of the i-th chemical element; n is the number of chemical elements with $\text{K}_c > 1.5$.

Elements with extremely low background content are not considered.

According to the guidelines for assessing the degree of danger of soil contamination with chemicals “MU 4266-87”, there are four categories of danger of chemical contamination of soils according to the values of the total contamination index Z_c: permissible ($Z_c < 16$); moderately dangerous ($16 < Z_c < 32$); dangerous ($32 < Z_c < 128$); extremely dangerous ($Z_c > 128$).

The values of the regional background were calculated from the geometric mean content of mobile forms of trace elements in a series of 212 soil samples, which included samples of surface soil horizons from natural undisturbed landscapes of the Khannya-Nakyn interfluve outside the impact zone of mining and beneficiation facilities [43, 44].

The obtained quantitative data were processed using Microsoft Excel 2016, OriginPro 8.5.1 software. Statistical analysis was performed using Statistica 13.0. Maps of total soil cover contamination were compiled using the ArcGIS 9.0 software.

Results and discussion. The Nakyn kimberlite field incorporates several highly diamondiferous kimberlite bodies, including the Botuobinskaya (discovered in 1994), Nyurbinskaya (1996) pipes, the Markhinskaya (1999), Mayskaya (2006) dykes, and the Botuobinskoye and Nyurbinskoye placers. At present, two kimberlite pipes, Nyurbinskaya and Botuobinskaya, are being mined open pit by the NMPD. The infrastructure includes two beneficiation plants (BP), N 15 and N 16, a geological factory N 17, a shift camp for more than 1000 people, a warehouse for explosive materials, runways. Surface technogenic storages of mining products, dumps of waste rocks, and that of beneficiation, tailings, are developed.

Permafrost soils are attributed to the trunk of primary, postlithogenic, organogenic, and synlithogenic soil formation and represent different subtypes of cryogenic soils. The structure of the soil cover of the Nyurba Mining and Processing Division industrial site, as well as the entire area of the Khannya-Nakyn interfluve, is dominated by cryozems, 84 % of the total area, which are characterized by a thin, weakly differentiated soil profile with pronounced cryoturbation, leading to disruption of the integrity of genetic horizons and mixing of soil material [44]. Table 2 shows the main physical and chemical properties of cryozems on the example of three soil sections, the most common cryozem types in the area.

Table 2

Main physical and chemical properties of the dominant types of cryozems in the Nakyn kimberlite field

Horizon index	Boundaries of horizons, sampling depth, cm	Soil type	pH_{aq}	Humus, %	C_{org}, %	Total nitrogen, %	C:N	Physical clay (<0.01 mm), %
AO	0-6(14)	Homogeneous suprapermafrost-gleyic cryozem	5.0±0.3	6.8±0.3	3.94±0.19	0.20±0.01	19.7	23.2±1.2
A_{cr}	6(14)-43(50)		6.2±0.3	1.4±0.07	0.81±0.04	0.156±0.008	5.08	26.1±1.3
CR_g	43(50)-80(83)		7.0±0.4	1.9±0.1	1.10±0.06	0.125±0.006	8.48	28.2±1.4
$C_g\perp$	80(83)-∞		7.0±0.4	0.9±0.05	0.52±0.03	0.125±0.006	4.02	11.0±0.6
AO	0-5(10)	Homogeneous humus-gley cryozem	5.1±0.3	8.8±0.4	5.10±0.26	0.156±0.008	31.9	30.0±1.5
CR_g	5(10)-35(45)		6.4±0.3	1.4±0.07	0.81±0.04	0.156±0.008	5.08	31.6±1.6
$C\underline{\downarrow}$	35(45)-∞		7.2±0.4	2.1±0.1	1.22±0.06	0.168±0.008	7.17	30.1±1.5
AK	0-40(42)	Gleyic podzolized cryozem	5.3±0.3	0.8 ±0.04	0.46±0.02	0.156±0.008	2.90	13.5±0.7
ELB	40(42)-61(72)		6.7±0.3	0.6±0.03	0.35±0.02	0.156±0.008	2.18	13.4±0.7
$C_g\perp$	61(72)-∞		7.0±0.4	1.9±0.10	1.10±0.06	0.168±0.008	6.48	20.5±1.0

Note: AO – coarse humus horizon; A_{cr} – accumulative-humus cryoturbated horizon; CR_g – cryoturbated horizon with signs of gleying; $C_g\perp$ – soil-forming rock with the presence of icy permafrost; $C\underline{\downarrow}$ – soil-forming rock with the presence of dry permafrost; AK – cryohumus horizon; ELB – eluvial podzolized horizon [45].

The soil cover has a predominantly acid reaction of the soil medium in the upper organogenic horizons and changes towards alkalinity down the profile. High values of humus determine the presence of moderately and weakly decomposed organic residues in soils, which is typical for soils in the northern regions. The estimation of the carbon to nitrogen ratio indicates a weak decomposition of plant residues. In the soil profile, cryozems have a sharply decreasing, bimodal, and increasing character of distribution. The presence of a significant amount of organic matter in the lower horizons is associated with permafrost destruction, i.e., mixing and its tongues along permafrost cracks.

The soil profile of cryozems has a two-member structure in terms of granulometric composition with a sharp decrease in the physical clay content down the soil profile due to an increase in the content of fractions with a diameter of 0.25-0.05 mm to 70 % in suprapermafrost-gleyic and humus-gley cryozems. In podzolized subtypes, on the contrary, their content decreases to 56 % [46].

The content of mobile forms of heavy metals in cryozems does not differ significantly by types (Table 3). In general, cryozems are distinguished by the presence of two maxima in the intra-profile distribution of mobile forms of trace elements: biogenic accumulation in the upper soil layer, followed by a decrease down the profile and the second peak in the suprapermafrost horizon. Biogenic accumulation in cryozems, as a rule, is characteristic of mobile forms of Mn, Zn, Co, Ni, Cd, As. Single cases of accumulation of mobile forms of Cu in the upper organogenic horizons are noted. Cryozems of natural landscapes in the study area outside the impact zone of mining operations are characterized by biogenic accumulation of Ni, Mn and Cd and suprapermafrost accumulation of Cr, Ni, Co, Mn, Cu. Moreover, the content of trace elements in the suprapermafrost horizons is higher than in the upper organogenic ones.

Table 3

Average content of mobile forms of trace elements in the dominant types of cryozems of the Nakyn kimberlite field

Horizon index	Mobile forms of trace elements, mg/kg								
	Pb	Ni	Mn	Cd	Co	Cr	Zn	Cu	As
Background, *n* = 212	2.88	1.77	13.19	0.03	2.14	4.70	6.31	11.5	0.22
	Homogeneous suprapermafrost-gleyic cryozem, *n* = 16								
AO	3.8±0.9 0.4-1.5	**2.6**±0.6 5.2-5.6	**22.9**±5.5 7.2-215.1	0.023±0.006 0.015-0.245	1.5±0.4 0.9-2.6	2.2±0.5 0.9-4.9	4.5±1.1 1.0-32.6	4.8±0.02 1.2-6.1	0.2±0.1 0.02-0.33
A$_{cr}$	2.1±0.5 0.5-1.8	**5.3**±1.2 1.1-6.9	**41.8**±10.0 16.5-490.1	0.011±0.003 0.003-0.064	2.4±0.6 0.9-3.6	2.6±0.6 0.8-5.1	6.8±1.6 3.2-13.5	6.7±1.6 1.5-17.7	<0.05
CR$_g$	2.3±0.5 0.4-1.3	**5.0**±1.2 0.8-7.2	**46.5**±11.2 13.9-138.6	0.014±0.003 0.001-0.023	2.5±0.6 0.4-6.2	2.5±0.6 1.2-5.2	**7.5**±1.8 3.8-13.4	8.1±1.9 0.7-30.0	0.1±0.02 0.03-0.12
C$_g$⊥	1.4±0.3 0.2-0.6	**3.8**±0.9 2.1-6.2	**43.8**±10.5 23.5-69.2	0.016±0.004 0.013-0.039	2.2± 0.5 1.4-3.9	3.3±0.8 1.3-9.3	6.2±1.5	3.9±0.9 2.5-7.9	<0.05
	Homogeneous humus-gley cryozem, *n* = 11								
AO	**4.2**±1.01 1.4-12.7	**4.5**±1.0 2.0-12.7	**55.8**±13.4 45.1-108.7	0.022±0.005 0.017-0.124	2.3± 0.5 1.3-9.8	2.3±0.5 1.1-47.0	3.7±0.9 1.1-37.9	7.7±1.9 5.4-11.1	0.2±0.1 0.07-0.23
CRg	2.8±0.7 0.9-2.2	**4.2**±1.0 1.5-5.9	**38.9**±9.3 57.9-102.7	0.008±0.002 0.003-0.035	1.9±0.5 1.2-2.4	2.2±0.5 1.7-8.2	6.3±1.5 2.4-14.9	7.9±1.9 3.6-10.7	<0.05
C$\underline{\downarrow}$	2.9±0.7 0.5-2.1	**5.1**±1.2 2.9-6.9	**39.4**±9.05 68.8-124.5	0.015±0.004 0.011-0.052	2.3±0.5 1.9-3.5	2.1±0.5 1.3-11.3	6.9±1.6 1.7-15.1	10.4±2.5 4.9-18.7	<0.05
	Gleyic podzolized cryozem, *n* = 5								
A	2.6±0.6 0.1-1.1	1.5±0.4 0.6-28.5	15.2±3.4 6.3-186.5	0.006±0.001 0.001-0.126	1.5±0.4 0.6-7.4	1.7±0.4 0.9-3.7	4.5±1.1 3.5-46.1	2.1± 0.5 0.7-5.3	<0.05
ELB	2.2± 0.5 0.4-2.1	**3.4**±0.8 1.1-7.8	**27.4**±6.6 9.2-97.7	0.008±0.002 0.004-0.153	2.2±0.5 0.4-9.7	2.1±0.5 1.2-3.8	5.1±1.2 2.7-15.1	2.8±0.7 0.6-3.5	<0.05
C$_g$⊥	2.2±0.5 0.4-1.2	**4.7**±1.1 0.9-3.9	**39.6**±9.5 19.5-87.5	0.019±0.005 0.006-0.193	2.5±0.6 0.6-7.3	1.8±0.4 1.3-5.9	7.1±1.7 3.1-11.9	4.7±1.1 0.5-10.4	<0.05

Notes: 1. Geometric mean values *m*±*s* are above the line, min-max are below the line; values in bold are above background levels. 2. *n* is the number of similar soil sections.

A different degree of correlation of mobile forms of heavy metals with humus content, pH values, and granulometric composition was revealed, which characterizes the selectivity of the combination of an element (or a group of elements) with the main soil components (Table 4). A significant positive correlation of As and Pb with the organic matter content, and Cu and Ni with the physical clay content was observed. A weak correlation was noted for Ni and Zn with pH, Mn and Cd with organic matter, Mn, Cd, and Pb with physical clay. It was found out in [44] that the fractions of fine dust and silt in cryozems bind the greatest number of elements: Zn, Ni, Cr, Cu, Pb, and As.

A consistent analysis of the content of mobile forms of trace elements in cryozems throughout the Nakyn kimberlite field showed patterns of intra-profile distribution: in the upper part of the soil profile, associated with biogenic accumulation, and in the lower part of the soil profile, a consequence of the influence of both underlying rocks and cryogenic processes with tongues along frost cracks. Due to the close occurrence of permafrost, a kind of suprapermafrost geochemical barrier is formed, where the main accumulation of trace elements occurs.

Table 4

Correlative matrix of the dependence of the content of trace elements on some physical and chemical parameters in the cryozems of the Nakyn kimberlite field (*n* = 436)

	pH	C_{org}	PC	Mn	Cu	Zn	Cd	Co	Cr	Ni	As	Pb
pH	1											
C_{org}	–0.37	1										
PC	0.35	0.45	1									
Mn	–0.01	0.42	0.35	1								
Cu	0.33	0.20	0.69*	0.23	1							
Zn	0.37	–0.23	0.17	–0.26	0.51*	1						
Cd	0.25	0.40	0.40	0.03	0.54*	0.38	1					
Co	0.14	–0.05	0.12	0.15	0.52*	0.81*	0.31	1				
Cr	0.02	–0.04	–0.08	0.30	–0.24	–0.07	–0.32	0.04	1			
Ni	0.46	–0.02	0.5*	–0.09	0.74*	0.88*	0.63*	0.72*	–0.17	1		
As	–0.33	0.84*	0.32	0.20	0.23	–0.20	0.46	–0.07	–0.06	0.01	1	
Pb	–0.34	0.72*	0.41	0.26	–0.13	–0.37	–0.04	–0.33	0.22	–0.31	0.57*	1

Notes: Correlation index values: to 0.2 – very weak correlation; to 0.5 – weak; to 0.7 – medium; to 0.9 – high; over 0.9 – very high (Nasledov A. IBM SPSS Statistics 20 and AMOS: professional statistical data analysis. St. Petersburg: Piter, 2013. 416 p.); PC – physical clay; * – statistical significance at $P < 0.01$.

At the present stage of research, the geochemical environmental situation is due to the combined influence of large-scale epigenetic processes of the tectonic-magmatic structure of the Nakyn kimberlite field and technogenic impact on ecosystem components, primarily on the soil cover. It was previously found out [47] that the decisive role in the formation of natural geochemical anomalies in the soil cover at the regional level is played by the weathering products of the rocks of the trap formation in the Khannya-Nakyn interfluve, kimberlites with the accumulation of Cr, Co, Ni and dolerites with the accumulation of Mn Li, Be, Sn. Natural geochemical anomalies in the soil cover are well identified from the materials of secondary scattering fluxes.

The regional geochemical soil anomaly corresponds to the structure of the kimberlite ore field, correlates quite clearly with the position of the endogenous anomaly at the level of the Early Paleozoic carbonate-terrigenous rocks, and is probably a telescoped geochemical reflection through the Early Jurassic sediments at the level of the modern erosional truncation [47]. The manifestation of natural anomaly of soils in the Nakyn kimberlite field in the microelement composition is determined by the increased concentrations of gross and mobile forms of elements typomorphic to kimberlites – Cr, Ni, Co, Mn, Cu. The composition of mobile forms is absolutely dominated by Mn.

Geochemical spectra built on the basis of concentration indices made it possible to reveal the degree of transformation of the elemental composition of soils over the observation period (Table 5). In the impact zone, the preserved areas with an undisturbed soil profile have high concentrations of mobile forms of Mn, Ni, Zn Co. The concentration indices vary in very wide limits. It was found out that soils falling into the zone of direct impact of technogenic facilities are characterized by surface accumulation of the same spectrum of trace elements as the grounds of technogenic landscapes (quarries, dumps, tailings and embankments for various purposes: $Mn_{28.0} > Zn_{8.0} > Ni_{7.7} > Cr_{6.8} > Co_{4.2} > As_{2.0}$ [48]).

Table 5

Comparative characteristics of the trace element composition of cryozems in key areas of the industrial site of the NMPD with the maximum Z_c value according to the research data of 2007 and 2018

Observation point number	Sampling location	Observation points coordinates	Trace element spectrum by years of observation		Z_c of mobile forms
			2007	2018	
In the impact zone of waste rock dumps					
19	1 m W from dump N 2	N 64 59.595 E 117 03.220	$\mathrm{Mn}_{4.3}\rightarrow\mathrm{Ni}_{2.9}\rightarrow\mathrm{Co}_{2.4}$	$\mathrm{Mn}_{69.7}\rightarrow\mathrm{Ni}_{4.5}\rightarrow\mathrm{Zn}_{4.1}\rightarrow\mathrm{Cd}_{3.4}\rightarrow\mathrm{Co}_{1.9}$	$\frac{9.6^{**}}{83.6}$
35	5 m N from dump N 1	N 65 02.361 E 117 05.320	$\mathrm{Mn}_{2.6}\rightarrow\mathrm{Ni}_{1.9}$	$\mathrm{Mn}_{669.4}\rightarrow\mathrm{Ni}_{16.11}\rightarrow\mathrm{Zn}_{7.3}\rightarrow\mathrm{Cd}_{4.2}\rightarrow\mathrm{Co}_{3.4}$	$\frac{4.5}{700.4}$
16	1.4 km E from dump N 1	N 65 02.434 E 117 07.943	$\mathrm{Mn}_{6.8}\rightarrow\mathrm{Ni}_{2.3}$	$\mathrm{Mn}_{186.8}\rightarrow\mathrm{Zn}_{4.7}\rightarrow\mathrm{Ni}_{2.0}$	$\frac{9.1}{193.5}$
In the impact zone of the beneficiation plants tailings					
32	50 m SE from tailings of BP N16	N 65 01.239 E 117 08.272	$\mathrm{Mn}_{6.4}\rightarrow\mathrm{Ni}_{3.1}\rightarrow\mathrm{Zn}_{2.7}$	$\mathrm{Mn}_{160.4}\rightarrow\mathrm{Zn}_{4.7}\rightarrow\mathrm{Ni}_{2.9}\rightarrow\mathrm{Cd}_{2.5}$	$\frac{12.2}{170.4}$
11	2.7 km S from tailings of BP N 15, summit of the watershed	N 64 58.731 E 117 08.676	$\mathrm{Mn}_{8.7}$	$\mathrm{Mn}_{290.4}\rightarrow\mathrm{Zn}_{5.4}\rightarrow\mathrm{Ni}_{3.8}\rightarrow\mathrm{Co}_{3.5}\rightarrow\mathrm{Cd}_{3.0}$	$\frac{8.7}{306.1}$
14	2.5 km E from tailings of BP N16	N 65 00.837 E 117 11.509	$\mathrm{Mn}_{10.6}\rightarrow\mathrm{Co}_{5.3}\rightarrow\mathrm{Ni}_{4.8}\rightarrow\mathrm{Cd}_{2.0}$	$\mathrm{Mn}_{141.4}\rightarrow\mathrm{Zn}_{2.5}$	$\frac{22.7}{143.9}$
31	150 m SE from tailings of BP N15	N 65 00.477 E 117 07.173	$\mathrm{Mn}_{3.5}\rightarrow\mathrm{Co}_{1.8}\rightarrow\mathrm{Ni}_{1.7}$	$\mathrm{Mn}_{127.0}\rightarrow\mathrm{Cr}_{10.0}\rightarrow\mathrm{Ni}_{7.2}\rightarrow\mathrm{Zn}_{6.0}\rightarrow\mathrm{Co}_{4.6}\rightarrow\mathrm{Cd}_{4.1}$	$\frac{7.0}{158.9}$
In the impact zone of quarries					
34	15 m SE from the Nyurbinskaya pipe quarry	N 65 01.452 E 117 05.334	–*	$\mathrm{Mn}_{27.9}\rightarrow\mathrm{Zn}_{8.0}\rightarrow\mathrm{Ni}_{7.7}\rightarrow\mathrm{Cr}_{6.8}\rightarrow\mathrm{Co}_{4.2}\rightarrow\mathrm{As}_{2.0}$	$\frac{2.9}{56.7}$
61	10 m SE from Botuobinskaya pipe quarry	N 65 00.110 E 117 02.819	–	$\mathrm{Mn}_{119.1}\rightarrow\mathrm{Zn}_{4.9}\rightarrow\mathrm{Ni}_{4.8}\rightarrow\mathrm{Cd}_{3.2}\rightarrow\mathrm{Co}_{2.5}$	$\frac{1.5}{134.2}$

---

* – no excess of background parameters, $K_c \leq 1.5$; ** – 2007 value above the line, 2018 below the line.

At the time of the study, the industrial site of the Nyurba MPD had a multielement nature of contamination with the imposition of halos of natural and technogenic anomalies. Based on the estimation of the total indicator of soil cover contamination by the content of mobile forms of trace elements, a spatial increase in the contrast of anomalies was revealed (Fig.2). The increase trend has a northwest and southeast direction. The geochemical environmental situation by 2018 has changed a lot with the predominance of a highly dangerous category of soil cover contamination, the halos of which occupy about 260.9 km^2.

Technogenic anomalies are confined to technogenic landscapes and are noted for active accumulation of precisely mobile forms of trace elements in the surface organogenic soil horizons. The content of mobile forms in the surface organogenic soil horizons increases in elements genetically related to the rocks of the mafic composition, kimberlites and dolerites (Fig.3). In 2007, at the initial stage of monitoring, the mobile forms of lead (40.6 %) differ in the maximum degree of mobility; by 2018, elements typomorphic to kimberlites and rocks of the trap formation, confined to facilities of mining, quarries, and beneficiation, tailings. The maximum degree of mobility is noted for Mn, 2007 7.3 % and 2018 47.8 %. The minimum mobility variations were found in As, 7.1 % in 2007 and 9.3 % in 2018.

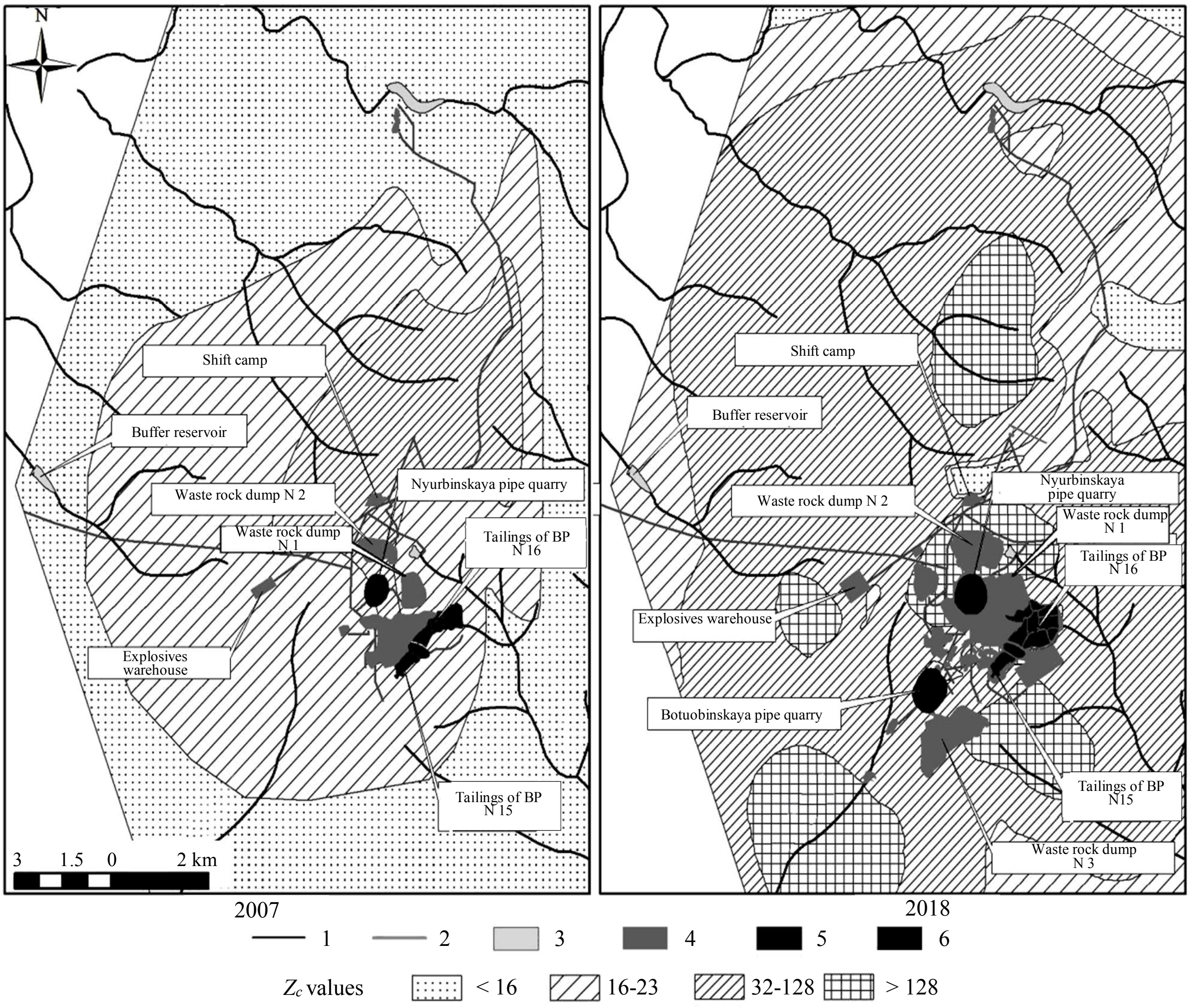

Fig.2. Dynamics of the geochemical environmental state of the soil cover in terms of Z_c for 2007-2018

1 – rivers; 2 – roads; 3 – anthropogenically transformed areas; 4 – waste rock dumps;
5 – hydraulic facilities, tailings; 6 – kimberlite pipe quarries

An analysis of the concentration factors and the degree of the elements mobility made it possible to conclude that the main Z_c -forming elements are Mn, Zn, Ni.

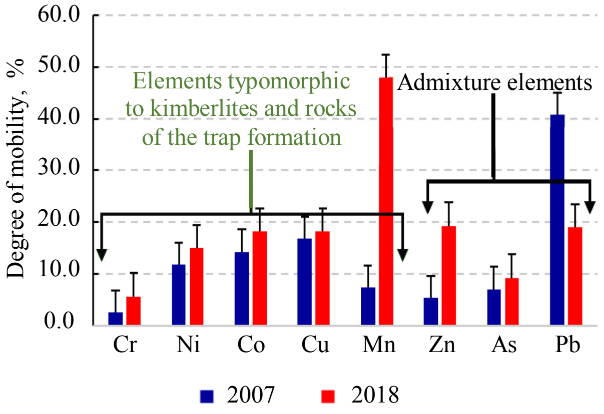

Fig.3. Degree of mobility of trace elements in the surface layer of soils of the NMPD industrial site by years of investigations

The technogenic anomalies in the soil cover of an industrial site can be, among other things, the result of atmospheric inputs of fine-grained products of the dust component during mass explosions in quarries, during the technological ore beneficiation, dusting of waste rock dumps or other embankments. For example, dispersion of the solid phase of dust emissions in the direction of the prevailing winds leads to the formation of soils with abnormally high contents of chemical elements. The formation in the soil cover of technogenic anomalies associated with the aerial transport of finely dispersed suspension is observed, for example, in the formed Sibaysky and

Uchalinsky geotechnical systems (GTS), located in the Republic of Bashkortostan. Colleagues who analysed the state of soils in the Bashkir Trans-Urals came to similar conclusions [20]. They attribute the influx of heavy metals into soils with aerial fallout of sulphide material from the pipes of the beneficiation plant and aeolian transport of sulphide-silicate material from dumps and tailings.

The technogenic anomalies identified by the authors are superficial. Therefore, to analyse the spatial relationship of the anomalies formed in the soil cover with the supposed sources of their occurrence, it is necessary to consider in more detail some climatic features of the Khannya-Nakyn interfluve. Climatically, the area belongs to the subarctic zone of the Siberian region [44]. Climatic conditions are described by data from the nearest meteorological stations of the Yakutsk Department for Hydrometeorology and Environmental Monitoring, Chumpuruk and Eyik, 50 km to the south and 112 km to the north, respectively. Available meteorological parameters are given on the websites www.meteo.ru and rp5.ru. The climate is sharply continental with long (eight months) winters with frosty dry weather (average January temperature –38 °C) determined by the prevailing Siberian anticyclone and short relatively warm summers (average July temperature 16.8 °C). The long-term average annual air temperature is –10.2 °C (Fig.4). The average annual precipitation is quite low, about 250 mm per year, of which about 200 mm falls during the warm period of the year (May-September). The graphs show an increase in both heat supply and humidity. Snow cover with an average annual thickness of 50 cm is formed in the last ten days of September and disappears in May; the duration of its stable existence is on average 216 days. The seasonally thawed layer is from 0.2 to 2.5 m, depending on the geomorphological and weather conditions of the year. The average wind speed, according to the Chumpuruk and Eyik meteorological stations, is 1.5 and 2.2 m/s. The highest average monthly wind speeds occur in April and May (Chumpuruk 2.0 and Eyik 2.6-2/7 m/s). Windless weather occupies 30 and 15 % of the year, respectively.

The degree of dusting of dumps increases with their height; their dusting is possible at a wind speed of more than 5 m/s [49]. According to the Chumpuruk weather station, in 2005-2019, in dry

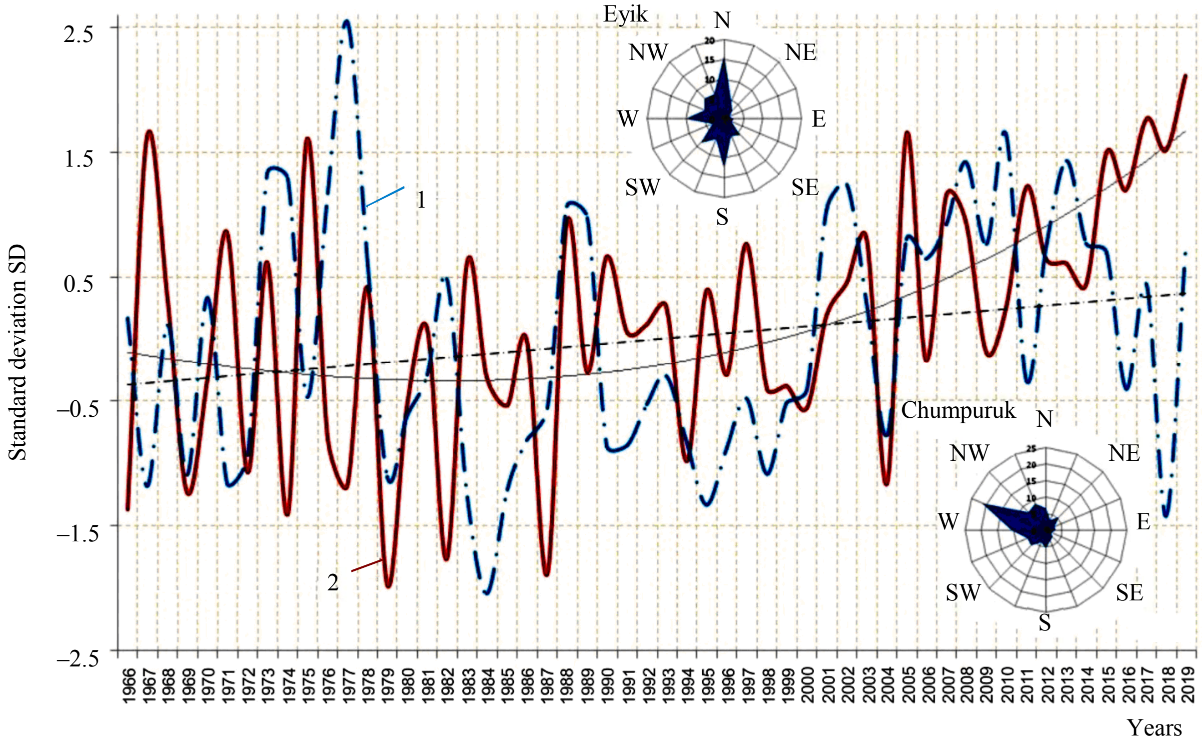

Fig.4. Graph of the variation of average annual air temperatures and the amount of annual precipitation according to the Chumpuruk weather station

1 – annual precipitation; 2 – average annual temperatures

weather, wind with a speed of 5 m/s or more was observed in 15-145 cases per year (57 on average). According to the Eyik weather station, there are an average of 370 cases per year. Strengthening of the wind is associated with the intensification of cyclonic activity, for this area more often of the western and north-western direction.

In the spring, there are separate landfalls of southern cyclones in Yakutia. In addition to circulation factors, the wind regime is influenced by the location of the weather station and, above all, by the topography. For the Chumpuruk meteorological station, the main wind direction coincides with the direction of the valley; the data of the Eyik meteorological station are significantly affected by its location on the northern coast of a large cognominal lake.

It turns out that in order to characterize the Nakyn field area, on the basis of geographical environmental analysis of climatic factors, by the number of strong winds, one can be guided by the data from the Chumpuruk weather station, and by the wind direction, by the data from the Eyik weather station. In this case, the main large-scale source of material for dust scattering and the formation of surface technogenic contamination of the soil cover are waste rock dumps. In short time periods, a significant amount of pollutant may fall out at a distance from the dumps. In a long time period, the entire area adjacent to the industrial site should be subjected to air contamination.

The studies carried out made it possible to determine the regularities of the intra-profile and spatial distribution of trace elements in the soils of the Nakyn kimberlite field. The formation of technogenic anomalies in the soil cover, spatially linked to technogenically transformed landscapes, ground and underground technogenic storages, can be traced at the industrial sites of other mining and beneficiation plants in Yakutia [50, 51]. The soil cover of the Mirninsky, Daldynsky, Alakit-Markhinsky and Nakyn kimberlite fields, within which mining and beneficiation plants operate, differs in structure and some basic physical and chemical properties of soils, but is characterized by similar manifestations of natural geochemical anomalies in the soil cover. Technogenically transformed landscapes at the industrial sites of mining and beneficiation plants form contamination halos, as a rule, of a surface nature. The nature of contamination and the spatial aspect of technogenic anomalies is individual for each site under consideration. Therefore, the revealed patterns exist under the conditions of a real technogenic impact, where there is a high probability of the emergence of new additional factors that, superimposed on the existing ones, can adjust the microelement composition of soils and increase the halos of secondary technogenic contamination.

Over the eleven-year period of observation of the soil cover state in the Khannya-Nakyn interfluve, the geochemical environmental situation worsened with an increase in the area of soil contamination and the contrast of its manifestation. Due to the high cyclonic activity, the main source of the technogenic anomalies in the surface horizons of soils in the industrial site of the NMPD are waste rock dumps or technogenic surface storages. The high sorption capacity of the upper organogenic horizons of cryozems contributes to the intensive accumulation of trace elements, including heavy metals. Thus, the upper organogenic horizons of cryozems perform a protective function in relation to the contamination of the entire soil profile. This ability of trace elements coming from outside as a result of air transport to be firmly settled by soil organic matter is a factor that can provide a low risk of multielement contamination for the entire ecosystem, provided that the soil profile integrity is maintained.

Conclusion. The zonal soil types of the Nakyn kimberlite field are cryozems with varying degrees of manifestation of gleization and cryoturbation. A distinctive feature of the intra-profile distribution of mobile forms of trace elements in the studied types of cryozems is the presence of two maxima: biogenic accumulation in the upper organogenic horizon followed by a decrease down the profile and a second peak in the suprapermafrost horizon. Biogenic accumulation in the AO and A_{cr} horizons is characteristic of the mobile forms of Ni, Mn, and Cd; suprapermafrost accumulation in the CR horizon is characteristic of the mobile forms of Cr, Ni, Co, Mn, and Cu.

In grounds and soils subjected to technogenic impact, there is a redistribution in the composition of mobile forms of trace elements. Elements typomorphic to kimberlites take the first place. In general, the percentage of the content of mobile forms of almost all determined trace elements increases. The grounds are distinguished by anomalously high concentrations of mobile forms of Mn, Zn, Ni, Cr, Co, As with concentration indices varying over a very wide range. The cryozems of the impact zone in the preserved forest areas are characterized by surface accumulation of mobile forms of Mn, Ni, Zn, and Co.

In general, the soil cover of the NMPD industrial site at the time of the study is characterized by a multielement composition of natural and technogenic anomalies. Based on the estimation of the total index of soil cover contamination Z_c a spatial increase in highly and very highly contaminated areas was revealed. The main Z_c-forming elements that determine the high level of soil contamination are Mn, Zn, and Ni.

The natural anomaly in soils manifests itself in the regular distribution of mobile forms of trace elements in the soil stratum with accumulation in the upper organogenic and suprapermafrost horizons, the suprapermafrost accumulation is higher than the biogenic one, which is a consequence of the natural geological and geochemical conditions for the formation of kimberlite fields. In the zones of direct impact of infrastructure facilities of the mining and beneficiation plant, a large amount of fine clay fraction is concentrated on the surface, characterized by an increased content of Cr-Ni-Co and Cu-Mn associations, which is manifested in high concentrations of mobile forms of these elements in the surface horizons of soils.

The pattern of surface technogenic anomalies in soils corresponds to the direction of the prevailing western and north-western winds.

When the soil cover, the integrity of the soil profile are disturbed, and the mineral part of the soil profile is exposed, the geochemical conditions change, as a result of which most of the trace elements pass into a mobile state, water-soluble and acid-soluble forms, etc., i.e. become more accessible to plants, soluble in water, which creates tension in the overall environmental situation in the area affected by the mining and processing plant.

The results obtained are especially important for the measures for rehabilitation of the soil cover in the impact zone of mining and beneficiation plants, for geoenvironmental monitoring and assessing the landscape resistance to chemical contamination. These data will serve as the basis for predicting soil contamination with trace elements, including heavy metals.

REFERENCES

1. Žibret G., Gosar M., Miler M., Alijagić J. Impacts of mining and smelting activities on environment and landscape degradation – Slovenian case studies. *Land Degradation & Development*. 2018. Vol. 29. Iss. 12, p. 4457-4470. DOI: 10.1002/ldr.3198

2. Dhar A., Miller V.S., Wilkinson S.R., Naeth M.A. Substrate and Topsoil Impact on Soil Water and Soil Temperature in Arctic Diamond Mine Reclamation. *Soil Systems*. 2022. Vol. 6. Iss. 1. N 12. DOI: 10.3390/soilsystems6010012

3. Yurkevich N.V., Eltsov I.N., Gureev V.N. et al. Technogenic impact on the environment in the Russian Arctic on the example of the Norilsk industrial region. *Bulletin of the Tomsk Polytechnic University Geo Assets Engineering*. 2021. Vol. 332. N 12, p. 230-249 (in Russian). DOI: 10.18799/24131830/2021/12/3207

4. Bloodworth A.J., Scott P.W., McEvoy F.M. Digging the backyard: Mining and quarrying in the UK and their impact on future land use. *Land Use Policy*. 2009. Vol. 26, p. S317-S325. DOI: 10.1016/j.landusepol.2009.08.022

5. Newman J.E., Levasseur P.A., Beckett P., Watmough S.A. The impact of severe pollution from smelter emissions on carbon and metal accumulation in peatlands in Ontario, Canada. *Environmental Pollution*. 2023. Vol. 320. N 121102. DOI: 10.1016/j.envpol.2023.121102

6. Benidire L., Benidire L., Boularbah A. Impacts of mining activities on soil properties: case studies from Morocco mine sites. *Soil Science Annual*. 2020. Vol. 74. Iss. 4, p. 395-407. DOI: 10.37501/soilsa/133011

7. Xiu-Wu Zhang, Lin-Sheng Yang, Yong-Hua Li et al. Estimation of lead and zinc emissions from mineral exploitation based on characteristics of lead/zinc deposits in China. *Transactions of Nonferrous Metals Society of China*. 2011. Vol. 21. Iss. 11, p. 2513-2519. DOI: 10.1016/S1003-6326(11)61044-3

8. Wilkin R.T., Lee T.R., Beak D.G. et al. Groundwater co-contaminant behavior of arsenic and selenium at a lead and zinc smelting facility. *Applied Geochemistry*. 2018. Vol. 89, p. 255-264. DOI: 10.1016/j.apgeochem.2017.12.011

9. Belosheikina A.V., Talovskaya A.V., Yazikov E.G. Ecological and geochemical assessment of the state of the soil cover on the territory of the Sorsky Mining and Processing Plant (Republic of Khakassia). *Bulletin of the Tomsk Polytechnic University Geo Assets Engineering*. 2020. Vol. 331. N 1, p. 44-53 (in Russian). DOI: 10.18799/24131830/2020/1/2446

10. Demkova L., Tomas. J., Bobulska L. Assessment of soil heavy metal pollution in a former mining area – before and after the end of mining activities. *Soil and Water Research*. 2017. Vol. 12. Iss. 4, p. 229-236. DOI: 10.17221/107/2016-SWR

11. Slavikovsky O.V., Slavikovskaya Yu.O., Valiev N.G. Subsoil Capacity of Geo-Technologies as a Fundamental Factor of the Effect of Mining Complex to the Environment. *Izvestiya vuzov. Gornyi zhurnal*. 2011. N 2, p. 70-75 (in Russian).

12. Zenkov I.V. Review of foreign researches in the field of mining ecology. *Gornyi zhurnal*. 2016. N 10, p. 96-99 (in Russian). DOI: 10.17580/gzh.2016.10.20

13. Abiola O., Adegbola O., Hu R., Atta R. Assessment of trace metals contamination in stream sediments and soils in Abuja leather mining, southwestern Nigeria. *Acta Geochimica*. 2018. Vol. 37. Iss. 4, p. 592-613. DOI: 10.1007/s11631-017-0256-1

14. Xufeng Fei, Zhaohan Lou, George Christakos et al. The association between heavy metal soil pollution and stomach cancer: a case study in Hangzhou City, China. *Environmental Geochemistry and Health*. 2018. Vol. 40. Iss. 6, p. 2481-2490. DOI: 10.1007/s10653-018-0113-0

15. Sarapulova G.I. Environmental Geochemical Assessment of Technogenic Soils. *Journal of Mining Institute*. 2018. Vol. 234, p. 658-662. DOI: 10.31897/PMI.2018.6.658

16. Ushakova E.S., Karavaeva T.I., Belkin P.A. The Ecological State of Soils in Industrial Territories (on the Example of Berezniki, Perm Territory): Comparison of Domestic and Foreign Assessment Methods. *Bulletin of the Tomsk Polytechnic University Geo Assets Engineering*. 2020. Vol. 331. N 10, p. 58-70 (in Russian). DOI: 10.18799/24131830/2020/10/2850

17. Hu Zhenqi, Wang Peijun, Li Jing. Ecological Restoration of Abandoned Mine Land in China. *Journal of Resources and Ecology*. 2012. Vol. 3. Iss. 4, p. 289-296. DOI: 10.5814/j.issn.1674-764x.2012.04.001

18. Yanin E.P. Chemical composition and geochemical environmental of urban soils. Analytical review. *Problemy okruzhayushchei sredy i prirodnykh resursov*. 2020. N 2, p. 40-73 (in Russian). DOI: 10.36535/0235-5019-2020-02-3

19. Basova I.A., Ivatanova N.P., Kopylov A.B. Assessment of the ecological state of soils in regions with a developed mining industry. *News of the Tula State University. Natural Sciences*. 2012. N 1-2, p. 14-16 (in Russian).

20. Naeth M.A., Wilkinson S.R. Establishment of Restoration Trajectories for Upland Tundra Communities on Diamond Mine Wastes in the Canadian Arctic. *Restoration Ecology*. 2014. Vol. 22. Iss. 4, p. 534-543. DOI: 10.1111/rec.12106

21. Sena K., Barton C., Hall S. et al. Influence of spoil type on afforestation success and natural vegetative recolonization on a surface coal mine in Appalachia, United States. *Restoration Ecology*. 2015. Vol. 23. Iss. 2, p. 131-138. DOI: 10.1111/rec.12164

22. Shafigullina G.T., Udachin V.N., Aminov P.G., Filippova K.A. Geochemical Characteristics of Technogenic Soils in the Mining Landscapes of the South Urals. *Vestnik Akademii nauk Respubliki Bashkortostan*. 2015. Vol. 20. N 4 (80), p. 93-101 (in Russian).

23. Myga-Piątek U. Landscape management on post -exploitation land using the example of the Silesian region, Poland. *Environmental and Socio-economic Studies*. 2014. Vol. 2. Iss. 1, p. 1-8. DOI: 10.1515/environ-2015-0026

24. Oelofse S.H.H. Mine water pollution – acid mine decant, effluent and treatment: a consideration of key emerging issues that may impact the State of the Environment. Mining: Environment and Health Concerns, 2008, p. 83-91.

25. Zabergja-Ferati F., Mustafa M.K., Abazaj F. Heavy Metal Contamination and Accumulation in Soil and Plant from Mining Area of Mitrovica, Kosovo. *Bulletin of Environmental Contamination and Toxicology*. 2021. Vol. 107. Iss. 3, p. 537-543. DOI: 10.1007/s00128-021-03223-6

26. Fei Zang, Shengli Wang, Zhongren Nan et al. Accumulation, spatio-temporal distribution, and risk assessment of heavy metals in the soil-corn system around a polymetallic mining area from the Loess Plateau, northwest China. *Geoderma*. 2017. Vol. 305, p. 188-196. DOI: 10.1016/j.geoderma.2017.06.008

27. Xiao Qing, Zong Yutong, Lu Shenggao. Assessment of heavy metal pollution and human health risk in urban soils of steel industrial city (Anshan), Liaoning, Northeast China. *Ecotoxicology and Environmental Safety*. 2015. Vol. 120, p. 377-385. DOI: 10.1016/j.ecoenv.2015.06.019

28. Nevedrov N.P. Profile distribution and migration of heavy metals in the soils of the Kursk agglomeration (model experiments). *South of Russia: ecology, development.* 2020. Vol. 15. N 1, p. 60-68 (in Russian). DOI: 10.18470/1992-1098-2020-1-60-68

29. Yuebing Sun, Qixing Zhou, Xiaokui Xie, Rui Liu. Spatial, sources and risk assessment of heavy metal contamination of urban soils in typical regions of Shenyang, China. *Journal of Hazardous Materials*. 2010. Vol. 174. Iss. 1-3, p. 455-462. DOI: 10.1016/j.jhazmat.2009.09.074

30. Long Zhao, Yafei Xu, Hong Hou et al. Source identification and health risk assessment of metals in urban soils around the Tanggu chemical industrial district, Tianjin, China. *Science of The Total Environment*. 2014. Vol. 468-469, p. 654-662. DOI: 10.1016/j.scitotenv.2013.08.094

31. Aklambetova K.M. Environmental consequences of mineral deposit development and their impact on the natural environment. Aktualnye problemy zdorovya cheloveka i formirovanie sredy obitaniya: Materialy mezhdunarodnoi nauchno-prakticheskoi konferentsii, 22 maya 2002, Karaganda, Russia. Karaganda: Izd-vo KarGU, 2002, p. 23-27 (in Russian).

32. Fujun Niu, Zeyong Gao, Zhanju Lin et al. Vegetation influence on the soil hydrological regime in permafrost regions of the Qinghai – Tibet Plateau, China. *Geoderma*. 2019. Vol. 354. N 113892. DOI: 10.1016/j.geoderma.2019.113892

33. Prach K., Karešová P., Jírová A. et al. Do not neglect surroundings in restoration of disturbed sites. *Restoration Ecology*. 2015. Vol. 23. Iss. 3, p. 310-314. DOI: 10.1111/rec.12189

34. Mikhalchuk N.V. Mobile forms of heavy metals and trace elements in the soils of the carbonate series of the south-west of Belarus. *Proceedings of the National Academy of Sciences of Belarus. Chemical Sciences Series*. 2017. N 3, p. 90-97 (in Russian).

35. Gololobova A.G. Heavy Metal Mobility and Trace Elements in Permafrost Soils Under Anthropization. *International Research Journal*. 2020. N 12 (102). Part 2, p. 49-54 (in Russian). DOI: 10.23670/IRJ.2020.102.12.043

36. Targulyan V.O., Goryachkin S.V., Karavaeva N.A. et al. Soil memory: soil as a memory of biosphere-geosphere-anthropogenic interactions. Moscow: Izd-vo LKI, 2008, p. 692 (in Russian).

37. Rusanova G., Shakhtarova O. Structural Organization and Matter Differentiation of Bolshezemelskaya Tundra South-East Automorphic Soils. *Tomsk State University Journal of Biology*. 2012. N 3 (19), p. 18-32 (in Russian).

38. Gorev N.I., Gerasimchuk A.V., Protsenko E.V., Tolstov A.V. Tectonic aspects of the structure of the Vilyuisko-Markhinskaya zone, their use in predicting kimberlite fields. *Nauka i obrazovanie*. 2011. N 3, p. 5-10 (in Russian).

39. Ladonin D.V. Heavy metal compounds in soils, problems and methods of study. *Pochvovedenie*. 2002. Vol. 35. N 6, p. 605-614 (in Russian).

40. Syso A.I. Patterns of the distribution of chemical elements in soil-forming rocks and soils of Western Siberia. Novosibirsk: Izd-vo Sibirskogo otdeleniya RAN, 2007, p. 227 (in Russian).

41. Osinseva E.V., Agisheva S.T., Gorbunova E.M. et al. Reference Materials System of Scientific Methodical Centre of State Service of Reference Materials for Composition and Properties of Substances and Materials Ural Research Institute for Metrology. *Standartnye obraztsy – Reference materials*. 2015. N 2, p. 31-55 (in Russian).

42. Saet Yu.E., Revich B.A., Yanin E.P. Environmental geochemistry. Moscow: Nedra, 1990, p. 335 (in Russian).

43. Legostaeva Ya.B., Ksenofontova M.I., Dyagileva A.G. Geochemical environmental monitoring of the soil cover in the impact zone of the Nyurba Mining and Processing Division. *Gornyi zhurnal*. 2014. N 4, p. 117-121 (in Russian).

44. Gololobova A.G., Legostaeva Ya.B. Heavy metals in cryozems of Western Yakutia. International Multidisciplinary Scientific GeoConference Surveying Geology and Mining Ecology Management, SGEM. 2019. Vol. 19. N 3.2, p. 239-246. DOI: 10.5593/sgem2019/3.2/S13.032

45. Field manual of Russian soils. Moscow: Pochvennyi institut im. V.V.Dokuchaeva, 2008, p. 182 (in Russian).

46. Dyagileva A.G. Resistance to chemical contamination of cryozems in Western Yakutia. Avtoref. dis. ... kand. biol. nauk. Ulan-Ude: Institut obshchei i eksperimentalnoi biologii Sibirskogo otdeleniya RAN, 2015, p. 23 (in Russian).

47. Yagnyshev B.S., Yagnysheva T.A., Zinchuk M.N., Legostaeva Ya.B. Environment of Western Yakutia (geochemistry of geosystems: state and problems). Yakutsk: Izd-vo Yakutskogo nauchnogo tsentra Sibirskogo otdeleniya RAN, 2005, p. 432 (in Russian).

48. Legostaeva Ya.B., Gololobova A.G. Long-term geochemical monitoring of the soil cover in the impact zone of diamond mining enterprises: a case study in the Nakyn kimberlite field, Russia. *Environmental Monitoring and Assessment*. 2021. Vol. 193. Iss. 6. N 337. DOI: 10.1007/s10661-021-09087-x

49. Amosov P.V., Baklanov A.A., Masloboev V.A. The results of the assessment of air pollution during dusting of the tailings (based on three-dimensional modeling). *Minerals and Mining Engineering*. 2017. N 6, p. 87-94 (in Russian).

50. Khovanskaya M.A., Kosinova I.I. Influence of mining and processing activity on soil of Ajhalskiy area (Sakha-Yakutia). *Proceedings of Voronezh State University. Series: Geology*. 2010. N 1, p. 282-285 (in Russian).

51. Legostaeva Ya.B., Gololobova A.G. Features of distribution of microelements in soils of background and impact zones at diamond mining sites in the North-West of the Siberian Platform. *Bulletin of the Tomsk Polytechnic University Geo Assets Engineering*. 2021. Vol. 332. N 9, p. 142-153 (in Russian). DOI: 10.18799/24131830/2021/9/3364

***Authors*: Yana B. Legostaeva,** *Candidate of Biology, Leading Researcher, https://orcid.org/0000-0002-1556-9182* (*Diamond and Precious Metal Geology Institute, Siberian Branch, RAS, Yakutsk, Russia*), **Anna G. Gololobova**, *Candidate of Biology, Senior Researcher, nuta0687@mail.ru, https://orcid.org/0000-0003-0813-5404* (*Diamond and Precious Metal Geology Institute, Siberian Branch, RAS, Yakutsk, Russia*), **Vladimir F. Popov**, *Associate Professor, https://orcid.org/0000-0001-9854-2825* (*M.K.Ammosov North-Eastern Federal University, Yakutsk, Russia*), **Victor S. Makarov**, *Candidate of Biology, Senior Researcher, https://orcid.org/0000-0002-4781-9027* (*Institute of Applied Ecology of the North, M.K.Ammosov North-Eastern Federal University, Yakutsk, Russia*).

The authors declare no conflict of interests.

ISSN 2411-3336; e-ISSN 2541-9404

JOURNAL OF MINING INSTITUTE

Zapiski Gornogo instituta

Journal homepage: pmi.spmi.ru

Research article

Uranium in man-made carbonates on the territory of Ufa

Iskhak M. FARKHUTDINOV[1,2], **Rustam R. KHAYRULLIN**[3]✉, **Bulat R. SOKTOEV**[4], **Anastasia N. ZLOBINA**[5], **Elena I. CHESALOVA**[1], **Anvar M. FARKHUTDINOV**[6], **Andrey V. TKACHEV**[1]

[1] *Vernadsky State Geological Museum of the RAS, Moscow, Russia*
[2] *OOO RN-BashNIPIneft, Ufa, Republic of Bashkortostan, Russia*
[3] *Ufa Federal Research Centre of the RAS, Ufa, Republic of Bashkortostan, Russia*
[4] *Tomsk Polytechnic National Research University, Tomsk, Russia*
[5] *Bashkir State University, Ufa, Republic of Bashkortostan, Russia*
[6] *CY Cergy Paris Université, Cergy-Pontoise, France*

***How to cite this article*:** Farkhutdinov I.M., Khayrullin R.R., Soktoev B.R., Zlobina A.N., Chesalova E.I., Farkhutdinov A.M., Tkachev A.V. Uranium in man-made carbonates on the territory of Ufa. Journal of Mining Institute. 2023. Vol. 260, p. 226-237. DOI: 10.31897/PMI.2023.4

***Abstract*.** The paper presents the results of analyzing uranium content in man-made carbonates (scale crusts) on the territory of Ufa based on examination of 42 samples. The median uranium content in the investigated samples stands at 1.44 mg/kg, which is significantly lower than the background values (scales from the Lake Baikal water, a clarke of sedimentary carbonate rocks) and data on other settlements of the Republic of Bashkortostan. Low values of uranium content are probably associated with the effects of the three leading factors, i.e. specific subsurface geology of the territory (gypsum, limestone); types of water supply; water treatment processes for the centralized type of water supply. Spatial distribution of uranium in man-made carbonates is characterized with uniformity, which is disturbed in two cases, i.e. a change of the water supply type (from centralized to individual); and material of the vessels used for boiling the water. No significant differences were detected when comparing samples of man-made carbonates associated with different sources of water supply (the bucket and infiltration types of water intake) and the types of household filters.

***Keywords*:** man-made carbonates; scale crust; potable water; geochemistry; environmental geochemistry; medical geology; Republic of Bashkortostan; Southern Urals; East European Platform; uranium

Acknowledgment. Analysis of the uranium content in man-made carbonates was carried out as part of the Tomsk Polytechnic University development programme. Data processing was performed within the framework of implementation of the Russian Science Foundation grant (project N 22-27-00748).

Received: 15.04.2022 ***Accepted: 17.11.2022*** ***Online: 26.01.2023*** ***Published: 25.04.2023***

Introduction. Water is one of the main sources of chemical elements for the human body [1, 2]. Both excess and deficiency of these elements can have a negative impact on health, triggering a number of possible diseases [3-5].

The hazards of uranium result from a combination of three effects [6], i.e. its toxic, radioactive and carcinogenic action [7-9]. At the same time, it does not perform any known biological functions [6, 10, 11]. Also the daughter products of uranium decay, of which radon, a radioactive gas, is the best known [12-14], produce predominantly negative effects. Studies have shown that radon can cause lung cancer, leukemia and other oncological diseases [15-17].

When ingested with water in low concentrations, uranium does not cause any significant harm as a radionuclide, but it can affect the human body as a toxic chemical element [18]. A number of studies show that high background levels of uranium in drinking water can cause renal cell carcinoma, kidney failure and other diseases [6, 19, 20]. Therefore, geochemical investigations of potable water for excessive concentrations of chemical elements, including uranium, are an important field of geoecology, medical geology, and toxicology [6, 21, 22]. Identification of such anomalies at the regional and local levels can seriously contribute to the prevention of chronic diseases caused by environmental factors of both natural and man-made origin.

Studies conducted in several regions of the Russian Federation (the Irkutsk, Tomsk and Chelyabinsk Regions, the Altai and Buryat Republics) and Kazakhstan (the Pavlodar Region) have shown that one of the indirect indicators of potable water quality are man-made carbonates (scale) that are formed when water is boiled in households [23-26]. These studies show that, in terms of material composition, the scale formed in domestic water boiling consists mainly of different variations of calcium carbonate. X-ray powder diffractometry and scanning electron microscopy confirm this by indicating that the main mineral phases in the scale are calcite or aragonite [24, 25], while the content of other mineral phases ranges within first few percent. This is explained by the fact that mainly hydrocarbonate calcium and magnesium-calcium waters are used for potable water supply.

In natural conditions the uranium geochemistry is quite versatile [27] and depends on a number of physical and chemical parameters, i.e. pH, Eh, presence of complexing compounds (carbonates, phosphates, sulphates, etc.) [28-30]. Under oxidizing conditions, uranium is most commonly found in its hexavalent form (U^{6+}) as uranyl ion (UO_2^{2+}), which forms more stable complexes and has higher mobility in natural waters [30]. When carbonate ions are present, uranyl ions easily associate with them producing $(UO_2)(CO_3)^0$, $(UO_2)(CO_3)_2^{2-}$, $UO_2(CO_3)_3^{4-}$ compounds [31-33], and precipitates with basic carbonate minerals (calcite, aragonite, dolomite) [34-36]. Deposition of uranium from solutions is usually associated with higher evaporation rates or local oversaturation [33, 37], which is observed in the case of potable water boiling (combination of the thermodynamic and evaporation geochemical barriers).

At the same time, studies of parallel samples of water and man-made carbonates on the territory of the Tomsk and Pavlodar regions, as well as in the Baikal area show that there is a positive correlation between the uranium content in water and in the man-made carbonates (the linear correlation indicator varies from 0.62 to 0.96).

The purpose of this research is to analyze the content of uranium in man-made carbonates (potable water scales) on the territory of Ufa. This study is a logical continuation of works to assess the geo-ecological situation in the Republic of Bashkortostan from the standpoint of medical geology [38].

Geologically, Ufa is located within the eastern margin of the East European Platform (the Russian Plate) (Fig.1). Most of the territory of the city is located on a flat plateau-like elevation with steep slopes, bounded on the west, south and east by the valleys of the Ufa and Belaya rivers, also known as the Ufa Peninsula. The Archean crystalline basement is overlain by a thick (about 8 km) layer of sedimentary rocks in this area. Permian, Neogene and Quaternary sediments are recorded within the city boundaries [39].

The Permian System within the territory of Ufa is represented with the Kungurian and Ufimian Stages of the lower Series. The Kungurian Stage includes light grey gypsum and anhydrite with interbeds of gypsiferous clays and dolomite, found at the base of steep riverbanks. The thickness of the sediments is up to 340 m. The Ufa Stage is represented with frequent interbedded limestones, clayey dolomites, marls, clays, siltstones and sandstones with an overall thickness ranging within 15-25 m and up to 60 m in some areas.

Neogene sediments are represented with the Kinel Formation in the valleys of the Belaya and Ufa Rivers, as well as the poorly defined Akchagyl and Apsheron Stages in the Belo-Ufimsk interfluve area. The Kinel Formation includes heavy clays, sands and gravels up to 70-100 m in total thickness. The Akchagyl and Apsheron Stages are composed of reddish-brown and greyish-brown heavy clays with interbands of sand in the lower part with a total thickness of 50 m [39].

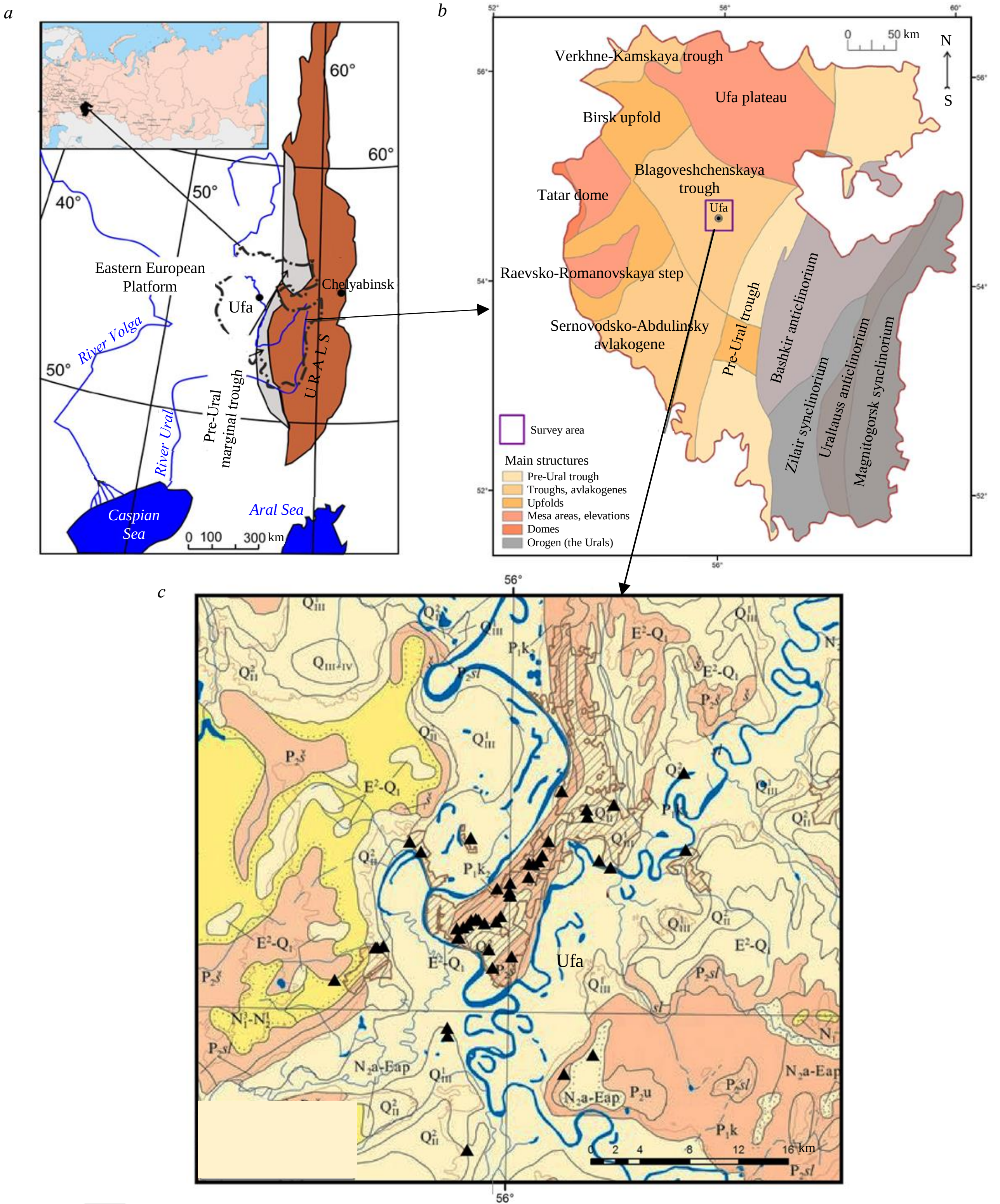

Q	Quaternary System. Holocene: Q_{IV}, $Q_{III\text{-}IV}$ – upper part of the upper regional stage; Q^1_{III} – lower part of the upper regional stage; Q^2_{II} – medium regional stage; E^2-Q_I – upper Eo-pleistocene – lower regional stage of Neo-Pleistocene
N_2^2a-Eap	Upper Holocene, Akchagyl Stage, Eo-pleistocene, Apsheron Stage
N_1^3-N_2^1	Neogene System: N_1-N_2 – Upper Miocene – Lower Pliocene
P_1u	Permian System. Ufimian Stage. Upper Substage: P_2s – Sheshma Formation; P_2sl – Solikamsk Formation
P_1k	Kungurian Stage, Upper Substage
▲	Sampling points

Fig.1. Subsurface geology of the survey area: *a* – location of the survey area; *b* – tectonic zoning of the Republic of Bashkortostan (State Geological Map, sheet N40(41), scale 1:1,000,000 (2001); *c* – a fragment of the geological map of the Republic of Bashkortostan with indication of sampling points, scale 1:500,000 (2011)

Quaternary sediments in the Belaya and Ufa river valleys are made up of alluvial gravels and sands with a thickness of 10-15 m overlain by periglacial clayey sediments (sandy loams, loams, clays) ranging from 1-3 to 15-20 m, while within the Belo-Ufa interfluve area the sediments are alluvial-deluvial (clays, loams) and their thickness varies from 0.5-2 to 10-15 m [39].

The city's drinking water supply is based on the waters of the Ufa River, as well as groundwater available both in the river valleys (Belaya, Ufa, Shugurovka) and in the interfluve area. According to research data, there exist noticeable differences in the groundwater composition in the southern and northern parts of the city. The chemical composition of groundwater in the southern (residential) part of the city is predominantly bicarbonate, sulphate-hydrocarbonate and hydrocarbonate-chloride magnesium-calcium, magnesium-calcium-sodium. The water salinity is 0.66-1.29 g/l, pH 7.2-7.62. The content of trace elements is below the maximum permissible concentration, and the main indicator of groundwater pollution in this part of the city is nitrogen compounds, as the concentration of nitrate-ion in wells of private houses reaches 1100-1530 mg/dm^3. Some areas are noted to have excessive levels of Cr, Hg, petroleum products, phenols and other chemical elements and organic compounds [40].

In the northern (industrial) part of the city, the groundwater is sulphate-hydrocarbonate, hydrocarbonate-chloride and chloride-hydrocarbonate calcium, calcium-sodium, sodium-calcium, sodium-magnesium-calcium, ammonium-sodium. The type of water changes from sulphate-sodium to magnesium-chloride and calcium-chloride with salinity rising up to 6-11.5 g/dm^3 [40]. The radiation safety indicators comply with the standards, i.e. the total α-radioactivity is below 0.02 Bq/L with the relevant standard level being 0.2 Bq/L, while the total β-radioactivity is less than 0.1 Bq/L with the standard of 1.0 Bq/L [41].

Water is supplied to households in Ufa by the Ufavodokanal State Unitary Enterprise. The territory of the city is provided with centralized water supply and sewerage systems, which comprises seven large-scale water intakes. i.e. an open river water intake (Northern, the bucket-type) and six infiltration-type water intakes with a total capacity of 613 thousand m^3/day [41]. Potable water, supplied to the population, meets the requirements of the state standards [42].

Methods. *Sampling.* Data on the uranium content in 42 samples of salt sediments from potable water were analyzed within the city territory, 36 of which were taken from households with centralized water supply, and 6 from water wells and boreholes. A comparative analysis was made using data on the uranium content in samples of man-made carbonates collected in the territory of the Ufa district (28 samples from 18 settlements). Data available for other settlements in the Republic of Bashkortostan, mainly for the cities [43, 44], were used randomly. The samples were collected in conformity with the available recommendations [45]. The sampling was done from various vessels, i.e. enameled and electric kettles, pots, samovars, which are used for boiling water from both centralized and individual (water wells, boreholes) water supply sources. The following criteria were also considered while sampling: the time of scale formation, i.e. when the vessels were last decalcified before the sampling, the depth of the water supply source and whether a filter was used.

Studies carried out in different locations [23-25] have proved the efficiency of using the scale crust as an indirect indicator of the potable water quality. Correct sampling minimizes the impact of factors such as type of vessels and the time of scale formation. The leading factors in this case are the type and the source of water supply as well as the use of a filter.

Analytical methods. The uranium content in man-made carbonates was analyzed using the instrumental neutron activation analysis in the nuclear geochemical laboratory of the “Uranium Geology” International Innovative Research and Education Center that uses the IRT-T nuclear research reactor at the Tomsk Polytechnic University (Accreditation Certificate N RA.RU.21АБ27 dated 08.04.2015, analysts: A.F.Sudyko, L.F.Bogutskaya).

X-ray powder diffractometry was used to analyze the material composition of the man-made carbonates. Seven randomly selected scale samples were analyzed using the X-ray phase analysis with the Bruker D2 Phaser X-ray diffractometer. The X-ray images were obtained in the Bragg – Brentano geometry. The following imaging parameters were used: anode material – Cu (copper), X-ray tube voltage – 30 kV, current – 10 mA, imaging angles 2ϴ – from 10 to 70°, imaging step – 0.02°, exposure time – 1 s per point, rotation – 20 rpm. The obtained diffractograms were interpreted using the DIFFRAC.Eva and TOPAS software suites based on the PDF-2 X-ray powder diffractometry databases of International Center for Diffraction Data (ICDD, Denver, USA).

The data were processed with the Statistica 8.0 and Microsoft Excel 2016 software packages. Statistical processing of the data included calculation of the following parameters: arithmetic mean, standard error, geometric mean, median, mode, minimum and maximum values, standard deviation, coefficient of variation, skewness ratio, degree of excess and their standard errors. In data processing, values below the detection limit (0.1 mg/kg) were replaced by half the value (0.05 mg/kg). Since the nature of uranium distribution in the studied selection does not match normal distribution according to various tests (Kolmogorov – Smirnov, Lilliefors, chi-squared tests), the mean value was taken to equal the median calculated without taking into account the outstanding samples, although they are shown in the discussion of the results obtained. Geochemical specialization of the man-made carbonates and the patterns of uranium accumulation in them were determined by comparing with the background values, i.e. a clarke of sedimentary carbonate rocks – 2.2 mg/kg [46], scale from Lake Baikal water obtained by the authors – 4.51 mg/kg [47].

Maps of spatial distribution of natural radioactive elements were built using the ArcGIS 10.3 software in Spatial Analyst module with the Inverse Distance Weighted Interpolation method. The choice of interpolation method was based on a relatively small number of survey points and their uneven spatial distribution. The values were approximated as weighted averages within a certain distance. The nearest objects have a greater weight, while the distant ones have a relatively low influence on the calculations (the weights are inversely proportional to the measure of distance).

Discussion of results. *Material composition of man-made carbonates.* The performed diffractometry studies of seven randomly selected scale samples show that all the samples are made up of various calcium carbonate modifications: the dominant mineral in four samples is calcite, i.e. its rhombohedral modification, and in the remaining three samples the main mineral is aragonite in orthorhombic modification. These data agree well with previous studies of the man-made carbonates in other territories (the Tomsk, Irkutsk, Pavlodar Regions and the Republic of Buryatia) [23-25].

Based on analyzing 42 samples of man-made carbonates collected on the territory of Ufa, the median content of uranium is 1.44 mg/kg ranging from 0.05 (half the detection limit by the instrumental neutron activation analysis) up to 28.9 mg/kg. It should be noted that the distribution of uranium in the studied sample selection is relatively homogeneous, as values of the arithmetic mean (1.82 mg/kg), geometric mean (1.3 mg/kg) and median content are quite close. The coefficient of variation for this selection (N = 42) is 82 %. The median content is significantly lower than in the background values which are used in comparative analysis to study of the man-made carbonates, i.e. the scale crust from Lake Baikal water (4.51 mg/kg) [47] and sedimentary carbonate rocks (2.2 mg/kg) [46]. The median content of uranium in the man-made carbonates within the territory of Ufa is significantly lower than the average value for the Republic of Bashkortostan, i.e. 5.4 mg/kg [44], as well as in other studied areas: the Tomsk region (1.9 mg/kg) and the Pavlodar region (27.4 mg/kg), the Baikal region (21.1 mg/kg), the Altai Republic (10.7 mg/kg) [47].

The low content of uranium in the man-made carbonates may be due to the specific features of subsurface geology within the territory of the city, as most of the city is located in the areas of gypsum and limestone distribution. A similar trend was previously revealed on the Ufa plateau, located in the northern part of the Republic [43, 44]. This factor, i.e. the subsurface geology, is more evident when comparing the obtained results with the data on the uranium content in the man-made carbonates from other large settlements of the Republic of Bashkortostan, mainly from the cities (Table 1).

Table 1

Uranium content in samples of man-made carbonates from various settlements

Settlement name	Number of samples	Content, mg/kg	Rocks/soils encountered on the day surface
Sibay	4	6.21	D_2kr_2 – Karamalytash Formation. Upper Subformation. Dacites, rhyodacites, basalts and their lava-breccias, hyaloclastites and calc-sinters, andesite-basalts, silicate tuffites, cryolites, and jaspers (over 750 m); D_3-C_1zl – Zilair Formation. Sandstones, silty sandstones, siltstones, often calcareous, siliceous-clayey and carbonaceous-clayey schists, rarely gravelites, silicate tuffites, limestones, underlain by olistostrome layers (up to 2700 m); aQ_{II} – alluvial sediments. Gravels, sands, pebbles, sandy loams, loams (up to 10 m); aQ_{III} – alluvial sediments. Sands, clays, siltstones, loams, pebbles (up to 12 m)
Sterlitamak	4	6.88	N_2^3ak+ap – Akchagyl and Apsheron Stages. Clays, siltstones, sands, pebbles; Q^1_{III} – clays, loams, sands, pebbles; $Q^2_{III}+Q_{IV}$ – Upper Quaternary, upper part and recent sediments. Topsoils, peats, loams, sands, pebbles
Oktyabrsky	14	8.5	P_1šš – Ufimian Stage. Sheshma Horizon. Sheshma Formation – sandstones, siltstones, pudding rocks, marls, limestones, dolomites, and gypsums; P_2kz_1 – Kazan Stage. Upper Substage – clays, marls, limestones, dolomites, siltstones, sandstones, pudding rocks, gypsums, anhydrites; P_2ur – Tatar Stage. Lower Substage. Urzhum Horizon. Urzhum Series – clays, limestones, dolomites, marls, siltstones, sandstones
Kumertau	12	9.3	T_1 – pudding rocks, sandstones with bands of clays and siltstones; T_3sr – Surkai Formation. Clays with bands of siltstones and sandstones; $N^3_2 + Q_1s$ – Obschesyrt Formation. Clays, loams with lenses of sands and pebbles
Akyar	9	10.2	$J_{1–2}bm$ – Baymak Formation. Mica and carbonaceous clays, siltstones, clayey and mica sands, rare interbeds of brown coals, lenses of siderites; below this layer – sandy-gravely pebbles, carbonaceous clays with interbeds of coals, interbeds of brown-iron ores (30-270 m); aQ_H^1 – Lower Holocene. Alluvial deposits of the high floodplain. Sandy loams, loams, sands, gravel, pebbles (up to 24 m)
Tuimazy	7	11.9	P_1šš – Ufimian Stage. Sheshma Horizon. Sheshma Formation – sandstones, siltstones, pudding rocks, marls, limestones, dolomites, and gypsums; P_2kz_1 – Kazan Stage. Lower Substage – clays, marls, limestones, dolomites, siltstones, sandstones, pudding rocks, gypsums, anhydrites; P_2kz_2 – Kazan Stage. Upper Substage – clays, marls, limestones, dolomites, siltstones, sandstones, pudding rocks, rock salt, gypsums, anhydrites
Davlekanovo	4	17.5	P_1šš^1 – Ufimian Stage. Sheshma Horizon. Lower Formation. Pudding rocks, sandstones, siltstones, argillites (Kamyshin layers); P_1šš^2 – Ufimian Stage. Sheshma Horizon. Middle Formation. Argillites, siltstones, dolomites, limestones, sandstones (Buraev layers); N_2kn – Kinel Formation. Clays, sands and pebbles; $N_2^3ak_2 + ap$ – Akchagyl Middle Substage and Apsheron Stage. Clays, loams, sands, pebbles
Akhunovo	2	22.7	$\gamma\delta Pz_3$ – granodiorites and plagiogranites
Chekmagush	10	27.8	P_1šš^2 – Ufimian Stage. Sheshma Horizon. Middle Formation. Pudding rocks, sandstones, siltstones, argillites, marls, limestones (Buraev layers); P_1šš^3 – Ufimian Stage. Sheshma Horizon. Upper Formation. Pudding rocks, sandstones, siltstones, argillites with lenses of gypsums, dolomites, limestones (Chekmagushev layers)

The obtained data make it possible to conclude that the leading role in the variations of uranium content in the man-made carbonates is played by the specific features of subsurface geology on this territory. Thus, in the Davlekanovo and Chekmagush settlements the uranium concentration reached 17.5 and 27.8 mg/kg respectively, which may be due to uranium intake from the Lower Permian redbed sandstones, shallow crystalline basement, as well as the occurrence of oil fields in these areas, which contributes to the migration of uranium together with oil from deeper layers. A higher content of uranium (22.7 mg/kg) in the scale was also found in samples from the Akhunovo village, located on the Akhunovsky granite massif [43, 44].

When comparing data on the uranium content in the samples from Ufa and settlements of the Ufa district it should be noted that the samples collected in the district are characterized with a higher median content of uranium. Samples of the man-made carbonates were obtained in 18 settlements within the boundaries of the Ufa district. The uranium content varies from 1.2 (Mokrousovo) to 14.5 mg/kg (Nagaevo, Nikolaevka). The median content for samples from settlements in the Ufa district was 4.9 mg/kg, which is more than three times higher than the median concentration in samples from the city of Ufa.

One of the likely factors that explains such a big difference is the type of water supply: the vast majority of scale samples from the city of Ufa were collected in households with centralized water supply, while in the settlements of the Ufa district the samples were mostly collected in households with individual water supply (water wells, boreholes, springs, etc.). Availability of the centralized water supply significantly affects the use of various water treatment systems. Thus, at the Northern water intake the Ufavodokanal State Unitary Enterprise uses sorption treatment of water with powdered activated carbon, cyclic pressure-tank filters, high-rate filters with burnt rock as a locally produced filtering material [41].

The spatial distribution of uranium was assessed based on the results of defining the uranium content in samples collected on the territory of Ufa. Analysis of the schematic map in Fig.2 shows that there exists a homogeneous distribution of uranium in the man-made carbonates. Deviations were registered in individual points (southern part of the city, the left bank, the suburbs) where concentrations reach 29 mg/kg. These deviations are probably related to the following two factors: the material of the vessels where the water was boiled (Fig.2, location 1); the individual type of water supply (a well) (Fig.2, location 2). The probable impact of the vessel material is explained by the fact that within the same household, in addition to this particular sample that was collected for an all-metal kettle, three more samples were also obtained from three other kettles with the uranium content of 0.99; 1.25; and 1.31 mg/kg.

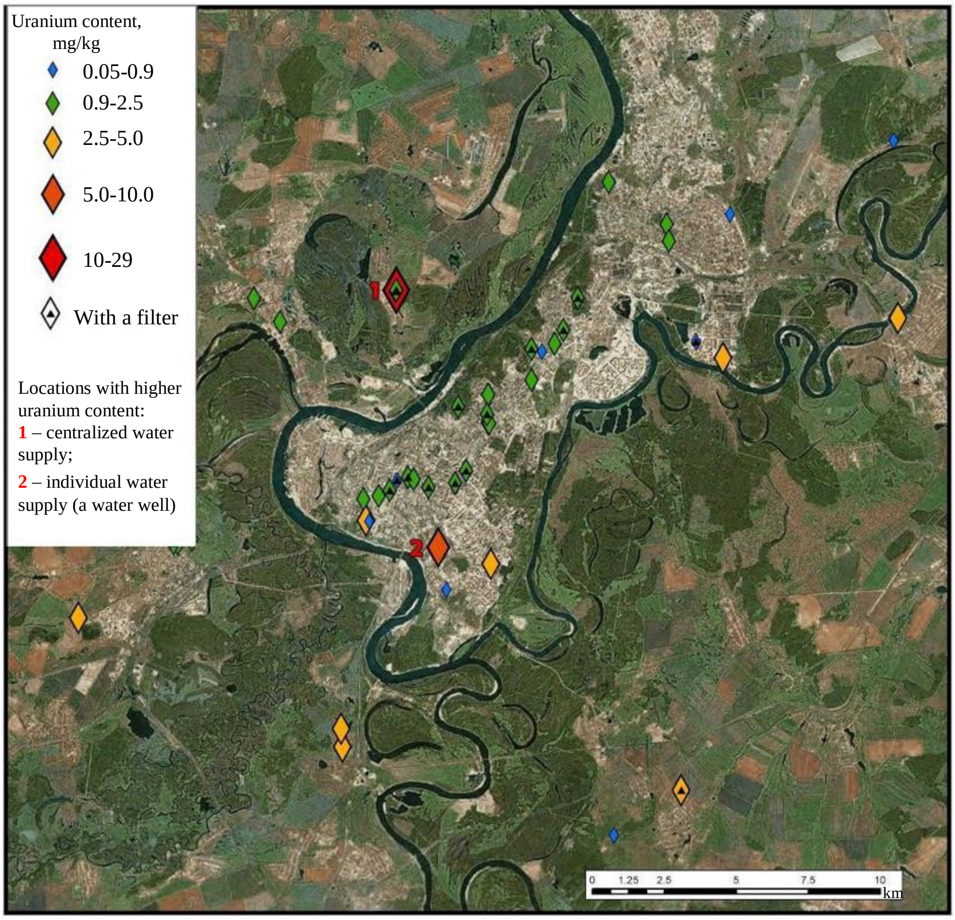

Fig.2. Spatial distribution of uranium content in samples of man-made carbonates collected in the city of Ufa

Data from 18 settlements in the suburban area of Ufa (Table 2) were taken for comparison. Individual water supply sources (water wells, boreholes, springs, etc.) are mainly developed within its boundaries. Analysis of the spatial distribution of uranium in the man-made carbonate samples in the territory of the Ufa district shows its heterogeneous nature (Fig.3). Halos of high concentrations of this chemical element are confined to the western and southwestern parts of the district (Bulgakovo, Dmitrievka, Marmylevo, Nikolaevka, Taptykovo, Nagaevo, Yumatovo), where the average content of uranium exceeds 10 mg/kg (Table 2).

In terms of their geological distribution within the territory of Ufa district, halos of the increased uranium content in the man-made carbonates are confined to the areas of loamy and clayey sediments (Upper Pliocene, Pleistocene, Holocene). A significant effect of the subsurface geology within this territory is explained by the fact that the vast majority of the man-made carbonate samples were obtained in households with individual water supply sources that do not typically have water treatment systems other than potable water filters (such as pitcher filters).

Effects of the water supply type (centralized/individual) and the filtering processes. Surveys conducted in the Tomsk and Pavlodar regions indicate that there exist significant differences regrading accumulation of chemical elements in the man-made carbonates depending on the type of the water supply source: in the case of the centralized water supply, concentrations of most chemical elements are significantly lower than those in water from the individual water supply sources [23, 24].

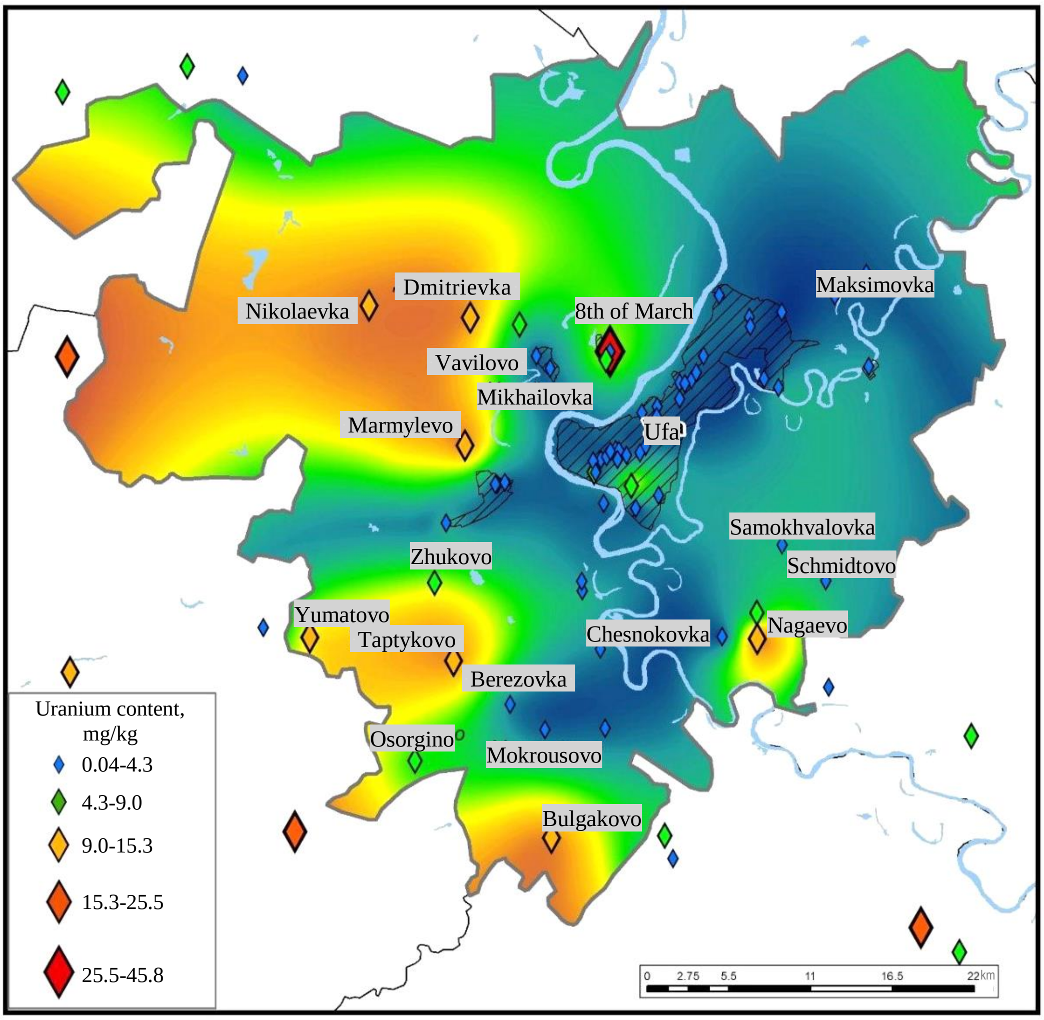

Fig.3. Spatial distribution of uranium content in samples of man-made carbonates collected in the territory of the Ufa district

Table 2

Uranium content in man-made carbonates from various settlements in the Ufa district

Settlement name	Number of samples	Content, mg/kg	Rocks/soils encountered on the day surface
Maksimovka	1	0.87	Q^1_{III} – Upper Quaternary, lower part. Loams, sandy loams, sands, pebbles
Mokrousovo	1	1.2	N_2kn – Kinel Formation. Clays, sands, pebbles
Chesnokovka	1	2.2	P_1ir – Kungurian Stage. Irensky Horizon. Anhydrites, gypsums, dolomites; P_1sk – Ufimian Stage. Solikamsk Horizon. Argillites, siltstones gypsified, limestones, dolomites; $P_1\check{s}\check{s}^1$ – Ufimian Stage. Sheshma Horizon. Lower Formation. Pudding rocks, sandstones, siltstones, argillites (Kamyshin layers); N_2kn – Kinel Formation. Clays, sands, pebbles
Berezovka	1	2.3	N_2kn – Kinel Formation. Clays, sands, pebbles
Mikhailovka	2	2.9	P_1u – Ufimian Stage. Limestones, marls, clays, siltstones, sandstones; N_2^3ak – Akchagyl Stage. Clays, siltstones, sands, pebbles; Q^1_{III} – Upper Quaternary, lower part. Loams, sands, pebbles; Q^2_{II} – Middle Quaternary sediments, upprt part. Clays, loams, sands, pebbles
Samokh-valovka	1	3.4	Q^1_{III} – Upper Quaternary, lower part. Loams, sandy loams, sands, pebbles; Q^2_{III} + Q_{IV} – Upper Quaternary, upper part and recent sediments combined. Loams, sands, muds, peats, pebbles
Schmidtovo	2	3.97	P_1kg – Kungurian Stage. Poorly defined sediments. Gypsums, anhydrites, salts, limestones
Vavilovo	1	5.2	N_2^3-Q_1 – Upper Pliocene – Lower Quaternary sediments. Sandy clays and loams with marl nodules, in some places with pebbles at the base
Osorgino	1	6.8	N_2^3akk – Akchagyl Stage. Middle Substage. Akkulayevsky Horizon. Sands, siltstones, clays, pebbles
8th of March	4	8.1	Q^1_{III} – Upper Quaternary, lower part. Loams, sands, pebbles; Q^2_{III}+Q_{IV} – Upper Quaternary, upper part and recent sediments. Topsoils, peats, loams, sands, pebbles
Zhukovo	4	8.5	$P_1\check{s}\check{s}^1$ – Ufimian Stage. Sheshma Horizon. Lower Formation. Pudding rocks, sandstones, siltstones, argillites (Kamyshin layers); P_1sk – Ufimian Stage. Solikamsk Horizon. Argillites, siltstones gypsified, limestones, dolomites; N_2kn – Kinel Formation. Clays, sands, pebbles
Yumatovo	1	10.4	$P_1\check{s}\check{s}^1$ – Ufimian Stage. Sheshma Horizon. Lower Formation. Pudding rocks, sandstones, siltstones, argillites (Kamyshin layers); $P_1\check{s}\check{s}^2$ – Ufimian Stage. Sheshma Horizon. Middle Formation. Argillites, siltstones, dolomites, limestones, sandstones (Buraev layers)
Taptykovo	1	13.4	P_1sk – Ufimian Stage. Solikamsk Horizon. Argillites, siltstones gypsified, limestones, dolomites; $P_1\check{s}\check{s}^1$ – Ufimian Stage. Sheshma Horizon. Lower Formation. Pudding rocks, sandstones, siltstones, argillites (Kamyshin layers); $P_1\check{s}\check{s}^2$ – Ufimian Stage. Sheshma Horizon. Middle Formation. Argillites, siltstones, dolomites, limestones, sandstones (Buraev layers); N_2kn – Kinel Formation. Clays, sands, pebbles
Dmitrievka	1	13.6	N_2^3-Q_1 – Upper Pliocene – Lower Quaternary sediments. Sandy clays and loams with marl nodules, in some places with pebbles at the base; N_2^3ak – Akchagyl Stage. Clays, siltstones, sands, pebbles
Bulgakovo	1	14.0	N_2kn – Kinel Formation. Clays, sands, pebbles
Marmylevo	1	14.1	P_1u – Ufimian Stage. Limestones, marls, clays, siltstones, sandstones; N_2^3ak – Akchagyl Stage. Clays, siltstones, sands, pebbles
Nagaevo	3	14.5	N_2^{2+3} – Middle and Lower Pliocene combined. Pebbles, sands, clays, ferruginous pudding rocks
Nikolaevka	1	14.5	P_1u – Ufimian Stage. Limestones, marls, clays, siltstones, sandstones

For this study, the selected man-made carbonate samples from Ufa were divided into two groups depending on the type of water supply. The results obtained make it possible to claim that the centralized water supply systems significantly reduce the uranium content in the man-made carbonates (4.0 mg/kg with the individual water supply, and 1.4 mg/kg with the centralized water supply) (Table 3). Decrease of uranium concentration is related to the water treatment processes used by water services company including the Ufavodokanal State Unitary Enterprise (sorption treatment of water with powdered activated carbon, cyclic pressure-tank filters, high-rate filters with burnt rock as a locally produced filtering material).

Table 3

Uranium content in man-made carbonates on the territory of Ufa depending on the type of water supply and filtering processes

Type of water supply	Number of samples	Median content of uranium, mg/kg
Centralized water supply:	35	1.4
with a filter	15	1.34
without a filter	19	1.43
Individual water supply	5	4.0

A wider introduction and development of the centralized type of water supply and, accordingly, methods of water pre-treatment (physical, chemical, physicochemical) can reduce not only the content of uranium, but also that of other chemical elements. It is especially important for rapidly developing urbanized areas, which include the territory of Ufa. This issue acquires a special significance in case the water supply source is confined to groundwater in quaternary sediments, as they are more vulnerable to man-made impact, including chemical, physical and biological contamination. This poses a serious threat to the health of the local population.

A possible impact of the original water source has been assessed. It is known that the water supply system of Ufa is based on the operation of eight water intakes (groundwater and river-type). The largest of them are the Southern water intake, with the maximum capacity of 240 thousand m^3/day, and the Northern the bucket-type with 200 thousand m^3/day. A total of 10 samples were collected to assess the possible impact of the original source of water supply: 5 in the northern part of the city and 5 in the southern part. The results turned out to be close in their values, i.e. 1.3 mg/kg in the north and 1.1 mg/kg in the south.

The study considers a possible influence of the household filtration process on the uranium content in the man-made carbonates: during the sampling the household owners were asked to provide information on the use of filters. A sufficient size is available only for samples collected from the centralized water supply: 15 samples with prefiltering prior to boiling (the Aquaphor, Barrier, and Geyser filter brands); 19 samples without prefiltering. The differences were minimal: 1.34 mg/kg for the samples where prefiltering was performed; 1.43 mg/kg for the samples without prefiltering. The study did not address the effect of the internal filtering material, as in each particular case the filter can be designed to entrap different substances.

Conclusion. The following conclusions were made based on the survey results:

- the average content of uranium in the man-made carbonates on the territory of Ufa is 1.44 mg/kg, which is three times lower than in the scale from the water of Lake Baikal, i.e. 4.51 mg/kg;
- the low values of uranium content in the scale are associated with the specific features of subsurface geology in the area, as most of the city is located within a distribution zone of gypsums and limestones;
- spatial distribution of uranium is described as homogeneous;
- significant differences were found between the uranium content in scale samples from the centralized (1.4 mg/kg) and the individual (4.0 mg/kg) types of water supply;
- no significant differences were revealed between the uranium content in the scale when comparing different sources of centralized water supply (the Northern bucket-type and the Southern infiltration water intakes) and the use of home filters.

The detected level of uranium content in the man-made carbonates on the territory of Ufa can be characterized as non-hazardous, since other investigations on the territory of the Pavlodar Region have shown that the maximum permissible concentration of uranium in water (0.015 mg/l according to SanPiN 1.2.3685-21) correlates with its content in the man-made carbonates (about 30 mg/kg) [24].

The authors are grateful to Professor L.P.Rikhvanov for his support of this research, to A.F.Sudyko and L.V.Bogutskaya from the Department of Geology at the Engineering School of Natural Resources of the Tomsk Polytechnic University for their analytical studies, and to the residents of the Republic of Bashkortostan who took part in this investigation.

REFERENCES

1. Baranovskaya N.V., Rikhvanov L.P., Ignatova T.N. et al. Essays on Geochemistry. Tomsk: Tomskii politekhnicheskii universitet, 2015, p. 378 (in Russian).

2. WHO. Guidelines for Drinking-water Quality: Fourth Edition Incorporating the First Addendum. Geneva: World Health Organization, 2017, p. 541.

3. Patel A.I., Hecht C.E., Cradock A. et al. Drinking Water in the United States: Implications of Water Safety, Access, and Consumption. *Annual Review of Nutrition*. 2020. Vol. 40, p. 345-373. DOI: 10.1146/annurev-nutr-122319-035707

4. McDonough L.K., Meredith K.T., Nikagolla C., Banati R.B. The influence of water-rock interactions on household well water in an area of high prevalence chronic kidney disease of unknown aetiology (CKDu). *Npj Clean Water*. 2021. Vol. 4. N 2. DOI: 10.1038/s41545-020-00092-0

5. Miller J., Workman C.L., Panchang S.V. et al. Water Security and Nutrition: Current Knowledge and Research Opportunities. *Advances in Nutrition*. 2021. Vol. 12. Iss. 6, p. 2525-2539. DOI: 10.1093/advances/nmab075

6. Bjørklund G., Semenova Y., Pivina L. et al. Uranium in drinking water: a public health threat. *Archives of Toxicology*. 2020. Vol. 94, p. 1551-1560. DOI: 10.1007/s00204-020-02676-8

7. Keith S., Faroon O., Roney N. et al. Toxicological Profile for Uranium. Agency for Toxic Substances and Disease Registry (US). Atlanta: Agency for Toxic Substances and Disease Registry, 2013, p. 526.

8. Bjørklund G., Christophersen O.A., Chirumbolo S. et al. Recent aspects of uranium toxicology in medical geology. *Environmental Research*. 2017. Vol. 156, p. 526-533. DOI: 10.1016/j.envres.2017.04.010

9. Ning Gao, Zhihui Huang, Haiqiang Liu et al. Advances on the toxicity of uranium to different organisms. *Chemosphere*. 2019. Vol. 237. N 124548. DOI: 10.1016/j.chemosphere.2019.124548

10. Konietzka R. Gastrointestinal absorption of uranium compounds – A review. *Regulatory Toxicology and Pharmacology*. 2015. Vol. 71. Iss. 1, p. 125-133. DOI: 10.1016/j.yrtph.2014.08.012

11. Minghao Ma, Ruixia Wang, Lining Xu et al. Emerging health risks and underlying toxicological mechanisms of uranium contamination: Lessons from the past two decades. *Environment International*. 2020. Vol. 145. N 106107. DOI: 10.1016/j.envint.2020.106107

12. Vengosh A., Coyte R.M., Podgorski J., Johnson T.M. A critical review on the occurrence and distribution of the uranium- and thorium-decay nuclides and their effect on the quality of groundwater. *Science of the Total Environment*. 2022. Vol. 808. N 151914. DOI: 10.1016/j.scitotenv.2021.151914

13. Darby S., Hill D., Auvinen A. et al. Radon in homes and risk of lung cancer: collaborative analysis of individual data from 13 European case-control studies. *British Medical Journal*. 2005. Vol. 330. DOI: 10.1136/bmj.38308.477650.63

14. Kheifets L., Swanson J., Yuan Y. et al. Comparative analyses of studies of childhood leukemia and magnetic fields, radon and gamma radiation. *Journal of Radiological Protection*. 2017. Vol. 37. N 2, p. 459-491. DOI: 10.1088/1361-6498/aa5fc7

15. UNSCEAR: sources, effects and risks of ionizing radiation UNSCEAR 2017. Report to the General Assembly Scientific Annexes A and B. New York: United Nations Publication, 2018. 184 p.

16. Zlobina A.N., Rikhvanov L.P., Baranovskaya N.V. Radioecological Hazard for the Population Living in the Regions with High Radioactive Granites. *Bulletin of the Tomsk Polytechnic University. Geo Assets Engineering.* 2019. Vol. 330. N 3, p. 111-125 (in Russian). DOI: 10.18799/24131830/2019/3/172

17. Maier A., Wiedemann J., Rapp F. et al. Radon Exposure – Therapeutic Effect and Cancer Risk. *International Journal of Molecular Sciences*. 2021. Vol. 22. Iss. 1. N 316. DOI: 10.3390/ijms22010316

18. Sahoo S.K., Jha V.N., Patra A.C. et al. Scientific background and methodology adopted on derivation of regulatory limit for uranium in drinking water – A global perspective. *Environmental Advances*. 2020. Vol. 2. N 100020. DOI: 10.1016/j.envadv.2020.100020

19. Zamora M.L., Tracy B.L., Zielinski J.M. et al. Chronic Ingestion of Uranium in Drinking Water: A Study of Kidney Bioeffects in Humans. *Toxicological Sciences*. 1998. Vol. 43. Iss. 1, p. 68-77. DOI: 10.1006/toxs.1998.2426

20. Gandhi T.P., Sampath P.V., Maliyekkal S.M. A critical review of uranium contamination in groundwater: Treatment and sludge disposal. *Science of the Total Environment*. 2022. Vol. 825. N 153947. DOI: 10.1016/j.scitotenv.2022.153947

21. Rikhvanov L.P., Baranovskaya N.V., Sudyko A.F. Chemical elements in the human body as the basis for implementation of medical geology concepts. *Gornyi zhurnal*. 2013. N 3, p. 37-42 (in Russian).

22. Farkhutdinov I., Farkhutdinova L., Zlobina A. et al. Historical aspects of medical geology. *Earth Sciences History*. 2020. Vol. 39. Iss. 1, p. 172-183. DOI: 10.17704/1944-6187-39.1.172

23. Mongolina T.A., Baranovskaya N.V., Soktoev B.R. Ultimate composition of salt scales in potable waters of the Tomsk Region. *Izvestiya Tomskogo politekhnicheskogo universiteta*. 2011. Vol. 319. N 1, p. 204-211 (in Russian)

24. Arynova Sh.Zh. Ultimate composition of salt formations from natural fresh waters as an indicator of ecological safety of water consumption: Avtoref. dis. … kand. geol.-mineral. nauk. Tomsk: Natsional'nyi issledovatel'skii Tomskii politekhnicheskii universitet, 2016, p. 22 (in Russian).

25. Soktoev B.R., Rikhvanov L.P., Matveenko I.A. Mineralogical and geochemical characteristics of drinking water salt deposits. XIX International Scientific Symposium in honor of Academician M.A.Usov "Problems of Geology and Subsurface Development", 6-10 April 2015, Tomsk, Russia. IOP Conference Series: Earth and Environmental Science. 2015. Vol. 27. N 012042. DOI: 10.1088/1755-1315/27/1/012042

26. Winde F., Erasmus E., Geipel G. Uranium contaminated drinking water linked to leukaemia – Revisiting a case study from South Africa taking alternative exposure pathways into account. *Science of the Total Environment*. 2017. Vol. 574, p. 400-421. DOI: 10.1016/j.scitotenv.2016.09.035

27. Evseeva L.S., Perel'man A.I., Ivanov K.E. Geochemistry of uranium in the hypergenesis zone. Moscow: Gosatomizdat, 1974, p.278 (in Russian).

28. Langmuir D. Uranium solution-mineral equilibria at low temperatures with applications to sedimentary ore deposits. *Geochimica et Cosmochimica Acta*. 1978. Vol. 42. Iss. 6, p. 547-569. DOI: 10.1016/0016-7037(78)90001-7

29. Silva R.J., Nitsche H. Actinide environmental chemistry. *Radiochimica Acta*. 1995. Vol. 70-71, p. 377-396. DOI: 10.1524/ract.1995.7071.special-issue.377

30. Mühr-Ebert E.L., Wagner F., Walther C. Speciation of uranium: Compilation of a thermodynamic database and its experimental evaluation using different analytical techniques. *Applied Geochemistry*. 2019. Vol. 100, p. 213-222. DOI: 10.1016/j.apgeochem.2018.10.006

31. Cumberland S.A., Douglas G., Grice K., Moreau J.W. Uranium mobility in organic matter-rich sediments: A review of geological and geochemical processes. *Earth-Science Reviews*. 2016. Vol. 159, p. 160-185. DOI: 10.1016/j.earscirev.2016.05.010

32. Geskeis H., Lützenkirchen J., Polly R. et al. Mineral-water interface reactions of actinides. *Chemical Reviews*. 2013. Vol. 113. Iss. 2, p. 1016-1062. DOI: 10.1021/cr300370h

33. Gurzhiy V.V., Kalashnikova S.A., Kuporev I.V., Plášil J. Crystal chemistry and structural complexity of the uranyl carbonate minerals and synthetic compounds. *Crystals*. 2021. Vol. 11. Iss. 6. N 704. DOI: 10.3390/cryst11060704

34. Elless M.P., Lee S.Y. Uranium solubility of carbonate-rich uranium-contaminated soils. *Water, Air, and Soil Pollution*. 1998. Vol. 107, p. 147-162. DOI: 10.1023/a:1004982515941

35. Kelly S.D., Rasbury E.T., Chattopadhyay S. et al. Evidence of a stable uranyl site in ancient organic-rich calcite. *Environmental Science and Technology*. 2006. Vol. 40. Iss. 7, p. 2262-2268. DOI: 10.1021/es051970v

36. Rihs S., Sturchio N.C., Orlandini K. et al. Interaction of uranyl with calcite in the presence of EDTA. *Environmental Science and Technology*. 2004. Vol. 38. Iss. 19, p. 5078-5086. DOI: 10.1021/es049847b

37. Zhiwei Niu, Xiaoyan Wei, Shirong Qiang et al. Spectroscopic studies on U(VI) incorporation into $CaCO_3$: Effects of aging time and U(VI) concentration. *Chemosphere*. 2019. Vol. 220, p. 1100-1107. DOI: 10.1016/j.chemosphere.2019.01.010

38. Farkhutdinova L.M., Farkhutdinov I.M. The Republic of Bashkortostan as a Ground for Research in Medical Geology. *Herald of the Academy of Sciences of the Republic of Bashkortostan*. 2017. Vol. 23. N 2 (86), p. 83-92 (in Russian).

39. Abdrakhmanov R.F., Buryachok O.V., Bakhtiyarov S.A. Formation of groundwaters in the city of Ufa. *Geologicheskii sbornik*. 2011. Vol. 9, p. 262-275 (in Russian).

40. Abdrakhmanov R.F. Hydrogeochemistry of Urban Territories in the Southern Fore-Ural Areas. *Geochemistry International*. 2019. Vol. 57. N 7, p. 812-820. DOI: 10.1134/S0016702919070036741

41. Quality of potable water. URL: https://www.ufavodokanal.ru/voda/water-quality (accessed 16.03.2021) (in Russian).

42. Valeev T.K., Sulejmanov R.A., Egorova N.N. et al. The Hygienic Characteristic of Risk of Influence of Quality of Water on Health of the Population of Large Industrial Centre. *Meditsina truda i ekologiya cheloveka*. 2016. N 3, p. 11-17 (in Russian).

43. Farkhutdinov I.M., Soktoev B.R., Rikhvanov L.P. Influence of Geological Factors on Uranium and Thorium Distribution in Drinking Water Salt Deposits (Republic Of Bashkortostan). *Bulletin of the Tomsk polytechnic university. Geo assets engineering*. 2020. Vol. 331. N 4, p. 16-27 (in Russian). DOI: 10.18799/24131830/2020/4/2590

44. Farkhutdinov I., Soktoev B., Zlobina A. et al. Influences of geological factors on the distribution of uranium in drinking water limescale in the junction zone of the East European Platform and the Southern. *Chemosphere*. 2021. Vol. 282. N 131106. DOI: 10.1016/j.chemosphere.2021.131106

45. Rikhvanov L.P., Yazikov E.G., Baranovskaya N.V., Yankovich E.P. Patent N 2298212 RF. A method to determine areas of environmental pollution with uranium. Pub. 27.04.2007. Bul. N 12. (in Russian)

46. Grigorev N.A. Distribution of chemical elements in the upper part of the continental crust. Ekaterinburg: UrO RAN, 2009, p. 382 (in Russian).

47. Soktoev B.R., Rikhvanov L.P., Arynova Sh.Zh., Baranovskaya N.V. Natural radioactive elements (Th, U) in salt scales of natural fresh waters. Materialy V Mezhdunarodnoi konferentsii “Radioaktivnost' i radioaktivnye elementy v srede obitaniya cheloveka”, 13-16 sentyabrya 2016, Tomsk, Rossiya. OOO “STT”, 2016, p. 599-603 (in Russian).

***Authors*: Iskhak M. Farkhutdinov,** *Candidate of Geological and Mineralogical Sciences, Academic Secretary, General Manager, https://orcid.org/0000-0001-8494-8154* (*Vernadsky State Geological Museum of the RAS, Moscow, Russia; OOO RN-BashNIPIneft, Ufa, Republic of Bashkortostan, Russia*), **Rustam R. Khayrullin,** *Leading specialist, hairullinrr@mail.ru, https://orcid.org/0000-0002-1318-2718* (*Ufa Federal Research Centre of the RAS, Ufa, Republic of Bashkortostan, Russia*), **Bulat R. Soktoev,** *Candidate of Geological and Mineralogical Sciences, Associate Professor, https://orcid.org/0000-0002-4102-4282* (*Tomsk Polytechnic National Research University, Tomsk, Russia*), **Anastasia N. Zlobina,** *Candidate of Geological and Mineralogical Sciences, Senior Lecturer, https://orcid.org/0000-0003-2748-8088* (*Bashkir State University, Ufa, Republic of Bashkortostan, Russia*), **Elena I. Chesalova,** *Researcher, https://orcid.org/0000-0003-3479-7241* (*Vernadsky State Geological Museum of the RAS, Moscow, Russia*), **Anvar M. Farkhutdinov,** *Candidate of Geological and Mineralogical Sciences, Researcher, https://orcid.org/0000-0003-4451-6052* (*CY Cergy Paris Université, Cergy-Pontoise, France*), **Andrey V. Tkachev,** *Doctor of Geological and Mineralogical Sciences, Chief Researcher, https://orcid.org/0000-0001-9714-8404* (*Vernadsky State Geological Museum of the RAS, Moscow, Russia*).

The authors declare no conflict of interests.

ISSN 2411-3336; e-ISSN 2541-9404

JOURNAL OF MINING INSTITUTE

Zapiski Gornogo instituta

Journal homepage: pmi.spmi.ru

Research article

Use of the UNIFAC model in the calculation of physicochemical properties of ecotoxicants for technological and ecoanalytical purposes

Vladimir G. POVAROV, Ignatyi I. EFIMOV ✉
Saint Petersburg Mining University, Saint Petersburg, Russia

How to cite this article: Povarov V.G., Efimov I.I. Use of the UNIFAC model in the calculation of physicochemical properties of ecotoxicants for technological and ecoanalytical purposes. Journal of Mining Institute. 2023. Vol. 260, p. 238-247. DOI: 10.31897/PMI.2023.41

Abstract. Modern development vector of environmental monitoring leads to elaboration of analytical methods for qualitative and quantitative analysis of different ecotoxicants. Many studies face the lack of information on isomers and homologues of already studied compounds. This problem cannot always be solved experimentally due to the difficulty of separating or synthesizing certain compounds; the use of group theories of solutions will help partly; using them, solubility in water or partition coefficient between two immiscible solvents is calculated for ecotoxicants. These parameters are important for solving the analytical and ecological problems. The partition coefficient in the octanol – water system is associated with a possibility of accumulation of different compounds in living organisms; the partition coefficient in the hexane – acetonitrile system can be used in gas chromatographic analysis. Solubility in water is closely associated with accumulation of ecotoxicants in water bodies, as well as with their ability to be transferred. This paper presents the capabilities of the UNIFAC model for solving physicochemical problems using the example of calculating the properties of real ecotoxicants on the basis of the available thermodynamic data. All the obtained calculated values were compared with those determined experimentally. In the case of pyrene derivatives, solubility data were obtained for the first time using a correlation group model to calculate the heat of fusion and melting temperature.

Keywords: UNIFAC; ecology; GCMS; identification; solubility; partition coefficient

Received: 27.01.2023 ***Accepted: 03.04.2023*** ***Online: 13.04.2023*** ***Published: 25.04.2023***

Introduction. Determination of physicochemical properties of ecotoxicants is an important task from the viewpoint of ecology and physical chemistry. Among such properties is the partition coefficient of a substance between two immiscible solvents, solubility in water, and octanol – water partition coefficient. Information about the partition coefficients in two-phase solvent systems can be used in sample preparation for extraction and subsequent analysis of toxic compounds [1, 2]. The partition coefficient octanol – water is of particular importance since it is associated with the ability of substances to penetrate through organic membranes [3]. Solubility in water is closely related to the ability of a substance to accumulate in water bodies, as well as to penetrate into groundwater [4]. All these physicochemical properties were studied only for a number of ecotoxicants, since some substances are either extremely difficult to separate in pure form, or they have not yet been synthesized. There are a large number of isomers and homologues for ecotoxicants, which are also toxic [5, 6]. An urgent problem is the development of methods for predicting the physicochemical properties of individual compounds based on their presumed structure.

The most common methods for predicting the properties of chemical compounds are the group approach methods. In these methods, the molecules are separated into fragments, most often functional groups. The most actively applied model realising this approach is the UNIFAC model [7]. It allows calculating the activity coefficients of individual components in a complex mixture by dividing them into separate fragments. For organic molecules, this approach is efficient since they are built from a limited set of functional groups. A set of groups CH_3, CH_2, CH, C and OH allows designing any alkane, cycloalkane or aliphatic alcohol, including a polyhydric one. For example, *n*-hexane (CH_3-$(CH_2)_4$-CH_3) consists of two CH_3 groups and four CH_2 groups. Ethanol contains one CH_3, one CH_2 and one OH group. Adding a group for ethers (C-O-C) and for esters (R_1OOR_2) it is possible to build molecules not only of ethers and esters, but also of hydroxyethers and hydroxyesters. For the consideration of amines, the NH_2 group is introduced, and for aromatic compounds, two groups of aromatic carbon are introduced – ACH – aromatic carbon with a hydrogen atom and AC – aromatic carbon without a hydrogen atom.

Some substances (CH_3OH, H_2O, CH_3CN) are distinguished as separate groups. Usually, these are the parent compounds of homologous series or substances that differ markedly in their properties from the typical organic substances. The ability to calculate the activity coefficients of components in the mixture allows estimating a large number of physicochemical properties using the equations of chemical thermodynamics. Using Raoult's law, it is possible to describe the liquid – vapour equilibrium, which is applied in modelling of rectification, distillation and evaporation [8, 9]. The Schroeder equation allows describing solubility in mixed solvents [10]. In the UNIFAC model, the activity factor is broken down into two components:

$$\ln\gamma = \ln\gamma_{comb} + \ln\gamma_{res}, \tag{1}$$

where γ is the activity coefficient; γ_{comb} – combinatorial component of the activity coefficient; γ_{res} – residual component of the the activity coefficient.

The combinatorial component takes into account the difference in the shape of molecules. The residual component is associated with energy interactions between molecules in solution. An obvious presence of the combinatorial component makes it possible to describe the properties of solutions of polymers and macromolecules [11]. In practice, all the parameters, which are necessary for the model, are determined by regression of experimental data based on liquid – vapour, liquid – liquid and solubility equilibria. Such an approach to describing the properties of multicomponent systems can be efficiently used in environmental monitoring and chemical analysis; further, it will be shown by the example of calculating the solubility and partition coefficients.

Methods. *Chromatographic analysis*. Chromatographic measurements were conducted on a Shimadzu GC-QP2010SE chromato-mass spectrometer equipped with an RTX-5MS column (30 m×0.25 mm×0.25 μm) of Restek Company. The chromatograph operated in a constant flow rate mode (1.03 ml/min). Helium was the carrier gas. Evaporator temperature was 250 °C. Injection volume was 1 μl, reset 20:1. The oven program consisted of an initial isotherm of 50 °C (for 10 min), then the temperature raised to 290 °C at a rate of 10 °C/min and was maintained for 10 min. Temperature of the ion source of mass detector equalled 200 °C, interface temperature was 290 °C. Mass scanning range was chosen as 45-500 m/z with imaging duration of 0.3 s.

Calculation of solubility according to the UNIFAC model. With a gradual change of the mole fraction of a component in solution from zero to one it is possible to find the equality point of both parts (if it exists at all). A smooth change in the composition of the solvent will correspond to a smooth change in the mole fraction of asphaltene. Thus, it is possible to construct a solubility isotherm using the Schroeder equation:

$$f = \left(\ln\left(\gamma_a x_a\right) + \frac{\Delta H_f}{R}\left(\frac{1}{T} - \frac{1}{T_f}\right)\right)^2, \tag{2}$$

where ΔH_f is the substance heat of fusion; T – temperature of the system; T_f – substance melting point; R – universal gas constant; x_a – mole fraction.

Calculation of the asphaltene solubility in one solvent was carried out by the dichotomy method (halving the segment). At each calculated point, the asphaltene activity coefficient was calculated according to the UNIFAC model, after which the error was determined from formula (2).

The calculation continued until the error became less than 10^{-20}. When calculating the solubility in two solvents, the solubility in one of the two-phase systems (in the absence of the third component) was taken as the first point. Then, there was a movement along the solubility line using the confidence interval method. The accuracy of the calculations was controlled by the calculation error.

Discussion of results. *Group approach in the calculation of partition coefficients for ecoanalytical purposes*. In gas chromatography-mass spectrometry (GCMS) analysis, some analytes might not be in the databases, which either completely excludes their identification or leads to erroneous identification. This problem is especially acute in analytical studies [12, 13] and in the development of modern technologies [14-16]. In this case, for many known ecotoxicants, several homologues or isomers can be proposed, which will have no less toxic properties, but will not be available in databases. For example, in the NIST MS 2018 mass spectra database, there are no mass spectra of any $C_{20}H_{18}$ tetramethyl pyrenes, although there are 16 substances with such a molecular formula in the database. These 16 spectra may well become a source of false identification, if tetramethyl pyrene is present in the analysed sample. At the same time, there are studies on the toxicity of pyrene [17], but the toxicity of its homologues was not investigated. If we take the extremely toxic 2,3,7,8-tetrachlorodibenzodioxine [18] as an example, there are no mass spectra of even a monomethyl derivative for it, and there are only two other substances with the same molecular formula. Due to the lack of information, any studies of the toxicity of such homologues and isomers will face the difficulty of their identification in complex matrices [19]. For this reason, it is important to identify the noninvestigated compounds and to increase the reliability of identification of the already studied compounds.

In practice other identification features can be used in addition to the mass spectrum. In case of identification on capillary columns the retention indices are applied [20], which make it possible to exclude the identification options that are unreliable for a given release time from the list of substances with similar mass spectra. It is possible to vary the ionization energy (in electron impact mass spectrometry, the energy of electrons in an ion source is varied). Sometimes, this makes it possible to reliably determine the molecular formula and even make reasonable assumptions about the structure of the analyte [21]. However, this significantly complicates the analysis and does not work well with substances with a weak intensity of molecular ion in the spectrum.

Back in the mid-1960s, it was proposed to use the partition coefficient K_d of a substance between two immiscible phases as an additional structure-dependent parameter for specifying the structure of molecules in gas chromatographic (GC) analysis [22]. Such a coefficient (concentration partition coefficient) is the ratio of the equilibrium concentrations of a substance distributed between two liquid phases. Examples of such phases are water – octanol, hexane – ethylene glycol solvent systems. During partition, polar substances will predominantly concentrate in a more polar solvent, and non-polar substances in a less polar one. If you take a mixture of methanol and heptane and distribute them between ethylene glycol and hexane, methanol will be collected in ethylene glycol, and heptane in hexane. If GC analysis of each phase is performed separately, then with equal volumes injected into the injector of the chromatograph, methanol partition coefficient can be calculated as the ratio of peak areas of methanol in the hexane and ethylene glycol phases:

$$K_{\mathrm{d}} = \frac{S_{\mathrm{hexane}}}{S_{\mathrm{eg}}}, \qquad (3)$$

where S_{hexane} is the peak area of the component in hexane phase; S_{eg} – peak area of the component in ethylene glycol phase.

On the one hand, this complicates the analysis, since now it is necessary to obtain two chromatograms instead of one. However, this allows solving several problems. First, each of the two chromatograms is simpler since not all sample components are present in the investigated phase. Secondly, by comparing the calculated partition coefficient of an unknown analyte with the known values, it can be used as an additional identification feature. Since the partition coefficient does not depend linearly on the retention index (which is also calculated from the chromatogram), the result is two independent identification features. When using mass spectrometric detector, it is possible to determine three independent identification features for each analyte. This methodology was successfully applied until the beginning of 1990 [23]. During this time, a number of important improvements were proposed. The list of the used solvent systems was expanded. First of all, this is due to hexane – acetonitrile system, an active use of which started in the analysis of essential oils and petroleum products [24]. In [25] a method for K_d measurement on the basis of an internal standard was proposed. A substance with a known partition coefficient was taken as a standard. Then, formula (3) for hexane – ethylene glycol pair of solvents is converted to the form

$$K_\mathrm{d} = K_\mathrm{st} \frac{S_\mathrm{hexane}}{S_\mathrm{eg}} \frac{S^\mathrm{st}_\mathrm{eg}}{S^\mathrm{st}_\mathrm{hexane}}, \tag{4}$$

where K_st is the partition coefficient of the standard; $S^\mathrm{st}_\mathrm{hexane}$ – peak area of the standard in the hexane phase; $S^\mathrm{st}_\mathrm{eg}$ – peak area of the standard in the ethylene glycol phase.

This modification makes it possible to avoid errors associated with inaccurate dosing of the sample into the chromatograph evaporator. Empirical formulas for calculating K_d of substances based on their known physicochemical properties, such as molecular weight, boiling point, number of carbon atoms in a molecule also appeared [26]. The LSER model [27, 28] that makes it possible to calculate the partition coefficients in previously studied solvent systems with a sufficiently high accuracy is most actively used in analytical practice. This made it possible to apply this method not only to confirm the results of identification, but also to check the assumptions about the structure of analyte molecules. However, the approach appeared to be much more efficient when the chromato-partition method was combined with group theories of solutions [29], which is due to a possibility of working with systems of solvents of variable composition. Group theories of solutions make it possible to estimate the partition coefficients for the non-investigated compounds.

Calculation of the activity coefficients of groups, and then of individual molecules, is rather complicated, but its result can be easily applied to the calculation of the K_d value. As an example, let us consider a system of α and β phases. For a two-phase equilibrium, the activities of any component i distributed between phases are equal to each other. Thermodynamic activity of a_i is equal to the product of the activity coefficient γ_i and the mole fraction of the component x_i, provided that it is normalized to a pure substance. Normalization is interpreted as a choice of composition at which the activity coefficient is assumed to be equal to one. Now, it is possible to write down the condition of thermodynamic equilibrium of phases:

$$\gamma_{\alpha,i} x_{\alpha,i} = \gamma_{\beta,i} x_{\beta,i}, \tag{5}$$

where α and β indicate the belonging of characteristics to phases α and β.

After transformations we get:

$$K_x = \frac{\gamma_{\alpha,i}}{\gamma_{\beta,i}} = \frac{x_{\beta,i}}{x_{\alpha,i}}. \tag{6}$$

K_x value is the ratio of mole fractions of the component in coexisting phases and differs from K_d value only by a simple factor equal to the ratio of molar volumes of the same phases,

$$K_\mathrm{d} = K_x \frac{V_\alpha}{V_\beta}, \tag{7}$$

where V_α and V_β are molar volumes of α and β phases.

Using equations (5)-(7) for any organic molecule that can be built from the known groups with the known parameters, it is possible to calculate the partition coefficient. The calculated value can then be compared with the measured value, and the assumptions about the structure of the analyte can be verified. It appears that the partition coefficient is a rather structure-sensitive parameter. Thus, for 3-carene and α-terpinene (general formula $C_{10}H_{16}$, both are components of the essential oil of coniferous plants), the Kovats retention indices are 1011 and 1018 [30]. Mass spectrum of these substances consists of ion series with the main masses 41-43; 77-79; 93; 121 and 136. In the conditions of routine GC-MS analysis on a 30-meter column, a difference in retention indices of 100 units corresponds to 1-2 min of time, i.e., the difference in the release time of these substances is from 3 to 6 s. This is not enough to reliably distinguish between substances. However, the situation changes when the partition coefficients are taken into account. For the hexane – acetonitrile system, K_d values are 6.7 and 4.3 for 3-carene and α-terpinene, respectively [23]. UNIFAC calculations give values of 7.5 and 4.4, which are extremely close to the experimental values. It is important to note that for any data set, the partition coefficient for 3-carene is 1.55-1.7 times higher than that for α-terpinene. This is a quite measurable difference and, therefore, the substances can be distinguished.

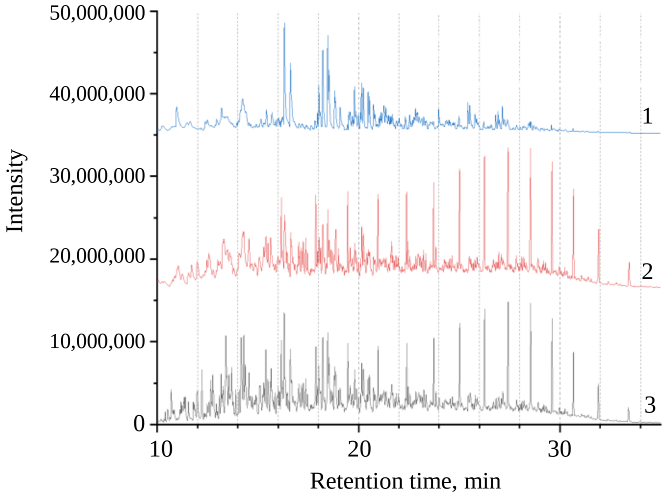

Fig.1. General view of chromatograms of equilibrium solutions of diesel fuel in acetonitrile (1); hexane (2) and initial diesel fuel (3).
Chromatograms are shifted from each other by a constant without distortion of peak heights

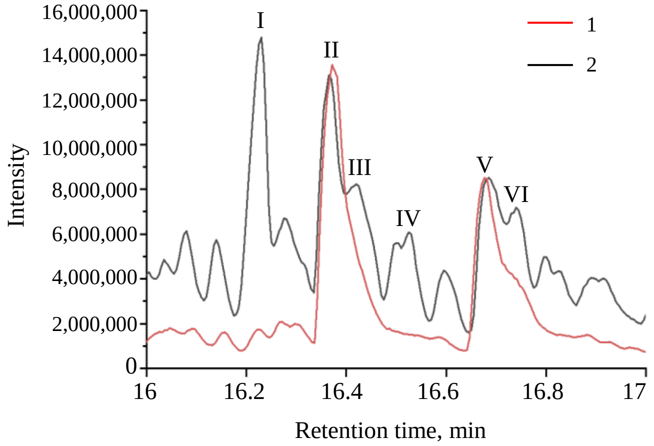

Fig.2. Section of chromatograms shown in Fig.1, in the interval of release time 16-17 min
1 – hexane extract; 2 – acetonitrile extract

One example of using this approach is the identification of polyaromatic compounds in middle-distillate petroleum products. Figure 1 illustrates the possibilities of the chromato-partition method. A sample of commercial diesel fuel was taken as an object. Six largest peaks in the centre of the chromatogram (1) are mono-, di- and trimethyl naphthalenes. Large peaks in the right part of the chromatogram (2) of the hexane phase are C_{14}-C_{22} n-alkanes. If there was no interphase partition, chromatogram (3) would be observed, obtained by summing lines 1 and 2 (original fuel). It can be seen that in this case, many peaks would simply overlap each other.

Figure 2 shows a section of the chromatogram of hexane and acetonitrile phases. Two large peaks can be found on the chromatogram of acetonitrile extract, while there are more of them in the hexane phase. Peak I is an n-alkane, peaks III and IV are isomeric alkanes, peaks II and V are isomers of methyl naphthalene, peak VI is an alkyl derivative of benzene with a long radical. There is a clear tendency of non-aromatic compounds to concentrate in the hexane phase, which makes it possible to analyse them separately and calculate the partition coefficient as an additional identification feature. In addition to identification of aromatic compounds, this approach can also be useful in the study of other fuel components [31].

Figure 3 shows the degree of correlation between the calculated and experimental values of the partition coefficients of methyl naphthalenes and anthracene. It can be seen that model calculations correlate well with experimental data. This makes it possible to use the partition coefficients calculated according to the UNIFAC model as an additional identification feature. In a similar way, it is possible to identify different polyaromatic and heterocyclic compounds: methyl derivatives of naphthalene, anthracene, fluorene, biphenyl, tetrahydro naphthalene, dibenzothiophene, dibenzofuran, carbazole [29].

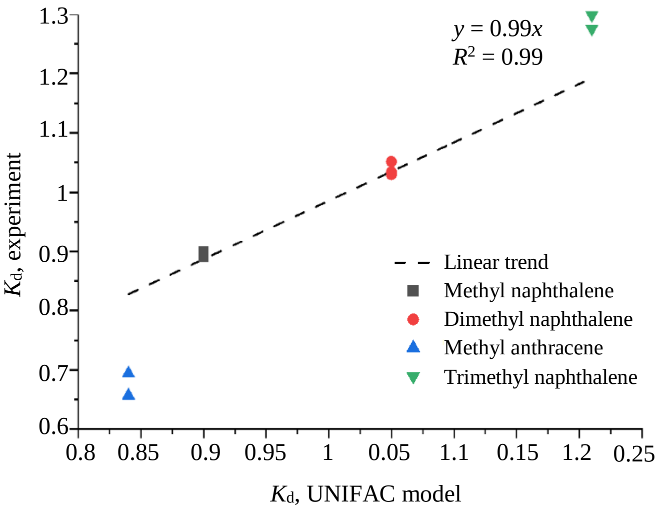

Fig.3. Calculated and experimental values of partition coefficients of some components of diesel fuel

Group approach in calculating the solubility of ecotoxicants in water and hydrocarbons. In mass spectrometry the use of partition coefficients is of an auxiliary nature, whereas in modelling of natural and technological processes these values are included in the list of the main ones. One of the most important indicators of any ecotoxicant is its solubility in water. However, if the substance is not in the database and is not isolated as a pure compound, the only way to estimate the solubility is to calculate it. Even if the solubility data are available, there is a possibility of experimental error due to the fact that the solubility of many ecotoxicants in water is very low (10-100 μg/l). The UNIFAC model makes it possible to calculate the solubility of such substances, for this it is necessary to take into account the effects of fusion of the substance under study. In practice such accounting is made using the Schroeder – van Laar equation. Since melting points of many important ecotoxicants are much higher than 0 °C, only the heat and fusion of the ecotoxicant should be taken into account when calculating the solubility in water. According to the Schroeder – van Laar equation, in this case, the activity of an ecotoxicant calculated according to the UNIFAC model in a solution, which is in equilibrium with a solid ecotoxicant, is related to the heat of fusion and melting temperature of the substance by the following formula:

$$\ln(\gamma x) = \frac{\Delta_f H}{R}\left(\frac{1}{T_f} - \frac{1}{T}\right). \tag{8}$$

It can be seen that the right side of formula (8) does not depend on the composition of solution. This means that it can be considered as a constant factor when calculating the total activity coefficient of the ecotoxicant:

$$\ln\gamma = \ln\gamma_{unifac} + \ln\gamma_f = \ln\gamma_{comb} + \ln\gamma_{res} + \ln\gamma_f. \tag{9}$$

With such a calculation of solubility, the main difficulty may be the lack of information on the heat of fusion of an ecotoxicant. However, it is possible to calculate these values using group contribution methods [32]. In such methods, a certain physical property of a substance is estimated as a linear combination of the contributions of individual molecular groups. For example, for the heat of fusion, the equation will look as:

$$\Delta_f H = H_{fus,0} + \sum_i N_i H_{fus,1} + \sum_j M_j H_{fus,2} + \sum_k O_i H_{fus,3}, \tag{10}$$

where N_i, M_j, O_i are the numbers of groups of the first, second and third order in the molecule; $H_{fus,1}$, $H_{fus,2}$, $H_{fus,3}$ – the contribution of each group to the heat of fusion; $H_{fus,0}$ – constant value.

First order groups are the simplest functional groups. For example, methyl (CH_3), hydroxo (OH) or aromatic with hydrogen (ACH). Groups of the second and third orders are combinations of simple groups; it is necessary to take them into account for correcting the obtained values with regard for the mutual influence of closely spaced groups or the shape of a molecule. Pyrene molecule in this calculation will consist of 16 groups of the first order (6 AC and 10 ACH) and 4 groups of the third order (two conjugations of aromatic rings according to the type of phenalene and two conjugations of aromatic rings of the phenanthrene type). The value calculated in this way is 421 K, which is extremely close to the experimentally determined value of 424 K [33].

Table 1 presents the results of solubility calculations for several important ecotoxicants and their homologues. It can be seen that the discrepancies between the calculated and experimental values are one order of magnitude. In the case of methyl and ethyl pyrene, the values were obtained using the calculated heat of fusion. Although a discrepancy of one order is significant for analytical practice, in the case of solubility estimation such accuracy will be sufficient. When working with the non-investigated substances, such an estimated calculation is, in fact, the only method for determining the solubility of ecotoxicants in mixed solvent systems.

Table 1

Examples of calculating the solubility of ecotoxicants according to the UNIFAC model (equation (8)

Substance	Formula	Equilibrium mole fraction	Heat of fusion, J/mol	Solubility, mg/l	Experimental solubility, mg/l
DDT, 1,1,1-trichloro-2,2-bis(4-chlorophenyl)ethane	$C_{14}H_9Cl_5$	$9.60\cdot10^{-9}$	26,280 [34]	$1.9\cdot10^{-1}$	$2.5\cdot10^{-2}$ [35]
DDE, 1,1-dichloro-2,2-bis(*p*-chlorophenyl) ethylene	$C_{14}H_8Cl_4$	$1.00\cdot10^{-7}$	23,550 [36]	1.8	$1.2\cdot10^{-1}$ [35]
Hexachloroethane	C_2Cl_6	$3.10\cdot10^{-6}$	9,750 [33]	$4.1\cdot10^{1.}$	$1.1\cdot10^{2}$ [37]
Hexachlorane	$C_6H_6Cl_6$	$3.1\cdot10^{-8}$	25,930 [38]	$5.0\cdot10^{-1}$	7.3 [39]
Benzpyrene	$C_{20}H_{12}$	$4.70\cdot10^{-11}$	14,700 [34]	$6.6\cdot10^{-4}$	$3.8\cdot10^{-3}$ [37]
Pyrene	$C_{16}H_{10}$	$2.50\cdot10^{-9}$	16,700 [33]	$2.8\cdot10^{-2}$	$1.3\cdot10^{-1}$ [37]
Methyl pyrene	$C_{17}H_{12}$	$1.60\cdot10^{-9}$	18,283*	$1.9\cdot10^{1}$	No data
Ethyl pyrene	$C_{18}H_{14}$	$1.30\cdot10^{-9}$	17,922*	$1.7\cdot10{,}000^{1}$	No data

---

*Values obtained from formula (10).

Group models of solutions are used to solve the environmental and technological problems in the calculation of solubility diagrams for hydrocarbon mixtures. Such a calculation itself would be a standard physicochemical problem if the researchers had exhaustive data on physicochemical properties of components. However, in practice the researchers face the lack of information about the system under consideration [40]. When preparing fuel for marine engines, fuel oil or other residual products of deep oil refining (oil tar, visbreaker tar) are often added to it. Since the solubility of high-molecular non-volatile products in fuels based on *n*-alkanes is low, for increasing it, it is necessary to add a diesel fraction with a high content of aromatic compounds to the fuel. The resulting fuel should be stable and, at the same time, meet a number of environmental and economic requirements [41]. Among the environmental constraints, one of the most important is low sulphur content in fuel (less than 0.5 wt.% according to the requirements of the International Maritime Organization). This value is easy to calculate if sulphur content in the residual product is known (sulphur content in the initial volatile diesel fractions is much lower and can usually be neglected) and the concentration of the residual product. Solubility in a mixture of alkanes and substituted arenes depends on their ratio and should be determined experimentally. The situation is complicated by the fact that such solutions are usually dark and can precipitate with time. For this reason, the calculation of the solubility of such compounds is an important ecological problem, which can also be solved using group models.

Molecular and group composition of the alkane-arene mixture can be determined from the data of GC-MS analysis. If the group and molecular composition of the residual product is known, it is possible to calculate its solubility using the Schroeder formula. The problem is that the residual products are also multicomponent, and it is customary to distinguish four main classes of compounds in their composition: paraffins, aromatic compounds, resins, and asphaltenes. This classification is based on SARA analysis. This is the procedure for successive isolation of the four above fractions using a set of solvents. Asphaltenes are the first to precipitate from the residual fuel; therefore, the remaining components only contribute to the change in the composition of the solvent. In order to correctly take into account these changes, it was proposed to use the average molecular weights of each of the above groups and the results of infrared (IR) spectroscopy and nuclear magnetic resonance (NMR). In this case, the molecular weight can be determined by cryoscopy or from the solvent vapour pressure.

At the stage of choosing a solvent for cryoscopy, UNIFAC model calculations are very useful. The UNIFAC model makes it possible to choose such a solvent, the solution of the substance in which will be close to ideal, for asphaltenes it appeared to be benzene. In addition to the average molecular weight, the elemental composition (or the equivalent average gross formula of the simulated compound) is needed for calculations, as well as IR or NMR spectra, which allow to determine the composition of the functional groups present in the compound. Based on these data, the group composition of an average molecule of asphaltene or hydrocarbon mixture can be obtained. As an example, Table 2 shows the group composition of asphaltenes of various compositions in the range of molecular weights 617-1,574 g/mol. The group composition was calculated based on the fact that only the AC, ACH, CH_2, and CH_3 groups are present in the asphaltene molecule. Thus, if the asphaltene empirical formula had the form C_NH_M, then the number of groups was calculated using the system of equations

$$\begin{cases} \mathrm{N}(\mathrm{AC}) + \mathrm{N}(\mathrm{ACH}) + \mathrm{N}(\mathrm{CH_2}) + 1 = \mathrm{N}; \\ \mathrm{N}(\mathrm{ACH}) + 2\mathrm{N}(\mathrm{CH_2}) + 3 = \mathrm{M}; \\ \mathrm{N}(\mathrm{ACH}):\mathrm{N}(\mathrm{AC}) = k, \end{cases} \tag{11}$$

where N(AC), N(ACH), and N(CH_2) are the numbers of UNIFAC groups comprised in one asphaltene molecule (the number of CH_3 groups is assumed to be one); k is the ratio of the number of ASN groups to the number of AC groups.

Parameter k can be estimated from the NMR spectroscopy data, or one of the known polyaromatic compounds can be taken as a sample. Thus, for benzopyrene $k = 11/8 = 1.375$. Such calculations can be performed even with N and M not rounded to integers and not rounding the obtained values of N(AC), etc. As an illustration of this method, Fig. 4 shows the solubility isotherms of asphaltenes with characteristics from Table 2 in mixtures of two diesel fractions. Fraction 1 consists mainly of alkanes and isoalkanes (98 wt.%), and fraction 2 of aromatic compounds (75 wt.%). As can be seen from the calculation results, asphaltenes dissolve better in highly aromatized fractions; also with an increase in molecular weight the solubility in alkane fractions decreases significantly.

Table 2

Data on composition and molecular weight of different asphaltenes [42]

Parameter	Sample 1	Sample 2	Sample 3
M_w, g/mol	617	1,135	1,574
C, wt.%	89.18	86.14	87.65
H, wt.%	5.68	6.39	6.5
S, wt.%	2.45	5.5	3.22
AC	20.9	33.1	46.5
ACH	15.9	25.3	35.6
CH_2	8.1	22.1	31.9
CH_3	1	1	1

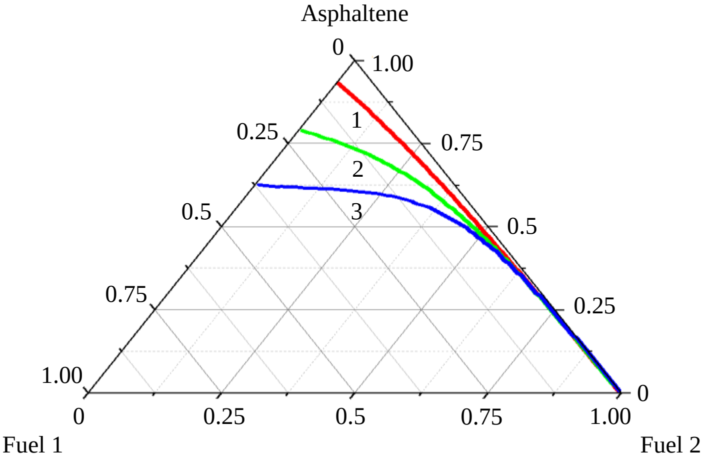

Fig.4. Calculated asphaltene solubility isotherms (1-3) from Table 2 at a temperature of 373 K

Conclusion. The given examples do not exhaust the application field of group theories of solutions for solving technological and ecoanalytical problems. The efficiency of such application depends on the availability and reliability of the physicochemical characteristics of the substances under study. These characteristics can be determined both experimentally and using different correlation dependences. In this work, it was demonstrated that the UNIFAC model can give satisfactory results when calculating the solubility of ecotoxicants in water and can also be used in the estimation of partition coefficients in two-phase systems.

REFERENCES

1. Ponomareva M.A., Cheremisina O.V., Mashukova Y.A., Lukyantseva E.S. Increasing the efficiency of rare earth metal recovery from technological solutions during processing of apatite raw materials. *Journal of Mining Institute*. 2021. Vol. 252, p. 917-926. DOI: 10.31897/PMI.2021.6.13

2. Sudarikov S.M., Yungmeister D.A., Korolev R.I., Petrov V.A. On the possibility of reducing man-made burden on benthic biotic communities when mining solid minerals using technical means of various designs. *Journal of Mining Institute*. 2022. Vol. 253, p. 82-96. DOI: 10.31897/PMI.2022.14

3. Cumming H., Rücker C. Octanol-Water Partition Coefficient Measurement by a Simple ^{1}H NMR Method. *ACS Omega*. 2017. Vol. 2. N 9, p. 6244-6249. DOI: 10.1021/acsomega.7b01102

4. Roy D.N., Goswami R., Pal A. The insect repellents: A silent environmental chemical toxicant to the health. *Environmental Toxicology and Pharmacology*. 2017. Vol. 50, p. 91-102. DOI: 10.1016/j.etap.2017.01.019

5. Gonçalves N.P.F., Vargaet Z., Nicol E. et al. Comparison of Advanced Oxidation Processes for the Degradation of Maprotiline in Water-Kinetics, Degradation Products and Potential Ecotoxicity. *Catalysts*. 2021. Vol. 11. Iss. 2. N 240. DOI: 10.3390/CATAL11020240

6. Pashkevich M.A., Kharko P.A. The use of a composite mix to remove metals from acidic drainage waters at tailings facilities. *Obogashchenie rud*. 2022. N 4, p. 40-47 (in Russian). DOI: 10.17580/or.2022.04.07

7. Fredenslund A., Jones R.L., Prausnitz J.M. Group-contribution estimation of activity coefficients in nonideal liquid mixtures. *AIChE Journal*. 1975. Vol. 21. N 6, p. 1086-1099. DOI: 10.1002/aic.690210607

8. Rodriguez-Donis I., Gerbaud V., Joulia X. Thermodynamic Insights on the Feasibility of Homogeneous Batch Extractive Distillation. 4. Azeotropic Mixtures with Intermediate Boiling Entrainer. *Industrial & Engineering Chemistry Research*. 2012. Vol. 51. N 18, p. 6489-6501. DOI: 10.1021/ie2019432

9. Seyf J.Y., Shojaeian A. Vapor-liquid (azeotropic systems) and liquid-liquid equilibrium calculations using UNIFAC and NRTL-SAC activity coefficient models. *Fluid Phase Equilibria*. 2019. Vol. 494, p. 33-44. DOI: 10.1016/J.FLUID.2019.04.029

10. Coto B., Suárez I., Tenorio M.J., Huerga I. Extraction of aromatic and polyaromatic compounds with NMP: experimental and model description. *Fluid Phase Equilibria*. 2022. Vol. 554. N 113293. DOI: 10.1016/J.FLUID.2021.113293

11. Pazuki G., Seyfi Kakhki S. A hybrid GMDH neural network to investigate partition coefficients of Penicillin G Acylase in polymer-salt aqueous two-phase systems. *Journal of Molecular Liquids*. 2013. Vol. 188, p. 131-135. DOI: 10.1016/j.molliq.2013.10.001

12. Raupov I., Burkhanov R., Lutfullin A. et al. Experience in the Application of Hydrocarbon Optical Studies in Oil Field Development. *Energies*. 2022. Vol. 15. Iss. 10. N 3626. DOI: 10.3390/EN15103626

13. Khalifa A.A., Bazhin V.Y., Ustinova Y.V., Shalabi M.E.K. Study of the kinetics of the process of producing pellets from red mud in a hydrogen flow. *Journal of Mining Institute*. 2022. Vol. 254, p. 261-270. DOI: 10.31897/PMI.2022.18

14. Kudinova A.A., Poltoratckaya M.E., Gabdulkhakov R.R. et al. Parameters influence establishment of the petroleum coke genesis on the structure and properties of a highly porous carbon material obtained by activation of KOH. *Journal of Porous Materials*. 2022. Vol. 29. Iss. 5, p. 1599-1616. DOI: 10.1007/S10934-022-01287-1

15. Leusheva E., Alikhanov N., Morenov V. Barite-Free Muds for Drilling-in the Formations with Abnormally High Pressure. *Fluids*. 2022. Vol. 7. Iss. 8. N 268. DOI: 10.3390/FLUIDS7080268

16. Sergeev V.V., Cheremisina O.V., Fedorov A.T. et al. Interaction Features of Sodium Oleate and Oxyethylated Phosphoric Acid Esters with the Apatite Surface. *ACS Omega*. 2022. Vol. 7. Iss. 3, p. 3016-3023. DOI: 10.1021/acsomega.1c06047

17. Bielská L., Kah M., Sigmund G. et al. Bioavailability and toxicity of pyrene in soils upon biochar and compost addition. *Science of the Total Environment*. 2017. Vol. 595, p. 132-140. DOI: 10.1016/J.SCITOTENV.2017.03.230

18. Mehrle P.M., Buckler D.R., Little E.E. et al. Toxicity and bioconcentration of 2,3,7,8-tetrachlorodibenzodioxin and 2,3,7,8-tetrachlorodibenzofuran in rainbow trout. *Environmental Toxicology and Chemistry*. 1988. Vol. 7. Iss. 1, p. 47-62. DOI: 10.1002/ETC.5620070108

19. Pashkevich M.A., Bykova M.V. Methodology for thermal desorption treatment of local soil pollution by oil products at the facilities of the mineral resource industry. *Journal of Mining Institute*. 2022. Vol. 253, p. 49-60. DOI: 10.31897/PMI.2022.6

20. Xiaoli Wei, Imhoi Koo, Seongho Kim, Xiang Zhang. Compound identification in GC-MS by simultaneously evaluating the mass spectrum and retention index. *The Analyst*. 2014. Vol. 139. Iss. 10, p. 2507-2514. DOI: 10.1039/C3AN02171H

21. Alam M.S., Stark C., Harrison R.M. Using Variable Ionization Energy Time-of-Flight Mass Spectrometry with Comprehensive GC×GC to Identify Isomeric Species. *Analytical Chemistry*. 2016. Vol. 88. Iss. 8, p. 4211-4220. DOI: 10.1021/acs.analchem.5b03122

22. Bowman M.C., Beroza M. Identification of Compounds by Extraction *p*-Values Using Gas Chromatography. *Analytical Chemistry*. 1966. Vol. 38. Iss. 11, p. 1544-1549. DOI: 10.1021/ac60243a022

23. Isidorov V.A., Zenkevich I.G., Dubis E.N. et al. Group identification of essential oils components using partition coefficients in a hexane-acetonitrile system. *Journal of Chromatography A*. 1998. Vol. 814. Iss. 1-2, p. 253-260. DOI: 10.1016/S0021-9673(98)00398-7

24. Tkachenko K.G., Zenkevich I.G. The Essential Oil of the Flowers of *Heracleum antasiaticum* Manden. Grown in Russia. *Journal of Essential Oil Research*. 1993. Vol. 5. Iss. 2, p. 227-228. DOI: 10.1080/10412905.1993.9698208

25. Berezkin V.G., Pankov A.G., Loshchilova V.D. Combined partition-chromatographic methods. *Chromatographia*. 1976. Vol. 9. Iss. 10, p. 490-496. DOI: 10.1007/BF02282661

26. Isidorov V.A., Kotowska U., Vinogorova V.T. GC Identification of Organic Compounds Based on Partition Coefficients of Their TMS Derivatives in a Hexane-Acetonitrile System and Retention Indices. *Analytical Sciences*. 2005. Vol. 21. Iss. 12, p. 1483-1489. DOI: 10.2116/analsci.21.1483

27. Poole C.F. Partition constant database for totally organic biphasic systems. *Journal of Chromatography A*. 2017. Vol. 1527, p. 18-32. DOI: 10.1016/j.chroma.2017.10.061

28. Poole C.F., Karunasekara T., Ariyasena T.C. Totally organic biphasic solvent systems for extraction and descriptor determinations. *Journal of Separation Science*. 2013. Vol. 36. Iss. 1, p. 96-109. DOI: 10.1002/jssc.201200709

29. Efimov I., Povarov V.G., Rudko V.A. Comparison of UNIFAC and LSER Models for Calculating Partition Coefficients in the Hexane-Acetonitrile System Using Middle Distillate Petroleum Products as an Example. *Industrial & Engineering Chemistry Research*. 2022. Vol. 61. Iss. 27, p. 9575-9585. DOI: 10.1021/acs.iecr.2c01093

30. Adams R.P., González-Elizondo M.S., González-Elizondo M., Slinkman E. DNA fingerprinting and terpenoid analysis of Juniperus blancoi var. huehuentensis (Cupressaceae), a new subalpine variety from Durango, Mexico. *Biochemical Systematics and Ecology*. 2006. Vol. 34. Iss. 3, p. 205-211. DOI: 10.1016/J.BSE.2005.11.004

31. Rekhletskaya E.S., Ershov M.A., Savelenko V.D. et al. Unraveling the Superior Role of Characterizing Methyl Ester of Isohexene as an Innovative High-Octane Gasoline Mixing Component. *Energy & Fuels*. 2022. Vol. 36. Iss. 19, p. 11829-11838. DOI: 10.1021/acs.energyfuels.2c01973

32. Marrero J., Gani R. Group-contribution based estimation of pure component properties. *Fluid Phase Equilibria*. 2001. Vol. 183-184, p. 183-208. DOI: 10.1016/S0378-3812(01)00431-9

33. Domalski E.S., Hearing E.D. Heat Capacities and Entropies of Organic Compounds in the Condensed Phase. Volume III. *Journal of Physical and Chemical Reference Data*. 1996. Vol. 25. Iss. 1, p. 1-525. DOI: 10.1063/1.555985

34. Acree W.E. Thermodynamic properties of organic compounds: enthalpy of fusion and melting point temperature compilation. *Thermochimica Acta*. 1991. Vol. 189. Iss. 1, p. 37-56. DOI: 10.1016/0040-6031(91)87098-H

35. Toxicological Profiles. ATSDR. URL: https://www.atsdr.cdc.gov/toxprofiledocs/index.html (accessed 02.11.2022).

36. Donnelly J.R., Drewes L.A., Johnson R.L. et al. Purity and heat of fusion data for environmental standards as determined by differential scanning calorimetry. *Thermochimica Acta*. 1990. Vol. 167. Iss. 2, p. 155-187. DOI: 10.1016/0040-6031(90)80476-F

37. IUPAC-NIST Solubility Database, Version 1.1. URL: https://srdata.nist.gov/solubility/ (accessed 30.05.2022). DOI: 10.18434/T4QC79

38. Sabbah R., Xu Wu An. Enthalpies de fusion et de sublimation de l'isomère γ d'hexachlorocyclohexane. *Thermochimica Acta*. 1991. Vol. 178, p. 339-341. DOI: 10.1016/0040-6031(91)80326-E

39. Richardson L.T., Miller D.M. Fungitoxicity of Chlorinated Hydrocarbon Insecticides in Relation to Water Solubility and Vapor Pressure. *Canadian Journal of Botany*. 1960. Vol. 38. N 2, p. 163-175. DOI: 10.1139/b60-015

40. Rogachev M.K., Aleksandrov A.N. Justification of a comprehensive technology for preventing the formation of asphalt-resin-paraffin deposits during the production of highlyparaffinic oil by electric submersible pumps from multiformation deposits. *Journal of Mining Institute*. 2021. Vol. 250, p. 596-605. DOI: 10.31897/PMI.2021.4.13

41. Gabdulkhakov R.R., Rudko V.A., Pyagay I.N. Methods for modifying needle coke raw materials by introducing additives of various origin (review). *Fuel*. 2022. Vol. 310. Part A. N 122265. DOI: 10.1016/J.FUEL.2021.122265

42. Gauthier T., Danial-Fortain P., Merdrignac I. et al. Studies on the evolution of asphaltene structure during hydroconversion of petroleum residues. *Catalysis Today*. 2008. Vol. 130. Iss. 2-4, p. 429-438. DOI: 10.1016/j.cattod.2007.10.005

***Authors*: Vladimir G. Povarov,** *Doctor of Chemical Sciences, Scientific Supervisor of the Project of the Administrative Staff of the Scientific Centre "Assessment of Technogenic Transformation of Ecosystems", https://orcid.org/0000-0001-6710-0514 (Saint Petersburg Mining University, Saint Petersburg, Russia)*, **Ignatyi I. Efimov,** *Postgraduate Student, efimov.ignaty@gmail.com, https://orcid.org/0000-0002-1748-7172 (Saint Petersburg Mining University, Saint Petersburg, Russia).*

The authors declare no conflict of interests.

ISSN 2411-3336; e-ISSN 2541-9404

JOURNAL OF MINING INSTITUTE

Zapiski Gornogo instituta

Journal homepage: pmi.spmi.ru

Research article

Production of biodiesel fuel from vegetable raw materials

Natalia K. KONDRASHEVA, Anzhelika M. EREMEEVA ✉
Saint Petersburg Mining University, Saint Petersburg, Russia

***How to cite this article*:** Kondrasheva N.K., Eremeeva A.M. Production of biodiesel fuel from vegetable raw materials. Journal of Mining Institute. 2023. Vol. 260, p. 248-256. DOI: 10.31897/PMI.2022.15

Abstract. One way to reduce the amount of harmful emissions from diesel fuel could be the replacement of part of the fuel with biofuel. Research is related to the production of biodiesel fuel in three ways: transesterification of vegetable oils; esterification of fat acids extracted from vegetable oil; and hydroprocessing of vegetable oils using catalysts in the diesel hydrotreatment process. Food and non-food oils, monatomic and diatomic alcohols were used to produce biodiesel fuel. Optimal parameters of vegetable oil transesterification have been determined: temperature; raw material ratio (oil/alcohol); mixing speed; time; type of process catalyst. The characteristics of the obtained biodiesel fuel samples were studied and compared with each other as well as with the requirements of EN 14214 "Automotive fuels. Fat acid methyl ethers for diesel engines. General technical requirements" and EN 590:2009 "EURO diesel fuel. Technical specifications". With regard to the physical and chemical characteristics of biodiesel fuel, the best way to produce it is by transesterification of vegetable oils. However, all fuels can be used as components of a blended environmentally friendly diesel fuel.

Keywords: biofuel; esterification; transesterification; hydroprocessing; vegetable oil; biodiesel fuel; complex ethers

Received: 20.01.2022 ***Accepted: 06.04.2022*** ***Online: 19.01.2023*** ***Published: 25.04.2023***

Introduction. Due to the shortage of oil reserves and the low level of oil refining (85 %), there is a need in European countries [1] to create technologies for the production of alternative fuels [2, 3]. Biodiesel is one of the most demanded fuels [4, 5], since most of the countries' transport sector consists of vehicles equipped with a diesel engine. Its main disadvantage is the amount of harmful emissions formed during the combustion of fuel, which is several times higher than the established standard. Therefore, most researchers consider the development of new types and compositions of biodiesel as a priority task.

Ethanol accounts for 74 % of all liquid biofuel, biodiesel for 22 % and green diesel for 4 %. The leaders in consumption of these fuels are the USA (46 %), Brazil (24 %), Europe and others (15 %) [6, 7].

In Russia, vehicles with diesel engine are in less demand than in Europe, but even there this form of transport is gaining popularity due to the obvious advantages of renewable biodiesel [8, 9], such as improved environmental properties (lower emissions of dispersed particles and volatile organic compounds during combustion [10], increased lubricity and high cetane number).

In European countries, the main raw material for biodiesel production is rapeseed oil, in the USA – soybean or corn oil, in Canada – canola oil, and some countries process palm oil to produce motor fuel component. The development of biofuels is increasing every year, for example, Emissions Reduction Alberta is investing in the development of a biodiesel plant in the Canadian province of Alberta.

Biodiesel testing and quality control have a special place in the biodiesel production process [11, 12]. New test methods according to American standards 14105 and ASTM D6584 are considered to be the most promising for assessing fuel quality. If a fuel fails to pass the quality test then it is refined and then retested. According to the European standard EN14214 [13] (Table 1) the following indicators, such as ether content, density, kinematic viscosity, flash point, sulphur content, cetane number, etc. are regulated in biodiesel. These indicators determine the possibility to use this type of fuel in the internal combustion engine: high viscosity impairs its pumping ability in the fuel supply system; low flash point of biofuel prevents timely ignition of the air-fuel mixture in the engine chamber.

Table 1

Basic requirements of EN14214 for biodiesel fuel [14]

Indicator	Test method	Maximum value	Minimum value
Ether content, %	EN 14103	–	96.5
Density at 15 °C, kg/m^3	EN ISO 3675, EN ISO 12185	900	860
Kinematic viscosity at 40 °C, mm^2/s	EN ISO 3104	5	3.5
Flash point in a closed crucible, °C	ISO/CD 3679	–	120
Sulphur content, ppm	EN ISO 20846, EN ISO 20884	10	–
Cetane number, units	EN ISO 5165	–	51

Methodology. The main methods of biodiesel production worldwide are: transesterification of vegetable oils and animal fats; esterification of fat acids extracted from vegetable oils; hydrogenation or hydroprocessing of vegetable oils [12, 15].

The esterification process of fat acids contained in vegetable oil is based on the interaction of organic acids with alcohols using a catalyst, leading to the formation of complex ethers [6]. The reaction follows a nucleophilic substitution mechanism [16-18] (Fig.1).

Organic acids (C15-C17) extracted from sunflower oil were used as raw material for the fuel. The second component for the synthesis was diatomic alcohol (ethylene glycol) and an acidic catalyst was used. After reaction time, the light ether phase (target product) was separated from the heavy phase – glycerol with catalyst [19] – by settling, centrifugation and distillation. After obtaining the fuel, the main characteristics of the product were studied and compared with the properties of raw material (Table 2).

The basic components of the synthesized fuel are ethers of fat acids contained in sunflower oil. Qualitative and quantitative composition for ester part of biodiesel was studied by chromatography-mass spectrometry (Agilent 5973, DB-Petro column, length 100 m) (Table 3). The content of ethers in the product was 77.78 % mass (Fig.2) [20, 21].

Table 3 shows that the best vegetable raw materials for the production of biodiesel are semi-dry oils, as the reacted acids are mainly linoleic, oleic and elaidic, which are contained in maximum quantity in this type of oil.

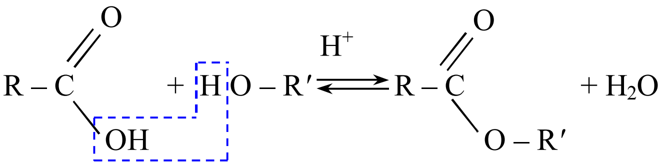

Fig.1. The mechanism for the esterification process of fat acids

Table 2

Operational characteristics of fat acids in sunflower oil and biodiesel fuel produced by esterification

Indicator	Biodiesel fuel	Fat acids of sunflower oil
Density at 20 °C, kg/m^3	914.00	909.78
Viscosity at 40 °C, mm^2/s	23.250	27.995
Flash point in a closed crucible, °C	112	115
Sulphur content, ppm	71	13
Lubricity (corrected wear spot diameter) at 60 °C, μm	202	157

Table 3

Component composition for the ester part of biodiesel fuel produced by esterification of sunflower oil fat acids with ethylene glycol

Name	Content, % mass
Methyl ether of linoleic acid	1.21
Methyl ether of oleic acid	0.49
Ethyl ether of linoleic acid	1.47
2,3-Dihydroxypropyl ether of linoleic acid	40.12
Oxyethyl ether of elaidic acid	24.48
Glycerol ether of elaidic acid	6.53
Oxyethyl ether of stearic acid	2.75
Cetyl ether of tranexamic acid	0.73

Once the synthesis is completed and the heavy phase is removed, the mixture requires additional purification because, in addition to the ester mixture, unreacted acids, alcohol and other compounds remain in the light phase (Fig.2). These substances must be removed as they can corrode engine parts and affect the oxidative stability of the fuel.

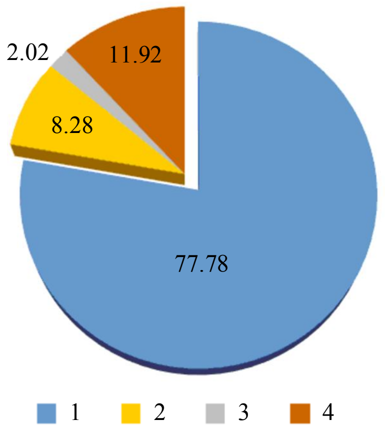

Fig.2. Group composition of biodiesel fuel produced by the esterification of sunflower oil fat acids with ethylene glycol

1 – ethers; 2 – acids; 3 – toluene; 4 – others, %

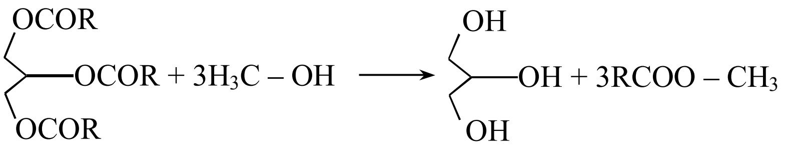

Fig.3. Transesterification process of vegetable oils

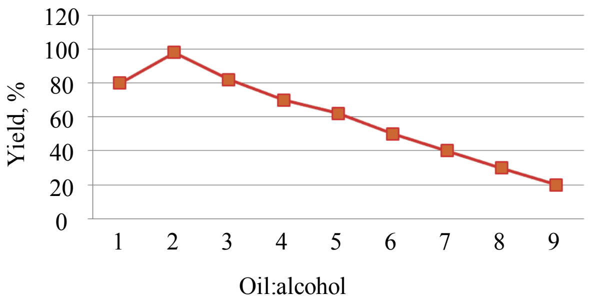

Fig.4. Yield curve of product on fractions of oil per share of alcohol

The second common method of biodiesel production consists of the transesterification of vegetable oils [22], a reaction of the interaction of triglycerides with alcohol leading to the formation of esters and glycerol (Fig.3) [23-25].

For synthesis of esters by transesterification, normal butyl alcohol, non-food raw material (red oil) and food oils (linseed and corn oil) were used. Concentrated sulphuric acid was chosen as a catalyst [1, 18]. The reagent mixture of ethylene glycol and vegetable oil was prepared in three-neck 250 ml flask. To choose the most suitable composition different ratios of the mixture were tried. Dependence of product yield on oil/alcohol ratio is shown in Fig.4.

The unit for the transesterification of vegetable oil consisted of an upper-drive mixer equipped with a water trap, a reverse water cooler, a sand bath and a thermometer. During the method testing for biodiesel production, temperature, mixing speed and time were the varying parameters of the process in addition to the raw material ratio (oil:alcohol). Mixing intensity was adjusted on mixer by setting 200, 250 and 300 rpm (Fig.5).

The transesterification of vegetable oil with diatomic alcohol was carried out at temperatures 140, 175 and 195 °C (Fig.6). The choice of the temperature range is due to the following reasons: at lower temperatures the reaction proceeds very slowly, higher temperatures require higher pressure, because the boiling point of diatomic alcohol is 197 °C.

The product yield also depends on the duration of the transesterification reaction of vegetable oils. The duration of the experiments was 150, 180, 200, 240 and 300 min (Fig.7).

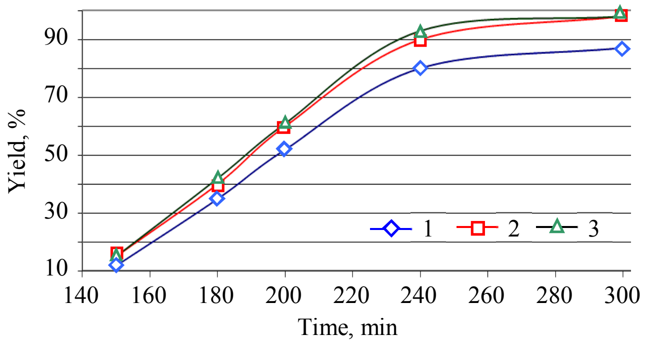

Fig.5. Curves for dependence of reaction rate on the mixing intensity at 195 °C

1 – 200; 2 – 250; 3 – 300 rpm

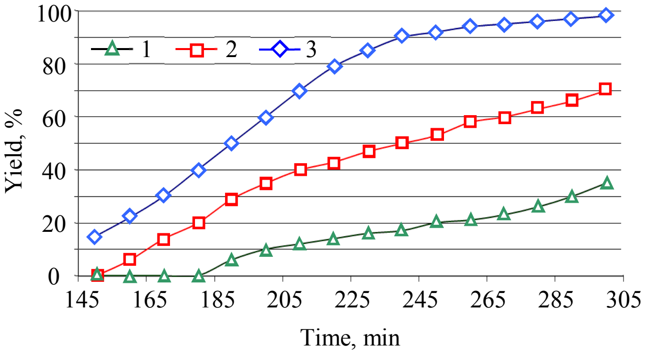

Fig.6. Curves for dependence of product yield on transformation time at a mixing speed of 250 rpm at different temperatures

1 – 140; 2 – 175; 3 – 195 °C

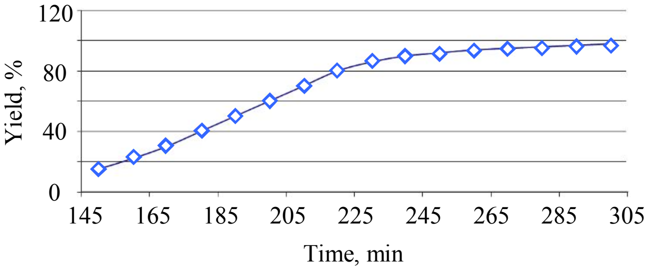

Fig.7. Curve for dependence of raw material conversion rate on mixing time at 195 °C

At the end of the experiments the product mixture was cooled down and settled for 3-4 days, then ether and glycerol phase were separated [5, 26, 27]. The main part of the acid after the reaction is concentrated in the glycerol phase [28]. The remaining part of the acid in the ether phase was neutralized with Na_2CO_3. The ether was flushed several times with hot water and separated into layers to separate the neutralized acid and water from the ether part. Then the ether was separated from the water in a separating funnel. The dewatered Na_2SO_4 was added to the separated ether for 60 min to remove any remaining water, followed by filtration.

The esterification products of red, linseed and corn oils were designated *n*-BERO (normal butyl ether of red oil), *n*-BELO (normal butyl ether of linseed oil) and *n*-BECO (normal butyl ether of corn oil), respectively (Table 4).

Table 4

Physical and chemical properties of butyl ether mixture obtained by by transesterification of red, linseed and corn oils

Indicator	*n*-BERO	*n*-BELO	*n*-BECO
Ether content, %	96.5	95	94
Density at 20 °C, kg/m^3	0.8766	0.8700	0.8758
Viscosity at 40 °C, mm^2/s	4.572	5.000	4.492
Flash point in a closed crucible, °C	150	135	120
Sulphur content, ppm	5.5	6.8	8.5
Cetane number, units	56	53	51
Lubricity at 60 °C, µm	553	601	592

Based on the data of Table 4, the best raw material for biodiesel production by transesterification method should be considered red oil, because *n*-BERO is characterized by the lowest values of sulphur content (5.5 ppm) and corrected wear spot diameter (553 µm). The mixture also has the highest flash point (150 °C) and cetane number (56 units).

The main components of the synthesized fuels are ethers of fat acids contained in vegetable oils. Qualitative and quantitative composition of ether part of biodiesel produced by transesterification of oil from red oil with *n*-butanol (Table 5) showed that the ether content in the yield was 60.03 % mass [14].

Table 5

Component composition of the ether part of biodiesel fuel, obtained by transesterification of red oil with n-butanol

Component	Content, % mass
Butyl ether:	
caprylic acid	0.90
capric acid	5.26
lauric acid	0.25
myristic acid	0.31
oleic acid	8.94
palmitic acid	10.43
pelargonic acid	0.87
acetic acid	1.86
elaidic acid	8.86
enanthic acid	0.86
Dibutyl ether:	
glutaric acid	0.23
pelargonic acid	0.49
sebacic acid	3.07
Methyl ether:	
linoleic acid	3.39
eicosenoic acid	6.36
Hexadecene ether of elaidic acid	6.57
Dimethylethyl ether of propenoic acid	0.49
Ether of Carbamic acid	0.89

Biodiesel fuel synthesized by the transesterification of red oil with *n*-butanol contains unreacted fat acids, unreacted alcohol and by-products in addition to complex ethers. Residual fat acids can be isolated from this fuel and introduced into anti-wear additives approved for use in Russia.

The third way of biodiesel fuel production consists in hydrocracking of lipids over sulphide or noble metal containing catalysts to form a mixture of hydrocarbons enriched with normal and *iso*-C15-C18 components. The main advantages of "green diesel" include full compatibility with oil diesel fuel [29], stability during storage because of the absence of oxygen-containing and unsaturated compounds, as well as environmental safety caused by the absence of aromatic hydrocarbons.

When triglycerides are hydroformed into diesel hydrocarbons, the following reactions take place [30]:

- hydrogenation of unsaturated bonds;
- hydrocracking with the formation of saturated fat acids and propane;
- deoxygenation of fat acids along the reactions of:
  – decarboxylation $R_x - COOH \rightarrow R_x - H + CO_2$;
  – hydrodecarbonylation $R_x - COOH + H_2 \rightarrow CO + H_2O + R_x - H$;
  – hydrogenation/dehydration $R_x - COOH + 3H_2 \rightarrow 2H_2O + R_x - CH_3$, where $x = 15, 17$;
- hydrocarbon isomerisation $n\text{-}R_x - CH_3 \rightarrow iso\text{-}R_x - CH_3$;
- hydrocarbon cracking $n\text{-}R_x - CH_3 \rightarrow n\text{-}R_y - CH_3 + n\text{-}R_z - CH_3$, where $y, z < x$.

Sunflower oil was used to produce biodiesel fuel samples using the hydrocracking method. The process was carried out in the boiling temperature range of the main fraction 180-360 °C on a $NiMo/Al_2O_3$ catalyst. The product was separated into three main fractions: gas fraction, water fraction and organic fraction. The main fuel characteristics of sample 1 "green diesel" synthesized using sulfide catalyst and sample 2 synthesized using noble metal based catalyst are presented in Table 6.

Table 6

Physical and chemical properties of "green diesel" samples obtained in the process of sunflower oil hydrocracking

Indicator	Sample 1	Sample 2
Density at 15 °C, kg/m^3	786.38	784.67
Sulphur content, ppm	50	0
Flash point in a closed crucible, °C	79	82
Lubricity at 60 °C, µm	582	606
Kinematic viscosity at 40 °C, mm^2/s	3.4273	3.2679
Fractional composition:		
at 250 °C, % vol.	4	4
at 350 °C, % vol.	96	98
95 % vol. is distilled at a temperature of, °C	355	304
Cetane number, units	79	80
Pour point, °C	16	4
Cloud point, °C	20	9
Content of fat acid methyl ethers, % vol.	–	–
Ash content, % mass	0.0083	0.0096

The main regulation document, according to which diesel fuel is produced at Russian refineries, is GOST R 52368-2005 "EURO diesel fuel. Technical Conditions". It meets all the requirements of the European standard EN 590 and limits the sulfur content in diesel fuel to 350 (Euro-3), 50 (Euro-4) and 10 ppm (Euro-5), and increases the cetane number to 51 (not less than 45 according to GOST 305-82).

Table 6 and parameters of the standard EN 590:2009 show that characteristics of samples 1 and 2 of "green diesel" do not meet the requirements of the standard by such indicators as the lubricity (exceeds the norm 1.5 times) and the cloud point of 20 and 9 °C, respectively (the standard is –22 °C). Qualitative and quantitative composition of diesel fraction (boiling range 150-350 °C), which is a part of samples 1 and 2, was studied (Table 7) by the method of gas chromatography (device Chromos, column DB-1, length 100 m).

Table 7

Component composition of diesel fractions for samples 1 and 2 obtained in the process of sunflower oil hydrocracking

Name	Content, % mass		Name	Content, % mass	
	Sample 1	Sample 2		Sample 1	Sample 2
iso-Decans	0.36	0.44	*n*-Pentadecans	2.87	3.15
iso-Decan	0.55	0.31	*iso*-Hexadecans	0.26	6.55
iso-Undecans	0.30	0.48	*n*-Hexadecan	4.74	2.89
iso-Undecan	0.39	0.28	*iso*-Heptadecans	1.57	24.26
iso-Dodecans	0.26	0.57	*n*-Heptadecan	32.36	27.63
n-Dodecan	0.30	0.24	*iso*-Octadecans	2.94	12.94
iso-Tridecans	0.17	0.59	*n*-Octadecan	49.22	13.43
n-Tridecan	0.26	0.26	*iso*-Nonadecans	1.22	1.74
iso-Tetradecans	0.18	0.63	*n*-Nonadecan	0.44	0.42
n-Tetradecan	0.28	0.22	*iso*-Eicosans	0.67	1.13
iso-Pentadecans	0.18	1.69	*n*-Eicosan	0.48	0.15
Total:				100.00	100.00

According to Table 7 the diesel fraction of sample 1 is dominated by *n*-heptadecan and *n*-octadecane, the content of which is 81.58 % mass. This composition causes high values of pour point (16 °C), cetane number (79 units) and poor lubricity (corrected wear spot diameter 582 μm) of the sample 1 "green diesel". On the contrary, the diesel fraction of sample 2 is dominated by *iso*-hexadecans, *iso*-heptadecans and *iso*-octadecans, their content reaching 43.75 % mass. Despite practically the same lubricating properties and cetane number, sample 2 has better low-temperature properties (lower pour point is 4 °C and cloud point is 9 °C). The advantage of sample 2 is the almost total absence of sulphur, so it can be used not only in Euro-5, but also in Euro-6 fuels.

Discussion of the results. Analysis of the characteristics of biodiesel fuels (Tables 2, 4, 6), shows that the best method for obtaining this type of fuel is the transesterification of vegetable oils, namely red oil, as almost all physical and chemical properties of this sample meet many requirements of EN 590:2009 standard for diesel fuel. Samples obtained by hydrocracking of vegetable oils need to be refined before they can be used in a diesel engine. Biodiesel fuel produced by the esterification of fat acids complies with the specifications of EN 590:2009. However, when comparing the characteristics of these fuels, it was found that after transesterification the fuel has better characteristics.

In the process of vegetable oil, transesterification with diatomic alcohol (ethylene glycol) in laboratory synthesis it is most rational to use temperature 195 °C, because with increasing of temperature the rate of target reaction is also increasing. However, because boiling point of ethyleneglycol is 197 °C, it is not reasonable to reach it. The longer the reaction time, the higher the selectivity of the process. Thus, time of reaction should be about 240 min, and further increasing of reaction time will make energy expenses considerably higher than target product obtained. The optimum composition is a ratio by mass (oil:alcohol) of 2:1, or 103:50 g.

Biodiesel fuel produced by the transesterification of vegetable oils is reasonable to use in engines in mixture with hydrotreated diesel fuel, otherwise engine reconstruction will be required, or engine life will be reduced, because pure biodiesel fuel has slightly higher viscosity than hydrotreated diesel fuel, and lubricating ability is worse [8, 31]. However, when using biodiesel fuel as a component of commercial diesel fuel [32], this indicator is improved more than twice.

In order to use samples 1 and 2 in a diesel engine as a commercial diesel fuel it is necessary to improve their characteristics to the requirements of EN 590:2009, namely research into improving their lubricating and low-temperature properties by introducing anti-wear and depressor-dispersant additives [33], which is a standard procedure in refineries when preparing commercial diesel fuel. This suggests that the technology will not become more expensive.

When using biodiesel fuel produced by transesterification and esterification, the environmental characteristics of the fuel are improved at the same time [13, 34]: the amount of sulphur remains at Euro-5 levels (less than 10 ppm); the carbon monoxide content in exhaust gases is reduced by 13-71 % at maximum engine load and by 26-48 % at partial load (75 %), depending on the number of rpm; the modified hydrocarbon concentration in exhaust gases is reduced by 5-31 % (at maximum load) and by 31-46 % (at partial load (75 %); exhaust gases smokiness is reduced to 65 %.

Conclusion. The considered ways of biodiesel fuel production from different plant raw materials will allow to expand the field of fuel resources and improve the quality of commercial fuels. One of the alternative options to bring the quality of fuel to the required standards is the compounding of the obtained samples with hydrotreated low-sulphur diesel fuel in a ratio of not less than 50 % mass of hydrotreated diesel fuel [5, 35-37]. Production of biodiesel using food raw materials such as corn and sunflower oil is not sustainable as it poses a great risk of food and fuel competition, leading to higher food prices and the threat of hunger. Non-food raw materials, such as red oil, are considered promising and environmentally friendly for biodiesel production.

REFERENCES

1. Litvinenko V.S., Sergeev I.B. Innovations as a Factor in the Development of the Natural Resources Sector. *Studies on Russian Economic Development*. 2019. Vol. 30, p. 637-645. DOI: 10.1134/S107570071906011X

2. Anchita K. HYDRO-IMP technology for upgrading of heavy petroleum. *Journal of Mining Institute*. 2017. Vol. 224, p. 229-234. DOI: 10.18454/PMI.2017.2.229

3. Kazamia E., Smith A.G. Assessing the environmental sustainability of biofuels. *Trends in plant science*. 2014. Vol. 19. Iss. 10, p. 615-618. DOI: 10.1016/j.tplants.2014.08.001

4. Dvoretsky S.I., Zazulya A.N., Nagornov S.A. et al. Biodiesel Production from Organic Raw Materia. *Problems of Contemporary Science and Practice Vernadsky University*. 2012. S2 (39), p. 126-135 (in Russian).

5. Sultanbekov R., Islamov Sh., Mardashov D. et al. Research of the influence of marine residual fuel composition on sedimentation due to incompatibility. *Journal of Marine Science and Engineering*. 2021. Vol. 9. Iss. 10. N 1067. DOI: 10.3390/jmse9101067

6. Korshunov G.I., Eremeeva A.M., Drebenstedt P. Justification of the use of a vegetal additive to diesel fuel as a method of protecting underground personnel of coal mines from the impact of harmful emissions of diesel-hydraulic locomotives. *Journal of Mining Institute*. 2021. Vol. 247, p. 39-47. DOI: 10.31897/PMI.2021.1.5

7. Pashkevich M.A. Classification and environmental impact of mine dumps. *Assessment, Restoration and Reclamation of Mining Influenced Soils*. 2017, p. 1-32. DOI: 10.1016/B978-0-12-809588-1.00001-3

8. Fernando S., Adhikari S., Kota K., Bandi R. Glycerol based automotive fuels from future biorefineries. *Fuel*. 2007. Vol. 86. Iss. 17-18, p. 2806-2809. DOI: 10.1016/j.fuel.2007.03.030

9. Hajjari M., Tabatabaei M., Aghbashlo M., Ghanavati H.J.R. A review on the prospects of sustainable biodiesel production: A global scenario with an emphasis on waste-oil biodiesel utilization. *Renewable Sustainable Energy Reviews*. 2017. Vol. 72, p. 445-464. DOI: 10.1016/j.rser.2017.01.034

10. Bezergianni S., Dimitriadis A. Comparison between different types of renewable diesel. *Renewable and Sustainable Energy Reviews*. 2013. Vol. 21, p. 110-116. DOI: 10.1016/j.rser.2012.12.042

11. Smirnova T.N., Podgaetskii V.M. Biodiesel – an alternative fuel for diesels. *Dvigatel*. 2007. N 2, p. 32-34.

12. Dzhevaga N.V., Borisova D.D. Analysis of Air Monitoring System in Megacity on the Example of St. Petersburg. *Journal of Ecological Engineering*. 2021. Vol. 22. Iss. 4, p. 175-185. DOI: 10.12911/22998993/134076

13. Nibin T., Sathiyagnanam A., Sivaprakasam S., Saravanan C. Investigation on emission characteristics of a diesel engine using oxygenated fuel additive. *Journal of the Institution of Engineers*, Part MC, Mechanical Engineering Division. 2005. Vol. 86, p. 51-54.

14. Wong K.C., Tan C.H. Volatile constituents of the flowers of Clerodendron fragrans (Vent.) R. Br. *Flavour fragrance journal*. 2005. Vol. 20. Iss. 4, p. 429-430. DOI: 10.1002/ffj.1457

15. Aghbashlo M., Tabatabaei M., Khalife E. et al. Exergoeconomic analysis of a DI diesel engine fueled with diesel/biodiesel (B5) emulsions containing aqueous nano cerium oxide. *Energy*. 2018. Vol. 149, p. 967-978. DOI: 10.1016/j.energy.2018.02.082

16. Fakas S., Papanikolaou S., Galiotou-Panayotou M. et al. Biochemistry and biotechnology of single cell oil. *New horizons in Biotechnology*. 2009, p. 38-60.

17. Halim R., Danquah M.K., Webley P.A. Extraction of oil from microalgae for biodiesel production: a review. *Biotechnology advances*. 2012. Vol. 30. Iss. 3, p. 709-732. DOI: 10.1016/j.biotechadv.2012.01.001

18. Litvinenko V.S. The Role of Hydrocarbons in the Global Energy Agenda: The Focus on Liquefied Natural Gas Resources 2020. *Resourses*. 2020. Vol. 9. Iss. 5, p. 59-81. DOI: 10.3390/resources9050059

19. Quispe C.A., Coronado C.J., Carvalho Jr. J.A. Glycerol: Production, consumption, prices, characterization and new trends in combustion. *Renewable sustainable energy reviews*. 2013. Vol. 27, p. 475-493. DOI: 10.1016/j.rser.2013.06.017

20. Loizzo M.R., Tundis R., Conforti F. et al. Comparative chemical composition, antioxidant and hypoglycaemic activities of Juniperus oxycedrus ssp. oxycedrus L. berry and wood oils from Lebanon. *Food chemistry*. 2007. Vol. 105. Iss. 2, p. 572-578. DOI: 10.1016/j.foodchem.2007.04.015

21. Ponomarenko T., Nevskaya M., Jonek-Kowalska I. Mineral ResourceDepletion Assessment: Alternatives, Problems, Results. *Sustainability*. 2021. Vol. 13. Iss. 2. N 862. DOI: 10.3390/su13020862

22. Gómez-Cuenca F., Gómez-Marín M., Folgueras-Díaz M.B. Effects of ethylene glycol ethers on diesel fuel properties and emissions in a diesel engine. *Energy conversion management*. 2011. Vol. 52. Iss. 8-9, p. 3027-3033. DOI: 10.1016/j.enconman.2011.04.017

23. Brady S., Tam K., Leung G., Salam C. Zero waste biodiesel: Using glycerin and biomass to create renewable energy. *UCR Undergraduate Research Journal*. 2008. Vol. 2 (5), p. 5-11.

24. De Torres M., Jimenez-Oses G., Mayoral J.A. et al. Glycerol ketals: Synthesis and profits in biodiesel blends. *Fuel*. 2012. Vol. 94, p. 614-616. DOI: 10.1016/j.fuel.2011.11.062

25. Strizhenok A.V., Korelskiy D.S. Estimation and reduction of methane emissions at the scheduled and repair outages of gas-compressor units. *Journal of Ecological Engineering*. 2019. Vol. 20. Iss. 1, p. 46-51. DOI: 10.12911/22998993/93943

26. Lapuerta M., Rodríguez-Fernández J., García-Contreras R. Effect of a glycerol-derived advanced biofuel–FAGE (fatty acid formal glycerol ester) – on the emissions of a diesel engine tested under the New European Driving Cycle. *Energy*. 2015. Vol. 93, p. 568-579. DOI: 10.1016/j.energy.2015.09.070

27. Mota C.J., da Silva C.X., Rosenbach Jr. N. et al. Glycerin derivatives as fuel additives: the addition of glycerol/acetone ketal (solketal) in gasolines. *Energy Fuels*. 2010. Vol. 24. Iss. 4, p. 2733-2736. DOI: 10.1021/ef9015735

28. Saengarun C., Petsom A., Tungasmita D.N. Etherification of glycerol with propylene or 1-butene for fuel additives. *The Scientific World Journal*. 2017. Vol. 2017. N 4089036. DOI: 10.1155/2017/4089036

29. Tóth C., Baladincz P., Hancsók J. Production of bio gas oil containing diesel fuel with upgraded cold flow properties by co-processing. *Chemical Engineering Transactions*. 2012. Vol. 29, p. 613-618. DOI: 10.3303/CET1229103

30. Mohammad M., Hari T.K., Yaakob Z. et al. Overview on the production of paraffin based-biofuels via catalytic hydrodeoxygenation. *Renewable and Sustainable Energy Reviews*. 2013. Vol. 22, p. 121-132. DOI: 10.1016/j.rser.2013.01.026

31. Dabbagh H., Ghobadi F., Ehsan M.R, Moradmand M. The influence of ester additives on the properties of gasoline. *Fuel*. 2013. Vol. 104, p. 216-223. DOI: 10.1016/j.fuel.2012.09.056

32. Burger J., Siegert M., Ströfer E., Hasse H. Poly (oxymethylene) dimethyl ethers as components of tailored diesel fuel: Properties, synthesis and purification concepts. *Fuel*. 2010. Vol. 89. Iss. 11, p. 3315-3319. DOI: 10.1016/j.fuel.2010.05.014

33. Mitusova T.N., Kondrasheva N.K., Lobashova M.M. et al. Influence of dispersing additives and blend composition on stability of marine high-viscosity fuels. *Journal of Mining Institute*. 2017. Vol. 228, p. 722-725. DOI: 10.25515/PMI.2017.6.722

34. Arteconi A., Mazzarini A., Di Nicola G. Emissions from ethers and organic carbonate fuel additives: a review. *Water, Air, Soil Pollution*. 2011. Vol. 221, p. 405-423. DOI: 10.1007/s11270-011-0804-y

35. Sultanbekov R., Nazarova M. The influence of total sediment of petroleum products on the corrosiveness of the metal of the tanks during storage. I International Conference “Corrosion in the Oil and Gas Industry”, 22-24 May 2019, Saint Petersburg, Russia. E3S Web of Conferences. 2019. N 01015. DOI: 10.1051/e3sconf/201912101015

36. Sultanbekov R., Nazarova M. Determination of compatibility of petroleum products when mixed in tanks. European Association of Geoscientists & Engineers, 25-29 March 2019, Tyumen, Russia. European Association of Geoscientists & Engineers, 2019. Vol. 2019, p. 1-5. DOI: 10.3997/2214-4609.201900614

37. Gendler S.G., Prokhorova E.A. Assessment of the cumulative impact of occupational injuries and diseases on the state of labor protection in the coal industry. *Mining Informational and Analytical Bulletin*. 2022. N 10-2, p. 105-116 (in Russian). DOI: 10.25018/0236_1493_2022_102_0_105

***Authors*: Natalia K. Kondrasheva,** *Doctor of Engineering Sciences*, *Head of Department*, *https://orcid.org/0000-0001-9340-4888* (*Saint Petersburg Mining University*, *Saint Petersburg*, *Russia*), **Anzhelika M. Eremeeva,** *Candidate of Engineering Sciences*, *Assistant Lecturer*, *eremeevaanzhelika@yandex.ru, https://orcid.org/0000-0002-9212-5534* (*Saint Petersburg Mining University*, *Saint Petersburg*, *Russia*).

The authors declare no conflict of interests.

ISSN 2411-3336; e-ISSN 2541-9404

JOURNAL OF MINING INSTITUTE
Zapiski Gornogo instituta
Journal homepage: pmi.spmi.ru

Research article

Assessment of the possibility of using iron-magnesium production waste for wastewater treatment from heavy metals (Cd^{2+}, Zn^{2+}, Co^{2+}, Cu^{2+})

Natalya Yu. ANTONINOVA ✉, **Artem V. SOBENIN**, **Albert I. USMANOV**, **Ksenia V. SHEPEL**
Institute of Mining of Ural Branch of RAS, Yekaterinburg, Russia

How to cite this article: Antoninova N.Yu., Sobenin A.V., Usmanov A.I., Shepel K.V. Assessment of the possibility of using iron-magnesium production waste for wastewater treatment from heavy metals (Cd^{2+}, Zn^{2+}, Co^{2+}, Cu^{2+}). Journal of Mining Institute. 2023. Vol. 260, p. 257-265. DOI: 10.31897/PMI.2023.34

Abstract. Relevant problems associated with treatment of industrial wastewater from heavy metal ions are considered. Due to industrial development, the amount of wastewater increases as well as the risks of heavy metals getting into surface and groundwater, accumulating in water bodies and becoming aggressive environmental pollutants, which affect the animal and human organisms. To assess the possibility of extracting metal ions (Cd^{2+}, Zn^{2+}, Co^{2+}, Cu^{2+}) from industrial wastewater and their further treatment, studies were carried out on redistribution of heavy metals in the "wastewater – waste" system using iron-magnesium production waste. Samples of the investigated waste weighing 0.1; 0.2; 0.5; 1; 1.5; 2 g were taken for wastewater volume of 50 ml per each subsample. Contact time varied from 5 to 180 min, waste fraction was 1 mm. The interaction process showed that the waste efficiently removes metal ions (Cd^{2+}, Zn^{2+}, Co^{2+}, Cu^{2+}) from industrial wastewater. The efficiency of removing a pollutant from the solution depends on the weight of the waste subsample, initial concentration of metal ions, and contact time.

Keywords: extraction; heavy metals; wastewater; removal of ions from solution; waste

Acknowledgment. The article was prepared under the state assignment N 075-00412-22 PR. Theme 2 (2022-2024) "Development of geoinformation technologies for assessing the protection of mining areas and predicting the development of negative processes in mineral resources management" (FUWE-2022-0002), reg. N 1021062010532-7-1.5.1.

Received: 28.10.2022 ***Accepted: 02.03.2023*** ***Online: 23.03.2023*** ***Published: 25.04.2023***

Introduction. The urgency of solving the problems of preventing environmental pollution by toxic elements is growing with industrial development. According to the Ministry of Nature of the RF, in 2021, the number of cases of extremely high pollution levels (EHP) increased by 15 % and of high levels of surface freshwater pollution (HP) in the RF increased by 12 % compared to 2020. Total number of cases of HP and EHP reached a maximum for the period 2012-2021, deviation of the annual value of the indicator from the average for 10 years was 14 %[*]. Sources of pollutants getting into water bodies are wastewater generated as a result of discharges from industrial enterprises and waste disposal sites (WDS) [1-4].

For many years of industrial development in the Ural region, mining industry of the Sverdlovsk Region remained one of the main components of economy, the development of which is accompanied by large-scale environmental pollution and accumulation of man-induced waste. Of particular hazard are the WDS of extraction and beneficiation of non-ferrous metals, in which metals are in a sulphide form, with the generation of the process of sulphuric acid leaching: dumps of off-balance ores; beneficiation products; waste of metallurgical conversion [5].

---

[*] On the state and protection of environment in the Russian Federation in 2021. State report. Moscow: Ministry of Nature of Russia; MGU named after M.V.Lomonosov, 2022, p. 684.

One of the examples of an area experiencing a significant technogenic impact is the group of Kabanskiye copper and sulphur pyrite deposits. The abandoned deposit lies on the eastern slope of the Middle Urals, about 15 km from the watershed ridge. Distance to the administrative centre of the Ural Federal District and the Sverdlovsk Region (Yekaterinburg) is 190 km. The approximate disturbed area is over 80 ha, of which 11 ha are water bodies.

The deposit was mined by the open pit method, leaving after completion of the work unreclaimed overburden dumps and two quarry excavations filled with acidic waters which are affected by underspoil waters with pH 2.33-3.10, content of zinc 50.12 mg/l, cobalt – 1.73 mg/l, cadmium – 0.20 mg/l, copper – 78.10 mg/l (Table 1).

Table 1

Elemental composition of the studied materials (gross content)

Chemical element	Iron-magnesium production waste, mg/kg	MPC/APC, mg/kg[*]	Chemical element	Underspoil waters "Kaban 1", mg/l	MPC, mg/l[**]
Cu	41.25±1.14	3/132	Cu^{2+}	78.10±2.94	0.001
Mg	175,000.00±3,498.32	–	Mg^{2+}	322.50±5.98	40
Fe	52,000.00±1,984.29	–	Fe^{3+}	147.71±3.94	0.1
Zn	77.70±1.84	23/220	Zn^{2+}	50.12±1.14	0.01
Cd	< 1	/2	Cd^{2+}	0.20±0.01	0.005
Co	119.75± 1.41	5/	Co^{2+}	1.73±0.01	0.01
Ni	3,083.00±48.13	4/80	Ni^{2+}	0.23±0.01	0.01
Ca	43,211.00±581.45	–	Ca^{2+}	33.20±0.99	180
K	30,140.00±787.40	–	K^{+}	5.26±0.96	50

---

[*] SanPiN 1.2.3685-21 "Hygienic standards and requirements for ensuring safety and (or) harmlessness of environmental factors for humans".

[**] Order of the Ministry of Agriculture of Russia dated 13.12.2016 N 552 (as amended on 10.03.2020) "On approval of water quality standards for water bodies of commercial fishery importance, including standards of maximum permissible concentrations of harmful substances in waters of water bodies of commercial fishery importance".

Zinc plays an important role in behaviour of various biochemical reactions, metabolism of proteins and nucleic acids, and is a cofactor of a large group of enzymes. Daily toxicity threshold for humans is about 600 mg [3]. Cadmium is toxic [3], irritating to the respiratory tract, and its long-term exposure can cause a severe dysfunction of kidneys, reproductive system, liver, brain, and central nervous system [4, 6]. The physiological role of cadmium is not well understood [3]. Copper and cobalt in high concentrations are also toxic and lead to adverse health effects [3, 7].

Neutralization of high concentrations of heavy metals can be achieved using various physical, chemical, and biological processes [8]. Common methods for removing metal ions from wastewater solution are precipitation, coagulation, ion exchange, and adsorption. Methods associated with precipitation and coagulation lead to formation of a large amount of sludge [9]. Ion exchange is expensive and requires preliminary wastewater treatment since the matrices of ion exchangers can become clogged during operation with various substances in wastewater [9]. Therefore, for ecological rehabilitation of technogenically polluted ecosystems, it is necessary to evaluate the efficiency of using inexpensive materials for wastewater treatment from heavy metals [10-12]. The materials that are widespread in the area of the source of industrial wastewater are of economic interest. Thus, the studies of the processes that determine the accumulation and migration of heavy metals in technogenically polluted ecosystems (especially in areas where industrial enterprises operate), the implementation of methods for detoxifying water resources based on the use of materials which contain production waste, are an intensely developing area of research [13, 14].

Many researchers [15, 16] studied the efficiency of using industrial waste to remove metals from wastewater solutions. The article [15] substantiates a possibility of using a magnesium-silicate reagent based on serpentinite magnesite, an overburden rock at the Khalilovskoye magnesite deposit, for an efficient multistage wastewater treatment. Thermally activated serpentine minerals can be used to neutralize and treat technogenic solutions, which contributes to precipitation of iron, aluminium, copper, and nickel. For copper, zinc, and nickel, the process of adsorption on the surface of reagent and coprecipitation is recorded.

In the study [16] the alkaline leach residual wire sludge (AWRS) was modified by heat treatment to produce an inexpensive and highly efficient material for removing Cu^{2+} and Ni^{2+} from wastewater. The results showed that the AWRS calcined at 700 °C demonstrated the maximum ability to remove Cu^{2+} and Ni^{2+}. Taking into account a low cost and a high efficiency of the AWRS, the sorbent developed by the authors offers good prospects for removing Cu^{2+} and Ni^{2+} from industrial wastewater solution.

Methods. As part of the research, the experiments were carried out on studying the selective removal of Cd^{2+}, Zn^{2+}, Cu^{2+}, Co^{2+} from a model solution using the material that represents unused resources in the form of iron-magnesium production waste, which forms in large quantities and is a pasty substance of red-brown colour (Table 1). Based on the results of experiments, the influence of the mass of waste subsample, initial concentration of metal ions and contact time for removal of metal ions from the solution of industrial wastewater by iron-magnesium production waste were analysed. Wastewater sampled in the summer of 2021 as part of the field studies within the boundaries of the depleted Kabanskoye deposit was chosen as a model solution (Table 1).

Experiments on redistribution of metals in the “*wastewater – waste*” *system.* The samples of iron-magnesium production waste were averaged by quartering and crushed to a fraction of 1 mm using test sieves and a porcelain mortar and pestle. The samples were dried in a drying oven (ShS-80-01-SPU, OOO “PriborUfa”, Russia). The samples were packed in synthetic fabric (perforation 0.025 mm).

Samples of industrial wastewater were taken into five-litre polyethylene bottles washed with distilled water. Samples were filtered using “blue ribbon” filters and stored in a refrigerator for 24 h. Preparation of wastewater samples for elemental analysis was carried out according to the NPDES method (Waste Water) [17].

Waste ashing was accomplished in MARS 5 Digestion Microwave System (CEM Corporation, USA) according to the EPA 3052 procedure [17]. 9 ml of HNO_3 and 3 ml of HF were added to the subsample of 0.5 g, the mixture was stirred, allowed to stand for 15 min, and the vessels were closed. EasyPrep vessels recommended by the manufacturer [17] were used. Temperature rising time to 180 °C was 6 min, temperature maintenance time was 10 min, and power was 1.800 W [17]. At the outlet, when diluted to 50 ml, a transparent sample was obtained without colour and particles.

Metal ion concentrations in wastewater, mineralized samples and obtained filtrates were determined by atomic absorption spectroscopy (AAS) in an air-acetylene flame (Varian AA 240 FS, Varian Australia Pty Ltd, Australia). Wavelengths used, nm: Cd 228.8; Zn 213.9; Co 240.7; Mg 202.6; Cu 324.7; Fe 248.3; Ni 232.0. Detection limits of elements in solution, µg/l: Cd 1.5; Zn 1.6; Cu 1.2; Mg 0.3; Fe 7.3; Ni 5.8; K 0.8; Ca 0.4.

Subsamples (0.1; 0.2; 0.5; 1; 1.5; 2 g) were weighed and placed in conical test tubes of the “falcon” type. Industrial wastewater of the volume of 50 ml was added to them. Then, the samples were stirred (99 rpm) for 120 min using an ELMI RM-1L rotary mixer (ELMI LTD, Latvia). The resulting solutions were filtered using “blue ribbon” filters. Industrial wastewater (50 ml) was added to 0.2 g subsamples, and the samples were stirred for 5 to 180 min. The resulting solutions were filtered using “blue ribbon” filters.

To construct isotherms and determine the effect of initial concentration of metal ions Cd^{2+}, Zn^{2+}, Cu^{2+}, Co^{2+} in solution on the efficiency of the wastewater treatment process, solutions were prepared with concentrations: 10; 30; 50; 100; 300; 500; 1,000 mg/l. Solutions were prepared from reagents of qualifications "extra pure" and SSS (state standard sample, initial concentration from 1 to 10 g/l). The interaction occurred at contact time of 120 min with subsample 0.2 g, 50 ml of solution, at room temperature and pH 2.3-2.5, regulated with NaOH and HNO_3. Hanna HI 99121 (Hanna Instruments, Germany) was used to determine pH and temperature. pH of the aqueous extract was determined at a weight ratio of the subsample and distilled water between them 1:5 (GOST 26423-85).

Static exchange capacity of waste q_e (mg/g) and the degree of pollutant extraction from solutions were calculated using the following equations:

$$\mathrm{SEC} = \frac{\left(C_{\mathrm{init}} - C_{\mathrm{equil}}\right)V}{g};$$

$$E = \frac{C_{\mathrm{init}} - C_{\mathrm{equil}}}{C_{\mathrm{init}}} \cdot 100,$$

where C_{init} is the initial concentration of copper ions in the solution, mg/l; C_{equil} – the equilibrium (residual) concentration of copper ions in the filtrate, which sets in in water after mixing of water and substrate, mg/l; g is the weight of a dry subsample of the substrate, g; V – volume of model solution added to waste, l.

The results of calculating the indicators of extraction degree of pollutants from the solution are given in Table 2.

Table 2

Results of chemical analysis of the obtained filtrates (50 ml, contact time 120 min)

Subsample, g	Content of chemical elements in filtrate, mg/l					pH
	Cd^{2+}	Zn^{2+}	Co^{2+}	Mg^{2+}	Cu^{2+}	
0.1	0.20±0.006	42.11±1.34	1.15±0.10	429.80±8.91	36.83±1.29	4.06±0.01
0.2	0.019±0.005	10.24±0.94	0.90±0.09	642.60±13.04	5.98±0.81	4.52±0.01
0.5	0.001±0.0007	0.12±0.011	< 0.005	849.60±14.01	0.09±0.005	5.87±0.01
1	< 0.0015	0.10±0.009	< 0.005	1,176.20±22.01	0.08±0.04	6.76±0.01
1.5	0.005.0.002	0.09±0.003	< 0.005	1,539.27±19.23	0.08±0.003	7.37±0.01
2	0.008±0.002	0.10±0.001	< 0.005	2,153.00±34.41	0.08±0.004	8.01±0.01

Discussion of results. To substantiate the possibility of using iron-magnesium production waste as a material for removing metals from wastewater solution, the following factors influencing the interactions were studied: initial concentration; contact time; waste dosage; pH of aqueous medium [18-20].

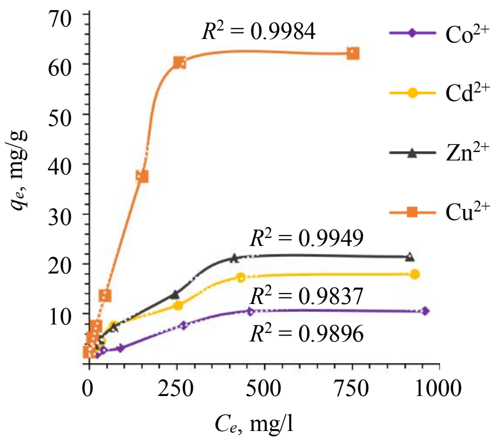

Fig.1. Effect of initial metal concentration in solution on wastewater cleaning process with iron-magnesium production waste

According to the results of elemental analysis, iron-magnesium production waste contains significant concentrations of the studied ions, mg/kg: Cu 41.25; Mg 175,000.00; Zn 77.70; Co 119.75. Industrial wastewater has an acidic medium (pH 2.33) and a high salinity. Content of the studied metal ions, mg/l: Cu 78.10; Zn 50.12; Co 1.73; Cd 0.20 (see Table 1).

Initial concentration of metal ions C_e (mg/l) is an important factor that controls the transfer of metal ions from aqueous solution to waste [21]. Its effect was studied in the range of 10-1,000 mg/l for Cd^{2+}, Zn^{2+}, Co^{2+}, Cu^{2+} at pH 2.3-2.5 (Fig.1). A model solution prepared from the GSS and reagents was used as a simulation of wastewater pollution.

The number of extracted metal ions q_e increases due to the growth of initial concentration of metal ions from 10 to 500 mg/l. Further growth of metal concentration in the solution to 1,000 mg/l does not increase the extraction efficiency (Fig.1). Thus, the results showing a linear dependence at the initial stage can be explained by the presence of available active centres, i.e., areas on the surface of iron-magnesium production waste that can interact with the studied metal ions or compete for a certain number in their initial concentration. Further, the number of active centres decreases, therefore, an increase in the concentration of metal ions in the solution over 1,000 mg/l will lead to saturation of waste areas and will not increase the treatment efficiency [9, 18, 19]. This necessitates research to assess the possibility of selective removal of the studied elements in terms of forming a cascade of biological ponds, taking into account the material composition of the bed and the composition of the filtration dam sensitive to each chemical element.

Study of the influence of interaction characteristics on the removal of metals from industrial wastewater solution. The time of equilibrium onset is an important parameter when conducting research on wastewater treatment [22, 23]. The maximum possible absorption of Cd^{2+}, Zn^{2+}, Co^{2+}, Cu^{2+} ions by iron-magnesium production waste depending on contact time was studied to determine the time of equilibrium onset. The effect of contact time on wastewater treatment was investigated using a constant concentration of the solution (Table 3) with different time intervals in the range of 5-180 min at room temperature. Elemental composition of the filtrates obtained as a result of interaction of iron-magnesium production waste with wastewater is given in Table 3.

Table 3

Results of chemical analysis of the obtained filtrates (50 ml, subsample 0.2 g)

Contact time, min	Content of chemical elements in filtrate, mg/l							pH
	Cd^{2+}	Zn^{2+}	Co^{2+}	Mg^{2+}	Cu^{2+}	Fe^{3+}	Ni^{2+}	
5	0.19±0.001	43.01±1.09	1.06±0.003	530.88±14.03	43.19±1.32	1.55±0.030	0.23±0.011	4.05±0.012
10	0.18±0.001	39.48±0.98	1.03±0.003	539.84±13.12	19.18±1.01	0.03±0.003	0.22±0.010	4.10±0.014
15	0.17±0.001	38.48±0.67	1.03±0.003	558.40±12.05	17.85±0.78	0.09±0.002	0.21±0.009	4.33±0.011
30	0.18±0.001	37.52±0.70	1.03±0.003	604.24±15.09	16.85±0.81	< 0.0073	0.13±0.014	4.78±0.015
60	0.04±0.007	10.62±0.79	1.02±0.004	1,076.88±21.87	6.74±0.77	< 0.0073	0.05±0.001	4.89±0.011
120	0.03±0.007	9.61±0.91	1.03±0.001	979.04±4.94	5.25±0.76	< 0.0073	< 0.0058	4.99±0.014
180	0.03±0.007	9.05±0.68	1.03±0.001	980.00±5.19	5.20±0.86	< 0.0073	< 0.0058	5.01±0.012

In order to assess the possibility of secondary pollution as a result of interaction of iron-magnesium production waste with a model solution of industrial wastewater, the obtained filtrates were also analysed for Fe^{3+} and Ni^{2+} (Table 3).

There is a dynamics in the decrease of concentrations of the studied elements depending on contact time and a possible absence of secondary pollution, provided that iron-magnesium production waste is used. The values of iron and nickel ions in the obtained filtrates do not exceed the initial ones. Figure 2 shows the effect of contact time on the removal degree of Cd^{2+}, Zn^{2+}, Co^{2+}, Cu^{2+} ions from filtrates using iron-magnesium production waste.

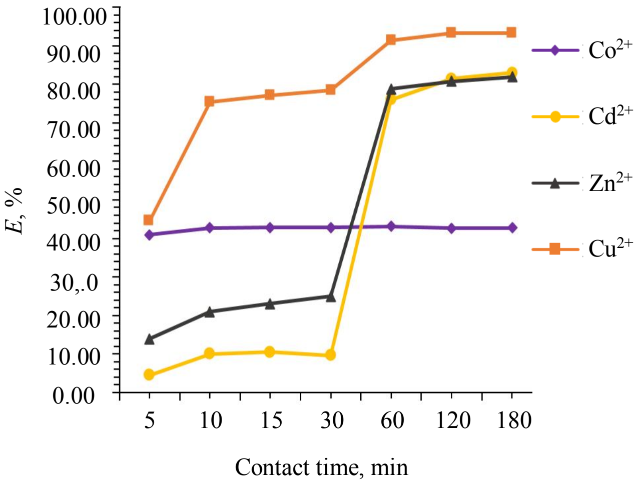

Fig.2. Effect of contact time on degree of metal ions extraction from solution

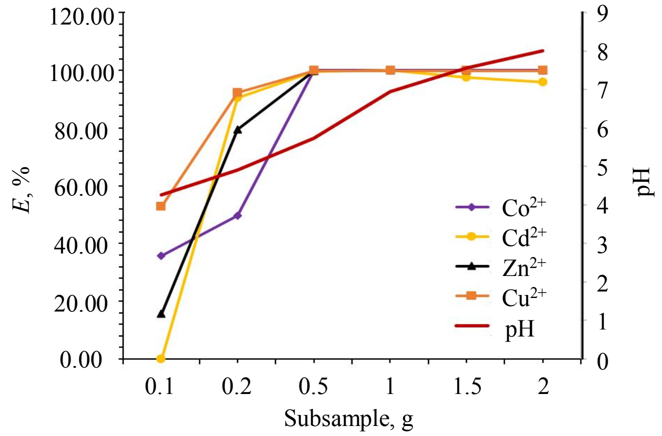

Fig.3. Influence of waste dosage and filtrate pH on the degree of ions extraction from solution

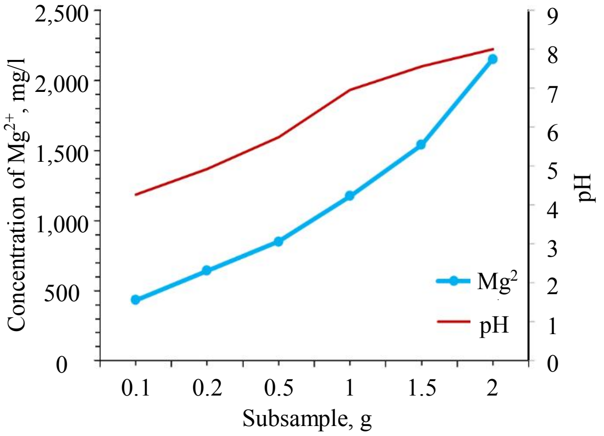

Fig.4. Change of filtrate pH relative to Mg^{2+} concentration in solution

Removal of the studied elements from solutions increases after 30 min of interaction with waste and reaches equilibrium at 120 min. An exception is Co^{2+} – the extraction degree for this element varies from 40.89 to 42.72 % and practically does not change with respect to a given time period. The efficiency of initial removal for copper, zinc and cadmium can be associated with the occurrence of a large number of free areas available on the waste surface. As the contact time increases, the number of active centres decreases, and further increase does not lead to significant changes in the treatment process [18, 19] (see Table 2).

pH of the medium [24, 25] affects both the chemical composition of the solution and the efficiency of the treatment process [26, 27]. An equally important parameter for metal extraction from solution is also the dosage of the material under study [28-30]. The effect of the waste dose on the treatment process should be optimized [31-33], since the mass of the waste affects the ability of the material to extract pollutants from the solution at a given initial waste concentration in operating conditions [34-36]. The process of extracting ions from solution was studied by varying the mass of waste from 0.1 to 2 g in 50 ml of solution with a constant concentration (see Table 1), constant stirring rate (99 rpm) for 120 min at room temperature. The effect of waste subsample on the removal of heavy metal ions from wastewater is shown in Fig.3.

Percentage of metal ions removal from the solution increases with a simultaneous increase in the dosage of waste (Fig.3). The minimum values of E indicator were recorded at waste dosage of 0.1 g and are, %: for Cd^{2+} 0; Zn^{2+} 15.78; Cu^{2+} 52.78; Co^{2+} 35.83; when the dosage is increased to 0.5 g, this indicator increases, %: Cd^{2+} 99.5; Zn^{2+} 99.74; Cu^{2+} 99.88; Co^{2+} 100 and reaches the equilibrium. Thus, in the graphs (Fig.2, 3) there is a tendency of increase in percentage of heavy metal ions removed from wastewater. Figure 4 shows the effect of pH on the concentration of magnesium ions in the filtrate depending on the weight of subsample of the investigated material.

pH increases depending on the weight of subsample of the investigated material: the larger the subsample, the higher the pH of the filtrates (see Table 2). This is due to the fact that iron-magnesium production waste has an alkaline pH of 8.7, since it contains a large amount of magnesium (Fig.4), thus diluting the acidic underspoil water with initial pH 2.33.

The results of elemental analysis of iron-magnesium production waste after interaction with model solution of industrial wastewater are given in Table 4. The data show the number of extracted metal ions under study by production waste from the solution on a dry weight basis. According to the obtained results, the number of detected metal ions in waste increases with time; the maximum values are recorded at contact time of 120 min, then a decrease in the values of metal ions in waste is observed (Table 4). The data show that in the composition of iron-magnesium production waste samples after interaction with industrial wastewater, with an increase in contact time from 5 to 120 min, Cd, Zn, Fe and Cu are found in higher concentrations than in initial samples. A significant decrease in Mg in the waste composition is also recorded.

Table 4

Results of elemental analysis of waste after interaction with wastewater (gross content)

Contact time, min	Content of chemical elements in waste, mg/kg					
	Cd	Zn	Co	Mg	Cu	Fe
5	1.20±0.03	120.54±1.23	100.00±1.75	10,021.32±1,948.24	351.21±25.04	61,819.25±2,948.47
10	1.25±0.03	127.50±1.41	131.75±2.37	16,822.50±2,821.52	407.75±21.48	73,386.34±3,645.75
15	2.21±0.09	615.54±29.47	135.11±2.04	28,983.21±3,948.63	885.37±36.94	64,528.73±3,562.74
30	3.00±0.14	844.04±41.22	140.25±3.17	32,430.64±4,958.01	3,354.01±138.04	68,945.50±3,465.39
60	3.75±0.02	1,035.09±28.98	169.24±4.08	27,562.21±4,756.06	4,137.50±241.10	69,746.25±2,547.05
120	3.78±0.16	1,041.66±21.84	154.32±5.19	24,842.30±2,484.05	3,775.32±194.90	61,207.93±2,567.93
180	3.54±0.17	663.99±17.38	96.22±2.28	17,594.54±1,875.75	1,499.55±53.10	62,641.50±2,857.05

Conclusion. Studies on redistribution of heavy metals in the “wastewater – waste” system using iron-magnesium production waste are given. The choice is due to the waste availability, since this is production waste forming in large amounts and is potentially cheap material for wastewater treatment. The enterprise, at which waste forms in the production process is not far from the facility (the depleted Kabanskoye deposit), which has a negative impact on the environment, this helps cutting the expenses on environmental protection measures and reducing the amount of waste to be disposed of at the WDS.

Treatment process showed that the waste efficiently removes metal ions (Cd^{2+}, Zn^{2+}, Co^{2+}, Cu^{2+}) from industrial wastewater. The removal efficiency depends on the weight of the waste subsample, contact time, initial concentration of metal ions in the solution and pH, and increases with growing dosage. The most efficient indicators of wastewater treatment from ions of the studied metals using iron-magnesium production waste are: contact time 120-180 min; dosage 4-10 g/l; initial concentration of metal ions (Cd^{2+}, Zn^{2+}, Co^{2+}, Cu^{2+}) in the solution not more than 500 mg/l.

The data obtained indicate a possibility of using iron-magnesium production waste to reduce the metallic aggressiveness of wastewater and are of great interest in the development of measures on wastewater treatment, in terms of forming a cascade of biological ponds, taking into account the material composition of the bed and the filtration dam sensitive to each chemical element. Thus, further research to find a possibility of involving industrial waste in the economic turnover for environmental purposes offers good prospects.

REFERENCES

1. Pashkevich M.A., Matveeva V.A., Danilov A.S. Migration of pollutants from the mining waste disposal territories on the Kola Peninsula. *Gornyi zhurnal.* 2019. N 1, p. 17-21 (in Russian). DOI: 10.17580/gzh.2019.01.04

2. Jiaping Paul Chen, Lawrence K. Wang, Mu-Hao S. Wang et al. Remediation of Heavy Metals in the Environment.1st Edition. Boca Raton: CRC Press, 2016, p. 540. DOI: 10.1201/9781315374536

3. Gabaraeva Z.G., Makieva D.C. The Effect of Heavy Metals on the Human Body. *Education and Law.* 2020. N 11, p. 302-304 (in Russian). DOI: 10.24411/2076-1503-2020-1114

4. Zhushan Fu, Shuhua Xi. The effects of heavy metals on human metabolism. *Toxicology Mechanisms and Methods*. 2020. Vol. 30. Iss. 3, p. 167-176. DOI: 10.1080/15376516.2019.1701594

5. Antoninova N.Yu., Rybnikova L.S., Slavikovskaya Yu.O., Shubina L.A. Environmental and Economic Aspects of Selecting Reclamation Directions for Industrial Mining and Metallurgical Waste Disposal Sites. *Russian Mining Industry.* 2022. N S1, p. 71-77 (in Russian). DOI: 10.30686/1609-9192-2022-1S-71-77

6. Genchi G., Sinicropi M.S., Lauria G. et al. The Effects of Cadmium Toxicity. *International Journal of Environmental Research and Public Health.* 2020. Vol. 17. Iss. 11. N 3782. DOI: 10.3390/ijerph17113782

7. Manisalidis I., Stavropoulou E., Stavropoulos A., Bezirtzoglou E. Environmental and Health Impacts of Air Pollution: a Review. *Frontiers in Public Health*. 2020. Vol. 8. DOI: 10.3389/fpubh.2020.00014

8. Sobenin I.V., Antoninova N.Yu., Usmanov A.I., Shepel K.V. Influence of material composition of biological pond bed on waste water treatment in mining and metallurgy industries. *Mining informational and analytical bulletin*. 2021. N 5-2, p. 273-282 (in Russian). DOI: 10.25018/0236_1493_2021_52_0_273

9. Chowdhury I.R., Chowdhury S., Mazumder M.A.J. et al. Removal of lead ions (Pb^{2+}) from water and wastewater: a review on the low-cost adsorbents. *Applied Water Science*. 2022. Vol. 12. Iss. 8. N 185. DOI: 10.1007/s13201-022-01703-6

10. Sadeghalvad B., Ahali Z., Azadmehr A. Modification of Natural Zeolite by Carboxylate Compounds and Minerals for Removal of Zinc Ions from Wastewater: Equilibrium and Kinetic Studies. *Arabian Journal for Science and Engineering*. 2016. Vol. 41. Iss. 7, p. 2501-2513. DOI: 10.1007/s13369-015-2003-4

11. Solache-Ríos M., Olguín M.T., Martínez-Miranda V. et al. Removal Behavior of Cobalt from Aqueous Solutions by a Sodium-Modified Zeolitic Tuff. *Water, Air & Soil Pollution*. 2015. Vol. 226. Iss. 12. N 420. DOI: 10.1007/s11270-015-2688-8

12. Singh S.A., Shukla S.R. Adsorptive removal of cobalt ions on raw and alkali-treated lemon peels. *International Journal of Environmental Science and Technology*. 2016. Vol. 13. Iss. 1, p. 165-178. DOI: 10.1007/s13762-015-0801-6

13. Kharko P.A., Matveeva V.A. Bottom sediments in a river under acid and alkaline wastewater discharge. *Ecological Engineering and Environmental Technology*. 2021. Vol. 22. Iss. 3, p. 35-41. DOI: 10.12912/27197050/134870

14. Pashkevich M.A., Kharko P.A. The use of a composite mix to remove metals from acidic drainage waters at tailings facilities. *Obogashchenie rud*. 2022. N 4, p. 40-47 (in Russian). DOI: 10.17580/or.2022.04.07

15. Kremenetskaya I.P., Ivanova T.K., Gurevich B.I. et al. Separate deposition of metals from highly concentrated solutions with granulated magnesia-silicate reagent. *Vestik MGTU*. 2021. Vol. 24. N 1, p. 118-130 (in Russian). DOI: 10.21443/1560-9278-2021-24-1-118-130

16. Ming Kong, Longmian Wang, Jianying Chao et al. Removal of Cu^{2+} and Ni^{2+} from Wastewater by Using Modified Alkali-Leaching Residual Wire Sludge as Low-Cost Adsorbent. *Water, Air & Soil Pollution*. 2019. Vol. 230. Iss. 3. N 65. DOI: 10.1007/s11270-018-4071-z

17. MARS 6. Microwave Acid Digestion. Method Note Compendiumod. URL: http://cem.com/media/contenttype/media/literature/MetNote_MARS6_Compendium.pdf (accessed 09.09.2022).

18. Faisal A.A.H., Nassir Z.S., Rashid H.M. et al. Neural network for modeling the capture of lead and cadmium ions from wastewater using date palm stones. *International Journal of Environmental Science and Technology*. 2022. Vol. 19. Iss. 11, p. 10563-10576. DOI: 10.1007/s13762-021-03883-1

19. Saranya S., Gandhi A.D., Suriyakala G. et al. A biotechnological approach of Pb (II) sequestration from synthetic wastewater using floral wastes. *SN Applied Sciences*. 2020. Vol. 2. Iss. 8. N 1357. DOI: 10.1007/s42452-020-3172-7

20. Barragán-Peña P., Macedo-Miranda M.G., Olguin M.T. Cadmium removal from wastewater in a fixed-bed column system with modified-natural clinoptilolite-rich tuff. *Chemical Papers*. 2021. Vol. 75. Iss. 2, p. 485-491. DOI: 10.1007/s11696-020-01314-y

21. El-Shazly E.A.A., Dakroury G.A., Someda H.H. Kinetic and isotherm studies for the sorption of ^{134}Cs and ^{60}Co radionuclides onto supported titanium oxide. *Journal of Radioanalytical and Nuclear Chemistry*. 2021. Vol. 330 Iss. 1, p. 127-139. DOI: 10.1007/s10967-021-07956-w

22. Chang Y.S., Au P.I., Mubarak N.M. et al. Adsorption of Cu(II) and Ni(II) ions from wastewater onto bentonite and bentonite/GO composite. *Environmental Science and Pollution Research*. 2020. Vol. 27. Iss. 26, p. 33270-33296. DOI: 10.1007/s11356-020-09423-7

23. Afolabi F.O., Musonge P., Bakare B.F. Bio-sorption of a bi-solute system of copper and lead ions onto banana peels: characterization and optimization. *Journal of Environmental Health Science and Engineering*. 2021. Vol. 19. Iss. 1, p. 613-624. DOI: 10.1007/s40201-021-00632-x

24. Sosun Ali A., Mannan A. et al. Removal of toxic metal ions (Ni^{2+} and Cd^{2+}) from wastewater by using TOPO decorated iron oxide nanoparticles. *Applied Water Science*. 2022. Vol. 12. Iss. 5. N 86. DOI: 10.1007/s13201-022-01588-5

25. Khadem M., Husni Ibrahim A., Mokashi I. et al. Removal of heavy metals from wastewater using low-cost biochar prepared from jackfruit seed waste. Biomass Conversion and Biorefinery. 2022. DOI: 10.1007/s13399-022-02748-y

26. Babeker T.M.A., Chen Q. Heavy Metal Removal from Wastewater by Adsorption with Hydrochar Derived from Biomass: Current Applications and Research Trends. *Current Pollution Reports*. 2021. Vol. 7. Iss. 1, p. 54-71. DOI: 10.1007/s40726-020-00172-2

27. Abd-Elhamid A.I., Elgoud E.M.A., Aly H.F. Alginate modified graphene oxide for rapid and effective sorption of some heavy metal ions from an aqueous solution. *Cellulose*. 2022. Vol. 29. Iss. 11, p. 6231-6245. DOI: 10.1007/s10570-022-04656-w

28. Ajala M.A., Abdulkareem A.S., Tijani J.O. et al. Adsorptive behaviour of rutile phased titania nanoparticles supported on acid-modified kaolinite clay for the removal of selected heavy metal ions from mining wastewater. *Applied Water Science*. 2022. Vol. 12. Iss. 2. N 19. DOI: 10.1007/s13201-021-01561-8

29. Abdelbasir S.M., Khalek M.A.A. From waste to waste: iron blast furnace slag for heavy metal ions removal from aqueous system. *Environmental Science and Pollution Research*. 2022. Vol. 29. Iss. 38, p. 57964-57979. DOI: 10.1007/s11356-022-19834-3

30. Agunwamba J.C., Amu A.M., Nwonu D.C. An efficient biosorbent for the removal of arsenic from a typical urban-generated wastewater. *Environmental Monitoring and Assessment*. 2022. Vol. 194. Iss. 12. N 911. DOI: 10.1007/s10661-022-10631-6

31. Naseem K., Imran Q., Ur Rehman M.Z. et al. Adsorptive removal of heavy metals and dyes from wastewater using Azadirachta indica biomass. *International Journal of Environmental Science and Technology*. 2022. DOI: 10.1007/s13762-022-04389-0

32. Singh S., Kapoor D., Khasnabis S. et al. Mechanism and kinetics of adsorption and removal of heavy metals from wastewater using nanomaterials. *Environmental Chemistry Letters*. 2021. Vol. 19. Iss. 3, p. 2351-2381. DOI: 10.1007/s10311-021-01196-w

33. Zhang L., Zhang S., Wang C. et al. Hypoxanthine Modified Polyethylene Glycol Diglycidyl Ether Gel for Ciprofloxacin Adsorption. *Journal of Biomedical Research & Environmental Sciences*. 2021. Vol. 2. Iss. 4, p. 244-250. DOI: 10.37871/jbres1219

34. Yanhui Li, Bing Xia, Quansheng Zhao et al. Removal of copper ions from aqueous solution by calcium alginate immobilized kaolin. *Journal of Environmental Sciences*. 2011. Vol. 23. Iss. 3, p. 404-411. DOI: 10.1016/s1001-0742(10)60442-1

35. Joshi H.K., Vishwakarma M.C., Kumar R. et al. Adsorption of Cd^{2+} from synthetic wastewater by modified leaves of Eupatorium adenophorum and Acer oblongum: thermodynamics, kinetics and equilibrium studies. *Discover Water*. 2022. Vol. 2. Iss. 1. N 9. DOI: 10.1007/s43832-022-00018-6

36. Obuzdina M.V., Rush E.A. Simulation of sorption processes of wastewater treatment by modi-fied zeolites. *RUDN Journal of Ecology and Life Safety*. 2022. Vol. 30. N 3, p, 240-249 (in Russian). DOI: 10.22363/2313-2310-2022-30-3-240-249

Authors**: Natalya Yu. Antoninova,** *Candidate of Engineering Sciences, Head of Laboratory*, *natal78@list.ru*, *https://orcid.org/0000-0002-8503-639X* (*Institute of Mining of Ural Branch of RAS, Yekaterinburg, Russia*), **Artem V. Sobenin,** *Researcher*, *https://orcid.org/0000-0001-5513-5680* (*Institute of Mining of Ural Branch of RAS, Yekaterinburg, Russia*), **Albert I. Usmanov,** *Junior Researcher*, *https://orcid.org/0000-0002-3650-0467* (*Institute of Mining of Ural Branch of RAS, Yekaterinburg, Russia*), **Ksenia V. Shepel,** *Junior Researcher*, *https://orcid.org/0000-0002-2827-8421* (*Institute of Mining of Ural Branch of RAS, Yekaterinburg, Russia*).

The authors declare no conflict of interests.

ISSN 2411-3336; e-ISSN 2541-9404

JOURNAL OF MINING INSTITUTE
Zapiski Gornogo instituta
Journal homepage: pmi.spmi.ru

Research article

Efficiency of acid sulphate soils reclamation in coal mining areas

Natalya V. MITRAKOVA✉, **Elena A. KHAYRULINA**, **Sergei M. BLINOV**, **Anna A. PEREVOSHCHIKOVA**
Natural Science Institute, Perm State National Research University, Perm, Russia

How to cite this article: Mitrakova N.V., Khayrulina E.A., Blinov S.M., Perevoshchikova A.A. Efficiency of acid sulphate soils reclamation in coal mining areas. Journal of Mining Institute. 2023. Vol. 260, p. 266-278. DOI: 10.31897/PMI.2023.31

Abstract. During the development of coal deposits, acid mine waters flowing to the surface cause the formation of acid sulphate soils. We study the effectiveness of soil reclamation by agrochemical and geochemical methods at the site of acid mine water discharge in the Kizel Coal Basin, carried out in 2005 using alkaline waste from soda production and activated sludge. A technosol with a stable phytocenosis was detected on the reclaimed site, and soddy-podzolic soil buried under the technogenic soil layer with no vegetation on the non-reclaimed site. The buried soddy-podzolic soil retains a strong acid pH concentration $H_2O = 3$. A high content of organic matter (8-1.5 %) is caused by carbonaceous particles; the presence of sulphide minerals reaches a depth of 40 cm. Technosol has a slightly acid pH reaction $H_2O = 5.5$, the content of organic matter due to the use of activated sludge is 19-65 %, the presence of sulphide minerals reaches a depth of 20-40 cm. The total iron content in the upper layers of the technosol did not change (190-200 g/kg), the excess over the background reaches 15 times. There is no contamination with heavy metals and trace elements, single elevated concentrations of Li, Se, B and V are found.

Keywords: coal mining; discharge of mine waters; acid sulphate soils; technosol; reclamation; trace elements; total contamination index; index of geological accumulation of elements

Acknowledgment. The work was supported financially by the Ministry of Education and Science of the Russian Federation, project N FSNF-2020-0021.

Received: 04.11.2022 ***Accepted: 02.03.2023*** ***Online: 30.03.2023*** ***Published: 25.04.2023***

Introduction. Coal production is the leading factor in the transformation of the natural environment in the areas of coal mining [1-3]. Shaft coal mining is usually accompanied by pumping and discharge of mine waters, as well as the accumulation of large-tonnage overburden dumps [4, 5]. Coals and coal-bearing rocks contain a large amount of sulphide and organic sulphur. For example, the content of pyrite in overburden can reach 10-12 % [6]. Pyrite and other sulphides in the oxidizing conditions of the mine space and rock dumps are chemically unstable under the influence of water and the participation of microorganisms [7, 8], so acid waters enriched with sulphates are formed in the mine space and rock dumps.

Discharge of mine waters to the surface and formation of acid wastewater of rock dumps, as well as the transfer of particles of rock dumps by temporary water flows leads to technogenic impact on the soils in adjacent areas [9-11]. Wastewater from dumps and spills of mine waters are sources of trace elements entering surface waters, bottom sediments, and soils [4, 10, 12]. As a result, technogenic soils are formed with physical and chemical properties that are not characteristic of the original soils [9], with a strong acid reaction of the environment and an increased content of sulphates and trace elements in the surface layer [9, 12, 13]. Retention capacity of soils provides the possibility of secondary contamination of surface and ground waters with trace elements and sulphates [14].

Reclamation of dumps and disturbed areas, remediation of soils and higher vegetation is an important applied task in the remediation of technogenic ecosystems [15, 16].

Soil formation in mining areas depends on the climate and topography, chemical composition of the dump rocks, which are technogenic soil-forming rock [17, 18]. Acid sulphate soils occur in coal mining areas due to the inflow of mine and waste water enriched with sulphates. Overburden dumps are an additional source of organic matter. In natural conditions, the formation of acid sulphate soils is confined to substrates rich in sulphides. For example, sulphidization manifests itself as a result of the penetration of sea water into tidal marshes with anaerobic conditions and a high content of organic matter [19, 20].

The study of technogenic soil formation and the effectiveness of reclamation measures was carried out in the Kizel coal deposit (Perm Krai). Despite the detailed study of surface waters and bottom sediments [4, 21, 22], the current state of soils in self-spills and acid mine waters discharge sites in the Kizel Coal Basin (KCB) has not been practically investigated. In the 20s of the XXI century, attempts were made to study soils formed on dumps [23, 24], however, the study of soils formed on runoff from dumps and mine water runoff was not carried out even before the reclamation activities.

The purpose of this work is to investigate the original and reclaimed soils at the site of acid water discharge from the Shirokovskaya mine in order to assess the effectiveness of the reclamation carried out in 2005. The tasks are to study the morphological changes in soils and their classification; investigate the chemical properties of soils, make a geochemical assessment of soils by the content of trace elements.

Methods. *Description of the study area*. The Kizel Coal Basin is in the eastern part of the Perm Krai, its area is 1500 km^2, its length is about 150 km. Underground coal mining lasted about 200 years. From 1992 to the early 2000s, the mines were abandoned. In the KCB area, there are about 100 rock dumps. Earth remote sensing (ERS) methods established that the land area occupied by dumps is 260 ha [4]. Over 35 million m^3 of rocks were accumulated in the dumps during the mine operation. The lithology of the coal-bearing stratum, the mining and storage technology determined the heterogeneity in the mineral composition of the rocks of the dumps, in which about 60 minerals were found. Dumps consist of mudstones, siltstones, sandstones, limestones, coal, pyrite, and may contain wood and metal features [25]. The long-term operation of mines and their inappropriate abandonment led to negative consequences for surface and ground waters and soils. Self-spills of mine waters to the surface and runoff from dumps have a strong acid reaction, pH 2-3, are characterized by high concentrations of iron, aluminium, manganese, beryllium, the content of which is hundreds of times higher than the maximum permissible concentration (MPC) [4, 10, 26].

The study area belongs to the Ural geochemical province of the eluvial-transalluvial region of the residual mountain ranges of the western slope of the Middle Urals, to the Upper Yaiva landscape of high ridged and steeply sloping foothills on the Paleozoic carbonate and partially terrigenous rocks. The climate is moderate continental, the average annual rainfall is 700 mm. The KCB area belongs to the Western foothill region of heavy loamy podzolic, soddy-podzolic, and marshy soils. According to the botanical and geographical zoning, the study area belongs to the middle and southern taiga foothill fir-spruce and spruce-fir forests.

The sampling area is in the Kizel district of the Perm Krai, near the dump of the Shirokovskaya mine, 0.3 km from the village of Yuzhny Kospashsky (Fig.1).

Research objects. In 2021, two soil profiles were made at the site of acid mine water discharge at an altitude of 370 m above sea level. The sampling area is 350 m from the dump of the Shirokovskaya mine: section N 1 directly at the site of acid mine waters discharge, section N 2 at the reclaimed discharge site (Fig.2). Samples of soddy-podzolic soil were taken as a background; the pit was made in a secondary small-leaved forest 30 m from the site of the former discharge.

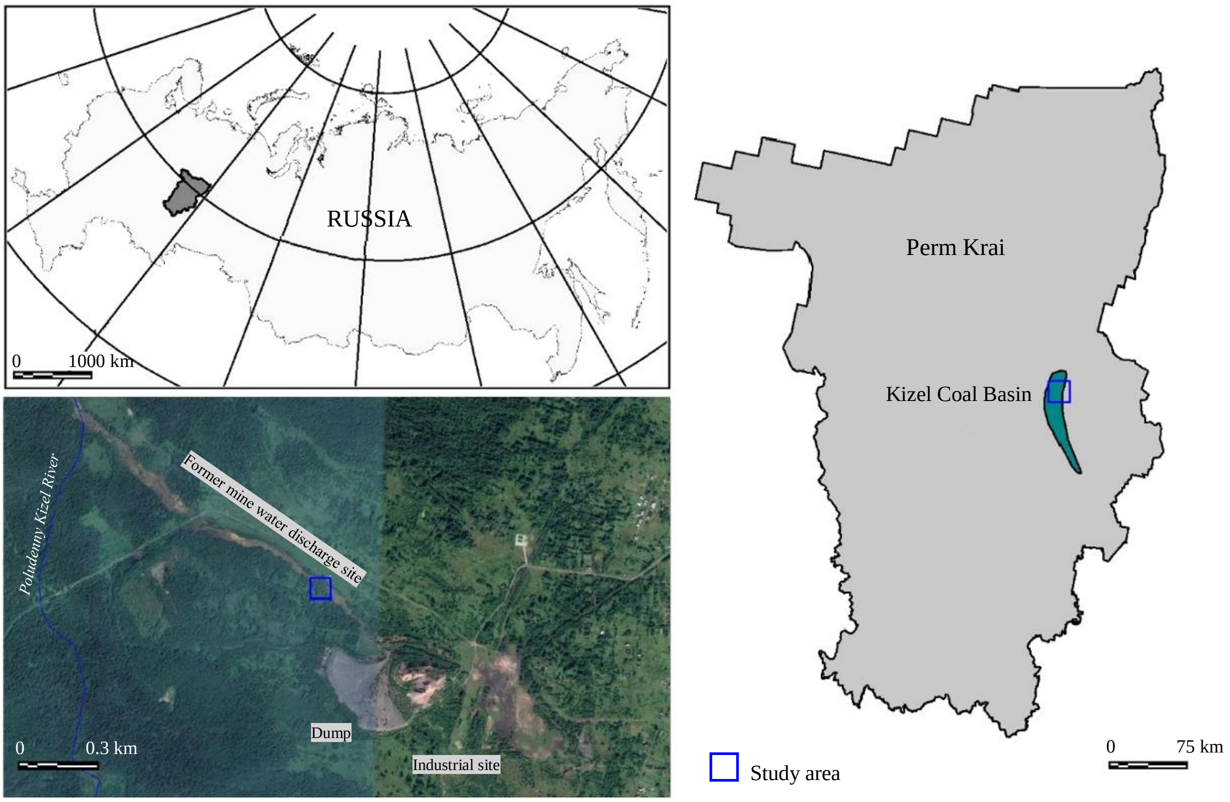

Fig.1. Geographical position of the Kizel Coal Basin

Location of section N 1

Location of section N 2

Fig.2. Sampling area

The acid mine water discharge site is a strip 10-90 m wide, extended in a north-western direction from the area of the former mine and the waste dump to the Poludenny Kizel River. The length of the site is about 1.8 km, its area in 2021, according to remote sensing data, was about 20 ha. The surface of the site has a red-brown colour and is characterized by a complete absence of vegetation. The remains of dead woody plants are noted.

The Shirokovskaya mine started its operation back in 1945, was abandoned at the end of the 1990s. Approximately in the mid-1980s, acid mine waters were neutralized with lime. As a result, a large amount of technogenic soils, consisting of finely dispersed iron hydroxides with crushed stone, grus, and sand of mine dumps, accumulated at the discharge site. The thickness of technogenic soils in some places can reach one metre.

Soil reclamation in a small area of the acid mine water discharge site near the Shirokovskaya mine dump was carried out about 17 years ago. It consisted in creating an artificial alkaline geochemical barrier that helps to reduce the migration of pollutants by transferring them into immobile forms [27]. To reduce the acidity of soils, alkaline wastes from OAO Berezniki Soda Plant (BSP) were used as a reactant. They consisted of finely dispersed $CaCO_3$ by more than 90 % and had no harmful admixtures. The activated sludge from the treatment facilities of OAO Metafrax (Gubakha) was used as organic matter [27]. The composition of the grass mixture for reclamation included reed canary grass *Phalaris arundinacea* L., red clover *Trifolium praténse* L., alfalfa *Medicago sativa* L., and couch grass *Elytrigia repens* (L). Reclamation measures on the soils with acid sulphate runoff led to a decrease in acidity from 2.7-3.0 to 5.0-6.0. Land reclamation in coal mining areas is often based on a decrease in acidity and an increase in fertility of technogenic soils in general. Reclamation includes fertilization to regulate nutrients, nitrogen, organic matter, as well as measures to improve the physical properties of soils [28]. In Europe, reclamation activities in dumps and mining areas are carried out for the emergence of sustainable tree plantations, which indicate the ecosystem restoration [1]. The introduction of lime during the reclamation of dumps is a fairly common method [28], as is the introduction of activated sludge as a fertile layer [29].

Currently, a stable phytocenosis was found on the reclaimed site, represented by young birches (genus *Betula*), willows (genus *Salix*), and alder (genus *Alnus*), as well as herbaceous plants of the sedge (genus *Carex*), graminaceous *Poaceae*, fireweed *Onagraceae*, pink *Caryophyllaceae* families, as well as mosses.

Sampling and research methods. In soil profiles, samples were taken to a depth of 80 cm with a step of 10 cm. Actual and exchangeable acidity was determined by the potentiometer. Determination of soil acidity in hydrogen peroxide was carried out for the oxidation of sulphide minerals present in dumps and runoff from them (R.Brinkman and L.J.Pons[1] proposed a preliminary pH limit of H_2O_2 = 2.5 for hazardous acid sulphate soils after peroxide treatment). Hydrolytic acidity was determined by the Kappen method (in 1M CH_3COONa extract), based on titration with 1 N alkali in the presence of phenolphthalein. Exchangeable acidity (EA), exchangeable aluminium Al_{ex} and exchangeable hydrogen N_{ex} were studied according to the Sokolov method, based on soil treatment with a 1M KCl solution, followed by titration of one part with alkali to discover the sum of exchangeable aluminium and hydrogen, the other part of the extract was titrated with alkali with adding fluoride to determine hydrogen ions. The content of organic matter was determined by spectrophotometry. The cation exchange capacity (CEC) was determined by the Bobko – Askinazi – Alyoshin method. The content of exchangeable calcium and exchangeable (mobile) magnesium was studied by complexometric titration. The content of mobile sulphur was determined by turbidimetry, mobile iron was determined by spectrophotometry with o-phenanthroline. Sulphate ions in the aqueous extract were determined by turbidimetry.

The microelement composition was determined by inductively coupled plasma spectrometry on an Elan 900 mass spectrometer, the particle size distribution was determined using a set of “Vibrotechnik” sieves and a laser diffraction particle size analyser Analysette 22 Micro Tec plus at the Centre for Unique Research Equipment of the Perm State National Research University.

---

[1] Brinkman R., Pons L.J. Recognition and prediction of acid sulphate soil conditions. Proceedings of an International Symposium. 1973, p. 169-203. URL: http://www.alterra.wur.nl/Internet/webdocs/ilri-publicaties/publicaties/Pub18_vol.1/pub18v1-h6.pdf (accessed 04.11.2022).

To assess the level of soil contamination with chemical elements, the *Igeo* index of geological accumulation of elements in soils was used, which links the content of elements of the natural soil background with the influence of human activity on the content of elements in technogenically disturbed soil. The index, widely used to assess the contamination of surface soil layers with trace elements [30, 31], was calculated for each element

$$Igeo = \log_2\left(\frac{Cn}{k}Bn\right),$$

where *Cn* is the content of the microelement in the soil; *Bn* is the local natural background content of the microelement in the soil; *k* is the index of background content compensation due to lithogenic factors, usually set equal to 1.5 [30, 31].

Igeo is divided into seven classes: $Igeo \leq 0$ – uncontaminated; $0 < Igeo < 1$ – uncontaminated to moderately contaminated; $1 < Igeo < 2$ – moderately contaminated; $2 < Igeo < 3$ – moderately contaminated to highly contaminated; $3 < Igeo < 4$ – highly contaminated; $4 < Igeo < 5$ – highly contaminated to very highly contaminated; $5 < Igeo$ – very highly contaminated.

An environmental assessment of the soil-vegetative layer (0-20 cm) according to the degree of total soil contamination with heavy metals was carried out using the contamination index Z_c, calculated according to SanPin 1.2.3685-21.

Discussion of the results. *Morphology and classification of soils.* Section N 1 was made on the unreclaimed site of acid mine water discharge. The soil profile consists of several layers (Fig.3, *a*). The upper layer is formed by technogenic material accumulated during the discharge of acid mine waters and their neutralization with lime, as well as mechanical deposition of sand and gruss of the dump rocks. Below the technogenic horizon, a profile of soddy-podzolic soil was found, consisting of humus, eluvial, transitional horizons, and horizon differentiated by texture.

The technogenic TCH layer is 0-33/33 cm, brown-orange, structureless, dense, viscous, clayey. The presence of sand and gruss of overburden rocks of the dump (2-10 mm) is noted, there are no pores, the boundary of the next layer is well defined. The volume of clastic particles is about 60 % of the soil mass.

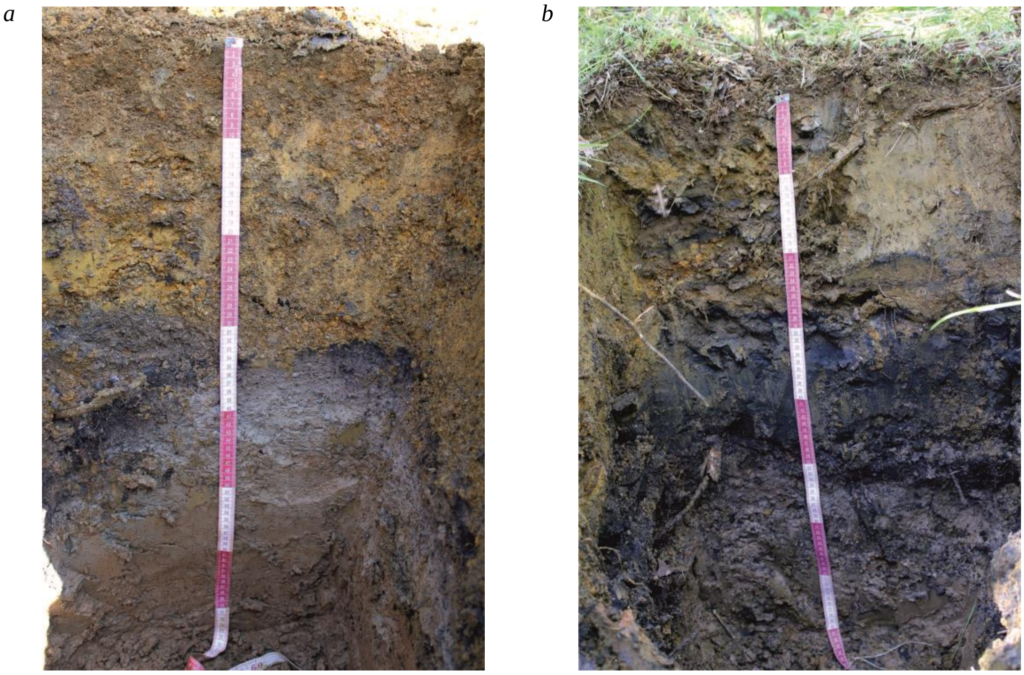

Fig.3. Soil profiles: *a* – soddy-podzolic soil buried under the technogenic layer; *b* – technosol

Humus horizon AY is 33-35/2 cm, dark grey, finely cloddy, clayey.

Eluvial horizon EL is 35-45/10 cm, pale-yellow, rusty spots on the soil pads, clayey, moist, unstructured in the field, when dry it breaks in one plane, which indicates layering.

Subeluvial horizon BEL is 45/60/15 cm, light yellow-pale, presence of ferruginous concretions, clayey, in a dry state breaks up into prisms, dense, porous.

Horizon differentiated by texture BT is 60-80/20 cm, pale-brown in dry state, reddish-brown in wet state, rusty stains, clayey, prismatic structure found in dry state. According to the classification and diagnostics of soils in Russia, the soil is diagnosed as a soddy-podzolic clayey soil buried under a technogenic layer.

According to the WRB[2] World reference base for soil resources, the soil is identified as Epitechno-leptic Technosols (Supraalbic, Epithionic, Clayic, Phytotoxic, Skeletic).

Profile N 2 is described on the reclaimed site. This soil has several layers of different colours (Fig.3, *b*). The soil is clayey, viscous, compacted. On the surface there are fallen leaves and grassy remains, below the leaves there is a technogenic horizon of brown-ochre colour, 29 cm thick, with black interlayers and reddish spots. At a depth of 20 cm, white inclusions are observed. Apparently, these are waste from soda production. From 29 to 52 cm, the colour of the profile becomes almost black, layering and lack of structure are observed. Below, to 80 cm, there is a grey-brown clayey unstructured layer. The soil was diagnosed as technosol on soddy-podzolic soil. This profile structure was formed as a result of the introduction of soda production waste and activated sludge, their mixing and migration along the profile over the next years. According to WRB, the soil is diagnosed as Technosols (Clayic, Histic, Gleyic). Both types of soils were formed under hydromorphic conditions in a trans-accumulative landscape.

The third profile is a typical soddy-podzolic clayey soil; under the humus horizon there is an eluvial horizon, then a transitional horizon, and then a horizon differentiated in texture; the presence of a thin litter is noted.

Chemical properties of soils. The soddy-podzolic soil buried under the technogenic layer to a depth of 30 cm has a strong acid reaction, pH H_2O = 3.0 (Fig.4, *a*), acidity decreases with depth; pH H_2O_2 to 30 cm does not exceed 2.5, which indicates the presence of sulphide minerals. High acidity is characteristic of the technogenic layer, which is represented by crushed matter of overburden dump rocks. Oxidation of sulphide minerals and acidification of the substrate occur due to the presence of pyrite in the mineral composition of rocks [4, 25]. The buried soddy-podzolic soil is characterized by an acid reaction, the acidity of the horizons corresponds to the acidity of the corresponding horizons in the background soil.

Technosol to 20 cm has a weak acid reaction, pH H_2O = 5.3-4.4; to a depth of 50 cm, the acidity sharply increases to pH H_2O = 3.3 (Fig.4, *b*). The indicators of actual acidity correlate with the pH values of H_2O_2; from a depth of 30-50 cm, sulphide minerals are present in the technosol, providing a strong acid soil reaction. The decrease in acidity in the upper layers of the technosol is caused by the soil neutralization as a result of the introduction of soda production waste during the reclamation.

The hydrolytic acidity H_{ha} of the entire profile of the soddy-podzolic soil buried under the technogenic layer and the background soil does not differ, its value is due to the presence of acid technogenic deposits and the properties of the soddy-podzolic buried soil. In the technosol, the value of hydrolytic acidity to 50 cm is lower than in the soddy-podzolic buried and background soil, which was promoted by the reclamation measures carried out (Table 1).

---

[2] World reference base for soil resources 2014 International soil classification system for naming soils and creating legends for soil maps. Rome, Italy: Food and Agriculture organization of the United Nations, 2015, p. 192.

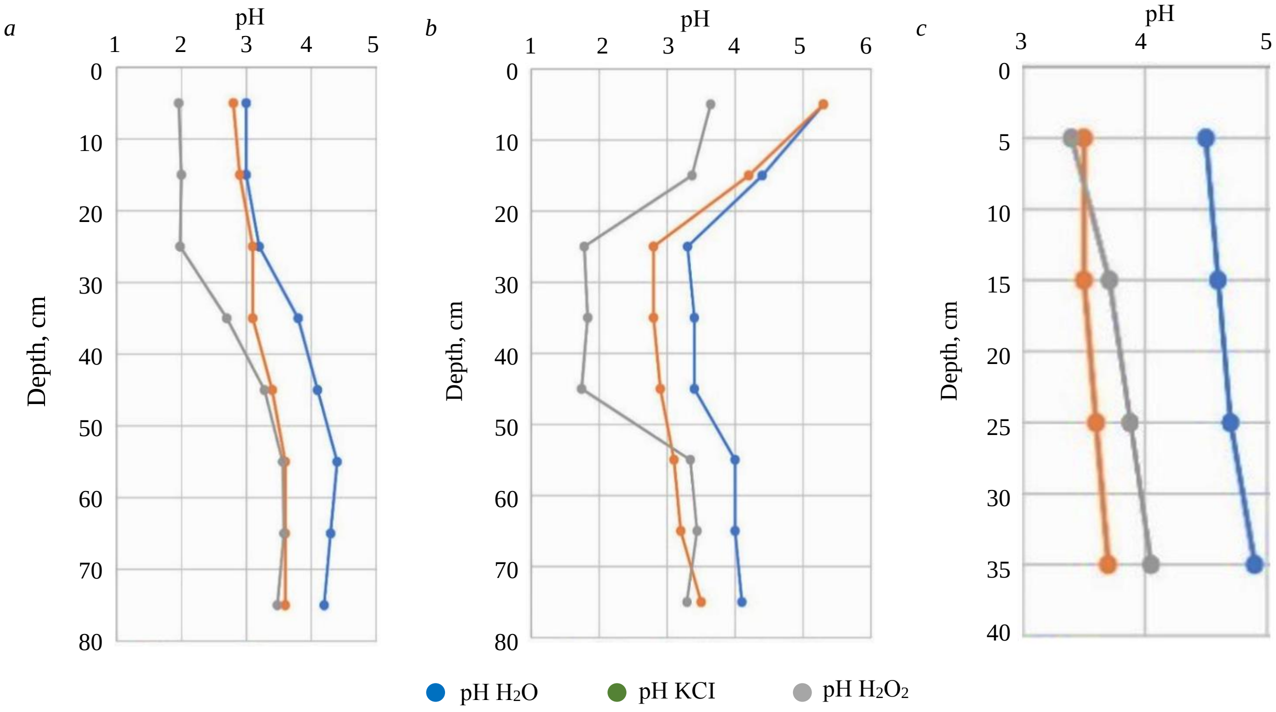

Fig.4. Soil acidity: *a* – soddy-podzolic, buried under the technogenic layer; *b* – technosol; *c* – background soddy-podzolic soil

Table 1

Soil chemical properties

Soil	Depth, cm	C_{org}, %	H_{ha}, mmol/100 g	CEC, mmol/100 g	Al_{ex}, mmol/100 g	EA, mmol/100 g	H_{ex}, mmol/100 g	SO_4^{2-}, mmol/100 g	Ca_{ex}, mmol/100 g	Fe_{mob}, (total), mg/kg	Fe_{tot}, g/kg	S_{mob}, mg/kg
Soddy-podzolic, buried under the technogenic layer	0-10	8.2	18.9	31.0	0.62	0.75	0.13	1.7	0.50	460	200.6	724
	10-20	6.5	18.1	25.0	0.59	0.69	0.15	1.6	0.50	530	200.8	698
	20-30	8.3	16.2	24.0	0.78	0.81	0.03	1.2	0.50	620	109.8	601
	30-40	4.7	24.7	22.0	6.11	7.45	1.34	1.1	0.88	200	18.7	182
	40-50	2.35	21.1	24.0	5.56	5.60	0.04	0.6	0.50	250	11.7	129
	50-60	1.5	12.5	20.0	5.33	7.30	1.91	0.7	1.00	180	13.3	158
	60-70	1.4	14.3	20.0	6.67	6.60	0	0.6	4.25	170	13.4	148
	70-80	2.2	16.2	13.0	5.22	5.90	0.62	0.8	1.38	170	16.0	43
Technosol	0-10	19.1	4.73	31.0	0.09	0.14	0.06	7.4	7.31	380	197.8	2000
	10-20	23.0	8.40	27.0	0.01	0.04	0.03	1.9	2.25	450	190.1	869
	20-30	41.4	14.2	23.0	1.89	2.00	0.11	0.9	1.19	310	66.3	331
	30-40	65.8	11.0	21.0	2.00	2.17	0.19	0.9	1.00	200	33.1	79
	40-50	65.8	13.7	22.0	2.44	2.51	0.04	0.7	1.06	220	41.9	349
	50-60	2.51	17.9	20.0	3.33	6.20	2.90	0.9	0.88	210	14.1	142
	60-70	1.4	15.8	24.0	6.56	6.60	0.06	0.8	0.50	260	17.3	117
	70-80	1.1	18.5	21.0	4.11	4.70	0.62	1.1	0.75	170	18.6	159
Soddy-podzolic (background)	0-10	5.0	26.4	13.0	4.78	5.0	0.17	0.05	3.25	430	13.5	12.9
	10-20	5.1	21.4	21.0	5.78	5.9	0.12	0.05	2.25	430	13.4	4.6
	20-30	6.1	20.8	19.0	5.78	5.9	0.13	0.05	2.75	360	11.6	0.2
	30-40	2.5	19.9	17.0	5.56	6.7	1.12	1.30	2.75	260	13.1	0.9

The maximum content of organic matter C_{org} is typical for 30-50 cm of the technosol layer, 65.8 %, in general, in the technosol to 50 cm, the amount of organic matter varies from 19.1 to 65.8 % (Table 1). This is due to the introduction of activated sludge during the reclamation and its migration along the profile over a 15-year period. The content of organic matter is about 8 % in the technogenic layer of soddy-podzolic buried soil, possibly due to the presence of carbonaceous particles. The cation exchange capacity in runoff soils has average values and exceeds the absorption capacity of the background soil.

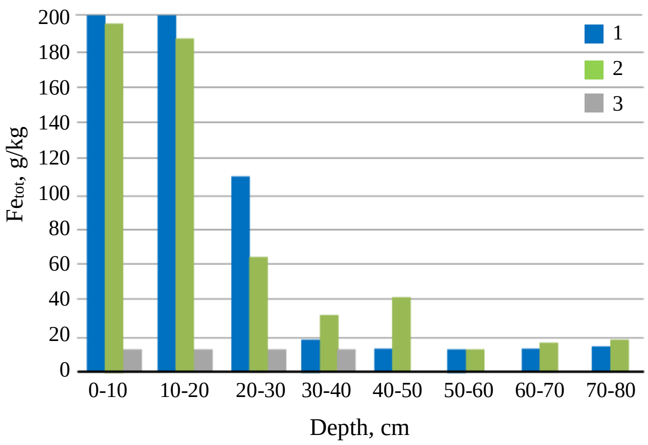

Fig.5. Total iron content

1 – soddy-podzolic soil buried under the technogenic layer; 2 – technosol; 3 – soddy-podzolic background soil

The exchangeable acidity and the content of Al_{ex} in the soils at the acid mine water discharge site are lower than in the background soils. This is due to the technogenic nature of acidity in the soddy-podzolic buried soil and technosol, namely, the presence of sulphide minerals. The technogenic layer of soddy-podzolic buried soil has a minimum value of exchangeable acidity along the profile from 0.75 to 0.81 mmol/100 g, while in the horizons of buried soddy-podzolic soil, exchangeable acidity corresponds to the background soil and is 6-8 mmol/00 g. The same trend is typical for H_{ex}.

The introduction of sludge and waste from soda production into the technosol provides low values of exchangeable acidity from 0.09 to 2.00 mmol/100 g to a depth of 40 cm. The amount of exchangeable calcium in the 0-10 cm layer of the technosol exceeds this indicator in the background and buried soils. In the soddy-podzolic soil buried under the technogenic layer, the amount of exchangeable calcium increases with depth, while in the technosol, on the contrary, it decreases.

The content of total iron Fe_{tot} in the upper 20-cm soil layer in the non-reclaimed and reclaimed sites is 15 times higher (200 g/kg) than in the humus horizon of the background soil (Fig.5, Table 1). The iron content decreases to the background level with depth in the soddy-podzolic soil buried under the technogenic layer and amounts to 11-13 g/kg (Fig.5).

According to Table 1, Fe_{tot} does not migrate down the profile, but remains in the substance of technogenic deposits. The amount of Fe_{tot} in the background soil corresponds to its content in the soddy-podzolic buried soil from a depth of 30 cm, which also indicates the absence of migration of the unreclaimed site in the soil. In the technosol, its increased content was noted to a depth of 50 cm, which is associated with the introduction of sludge and waste from soda production to the upper layer during the reclamation; then the technogenic material of the dump and the introduced substances were mixed. This ensured the penetration of the technogenic substance into the middle layers of the technosol and the high content of Fe_{tot} relative to the background. The content of mobile iron in soils decreases with depth; there are no significant differences from the background.

The amount of Fe_{tot} in soils in the former discharge site of acid mine waters is explained by the mineralogical features of overburden rocks, the main part of the minerals in which are unstable and readily soluble iron sulphates [25].

Sulphate ions predominate in the water extract of soils, their content varies from 0.7 to 1.9 mmol/100 g, except for the surface layer of technosol, 7.4 mmol/100 g (Table 1). The content of mobile sulphur S_{mob} in the studied soils does not differ and is hundreds of times higher than this indicator in the background soil. A correlation was found between the content of mobile sulphur and the content of total iron $R^2 = 0.71$. The source of mobile sulphur in technogenic soils is technogenic deposits from rock dumps, the material in which contains sulphur in sulphide, sulphate, and elemental forms [32].

The study of the particle size distribution in the soddy-podzolic buried soil showed its clayey composition (Fig.6). In the 0-10 cm layer of soddy-podzolic buried soil, a significant proportion (30 %) was gravel, about 10 % of which has a size of 5-10 mm or more. This indicates the presence of deposits on the surface of the acid mine waters discharge site containing fragments of overburden. With depth, the amount of gravel decreases. The predominant fraction to 40 cm is particles with a size of 1-0.1 mm, below, a fraction with a size of 0.05-0.01 mm.

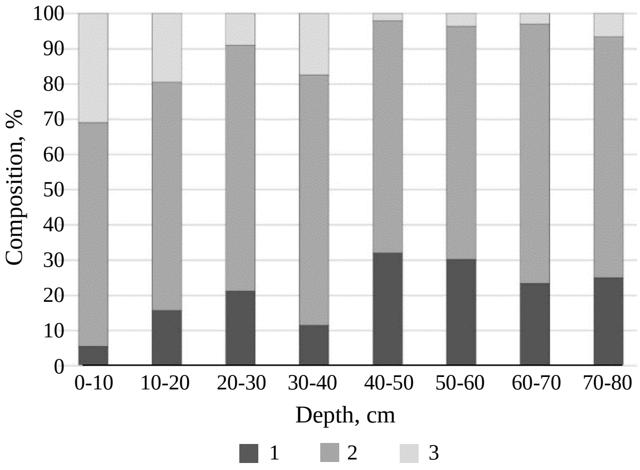

Fig.6. Particle size distribution of soddy-podzolic soil buried under the technogenic layer of soil
1 – physical clay; 2 – physical sand; 3 – gravel

The technosol also has a clayey composition, the presence of gravel in a 20-cm layer is noted, however, in a smaller amount than in the soddy-podzolic buried soil. Below 40 cm gravel is absent.

The properties of the buried soddy-podzolic soil correspond to those of the background soil. However, a 30-cm layer of technogenic deposits from the dump causes a sharply acid reaction of the soil environment pH H_2O = 3.0, reduced values of exchange-able aluminium and calcium, and an increased content of total iron relative to buried and background soils. It can be assumed that the buried soddy-podzolic soil was in a preserved state, its environmental properties did not undergo significant transformation. During reclamation, the technogenic soil layer of the acid mine water discharge site was mixed with the addition of sludge and carbonate-containing waste, which caused the deposit substance to enter deeper soil layers, which caused an even greater variation in properties. In the technosol, the actual (pH H_2O = 5.0) and hydrolytic acidity is lowered, sulphide minerals are neutralized in the upper part of the profile, the content of organic matter and exchangeable calcium is high, and the content of total iron is increased in most of the profile. Reclamation on the soils of the acid sulphate runoff site led to a decrease in acidity, an increase in the amount of organic carbon and absorption capacity. The improvement of soil properties in the reclaimed site led to the emergence of a stable phytocenosis.

Geochemical assessment of soils. The study of the content of trace elements (Cu, Zn, Co, Ni, Cd, Pb, V, Mn, Li, Be, B, Se, Al) included identifying the degree of contamination and distribution of trace elements along the profile of soils formed on the area of runoff from the coal dump, relative to background values, clarke according to Vinogradov, APC and the *Igeo* index.

The content of trace elements (Li, B, Fe, Co, As, Pb, Se) in the studied soils exceeds their background values (Table 2). This is due to the high content of trace elements in overburden rocks [33], as well as their high adsorption on iron hydroxides and organic matter. According to [34], heavy metals are sorbed on iron hydroxides; however, in organogenic soils, iron competes with heavy metals; iron hydroxides can be used as a geochemical sorption barrier for the accumulation of trace elements.

The content of Cu and Cd exceeds the approximate permissible concentrations (APC) for acid clayey soils; for V, an excess of MPC was found. For Zn, the excess is typical for a layer of 0-20 cm of the background soil, the excess for Co and Ni was found below the geochemical barriers in soils in the area of the runoff from the dump with depth along the profile.

The total contamination index Z_c, calculated for all the studied trace elements for the surface layers (0-10 and 10-20 cm) of the soddy-podzolic soil buried under the technogenic layer and technosol, indicates the absence of contamination.

The *Igeo* index was calculated for each element in the root layers (0-10, 10-20 cm) using the background content in the soddy-podzolic soil (Table 3). The studied samples of the soddy-podzolic buried soil are slightly contaminated with Li, B, V, and Se. The remaining elements had values less than zero, which indicates the absence of contamination in the studied soils. Thus, Se forms the geochemical orientation of the soil cover of the gold ore deposit area, the main minerals in which are pyrite, chalcopyrite, iron hydroxides, etc. [36]. The sources of Li and V are coals, while the main carriers of Li are illite and montmorillonite [37]. Due to weathering at sulphide ore features, Se, Li, V, and B can enter natural features, for example, into soils, which explains their presence in the technogenic alluvial soil layer in the dump runoff area.

Table 2

Trace elements content in soils of runoff from the coal dump

Soil	Depth, cm	pH KCl	Cu	**Zn**	**Co**	**Ni**	**Cd**	Pb	**V**	**Mn**	**Li**	**Be**	**B**	**Se**	**Al**	Z_c*
Soddy-podzolic buried under the technogenic layer	0-10	2.8	92.87	41.90	4.35	17.47	5.17	17.94	375.58	102.25	83.11	1.75	389.27	5.16	92.52	4.3
	10-20	2.9	120.48	43.20	3.95	17.42	5.02	21.49	425.81	86.80	82.12	1.68	383.43	5.27	90.87	5.0
	20-30	3.1	111.60	67.96	9.65	33.96	8.75	25.00	314.97	192.61	70.48	2.05	330.32	3.90	175.09	–
	30-40	3.1	102.72	92.71	15.35	50.49	12.49	28.52	204.14	298.42	58.83	2.41	277.22	2.54	259.31	–
	40-50	3.4	75.57	104.02	21.22	63.83	12.37	26.53	193.77	376.28	63.00	2.53	253.15	3.53	252.18	–
	50-60	3.6	66.60	92.84	21.44	60.76	11.01	25.00	174.95	455.23	58.53	2.98	242.54	1.50	243.43	–
	60-70	3.6	68.66	92.71	21.20	59.95	11.04	27.22	181.55	454.44	53.09	2.81	240.53	1.62	229.08	–
	70-80	3.6	64.76	89.28	24.96	57.35	11.61	31.13	190.58	7.82	47.66	2.86	215.34	1.99	221.62	–
Technosol	0-10	5.3	88.17	64.59	8.20	27.47	5.02	49.92	345.20	211.95	126.51	2.92	488.64	4.65	82.88	5.5
	10-20	4.2	85.60	61.89	7.98	26.57	4.98	47.97	330.54	204.39	121.00	2.76	468.10	4.25	84.19	5.5
	20-30	2.8	62.46	49.41	7.57	30.72	10.19	32.94	300.85	120.38	194.06	4.46	598.86	6.07	139.35	–
	30-40	2.8	71.17	53.09	9.13	37.40	10.75	30.00	303.38	112.03	249.31	5.87	711.17	4.47	146.68	–
	40-50	2.9	121.35	60.68	8.35	32.84	9.76	23.02	319.89	100.95	232.13	5.59	681.27	1.77	127.54	–
	50-60	3.1	79.61	83.93	18.44	60.68	10.49	25.40	204.55	641.08	74.77	2.64	333.30	1.33	285.55	–
	60-70	3.2	83.36	102.22	22.24	72.95	12.37	29.72	233.66	728.25	74.89	2.83	311.98	2.97	289.89	–
	70-80	3.5	72.30	106.10	25.40	75.56	9.49	28.09	242.79	573.03	71.69	3.23	283.38	1.96	262.14	–
Soddy-podzolic (background)	0-10	3.5	85.23	128.57	15.91	53.11	11.12	43.07	174.69	496.00	48.09	2.79	225.16	3.13	240.00	–
	10-20	3.5	79.25	126.99	15.88	53.13	11.21	33.53	176.53	511.51	44.66	2.54	221.45	3.40	226.94	–
	20-30	3.6	70.43	97.08	14.83	48.65	12.58	23.28	160.29	508.85	38.69	1.93	204.41	2.56	225.02	–
	30-40	3.7	68.08	99.73	20.29	65.23	10.74	21.95	175.05	399.31	41.80	1.95	184.34	1.79	226.71	–
Clarke according to Vinogradov [35]		–	47	83	18	58	0.13	16	90	1000	–	3.8	12	–	80,500	–
APC**/MPC		–	66/	110/	–	40/	1/	65/	/150	/1500	–	–	–	–	–	–

Notes. Trace elements are highlighted in bold, for which an excess was found in KCB rivers and bottom sediments according to the report (On the state and environmental protection of the Perm Krai in 2020. Perm: Ministry of Natural Resources and Environment of the Perm Krai, 2021, p. 288); * – Z_c calculated for layers 0-10, 10-20 cm (as root-inhabited) relative to the corresponding background values; ** – APC according to SanPin 1.2.3685-21 (pH KCl < 5.5).

Table 3

Results of statistical analysis of the geological accumulation index *Igeo*

Soil	**Li**	Be	**B**	Al	**V**	Mn	Co	Ni	Cu	Zn	**Se**	Cd	Pb
Technosol (medium)	0.8	<0	0.5	<0	0.4	<0	<0	<0	<0	<0	<0	<0	<0
Soddy-podzolic, buried under the technogenic layer (medium)	0.2	<0	0.2	<0	0.6	<0	<0	<0	<0	<0	0.1	<0	<0
Contamination level	1	–	1	–	1	–	–	–	–	–	1*	–	–

---

* Only for soddy-podzolic buried soil.

It should be noted that there is no intensive technogenic migration of elements down the soil profile. Pollutants, mainly Li, B, Be, Fe, V, are concentrated in the surface layers of soils in the area of acid mine water discharge and actively migrate with planar runoff in the form of suspended particles, together with dump minerals, into accumulative landscapes, fall into rivers, concentrate in bottom sediments, and migrate with water flows over long distances, as evidenced by the data in [4, 10, 38].

Conclusion. Due to the technogenic deposits, a soddy-podzolic soil buried under the technogenic layer was formed at the acid mine water discharge site, which, according to WRB, is defined as Epitechnoleptic Technosols (Supraalbic, Epithionic, Clayic, Phytotoxic, Skeletic). The profile and properties of a typical zonal soddy-podzolic soil are preserved under a 30-cm layer of technogenic deposits. The reclamation of this soil using activated sludge and alkaline waste from soda production led to the emergence of a technosol; according to WRB, the soil was diagnosed as Technosols (Clayic, Histic, Gleyic).

The soddy-podzolic soil buried under the technogenic layer has a sharply acid pH reaction H_2O = 3, which is an indicator of the presence of sulphide minerals. The high content of organic matter is due to the presence of carbonaceous particles (8-4.7 % in the layer formed by technogenic deposits); the exchange acidity of the technogenic layer is low; average absorption capacity is 31-20 mmol/100 g. Technosol is characterized by a less acid pH reaction H_2O = 4.5-5.5; the content of organic matter down to a depth of 50 cm varies from 19 to 65 %, which is due to reclamation activities. The cation exchange capacity is average, but the amount of exchangeable calcium in the technosol is higher than in the soddy-podzolic buried soil, as is the S_{mob} content. The Fe_{tot} content in the upper 30-cm soil layer of the acid mine water discharge site varies from 66 to 200 g/kg, which exceeds the background values by 8-15 times.

A study of the microelement composition showed an excess of Li, B, Fe, Co, As, Pb, Se content in the studied soils over the background values. An excess of APC for Cu, Cd and MPC for V was also found. However, a comprehensive assessment of geochemical environmental state of the surface layers of soils in acid mine water discharge site based on the Z_c and *Igeo* indices showed the absence of contamination by the studied trace elements, except for Li and B, as well as Se for the soddy-podzolic soil buried under the technogenic layer.

Reclamation led to an improvement in the physical and chemical properties of technogenic soils, a decrease in acidity and an increase in the organic matter content. Formation of a stable phytocenosis in the reclaimed site of acid mine water discharge indicates the effectiveness of this reclamation method.

REFERENCES

1. Ahirwal J., Maiti S.K. Assessment of soil properties of different land uses generated due to surface coal mining activities in tropical Sal (Shorearobusta) forest, India. *CATENA*. 2016. Vol. 140, p. 155-163. DOI: 10.1016/j.catena.2016.01.028

2. Arefieva O., Nazarkina A.V., Gruschakova N.V. et al. Impact of mine waters on chemical composition of soil in the Partizansk Coal Basin, Russia. *International Soil and Water Conservation Research*. 2019. Vol. 7. Iss. 1, p. 57-63. DOI: 10.1016/j.iswcr.2019.01.001

3. Xiaoyang Liu, Huading Shi, Zhongke Bai et al. Heavy metal concentrations of soils near the large opencast coal mine pits in China. *Chemosphere*. 2020. Vol. 244. N 125360. DOI: 10.1016/j.chemosphere.2019.125360

4. Maksimovich N.G., Pyankov S.V. The Kizel coal basin: ecological problems and solutions. Perm: Perm State National Research University, 2018, p. 288 (in Russian).

5. Chowdhury R.A., Sarkar D., Datta R. Remediation of Acid Mine Drainage-Impacted Water. *Current Pollution Reports*. 2015. Vol. 1. Iss. 3, p. 131-141. DOI: 10.1007/s40726-015-0011-3

6. Singh Kh.N., Narzary D. Geochemical characterization of mine overburden strata for strategic overburden-spoil management in an opencast coal mine. *Environmental Challenges*. 2021. Vol. 3. N 100060. DOI: 10.1016/j.envc.2021.100060

7. Welch C., Barbour S.L., Hendry M.J. The geochemistry and hydrology of coal waste rock dumps: A systematic global review. *Science of the Total Environment*. 2021. Vol. 795. N 148798. DOI: 10.1016/j.scitotenv.2021.148798

8. Zhihong Tu, Qi Wu, Hongping He et al. Reduction of acid mine drainage by passivation of pyrite surfaces: A review. *Science of the Total Environment*. 2022. Vol. 832. N 155116. DOI: 10.1016/j.scitotenv.2022.155116

9. Kostin A.S., Krechetov P.P., Chernitsova O.V., Terskaya E.V. Data on physico-chemical characteristics and elemental composition of gray forest soils (Greyzemic Phaeozems) in natural-technogenic landscapes of Moscow brown coal basin. *Data in Brief*. 2021. Vol. 35. N 106817. DOI: 10.1016/j.dib.2021.106817

10. Ushakova E., Menshikova E., Blinov S. et al. Environmental Assessment Impact of Acid Mine Drainage from Kizel Coal Basin on the Kosva Bay of the Kama Reservoir (Perm Krai, Russia). *Water*. 2022. Vol. 14. Iss. 5. N 727. DOI: 10.3390/w14050727

11. Shipilova A.M., Semina I.S. Features of physical properties of soil of technogenic landscapes of forest-steppe zone of Kuzbass. *News of the Ural State Mining University*. 2016. Vol. 3 (43), p. 25-28 (in Russian). DOI: 10.21440/2307-2091-2016-3-25-28

12. Sahoo P.K., Equeenuddin S.M., Powell M.A. Trace Elements in Soils around Coal Mines: Current Scenario, Impact and Available Techniques for Management. *Current Pollution Reports*. 2016. Vol. 2. Iss. 1, p. 1-14. DOI: 10.1007/s40726-016-0025-5

13. Grantcharova M.M., Fernández-Caliani J.C. Soil Acidification, Mineral Neoformation and Heavy Metal Contamination Driven by Weathering of Sulphide Wastes in a Ramsar Wetland. *Applied Sciences*. 2022. Vol. 12. Iss. 1. N 249. DOI: 10.3390/app12010249

14. Hulisz P., Różański S.Ł., Boman A., Rauchfleisz M. Can acid sulfate soils from the southern Baltic zone be a source of potentially toxic elements (PTEs)? *Science of the Total Environment*. 2022. Vol. 825. N 154003. DOI: 10.1016/j.scitotenv.2022.154003

15. Ye Yuan, Zhongqiu Zhao, Shuye Niu et al. Reclamation promotes the succession of the soil and vegetation in opencast coal mine: A case study from Robinia pseudoacacia reclaimed forests, Pingshuo mine, China. *CATENA*. 2018. Vol. 165, p. 72-79. DOI: 10.1016/j.catena.2018.01.025

16. Yu Feng, Jinman Wang, Zhongke Bai, Lucy Reading. Effects of surface coal mining and land reclamation on soil properties: A review. *Earth-Science Reviews*. 2019. Vol. 191, p. 12-25. DOI: 10.1016/j.earscirev.2019.02.015

17. Bragina P.S., Tsibart A.S., Zavadskaya M.P., Sharapova A.V. Soils on overburden dumps in the forest_steppe and mountain taiga zones of the Kuzbass. *Eurasian Soil Science*. 2014. Vol. 47. Iss. 7, p. 723-733. DOI: 10.1134/S1064229314050032

18. Zástěrova P., Marschalko M., Niemiec D. et al. Analysis of Possibilities of Reclamation Waste Dumps after Coal Mining. *Procedia Earth and Planetary Science*. 2015. Vol. 15, p. 656-662. DOI: 10.1016/j.proeps.2015.08.077

19. Fall L.A.C.A., Montoroi J.-P., Starh K. Coastal acid sulfate soils in the Saloum River basin, Senegal. *Soil Research*. 2014. Vol. 52. Iss. 7, p. 671-684. DOI: 10.1071/SR14033

20. Hulisz P., Kwasowski W., Pracz J., Malinowski R. Coastal acid sulphate soils in Poland: a review. *Soil Science Annual*. 2017. Vol. 68. Iss. 1, p. 46-54. DOI: 10.1515/ssa-2017-0006

21. Ushakova E., Menshikova E., Blinov S. et al. Distribution of Trace Elements, Rare Earth Elements and Ecotoxicity in Sediments of the Kosva Bay, Perm Region (Russia). *Journal of Ecological Engineering*. 2022. Vol. 23. Iss. 4, p. 1-16. DOI: 10.12911/22998993/146269

22. Pyankov S.V., Maximovich N.G., Khayrulina E.A. et al. Monitoring Acid Mine Drainage's Effects on Surface Water in the Kizel Coal Basin with Sentinel-2 Satellite Images. *Mine Water and the Environment*. 2021. Vol. 40. Iss. 3, p. 606-621. DOI: 10.1007/s10230-021-00761-7

23. Karakulieva A.A., Kondrateva M.A. Properties of Embryoses of Coal Mines Dumps of the Kizelovsky Basin. *Anthropogenic Transformation of Nature.* 2018. N 14, p. 156-159 (in Russian).

24. Berdinskikh S.Y., Botalov V.S., Romanov A.V., Zaitsev A.G. Agrochemical characteristics of the top layer of soil on coal heaps and the effect of clay formation on their natural overgrowth (on the example of the Kizelovsky coal basin). Environmental Safety in Conditions of Anthropogenic Transformation of the Environment, 21-22 April 2022, Perm, Russia. Perm State National Research University, 2022, p. 437-441 (in Russian).

25. Menshikova E., Osovetsky B., Blinov S., Belkin P. Mineral Formation under the Influence of Mine Waters (The Kizel Coal Basin, Russia). *Minerals.* 2020. Vol. 10. Iss. 4. N 364. DOI: 10.3390/min10040364

26. Menshikova E., Blinov S., Belkin P. et al. Dumps of the Kizel Coal Basin as a Potential Source of Rare and Rare-Earth Elements. Science and Global Challenges of the 21st Century – Science and Technology. Perm Forum 2021. Lecture Notes in Networks and Systems. Cham: Springer. 2022. Vol. 342, p. 352-361. DOI: 10.1007/978-3-030-89477-1_35

27. Krasilnikova S.A., Blinov S.M. Consequences of discharge of acidic mine waters in the Kizel coal basin. *Natural and technical sciences.* 2017. N 11 (113), p. 153-154 (in Russian).

28. Fernández-Caliani J.C., Giráldez M.I., Waken W.H. et al. Soil quality changes in an Iberian pyrite mine site 15 years after land reclamation. *CATENA.* 2021. Vol. 206. N 105538. DOI: 10.1016/j.catena.2021.105538

29. Nekrasova A.E., Bobrenko E.G., Knych A.I., Sologaev V.I. Reclamation of waste dump open joint-stock Company "Mine "Capital" of the Kemerovo region. *Bulletin of the Omsk State Agrarian University.* 2016. N 1 (21), p. 154-160 (in Russian).

30. Ghrefat H.A., Abu-Rukah Y., Rosen M.A. Application of geoaccumulation index and enrichment factor for assessing metal contamination in the sediments of Kafrain Dam, Jordan. *Environmental Monitoring and Assessment*. 2011. Vol. 178. Iss. 1-4, p. 95-109. DOI: 10.1007/s10661-010-1675-1

31. Martinez L.L.G., Poleto C. Assessment of diffuse pollution associated with metals in urban sediments using the geoaccumulation index (Igeo). *Journal of Soils and Sediments*. 2014. Vol. 14. Iss. 7, p. 1251-1257. DOI: 10.1007/s11368-014-0871-y

32. Maksimovich N.G., Meshcheryakova O.Yu., Berezina O.A. et al. Formation of acidic effluents from dumps of the Kizel coal basin (Perm Territory). Geological evolution of the interaction of water with rocks: Materials of the fourth All-Russian scientific conference with international participation. 17-20 August, 2020, Ulan-Ude, Russia. Ulan-Ude: Bulletin of the Buryat Scientific Center of the Siberian Branch of the Russian Academy of Sciences, 2020, p. 239-241. DOI: 10.31554/978-5-7925-0584-1-2020-239-241

33. Candeias C., Ferreira da Silva E., Salgueiro A.R. et al. The use of multivariate statistical analysis of geochemical data for assessing the spatial distribution of soil contamination by potentially toxic elements in the Aljustrel mining area (Iberian Pyrite Belt, Portugal). *Environmental Earth Sciences*. 2011. Vol. 62. Iss. 7, p. 1461-1479. DOI: 10.1007/s12665-010-0631-2

34. Yifan Lin, Jing Wang, Chunye Lin. Vertical changes in the geochemical distributions of iron, manganese and heavy metals in wetland soil cores from cold temperate zones in northeastern China. *Journal of Hazardous Materials Advances*. 2022. Vol. 6. N 100085. DOI: 10.1016/j.hazadv.2022.100085

35. Kasimov N.S., Vlasov D.V. Clarkes of Chemical Elements as Comparison Standards in Ecogeochemistry. *Bulletin of Moscow University. 2015. Series 5. Geography.* N 2, p. 7-17.

36. Mishankin A.Yu., Yazikov E.G., Filimonenko E.A., Sobyanin Yu.P. Mineral and geochemical features of the soil cover of the Vyun gold ore deposit (the republic of Sakha (Yakutia)). *Bulletin of the Tomsk Polytechnic University. Geo Assets Engineering.* 2021. Vol. 332. N 11, p. 98-109 (in Russian). DOI: 10.18799/24131830/2021/11/3381

37. Beilei Sun, Yunxia Liu, Lucie Tajcmanova et al. In-situ analysis of the lithium occurrence in the N 11 coal from the Antaibao mining district, Ningwu Coalfield, northern China. *Ore Geology Reviews*. 2022. Vol. 144. N 104825. DOI: 10.1016/j.oregeorev.2022.104825

38. Fetisova N. Study of Migration Forms of Metals in Rivers Affected by Acid Mine Drainage of the Kizel Coal Basin. *Bulletin of the Tomsk Polytechnic University. Geo Assets Engineering*. 2021. Vol. 332. N 1, p. 141-152 (in Russian). DOI: 10.18799/24131830/2021/1/3007

***Authors*: Natalya V. Mitrakova,** *Candidate of Biology, Senior Researcher, mitrakovanatalya@mail.ru, https://orcid.org/0000-0002-5571-7725* (*Natural Science Institute, Perm State National Research University, Perm, Russia*), **Elena A. Khayrulina,** *Doctor of Geography, Leading Researcher, https://orcid.org/0000-0002-9074-8551* (*Natural Science Institute, Perm State National Research University, Perm, Russia*), **Sergei M. Blinov,** *Candidate of Geological and Mineralogical Sciences, Leading Researcher, https://orcid.org/0000-0002-4953-3567* (*Natural Science Institute, Perm State National Research University, Perm, Russia*), **Anna A. Perevoshchikova,** *Junior Researcher, https://orcid.org/0000-0003-1769-7740* (*Natural Science Institute, Perm State National Research University, Perm, Russia*).

The authors declare no conflict of interests.

ISSN 2411-3336; e-ISSN 2541-9404

JOURNAL OF MINING INSTITUTE

Zapiski Gornogo instituta

Journal homepage: pmi.spmi.ru

Research article

Electric steelmaking dust as a raw material for coagulant production

Svetlana V. SVERGUZOVA[1], **Zhanna A. SAPRONOVA**[1], **Olga S. ZUBKOVA**[2]✉, **Anastasia V. SVYATCHENKO**[1], **Karina I. SHAIKHIEVA**[3], **Yulia S. VORONINA**[1]

[1] *Belgorod State Technological University named after V.G.Shukhov, Belgorod, Russia*
[2] *Saint Petersburg Mining University, Saint Petersburg, Russia*
[3] *Kazan National Research Technological University, Kazan, Russia*

How to cite this article: Sverguzova S.V., Sapronova Zh.A., Zubkova O.S., Svyatchenko A.V., Shaikhieva K.I., Voronina Yu.S. Electric steelmaking dust as a raw material for coagulant production. Journal of Mining Institute. 2023. Vol. 260, p. 279-288. DOI: 10.31897/PMI.2023.23

Abstract. The paper describes the issues associated with waste generated during steel production and processing, in particular the dust from electric arc furnaces (EAF). An effective solution for the disposal of such waste is its involvement in processing to obtain valuable products. This paper studies the physical and chemical properties of EAF dust produced during the smelting of metallized pellets and captured by the dust and gas cleaning system of the steel-smelting shop at the Oskol Electrometallurgical Combine, Belgorod Region. The results obtained in the study of the chemical and disperse compositions of dust, the microstructure of the surface made it possible to propose the use of dust as a raw material for coagulant production. The conditions of acid-thermal treatment of dust are determined, contributing to the partial dissolution of iron (II), (III), and aluminium compounds, which ensure the coagulation processes during wastewater treatment. Model solutions show high efficiency (> 95 %) of water treatment from heavy metal ions by modified EAF dust.

Keywords: dust from electric arc furnaces; acid treatment; iron ions; aluminium ions; zinc ions

Acknowledgment. The work was carried out under the federal program to support universities “Priority 2030” using equipment based at the Centre for High Technologies of the Belgorod State Technical University named after V.G.Shukhov.

Received: 16.11.2022 ***Accepted: 14.02.2023*** ***Online: 22.03.2023*** ***Published: 25.04.2023***

Introduction. Steel production and processing are associated with a large amount of industrial waste [1-3]. Most part of this waste does not find proper use and for this reason is stored in industrial landfills and temporary storage sites. The accumulation of a large amount of industrial waste and the need for its temporary storage cause a number of serious environmental and economic problems [4, 5]. An effective solution to these problems can be the involvement of this waste in the resource circulation as a feed for the production of various materials, which is a prerequisite for low-waste and waste-free technologies. Such an approach to the disposal and processing of man-made industrial waste contributes to solving the issues of resource and energy saving, makes it possible to expand the range of manufactured products, increase the raw material base and its diversity [6, 7]. In addition, the involvement in the production cycles of abandoned large-tonnage industrial waste will make it possible to release many hectares of land now under dumps and tailings and begin their reclamation and fertility recovery [8-10]. The importance of the indicated problem can be judged by the scale of mining and processing of iron ore. In 2013, Russia produced 102 Mt of iron ore, making it the fifth largest iron ore producer after China, Australia, Brazil, and India. According to Rosgeolfond, the country’s iron ore reserves for 2020 are estimated at about 112 Bt, with more than 60 % of the reserves in the Kursk Magnetic Anomaly (KMA) in the European part of Russia [11].

The KMA region is one of the largest iron ore (mainly magnetite and hematite) deposits on Earth. The area of iron ore deposits within the KMA is 120 thousand km^2. They are located in three regions of Russia (Kursk, Belgorod, and Orel) [12-14]. Rich ores were discovered in 1931. Mineralization is represented by ferruginous quartzites (banded iron formation) occurring together with various Early Precambrian metamorphic and igneous rocks [15, 16]. High iron zones were formed by hypergene enrichment of the upper horizons of the banded iron formation. The reserves of ferruginous quartzites with iron content of 32-37 % are more than 25 Bt, and the amount of enriched ores with iron content of 52-66 % exceeds 30 Bt. The deposits are developed by open-pit (Stoilensky, Lebedinsky, Mikhailovsky) and underground (Korobkovsky) mines [17].

Iron ore mining is sometimes viewed as mere mineral extraction, but the industry is fiercely competitive internationally and is currently under increased pressure to reduce costs due to the recent significant drop in iron ore prices. Despite modern advances, the international iron ore industry will have to develop alternative types of ores in the coming decades as the reserves of high iron ore around the world continue to dwindle. Magnetite and polymetallic ores, which are now mined in China, can act as a replacement. They have a complex mineral composition and fine grains.

More than 30 % of world steel is produced in electric arc furnaces [18]. During the steelmaking in such furnaces at temperatures above 1600 °C, many volatile components of the feedstock evaporate. This gas is cooled, and large particles are collected in cyclones, while smaller particles are captured in bag filters or electrostatic precipitators. Production of 1 ton of raw steel generated approximately 10-20 kg of EAF dust. It was estimated that 6 Mt of EAF dust is generated worldwide every year, while only 2.5 Mt of dust is recycled. EAF dust contains various metal elements, mainly depending on the type of scrap steel, iron ore, and smelting conditions. In general, the dust consists of 7-40 wt. % Zn and 30-45 wt. % Fe in the forms $ZnFe_2O_4$, ZnO, Fe_2O_3, and Fe_3O_4. Other minor metallic elements such as Mn, Al, and Cr are also present in EAF dust and therefore the dust is classified as a hazardous waste that must be properly disposed of or treated in accordance with the European Waste Catalogue and the List of Hazardous Waste. Obviously, the processing and disposal of EAF dust is an urgent task [18, 19].

The seriousness of the recycling management issue arises from the fact that EAF dust is generated in significant volumes and the amount is constantly increasing. The chemical composition of the dust varies depending on the type of raw material and steel produced, and these differences can be significant [20, 21]. Efforts were made around the world to stabilize EAF dust. There are studies on the use of dust with a high FeO content for asphalt modification, in cement mortars, to produce sintered bodies with promising mechanical properties [22-24]. Studies evaluating the use of EAF dust in ceramic and cement compositions show that although the dust properties may vary depending on the physical and chemical properties of the raw materials and process parameters, it is possible to develop process circuits and modify the waste (i.e., by hydrometallurgy, pyrometallurgy, etc.) considering the needs of the target application area [25-27].

Another well-known direction of management and processing of waste containing metals is leaching, or extraction, of valuable components with various reactants [28]. Selective extractants are used to separate certain metals from undesirable components and from each other or in groups [29-31]. The metal-containing filtrate is separated individually by solvent extraction using cationic, anionic, and neutral extractants. The hydrometallurgical method makes it possible to extract and purify metals in multi-element solutions [32-34]. Due to the specific chemical composition and high dispersion, such dust can be used to obtain coagulants suitable for wastewater treatment [35, 36].

The purpose of this work was a comprehensive study of the mineral composition and physical and chemical properties of electric steelmaking dust in the production of steel in electric arc furnaces at the Oskol Electrometallurgical Plant (Stary Oskol, Belgorod Region). When achieving the goal, we had to solve the following tasks:

- conduct comprehensive studies of the physical and chemical properties of EAF dust;
- determine the influence of conditions of acid treatment of dust on leaching of iron, zinc, aluminum from EAF dust;
- assess the possibility of using modified EAF dust as a coagulant in wastewater treatment.

Materials and methods. The studies used EAF dust formed during the melting of metallized pellets and captured in the dust and gas cleaning system of the steel-smelting shop at the Oskol Electrometallurgical Plant. EAF dust consists of a light fraction of metal-containing compounds and is a finely dispersed system of a multi-component composition. For dust treatment, concentrated hydrochloric acid was used. Hydrochloric acid was chosen as one of the well-known strong mineral acids, which does not release dangerous substances such as SO_2 or N_xO_y into the air.

To increase the reactivity of the dust, it was treated with hydrochloric acid at a temperature of 23 °C and boiled. Boiling was carried out in HCl solutions diluted 1:3 and 1:5 for 0.5; 2, and 3 h. After the end of boiling, the contents of the reaction vessels were quantitatively transferred into flasks with a capacity of 1 dm^3, filtered; the remaining precipitate was analysed using X-ray diffraction (XRD), and the concentrations of Fe_{tot}, Al, and Zn were determined in the solution.

Microstructural studies were carried out using a TESCAN MIRA 3 LMU electron microscope. This microscope has the possibility of high resolution (to 1 nm) and energy dispersive microanalysis, magnification from 4 to 1000000. The investigation was carried out at an accelerating voltage from 200 V to 30 kV with continuous adjustment. The maximum value of the probe current is 200 nA. The SE secondary electron detector of the Everhart – Thornley type was used to obtain topographic contrast images. We also used the AdvancedAztecEnergy (IE350)/ X-max80 energy-dispersive microanalysis system with a guaranteed spectral resolution on the Mn $K\alpha$ line of 127 eV. The electron source is a high brightness Schottky cathode. Resolution was 1 nm at 30 kV.

X-ray phase analysis of EAF dust ground in an agate mortar and pressed into a tablet was carried out using an ARL 9900 WorkStation X-ray fluorescence spectrometer with a built-in diffraction system.

Experimental studies on the treatment of model solutions were conducted out as follows. Model solutions were prepared containing Fe^{3+}, Fe^{2+}, Al^{3+}, Zn^{2+}, Cu^{2+} ions at concentrations of 10 mg/dm^3. To 100 cm^3 of model solutions, a dust suspension in an HCl solution was added in an amount of 0.5 to 4 cm^3, mixed for 30 min, and filtered. In the filtrate after treatment of the model solution, the residual concentration of the pollutant was determined by the atomic absorption method on the KVANT-Z.ETA-T device according to the M-MVI 539-03 method.

The particle size distribution of the dust was measured using a Micro Sizer 201 laser particle sizer, which makes it possible to study particles in the range from 0.2 to 600 μm. The bulk density was found by weighing a known volume of dust and dividing the mass found by the volume. To determine the true density, the pycnometric method was used in an alcohol solution. In order to measure the pH of the aqueous extract, 10 g of dust was added to 100 cm^3 of distilled water with a pH of 7; the contents of the laboratory container were boiled for 30 minutes, filtered through a paper filter, the pH of the medium was determined in the filtrate using an Akvilon I-500 device.

Statistical processing was carried out for the experimental data, Student's t-test was calculated for independent samples. The critical values of the t-test for $df = 8$ are 2.31 ($p = 0.05$), 3.36 (p = 0.01), and 5.04 (p = 0.001). Student's t-test for independent samples was calculated using the formula

$$t = \frac{\left|\overline{m_1} - \overline{m_2}\right|}{\sqrt{\frac{\sigma_1^2}{n_1} + \frac{\sigma_2^2}{n_2}}},$$

where $\overline{m_1}$ and $\overline{m_2}$ are the sample means; σ_1^2 и σ_2^2 are sample variance of samples; n_1 and n_2 are the number of experiments in each sample.

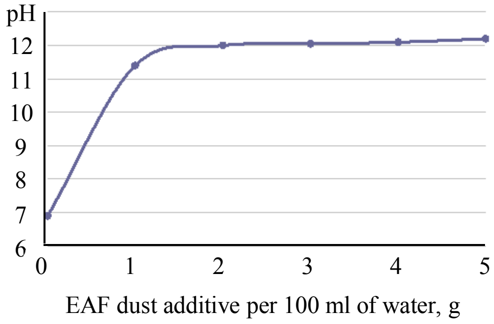

Fig.1. Change in the pH of the aqueous medium upon the addition of EAF dust

Discussion of the results. EAF dust of the current electric steelmaking is a finely dispersed system of complex composition of dark brown colour with a moisture content to 2.5 % and a bulk particle size (> 60 %) to 0.1 mm. Processing properties of EAF dust: bulk density ρ_{bulk} = 0.94 g/cm^3; true density ρ_{true} = 3.64 g/cm^3; pH of water extract 11.2; solubility in water 6.4 %; solubility in 1 n HCl is greater than 82.6 %. The graph of changes in the pH of the aqueous medium when the dust is added is shown in Fig.1. When the values of hydrate formation in the solution are reached, the heavy metal ions existing in the solution (and released from the dust) form poorly soluble hydroxides and are removed from the solution together with coagulation particles [37].

The mineral composition of the dust, according to XRF estimates, is represented by such compounds as Fe_3O_4 ($FeO \cdot Fe_2O_3$), Fe_2O_3, MgO, Al_2O_3, SiO_2, $Ca(OH)_2$. Compounds of di- and trivalent iron are mainly oxides, compounds that are poorly soluble in water and are not able to participate in exchange reactions in normal conditions [38].

Figure 2 shows X-ray diffraction patterns of initial dust and dust treated with acid diluted 1:3 for 0.5; 2, and 3 h, the ratio of dust to acid solution is 1:5.

Iron peaks in Fig.2, *b*, *c* are somewhat lower compared to Fig.2, *a*, which confirms the fact of dust dissolution and the transition of metals to a dissolved state. As expected, the lowest peaks are noted in Fig.2, *d*, which indicates the highest level of leaching of the slag components.

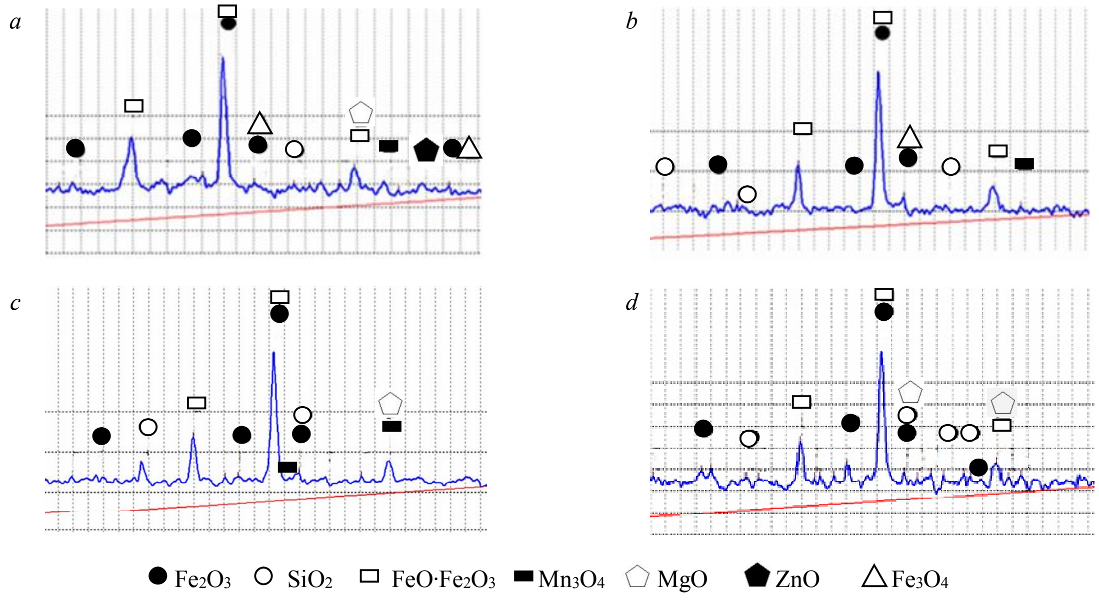

Fig.2. X-ray patterns of initial EAF dust (*a*) and dust treated with acid diluted 1:3 for 0.5 (*b*), 2 (*c*), 3 h (*d*)

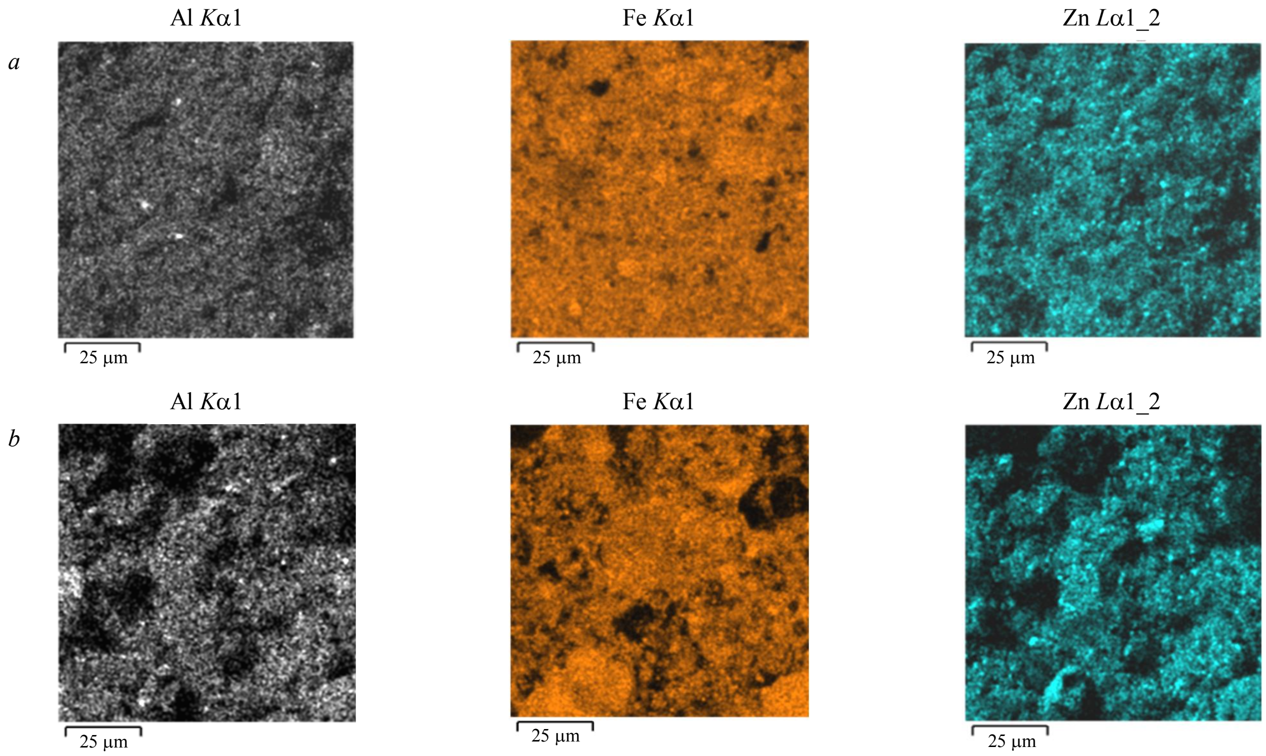

Fig.3. Multilayer maps of the energy-dispersive spectra of the dust surface after 180 min of boiling in HCl diluted 1:3 (*a*); 1:5 (*b*) and indicating sections of Fe, Al, and Zn

Multilayer maps of the energy dispersive spectra of the dust surface are shown in Fig.3.

Figure 4 shows micrographs of the dust particles surface and energy dispersive spectra for samples treated with HCl.

The average values of the elemental composition of EAF dust samples are presented in Table 1.

Table 1

Averaged values of the elemental composition of dust after acid treatment

Treatment temperature, °C	Treatment conditions		Initial content of elements, wt.%												
	Acid dilution	Treatment time, min	21.5 C	33.98 O	0.71 Na	1.99 Mg	0.29 Al	8.91 Si	1.72 S	1.75 Cl	1.14 K	1.1 Ca	2.51 Mn	40.12 Fe	4.87 Zn
23	1:5	30	17.13	30.82	0.68	1.62	0.22	8.02	0.65	1.55	0.29	0.22	2.31	34.42	3.42
	1:5	120	19.12	31.14	0.27	1.50	0.18	6.84	0.48	0.96	0.15	0.22	1.60	36.75	1.99
	1:5	180	18.04	31.08	0.09	1.25	0.06	4.88	0.13	0.78	0.09	0.06	1.13	35.72	1.87
	1:3	30	16.73	31.06	0.33	1.59	0.18	8.52	1.53	0.49	1.00	0.98	1.14	39.97	3.52
	1:3	120	11.93	31.78	0.27	1.44	0.16	6.67	0.94	0.43	0.66	0.46	1.79	36.19	2.50
	1:3	180	16.58	33.82	0.25	1.07	0.07	4.85	0.81	0.32	0.48	0.37	0.85	33.92	2.04
100	1:5	30	16.91	30.42	0.67	1.6	0.22	7.92	0.64	1.53	0.283	0.22	2.28	33.98	3.38
	1:5	120	18.87	30.74	0.263	1.48	0.18	6.75	0.47	0.95	0.15	0.22	1.58	36.28	1.96
	1:5	180	17.81	30.68	0.09	1.23	0.06	4.82	0.13	0.77	0.09	0.06	1.12	35.26	1.85
	1:3	30	16.52	30.66	0.33	1.57	0.18	8.41	1.51	0.48	0.99	0.97	1.13	39.46	3.47
	1:3	120	11.78	31.37	0.27	1.42	0.16	6.58	0.93	0.42	0.65	0.45	1.77	35.73	2.47
	1:3	180	16.37	33.39	0.25	1.06	0.07	4.79	0.80	0.32	0.47	0.37	0.84	33.48	2.01

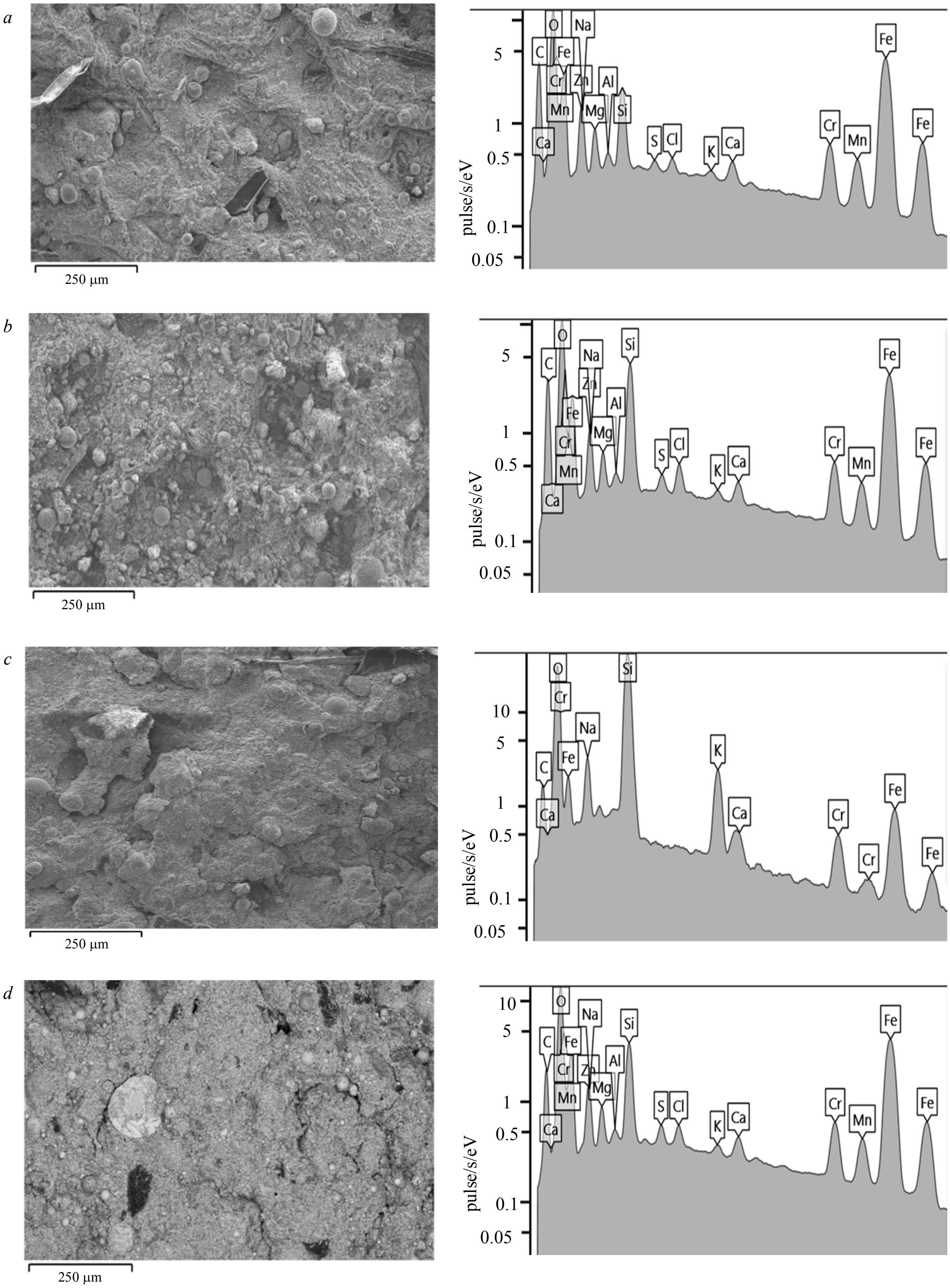

Fig.4. Dust surface in reflected electrons after boiling in HCl and energy dispersive spectrum: after 30 min of boiling with dilution 1:5 (*a*), 1:3 (*c*); after 180 min of boiling with dilution 1:5 (*b*), 1:3 (*d*)

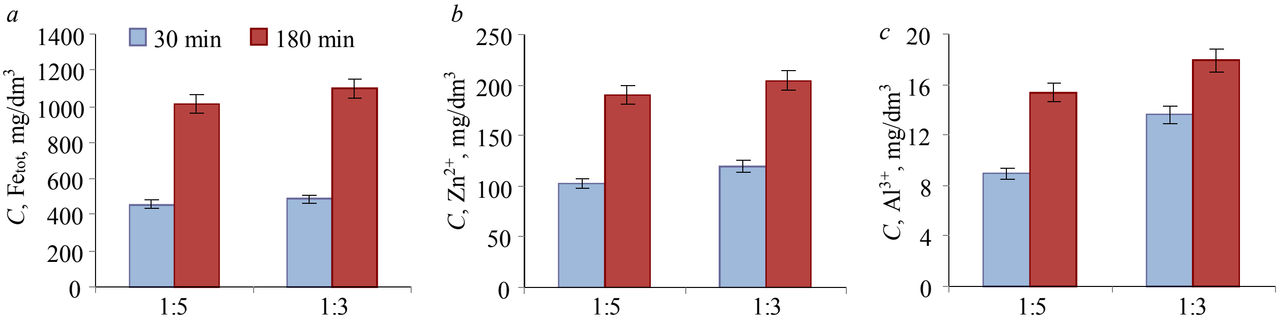

Fig.5. Leaching of iron (*a*), zinc (*b*), and aluminum (*c*) from EAF dust at different HCl concentrations

It follows from Table 1 that as the acid concentration and the treatment duration increase, the dust contains an ever smaller amount of elements, Mg, Al, Fe, Zn. Zn content in the dust also decreases as the treatment duration and the acid concentration increase. The preliminary experiments determined that 3 hours of EAF dust treatment is sufficient. A further increase in the duration of boiling leads to unjustified energy costs. Thus, at a 1:5 dilution, as the treatment time increases from 30 to 180 min, the Zn content in the dust decreases from 3.38 to 1.85 %. At a 1:3 dilution, as the treatment time increases from 30 to 180 min, the Zn content decreases from 3.47 to 2.01 %. Figure 5 shows the dependence of the intensity of leaching of Fe_{tot}, Al^{3+}, and Zn^{2+} ions on the acid solution concentration.

The resulting difference in the concentration of metal ions in solutions at different acid concentrations is statistically significant (Table 2). Thus, within the framework of this study, hydrochloric acid diluted 1:3; heat treatment temperature 100 °C; duration of boiling 180 min can be considered the best conditions for transferring Fe^{2+}, Fe^{3+}, Al^{3+}, Zn^{2+} ions into solution.

Modified dust can be used as a coagulation material for wastewater treatment [36].

Table 2

Student's *t*-test values

Treatment time, min	Acid dilution	*t*-test		
		Fe	Zn	Al
30	1:5	5.099	4.103	15.503
30	1:3			
180	1:5	23.86	14.356	18.721
180	1:3			

In an aqueous medium, Fe^{2+}, Fe^{3+}, Al^{3+} cations undergo hydrolysis according to the following tentative reactions:

$$Fe^{2+} + HOH \rightleftarrows [FeOH]^{+} + H^{+};$$

$$[FeOH]^{+} + HOH \rightleftarrows Fe(OH)_2 \downarrow + H^{+};$$

$$Fe^{3+} + HOH \rightleftarrows [FeOH]^{2+} + H^{+};$$

$$[FeOH]^{2+} + HOH \rightleftarrows [Fe(OH)_2]^{+} + H^{+};$$

$$[Fe(OH)_2]^{+} + HOH \rightleftarrows Fe(OH)_3 \downarrow + H^{+}.$$

The Al^{3+} ions are hydrolysed similarly to the Fe^{3+} ion:

$$Al^{3+} + HOH \rightleftarrows [AlOH]^{2+} + H^{+};$$

$$[AlOH]^{2+} + HOH \rightleftarrows [Al(OH)_2]^{+} + H^{+};$$

$$[Al(OH)_2]^{+} + HOH \rightleftarrows Al(OH)_3 \downarrow + H^{+}.$$

Zn^{2+} ions are hydrolysed similarly to Fe^{2+}.

As it is known, hydrolysis is the interaction of salt dissociation products with water to form large flakes, which can then be separated from the aqueous medium by decantation or filtration.

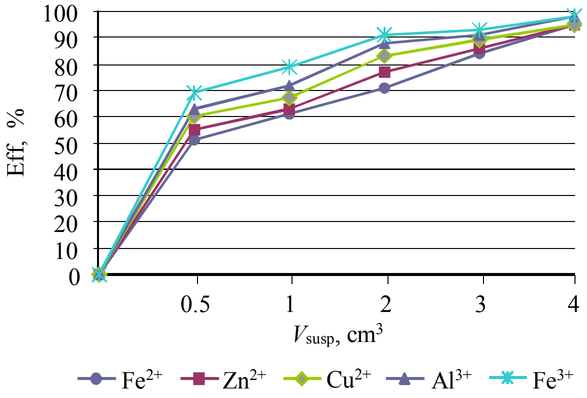

Fig.6. Dependence of treatment efficiency on suspension volume

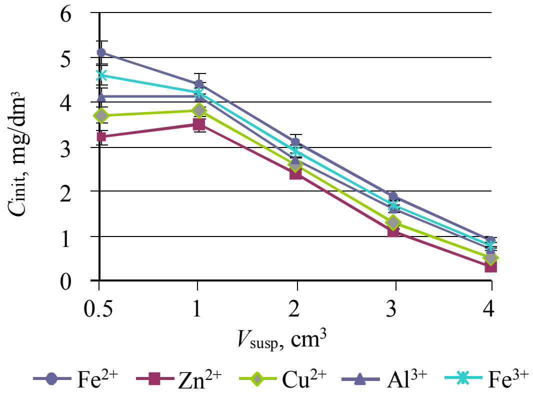

Fig.7. Influence of suspension volume on the content of metal ions in solution

In the practice of water treatment, salts $Al_2(SO_4)_3$, $AlCl_3$, $FeCl_3$, $Fe_2(SO_4)_3$, $FeSO_4$, $FeCl_2$ and their mixtures in various combinations are widely used as coagulants [36].

Wastewater from various industrial productions often simultaneously contain ions of many heavy metals, Ni^{2+}, Cu^{2+}, Cd^{2+}, Co^{2+}, Cr^{3+} etc. With an increase in the pH of the aqueous medium, these ions form poorly soluble hydroxides, $Ni(OH)_2$, $Cu(OH)_2$, $Cd(OH)_2$, $Co(OH)_2$, $Cr(OH)_3$, which, due to their high dispersion, form a stable hard-to-remove suspension. In this case, the use of coagulants makes it possible to extract suspended particles from a dispersed medium using coagulation and purify the solution to the specified requirements.

Due to the fact that the dust composition includes oxides such as CaO, Na_2O, K_2O, BaO, MgO, etc., when dust is added to the aqueous medium, they partially dissolve, which invariably leads to an increase in the pH of the medium. During acid treatment of dust, the pH of the medium also gradually increases over time due to the dissolution of alkaline components.

The results of studies presented in Fig.6 and 7 show that the treatment efficiency for all ions is at least 95 %. If it is necessary to achieve a lower residual concentration of metal ions, it is possible to use the second treatment stage.

Thus, EAF dust can be successfully used to obtain a coagulant suitable for use in water treatment. This conclusion is confirmed by experimental data. In the course of observations, large flakes of coagulated particles were noted after adding a coagulating suspension to a finely dispersed system. After coagulation, a rapid, even sedimentation was observed.

Conclusion. The prospects for the use of steel industry waste as a raw material for coagulant production are considered. According to the analysis of literary sources, the coagulation material obtained on the base of EAF dust can be used in wastewater treatment. It was determined that the recommended conditions for obtaining a coagulation mixture are HCl acid diluted 1:3, boiling duration is 180 min. These conditions lead to partial dissolution of dust and the transition of Fe^{3+}, Fe^{2+}, Al^{3+} ions into solution, causing a coagulation effect in the aqueous medium with respect to suspended fine particles. EAF dust after acid treatment is used as a coagulation mixture, which leads to wastewater treatment with a high efficiency of 95-98 %.

REFERENCES

1. Sizyakov V.M., Kozyrev B.A. Processing of formate solutions obtained from red mud leaching. *iPolytech Journal*. 2021. Vol. 25. N 5, p. 633-642 (in Russian). DOI: 10.21285/1814-3520-2021-5-633-642

2. Lebedev A.B., Utkov V.A., Bazhin V.Yu. Use of alumina production waste red mud during molten sulfur-containing slag granulation. *Metallurgist*. 2019. Vol. 63, p. 727-732. DOI: 10.1007/s11015-019-00882-z

3. Urbanovich N.I., Korneev S.V., Volosatikov V.I., Komarov D.O. Analysis of the composition and processing technologies of dispersed iron-containing waste. *Foundry Production and Metallurgy*. 2021. N 4, p. 66-69 (in Russian). DOI: 10.21122/1683-6065-2021-4-66-69

4. Aryngazin K.Sh., Stanevich V.T., Tleulesov A.K. et al. Research of Production Processes of Concrete Products on the Steelmaking Slags Basis. *Science and Technology of Kazakhstan*. 2018. N 4, p. 43-49 (in Russian).

5. Ruzavin A.A. Disposal of Steelmaking Slags by Accelerated Carbonation. *Bulletin of the South Ural State University. Seriya "Construction Engineering and Architecture"*. 2018. Vol. 18. N 3, p. 68-72 (in Russian). DOI: 10.14529/build180310

6. Duisekenov R.K., Mazdubai A.V. Dust and Sludge of Gas Cleaning Plants and Analysis of Ways of Their Utilization. *Science and Technology of Kazakhstan*. 2020. N 3, p. 29-37 (in Russian).

7. Belskii S.S., Zaitseva A.A., Tyutrin A.A. et al. Current state of steelmaking slag processing. *iPolytech Journal*. 2021. Vol. 25. N 6, p. 782-794 (in Russian). DOI: 10.21285/1814-3520-2021-6-782-794

8. Chukaeva M.A., Povarov V.G., Sverchkov I.P. Iron-Containing Metalworking Wastes as a Chemosorbent for Wastewater Treatment from Molybdenum Ions. *Moscow University Chemistry Bulletin*. 2020. Vol. 75. N 1, p. 36-42. DOI: 10.3103/S0027131420010058

9. Novichikhin A.V., Shorokhova A.V. Systematic processing of iron-ore waste in mining regions. *Steel in Translation*. 2017. Vol. 47, p. 456-462. DOI: 10.3103/S0967091217070105

10. Svergusova S.V., Sapronova Zh.A., Svyatchenko A.V. Iron-Containing Modeled Waste as Raw Material for Coagulant Receiving. *IOP Conference Series: Earth and Environmental Science*. 2019. Vol. 272. Iss. 3. N 032007. DOI: 10.1088/1755-1315/272/3/032007

11. Holmes R.J., Yifan Lu, Liming Lu. Introduction: overview of the global iron ore industry. Iron Ore. Mineralogy, Processing and Environmental Sustainability. Amsterdam: Elsevier, 2022, p. 1-56. DOI: 10.1016/B978-0-12-820226-5.00023-9

12. Taylor P.T., Kis K.I., Wittmann G. Satellite-altitude horizontal magnetic gradient anomalies used to define the Kursk Magnetic Anomaly. *Journal of Applied Geophysics*. 2014. Vol. 109, p. 133-139. DOI: 10.1016/j.jappgeo.2014.07.018

13. Gzogyan T.N., Gzogyan S.R. Material Composition of Rich Iron Ore Deposits of KMA. *Nauchnye vedomosti Belgorodskogo gosudarstvennogo universiteta. Seriya Estestvennye nauki*. 2018. Vol. 42. N 2, p. 131-141 (in Russian). DOI: 10.18413/2075-4671-2018-42-2-131-141

14. Khramtsov B.A., Bakaras M.V., Kravchenko A.S., Korneychuk M.A. Loose Dump Stability Control at Open Pit Iron Ore Mines of the Kursk Magnetic Anomaly. *Mining informational and analytical bulletin*. 2018. N 2, p. 66-72 (in Russian). DOI: 10.25018/0236-1493-2018-2-0-66-72

15. Oreshkin D., Proshlyakov A. Assessment of Ecological Parameters of Iron Ore Deposit Open-Cast Mining in Time Based on the Resource Approach. *Proceedings of the Siberian department of the section of earth sciences of the Russian academy of natural sciences. Geology, exploration and development of mineral deposits*. 2017. Vol. 40. N 4, p. 98-111 (in Russian). DOI: 10.21285/2541-9455-2017-40-4-98-111

16. Egger F. Implementation of a Dynamic Mining Strategy Following Changing Conditions in a Multipit, Multielement Blending Iron Ore Mining Operation. *BHM Berg- und Hüttenmännische Monatshefte*. 2011. Vol. 156, p. 325-329. DOI: 10.1007/ s00501-011-0014-3

17. Savko A.D., Ovchinnikova M.Yu. The Main Types and Mineral Composition of Bauxites of the Kursk Magnetic Anomaly. *Uchenye Zapiski Kazanskogo Universiteta. Seriya estestvennye nauki*. 2020. Vol. 162. N 2, p. 274-289 (in Russian). DOI: 10.26907/2542-064X.2020.2.274-289

18. Huimin Tang, Zhiwei Peng, Liancheng Wang et al. Facile synthesis of zinc ferrite as adsorbent from high-zinc electric arc furnace dust. *Powder Technology*. 2022. Vol. 405. N 117479. DOI: 10.1016/j.powtec.2022.117479

19. Karahan B.D. Carbon coated electric arc furnace dust prepared by one-pot pyrolysis: An effcient, low carbon footprint electrode material for lithium-ion batteries. *Materials chemistry and physics*. 2022. Vol. 287. N 126178. DOI: 10.1016/j.matchemphys.2022.126178

20. Mamdouh O., Timo F., Eetu-Pekka H. Selective Zinc Removal from Electric Arc Furnace (EAF) Dust by Using Microwave Heating. *Journal of Sustainable Metallurgy*. 2019. Vol. 5, p. 331-340. DOI: 10.1007/s40831-019-00222-0

21. Toporkova Yu.I., Bludova D., Mamyachenkov S.V., Anisimova O.S. A review of processing methods for electric arc furnace dust. *iPolytech Journal*. 2021. Vol. 25. N 5, p. 643-680 (in Russian). DOI: 10.21285/1814-3520-2021-5-643-680

22. Loaiza A., Colorado H.A. Marshall stability and flow tests for asphalt concrete containing electric arc furnace dust waste with high ZnO contents from the steel making process. *Construction and Building Materials*. 2018. Vol. 166, p. 769-778. DOI: 10.1016/j.conbuildmat.2018.02.012

23. *Aryngazin K., Abisheva A.* Use of recycled waste in the production of building materials. *Technobius*. 2022. Vol. 2. N 2. N 0020. DOI: 10.54355/tbus/2.2.2022.0020

24. Atroshchenko Yu.M., Nikishina M.B., Simonov R.V. Study of the strength characteristics of building composites using converter slags. *Endless light in science*. 2022. N 5-5, p. 161-165 (in Russian). DOI: 10.24412/2709-1201-2022-161-165

25. Korneeva E.V., Berdov G.I. Use of Electric Furnace Slag in Production of Clinkerless Cement. *Bulletin of the South Ural State University. Seriya "Construction Engineering and Architecture"*. 2018. Vol. 18. N 3, p. 35-40. (in Russian). DOI: 10.14529/build180305

26. Kauchur A.S., Sheleh V.K., Kauchur S.G. et al. Development of Terracot Ceramic Tiles Manufacturing Technology with use of Technogenic Products of Energy Complex. *Vestnik Vitebskogo gosudarstvennogo tekhnologicheskogo universiteta*. 2017. N 2 (33), p. 86-94 (in Russian).

27. Singh M., Saini B., Chalak H.D. An Overview on Waste Materials Used in Engineered Cementitious Composite. Smart Technologies for Sustainable Development. Cham: Springer, 2021. LNCE. Vol. 78, p. 213-222. DOI: 10.1007/978-981-15-5001-0_17

28. Montoya D.A., Pistofidis N., Giannakopoulos G. et al. Revisiting the iron-rich "ordinary Portland cement" towards valorisation of wastes: study of Fe-to-Al ratio on the clinker production and the hydration reaction. *Materials and Structures*. 2021. Vol. 54. N 30. DOI: 10.1617/s11527-020-01601-w

29. Shahbaz A. A systematic review on leaching of rare earth metals from primary and secondary sources. *Minerals Engineering*. 2022. Vol. 184. N 107632. DOI: 10.1016/j.mineng.2022.107632

30. Martins Th.A.G., Calda M.P.K., Tavares de Moraes V. et al. Recovering metals from motherboard and memory board waste through sulfuric leaching. *Journal of Environmental Chemical Engineering*. 2021. Vol. 9. Iss. 6. N 106789. DOI: 10.1016/j.jece.2021.106789

31. Fomina D.D., Danilov N.F. Leaching of Vanadium Compounds in the Processing of Vanadium Pentoxide Production Chemical Waste Using Sulfuric and Nitric Acids. *Vestnik Permskogo natsionalnogo issledovatel'skogo politekhnicheskogo universiteta. Khimicheskaya tekhnologiya i biotekhnologiya*. 2021. N 2, p. 77-93 (in Russian). DOI: 10.15593/2224-9400/2021.2.07

32. Voropanova L.A., Pukhova V.P. Extraction of Copper, Cobalt and Nickel Ions from Aqueous Solutions by Extractant Cyanex 272. *Journal of Mining Institute*. 2018. Vol. 233, p. 498-505. DOI: 10.31897/PMI.2018.5.498

33. Kioresku A.V. Intensification of Bacterial-Chemical Leaching of Nickel, Copper and Cobalt from Sulfide Ores Using Microwave Radiation. *Journal of Mining Institute*. 2019. Vol. 239, p. 528-535. DOI: 10.31897/PMI.2019.5.528

34. Awasthi A.K., Jinhui Li. An overview of the potential of eco-friendly hybrid strategy for metal recycling from WEEE. *Resources, Conservation & Recycling*. 2017. Vol. 126, p. 228-239. DOI: 10.1016/j.resconrec.2017.07.014

35. Svergusova S.V., Sapronova Zh.A., Svyatchenko A.V. et al. Coagulant on the base of industrial ferriferous waste for the preliminary treatment of multi-component sewage. III International Scientific and Technical Conference Energy Systems (ICES 2018), 29-30 November 2018, Belorgod, Russian Federation. IOP Conference Series Materials Science and Engineering, 2019. Vol. 552. N 012026. DOI: 10.1088/1757-899X/552/1/012026

36. Sverguzova S.V., Sapronova Zh.A., Svyatchenko A.V. Technology to produce iron-containing coagulant of steel production wastes for treatment rainwater. *Bulletin of Belgorod state technological university named after V.G.Shukhov*. 2016. N 12, p. 160-164 (in Russian). DOI: 10.12737/22652

37. Sverguzova S.V., Shaikhiev I.G., Porozhnyuk L.A. et al. Possible uses of solid waste from electric steel smelting – dust from electric arc furnaces. *Vestnik Kazanskogo tekhnologicheskogo universiteta*. 2014. Vol. 17. N 6, p. 199-201 (in Russian).

38. Ipanov D.Yu. Treatment of wastewater from phosphates and heavy metals by dust from electric arc furnaces: Avtoref. dis. … kand. tekhn. nauk. Penza: Penzenskaya gosudarstvennaya tekhnologicheskaya akademiya, 2015, p. 19 (in Russian).

***Authors*: SvetlanaV. Sverguzova**, *Doctor of Engineering Sciences, Head of Department, https://orcid.org/0000-0002-3845-8741* (*Belgorod State Technological University named after V.G.Shukhov, Belgorod, Russia*), **Zhanna A. Sapronova**, *Doctor of Engineering Sciences, Professor, https://orcid.org/0000-0003-1410-0179* (*Belgorod State Technological University named after V.G.Shukhov, Belgorod, Russia*), **Olga S. Zubkova**, *Candidate of Engineering Sciences, Researcher, zubkova-phd@mail.ru, https://orcid.org/0000-0002-5833-528X* (*Saint Petersburg Mining University, Saint Petersburg, Russia*), **Anastasia V. Svyatchenko**, *Senior Lecturer, https://orcid.org/0000-0002-2758-884X* (*Belgorod State Technological University named after V.G.Shukhov, Belgorod, Russia*), **Karina I. Shaikhieva**, *Postgraduate Student, Assistant Lecturer, https://orcid.org/0000-0003-1188-7885* (*Kazan National Research Technological University, Kazan, Russia*), **Yulia S. Voronina**, *Postgraduate Student, https://orcid.org/0000-0001-6125-0239* (*Belgorod State Technological University named after V.G.Shukhov, Belgorod, Russia*).

The authors declare no conflict of interests.

ISSN 2411-3336; e-ISSN 2541-9404

JOURNAL OF MINING INSTITUTE

Zapiski Gornogo instituta

Journal homepage: pmi.spmi.ru

Research article

Environmental geotechnology for low-grade ore mining with the creation of conditions for the concurrent disposal of mining waste

Igor V. SOKOLOV, Yuriy G. ANTIPIN, Artem A. ROZHKOV✉, Yuriy M. SOLOMEIN
Institute of Mining, Ural Branch of the RAS, Yekaterinburg, Russia

How to cite this article: Sokolov I.V., Antipin Yu.G., Rozhkov A.A., Solomein Yu.M. Environmental geotechnology for low-grade ore mining with the creation of conditions for the concurrent disposal of mining waste. Journal of Mining Institute. 2023. Vol. 260, p. 289-296. DOI: 10.31897/PMI.2023.21

Abstract. Due to the constantly deteriorating environmental situation in the regions with mining enterprises, the article considers the topical issue of disposing the maximum possible volume of waste from the mining and processing of low-grade ferrous ores through the creation of an effective underground environmental geotechnology. Traditional procedure with descending mining of reserves with a caving system does not allow waste to be disposed of in a gob. The idea is to use geotechnology based on the ascending order of mining the ore body, room excavation, leaving truncated pillars, and staggered arrangement of adjacent rooms in height, which makes it possible to form containers for waste disposal in the form of a cementless backfill. The main characteristics of the proposed procedure are investigated and compared with the traditional procedure of low-grade iron ores mining. It was established that from the point of view of the complete extraction of reserves and the unit costs for the preparatory-development operations, the processes are comparable, while in terms of the mining quality, the proposed option is much more efficient. Evaluation of environmental geotechnology by the criterion of waste disposal, performed according to the proposed methodology, showed that the combination of these technical solutions ensures the placement in the formed gob from 80 to 140% of all waste generated during the mining and beneficiation of low-grade iron ores.

Keywords: environmental geotechnology; underground geotechnology; disposal; waste; low-grade ores; ascending order; cementless backfill; environmental potential

Acknowledgment. The work was carried out under the State Assignment N 075-00412-22 PR. Topic 1 (2022-2024) (FUWE-2022-0005), reg. N 1021062010531-8-1.5.1.

Received: 17.10.2022 ***Accepted: 13.02.2023*** ***Online: 14.03.2023*** ***Published: 25.04.2023***

Introduction. The continuous accumulation of waste from mineral production, mining, and beneficiation leads to a significant deterioration of the environmental situation in the regions where mining and processing enterprises are located [1-3]. Over the past decade, the growth of these wastes in Russia has increased from 3.8 to 7.9 billion tons per year [4]. It is obvious that the problem of waste disposal is becoming more and more relevant both in terms of the environmental consequences of mineral management [5-7] and in terms of the economic efficiency of enterprises in the face of tougher environmental requirements [8-10]. The target of study in this paper is geotechnological methods for the disposal of waste from the mining and processing of mineral raw materials during underground mining, which would reduce the share of geoenvironmental measures, such as reclamation and neutralization.

All geotechnological methods of waste disposal are primarily based on their placement in the gob. In open pit mining, the main disposal methods are internal dumping, the use of the entire quarry bowl or its part for storing liquid and pasty waste, the preparation of man-made containers inside the quarry space or in dumps using overburden, dams, and gabion structures, etc. [11-13]. In underground mining, waste disposal is possible by using it as backfill material for infilling the gob [14, 15]. While remaining an integral part of underground geotechnology, backfill operations are mainly considered from the point of view of controlling rock pressure and increasing the completeness of the working excavation. In modern conditions, the need to apply an integrated approach to the development of deposits is obvious, when geotechnology with backfilling of gob should be considered in the aspect of providing favourable conditions for the disposal of mining and beneficiation waste, in other words, as an environmental geotechnology [16-18].

Thus, the development of an effective underground environmental geotechnology with the purposeful creation of conditions for the disposal of the maximum possible amount of waste is an urgent scientific and technical task.

Methodology. Due to the low content of the useful component with large volumes of mining, the issue of waste disposal is most acute in the development of high-output deposits. During the mining of non-ferrous metal ores, the backfill mass, as a rule, is formed by hardening mixtures based on a cement binder, and significant costs for backfill operations are justified by the complete and qualitative extraction of the mineral and the high recoverable value of the mined and beneficiated ore [19]. The disadvantages of the hardening backfill, in addition to the high cost, include the staged procedure for mining reserves, due to the significant period of strength gain of the backfill mass [20, 21]. To reduce the cost of the hardening backfill in the development of copper pyrite deposits, mixture compositions based on lime-slag binders were sought, which made it possible to abandon the use of cement and reduce the cost of backfill by 20-30 % [22]. Studies were carried out on the construction of a combined backfill mass from a dry and hardening backfill, which made it possible to reduce costs and intensify the process. However, it complicated the organization of backfilling [23]. There are developments on the partial strengthening of a dry backfill mass by injecting hardening solutions through special wells and its subsequent compaction by breaking the reserves of the adjacent room onto the compressed environment of the backfill mass [24].

Another direction was the construction of high-density man-made masses with a small proportion of hardening backfill (10-15 %) and mechanical compaction of rock fill by analogy with road construction. The disadvantage of the procedure is the need to use heavy road rollers in underground conditions and a certain procedure for erecting a backfill mass with an accurate layout, alternating parapets of certain sizes at a certain distance. It should be noted that the use of hardening mixtures, even in small quantities and regardless of their composition, entails organizational and technical complication and an increase in the cost of the entire geotechnology as a whole. However, the economic effect obtained during the mining of non-ferrous metal ores or rich ores makes it possible to use working systems with a hardening backfill for the development of high-output deposits with virtually no alternative.

In the mining of poor and ordinary ores of ferrous metals, in particular iron, the low recoverable value makes the use of a hardening backfill impractical. Such deposits, as a rule, are mined by working systems with the caving of ores and host rocks. The traditional procedure has significant advantages such as high labour productivity at the working excavation and low production costs; however, it is characterized by low ore recovery rates (losses and impoverishment to 20-30 %) and a large specific volume of preparatory-development operations (PDO) [25-27]. These factors affect its efficiency but make it possible to profitably develop low-grade iron ore deposits in modern economic conditions. The potential of this geotechnology in terms of waste disposal in the gob is practically zero [28]. Thus, the only way to increase the environmental potential of the geotechnology in such deposits is the use of workings systems with cementless backfill.

The use of a cementless backfill involves the formation of insulating interlevel (ILP) and interchamber (ICP) pillars, since the backfill does not have the necessary stability properties in the presence of lateral outcropping planes. ICPs can be either kept or worked out by mining systems with caving. The use of the ascending order of reserves mining makes it possible to withdraw from the ILP [29]. A significant part of the ore body is left in the form of remnant pillars or is mined using caving procedure that does not imply the conditions for waste disposal in the gob.

Thus, when designing an environmentally oriented mining system, one should be guided by the following principles:

- application of a room excavation, which allows to form a gob as a container for waste disposal;
- use of ascending order of reserves mining;
- the design of the system should provide the possibility of placing the maximum volume of waste in the form of a cementless backfill with a minimum volume of formed ore pillars;
- provision of recovery rates comparable with conventional procedure with ore and host rocks caving.

As a result, a variant of a sublevel-room mining system with cementless backfill was designed, which meets the main trends in improving underground ore mining as part of the development of environmental geotechnologies. The procedure provides for the division of the level into sub-levels, which are mined in ascending order by rooms located relative to neighbouring rooms with an offset in the vertical plane by half of the sublevel height and leaving remnant insulating pillars of a triangular or trapezoidal shape with a minimum width of the upper base (Fig.1).

Two faces carry out extraction of room reserves by sectional breaking of ore with opposite fans of holes and subsequent end withdrawal using load-haul-dump machines (LHD) with remote control (RC). After mining out the room, it is filled with backfill material. Mining dump trucks are used to transport cementless backfill to the room. The backfill mass formed by a mine bulldozer with RC by distributing and planning the rock over the entire area of the room, which makes it possible to create a drawing-off level of the overlying room.

The ascending order of mining the ore body, the staggered arrangement of the rooms in height and the leaving of insulating triangular pillars make it possible to isolate the mined room from the adjacent gob filled with waste, thereby forming a container for the construction of a cementless backfill mass, and the truncated shape of the remnant pillars minimizes their sizes.

Discussion of the results. The proposed option should not be inferior to the traditional procedure in terms of completeness and quality of extraction of subsoil reserves. Another important factor in any underground geotechnology is the specific volume of PDO, which has a significant impact on

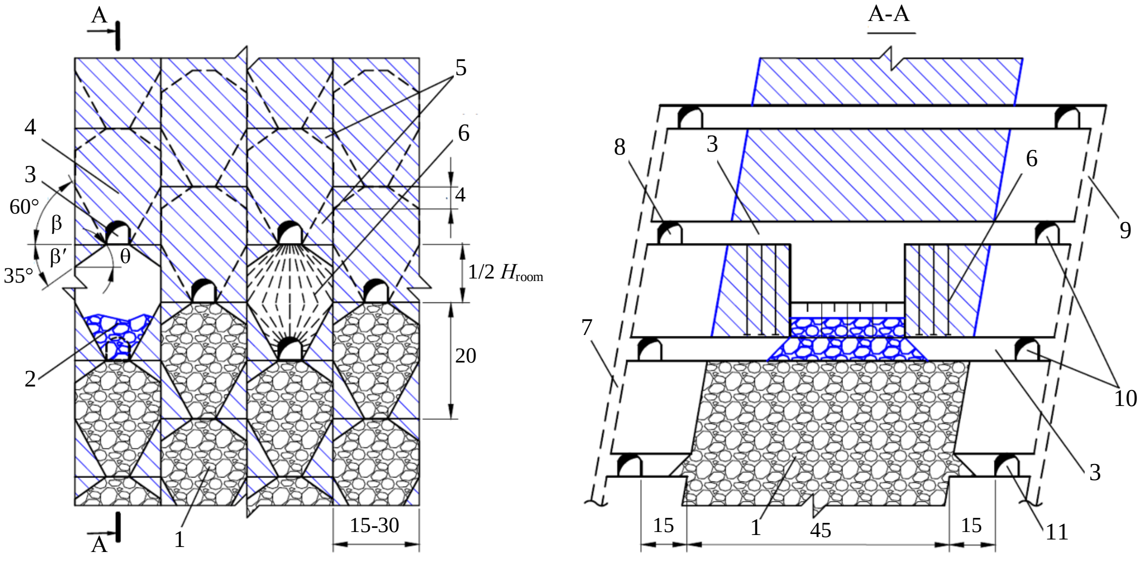

Fig.1. Sublevel-room mining system with ascending extraction and cementless backfill

1 – cementless backfill; 2 – broken ore; 3 – drill haulage ort; 4 – room; 5 – insulating pillar; 6 – blastholes; 7 – ascending ventilation hole; 8 – ventilation drift; 9 – ore pass; 10 – sublevel drift; 11 – level drift

the cost of driving preparatory-development workings. These factors and the volume of the emerging container for waste disposal significantly depend on the geometric parameters of the rooms, determined considering specific mining, geological, and geomechanical conditions. It is known that with an increase in the size of the stope rooms, technical and economic factors improve. Since the study is methodical in nature, we considered the range of change in the width of the room from 15 to 30 m at a constant height of 20 m. With an increase in the height of the rooms, it is very difficult to qualitatively design the pillars of a truncated shape, which ensure the stability of the cementless backfill mass [30].

The factors of the traditional system were determined with a rational ratio of the width and height of the panel, 15×20 m, 20×25, and 25×30 m [31] according to the generally accepted method [32]. With the proposed procedure, ore losses in truncated insulating pillars make up the bulk of the total operational losses during excavation of reserves. With an increase in the width of the room from 15 to 30 m, the losses in the pillars are halved (from 25 to 13 %), the losses of broken ore remain within 2-3 %.

Calculation of the specific volume of PDO, considering the increase in the width of the room or panel, was carried out as follows

$$\Delta V_{\text{pdo}} = \frac{\Sigma V_{\text{pdo}} \cdot 1000}{Q_{\min}}; \tag{1}$$

$$\Sigma V_{\text{pdo}} = S_{\text{d.h.o}} m + S_{\text{e}} l_{\text{e}} n_{\text{e}} + \left(S_{\text{avh}} + S_{\text{op}}\right) h_{\text{sl}} \frac{B}{L_{\text{pc}}} + S_{\text{sd}} B n_{\text{sd}}; \tag{2}$$

$$Q_{\min} = B h_{\text{sd}} m \gamma_{\text{o}} \frac{(1-\text{L})}{(1-\text{I})}, \tag{3}$$

where ΣV_{pdo} is the total volume of PDO in the room (panel), m^3; $Q_{\min}$ are mineable reserves of the room, t; $S_{\text{d.h.o.}}$, S_{e}, S_{avh}, S_{op}, S_{sd} – areas of the drill haulage ort, entry into the room, ascending ventilation hole, ore pass, and sublevel drift, m^2; m is the thickness of the ore body, m; l_{e} is the length of entry into the room, m; n_{e} is the number of entries to the room, pcs.; L_{op} is the distance between the ascending ventilation hole and the ore pass along the strike of the ore body, m; h_{sl} is the sublevel height, m; B is the room width, m; n_{sd} is the number of sublevel drifts, pcs.; γ_{o} – ore density, t/m^3; L – ore loss index, mon. units; I – ore impoverishment index, mon. units.

Comparison of indicators of losses and specific volume of PDO, characterizing the traditional (1) and the proposed option (2) depending on the width of the mining unit (panel or room), is shown in Fig.2.

An analysis of the graphs in Fig.2 shows that, in terms of the complete extraction of reserves and the unit costs for preparatory-development operations, the options are comparable. With an increase in the width of the mining units, the factors of losses and the specific volume of PDO for both options improve. The specific consumption of PDO is reduced due to the greater increase in the mineable reserves of the room (panel) to the increase in the PDO volume. Impoverishment during room excavation of a thick steeply dipping ore body in ascending order will be several times lower than during descending mining by a sublevel caving system with an end withdrawal (5-7 % vs. 25-30) due to the minimal admixture of waste rocks of the hanging side and the working excavation under the ore mass, and not the collapsed rocks.

As noted above, the traditional procedure with the caving of ore and host rocks does not have an environmental potential, since no cavities suitable for filling with waste are formed. To assess the environmental potential of the developed underground geotechnology, an appropriate criterion is proposed, the factor of waste disposal in the gob, which is the ratio of the filled volume of the room to the volume of waste generated during its mining

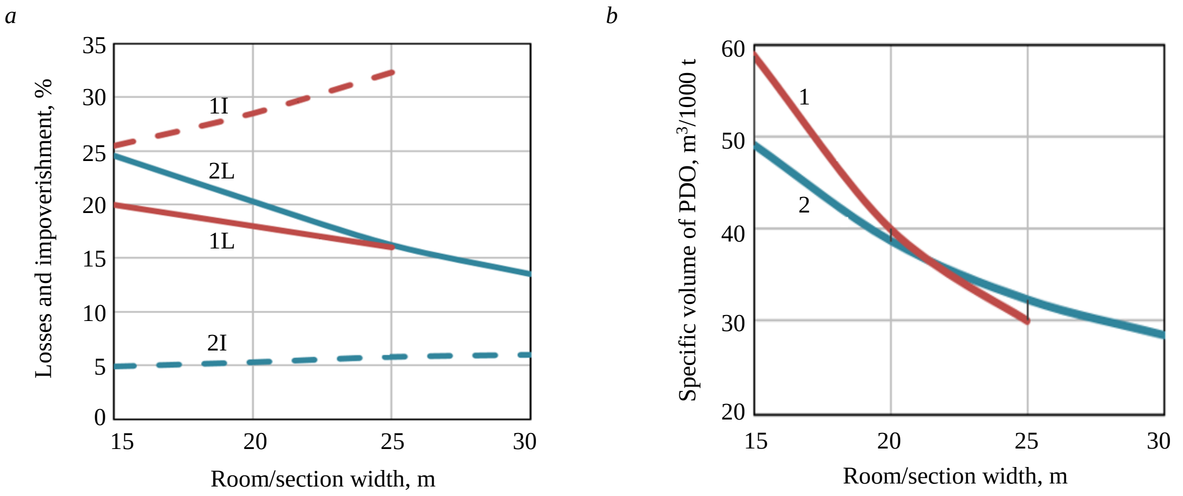

Fig.2. Comparison of ore recovery and specific consumption of PDO with traditional (1) and proposed (2) process options

$$\eta = \frac{V_{\text{op}} k_{\text{fil}}}{V_{\text{w}} k_{\text{shr}}}, \tag{4}$$

where V_{op} is the operating volume of the room, m^3; k_{fil} is the filling factor of the room, mon. units; k_{shr} is the factor of waste shrinkage, mon. units; V_{w} is the volume of waste generated during the mining of the room, m^3.

The operating volume of the room is determined considering the triangular shape of the pillars

$$V_{\text{op}} = \left(ah - b^2 \text{tg}\beta - b^2 \text{tg}\beta'\right) m, \tag{5}$$

where a is the room width, m; h is the room height, m; b is the pillar base width, m; β is the tilt angle of the triangular pillar in the lower part of the room, deg; β′ is the tilt angle of the triangular pillar in the upper part of the room, deg; m is the thickness of the steeply dipping ore body, m.

The angle β is determined by the pillar width, the sublevel height and is limited to half of this height. The angle β' is equal to the angle θ, which is assumed to be 1-2 degrees greater than the repose angle of the backfill mass being formed in the roof of the room.

The volume of waste generated during the mining of the room is determined considering the specific consumption of PDO and the procedure of two-stage beneficiation of iron ores using dry and wet magnetic separation methods [33, 34]:

$$V_{\text{w}} = V_{\text{rock}} + V_{\text{dms}} + V_{\text{wms}}, \tag{6}$$

where V_{rock} is the volume of rock from the preparatory-development operations, m^3; V_{dms} is the volume of dry magnetic separation waste, m^3; V_{wms} is the volume of wet magnetic separation waste, m^3.

As an example of assessing the environmental potential of the proposed procedure, a steeply dipping ore body with an average thickness of 45 m and an iron content in low-grade ores from 25 to 45 % is considered.

Approximate volumes of waste are presented as a function of the width of the room and the content of the useful component (Fig.3, *a*).

The graphs in Fig.3, *a* show that the volume of disposed waste grows with an increase in the room width due to an increase in the volume of mineable reserves in the extraction unit and decreases with an increase in the metal content in the ore. An increase in the intensity of the function with an increase in the width of the room occurs due to a decrease in the influence of the share of waste from drifting, and a decrease in the intensity of the function with an increase in the content of the useful component is due to an increase in impoverishment and a decrease in the quality gain in the beneficiation process at the stage of dry magnetic separation [35].

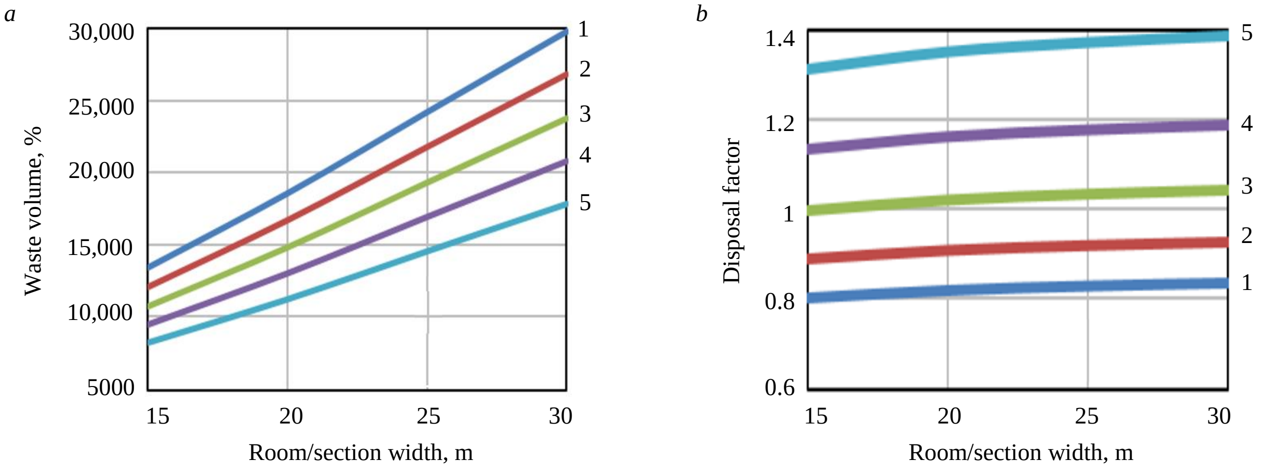

Fig.3. Dependence of the volume of waste generated during the mining of the room (*a*) and the disposal factor (*b*) on the width of the room and the content of the useful component in the ore

1 – Fe = 25 %; 2 – 30; 3 – 35; 4 – 40; 5 – 45

The values of the waste disposal factor determined for the developed environmental geotechnology depending on the width of the mining unit in the considered range of the content of the useful component in the ore are shown in Fig.3, *b*.

Figure 3, *b* shows that the factor values increase with the room width and the content of the useful component in the ore due to an increase in the volume of reserves and a decrease in the proportion of waste rock in the ore mass. A decrease in the intensity of the function with an increase in the room width occurs due to an improvement in the loss factor and a deterioration in the impoverishment factor.

The results of the study show that it is possible to use a significant amount of waste from the mining and processing of low-grade iron ores in specially formed storage rooms without a binder to consolidate and hold backfill material in a stable state (from 80 % in the worst to 140 % in the best of the considered cases). Also, when the iron content in the ore is more than 35 % ($\eta > 1$), the backfilled rooms may dispose more dry and solid waste than is generated as a result of their mining, which additionally enables to dispose the rock from the permanent workings or other mining waste already existing at the enterprise.

Conclusion. As part of the creation of environmentally oriented underground geotechnologies for the mining of low-grade ores, an environmental geotechnology was developed based on the working of a deposit in an ascending order, room extraction of reserves with a staggered arrangement of rooms in height, the formation of insulating pillars of a truncated shape, and the placement of mining waste in a gob in the form of cementless backfill. In addition to iron ore deposits, the developed procedure can be promising for deposits with low-grade ores of non-ferrous metals and apatite-nepheline raw materials similar in occurrence conditions.

Studies of the main factors of the proposed procedure and their comparison with the traditional procedure for mining low-grade iron ore, the system for developing sublevel caving, determined that in terms of the complete extraction of reserves and unit costs for drifting of preparatory-development workings, the procedures are comparable, while in terms of extraction quality, the developed version is much more efficient.

Evaluation of environmental geotechnology according to the criterion of waste disposal, performed according to the proposed methodology, showed that the sublevel-room working system with ascending excavation of rooms and cementless backfill provides placement in the formed gob from 80 to 140 % of all waste generated during the mining and beneficiation of low-grade iron ores with iron content alternating from 25 to 45 %.

Improvement of underground environmental geotechnologies and development of the methodology for their assessment with access to an integral environmental and economic criterion is the direction of further research by the authors.

REFERENCES

1. Pashkevich M.A. Classification and Environmental Impact of Mine Dumps. Assessment, Restoration and Reclamation of Mining Influenced Soils. London: Academic Press, 2017, p. 1-32. DOI: 10.1016/B978-0-12-809588-1.00001-3

2. Lima A.T., Mitchell K., O'Connell D.W. et al. The legacy of surface mining: remediation, restoration, reclamation and rehabilitation. *Environmental Science & Policy*. 2016. Vol. 66, p. 227-233. DOI: 10.1016/j.envsci.2016.07.011

3. Agboola O., Babatunde D.E., Fayomi O.S. et al. A review on the impact of mining operation: Monitoring, assessment, and management. *Results in Engineering*. 2020. Vol. 8. N 100181. DOI: 10.1016/j.rineng.2020.100181

4. Antoninova N.Yu., Shubina L.A. To the Question about the Features of Integrated Environmental Analysis Areas Experienced Local Technical Burden of Mining and Smelting Complex Enterprises. *Ecology and Industry of Russia*. 2017. Vol. 21. N 2, p. 52-56. DOI: 10.18412/1816-0395-2017-2-52-56

5. Arratia-Solar A., Svobodova K., Lèbre É., Owen J.R. Conceptual framework to assist in the decision-making process when planning for post-mining land-uses. *The Extractive Industries and Society*. 2022. Vol. 10. N 101083. DOI: 10.1016/j.exis.2022.101083

6. Boldy R., Santini T., Annandale M. et al. Understanding the impacts of mining on ecosystem services through a systematic review. *The Extractive Industries and Society*. 2021. Vol. 8. Iss. 1, p. 457-466. DOI: 10.1016/j.exis.2020.12.005

7. Kornilkov S.V., Antoninova N.Yu., Shubina L.A., Slavikovskaya Yu.O. Ecological Aspects of Choosing a Recultivation Scenario in Mineral Mining. *Mining Informational and Analytical Bulletin*. 2021. N 5-2, p. 218-230 (in Russian). DOI: 10.25018/0236_1493_2021_52_0_218

8. Onimisi A.H., Olanrewaju I.O. Environmental impacts of iron ore mining on quality of surface water andits health implication on the inhabitants of Itakpe. *International Journal of Current Multidisciplinary Studies*. 2016. Vol. 2. Iss. 6, p. 318-321.

9. Pashkevich M.A., Alekseenko A.V., Petrova T.A. Assessment and control of environmental and economic risk in the Novorossiysk industrial agglomeration. *Izvestiya Tulskogo gosudarstvennogo universiteta. Nauki o zemle*. 2018. N 1, p. 23-35 (in Russian).

10. Antoninova N.Yu., Rybnikova L.S., Slavikovskaya Yu.O., Shubina L.A. Environmental and Economic Aspects of Selecting Reclamation Directions for Industrial Mining and Metallurgical Waste Disposal Sites. *Russian Mining Industry*. 2022. N S1, p. 71-77 (in Russian). DOI: 10.30686/1609-9192-2022-1S-71-77

11. Trubetskoy K.N. Solution of the problem of ecological balance in open pit mineral mining. *Gornyi zhurnal*. 2018. N 6, p. 71-76 (in Russian). DOI: 10.17580/gzh.2018.06.15

12. Zoteev O.V., Kravchuk T.S., Pytalev I.A., Yakshina V.V. Study of the possibility of using gabion structures in the complex development of mining systems. *Izvestija Tulskogo gosudarstvennogo universiteta. Nauki o Zemle*. 2020. N 4, p. 179-189 (in Russian). DOI: 10.25635/h3068-0098-9195-n

13. Sakantsev G.G., Perekhod T.M., Sveshchinskaya N.A. Theoretical Bases of Waste-Free Technologies for Opencast Mining of Ore Deposits. *Problems of Subsoil Use*. 2019. N 3 (22), p. 86-94 (in Russian). DOI: 10.25635/2313-1586.2019.03.086

14. Kaplunov D.R., Yukov V.A. Principles of a Mine Transition to Sustainable and Environmentally Sound Development. *Mining Informational and Analytical Bulletin*. 2020. N 3, p. 74-86 (in Russian). DOI: 10.25018/0236-1493-2020-3-0-74-8615

15. Khayrutdinov M.M., Kuziev D.A., Kopylov A.B., Golovin K.A. Man-Made Waste in Backfill Mixtures – A Way to Reduce Environmental Impact. *Izvestija Tulskogo gosudarstvennogo universiteta. Nauki o Zemle*. 2022. N 1, p. 152-164 (in Russian). DOI: 10.46689/2218-5194-2022-1-1-152-164

16. Kaplunov D.R., Rylnikova M.V., Radchenko D.N. Scientific and Methodological Bases of Design of Ecologically Balanced Cycle of Comprehensive Exploitation and Conservation of the Earth's Reserves. *Mining Informational and Analytical Bulletin*. 2015. N S 4-2, p. 5-11 (in Russian).

17. Galchenko Yu.P. The Creation and Use of Ekogeo-Tehnology – As the Prospect of Environmental Engineering. *Mining Informational and Analytical Bulletin*. 2014. N S1, p. 211-227 (in Russian).

18. Litvinenko V., Naumov I., Bowbrick I., Zaitseva Z. Global guidelines and requirements for professional competencies of natural resource extraction engineers: Implications for ESG principles and sustainable development goals. *Journal of Cleaner Production*. 2022. Vol. 338. N 130530. DOI: 10.1016/j.jclepro.2022.130530

19. Danilov A.S., Horttanainen M.V., Matveeva V.A., Korelskiy D.S. Backfill of a mined-out gold ore deposit with the cemented rubber-cord and waste rock paste: environmental changes in aqueous media. *Journal of Ecological Engineering*. 2021. Vol. 22. Iss. 7, p. 190-203. DOI: 10.12911/22998993/138870

20. Wu D., Fall M., Cai S.J. Coupling temperature, cement hydration and rheological behaviour of fresh cemented paste backfill. *Minerals Engineering*. 2013. Vol. 42, p. 76-87. DOI: 10.1016/j.mineng.2012.11.011

21. Yowa G.G., Sivakugan N., Tuladhar R., Arpa G. Strength and rheology of cemented pastefill using waste pitchstone fines and common pozzolans compared to using portland cement. *International Journal of Geosynthetics and Ground Engineering*. 2022. Vol. 8. N 56. DOI: 10.1007/s40891-022-00400-3

22. Kalmykov V.N., Petrova O.V., Yanturina Yu.D. Assessment of technological reserves of sustainable development of mining engineering systems in underground development of ore deposits. *Mining Informational and Analytical Bulletin*. 2014. N S1-1, p. 69-78 (in Russian).

23. Allaberdin A.B., Mazhitov A.M., Pytalev I.A., Gavrishev S.E. analysis and evaluation of formation schemes of a combined artificial array for the storage-chamber development system. *Sustainable Development of Mountain Territories*. 2020. Vol. 12. N 3 (45), p. 436-443. DOI: 10.21177/1998-4502-2020-12-3-436-443

24. Mazhitov A.M., Volkov P.V., Krasavin A.V., Allaberdin A.B. Developing the Technology for the Formation of an Artificial Array with Specified Geotechnical Characteristics. *Izvestiya vysshikh uchebnykh zavedenii. Gornyi zhurnal*. 2019. N 2, p. 51-58 (in Russian). DOI: 10.21440/0536-1028-2019-2-51-58

25. Savich I.N. Application of systems with forced collapse in underground mining of ore deposits. *Mining Informational and Analytical Bulletin*. 2014. N S1, p. 366-373 (in Russian).

26. Sokolov I.V., Antipin Yu.G., Nikitin I.V. et al. Survey on Underground Geotechnology during Transition to the Development of Deep Reserves of Inclined Copper Pyrite Deposits. *News of the Ural State Mining University*. 2016. N 2 (42), p. 47-53 (in Russian). DOI: 10.21440/2307-2091-2016-2-47-53

27. Ross I.T. Benchmarking and its application for caving projects. Caving 2018: Proceedings of the Fourth International Symposium on Block and Sublevel Caving, 15-17 October 2018, Perth, Australia. Australian Centre for Geomechanics, 2018, p. 473-486. DOI: 10.36487/ACG_rep/1815_36_Ross

28. Falorni G., Del Conte S., Bellotti F., Colombo D. InSAR monitoring of subsidence induced by underground mining operations. Caving 2018: Proceedings of the Fourth International Symposium on Block and Sublevel Caving, 15-17 October 2018, Perth, Australia. Australian Centre for Geomechanics, 2018, p. 705-712. DOI: 10.36487/ACG_rep/1815_54_Falorni

29. Antipin Yu.G., Baranovsky K.V., Rozhkov A.A., Klyuyev M.V. Overview of Combined Underground Mining Systems for Ore Deposits. *Problems of Subsoil Use*. 2020. N 3 (26), p. 5-22 (in Russian). DOI: 10.25635/2313-1586.2020.03.005

30. Antipin I.G., Rozhkov A.A., Baranovskii K.V. Substantiation of the parameters of open stoping mining method with abandonment of unrecoverable pillars. *Izvestiya vysshikh uchebnykh zavedenii. Gornyi zhurnal*. 2021. N 4, p. 15-23 (in Russian). DOI: 10.21440/0536-1028-2021-4-15-23

31. Noriega R., Pourrahimian Y., Victor W.L. Optimization of the undercut level elevation in block caving mines using a mathematical programming framework. Caving 2018: Proceedings of the Fourth International Symposium on Block and Sublevel Caving, 15-17 October 2018, Perth, Australia. Australian Centre for Geomechanics, 2018, p. 363-372. DOI: 10.36487/ACG_rep/1815_25_Noriega

32. Mijalkovski S., Despodov Z., Mirakovski D., Adjiski V. Methodology for optimization of coefficient for ore recovery in sublevel caving mining method. *Podzemni radovi*. 2017. Vol. 30, p. 19-27. DOI: 10.5937/podrad1730019S

33. Pelevin A.E. Iron ore beneficiation technologies in Russia and ways to improve their efficiency. *Journal of Mining Institute*. 2022. Vol. 256, p. 579-592. DOI: 10.31897/PMI.2022.61

34. Feiwang Wang, Zhiqiang Zhao, Song Zhang et al. Performance assessment of an innovative precise low-intensity magnetic separator. *Minerals Engineering*. 2022. Vol. 187. N 107774. DOI: 10.1016/j.mineng.2022.107774

35. Tripathy S.K., Singh V., Rama Murthy Y. et al. Influence of process parameters of dry high intensity magnetic separators on separation of hematite. *International Journal of Mineral Processing*. 2017. Vol. 160, p. 16-31. DOI: 10.1016/j.minpro.2017.01.007

Authors: **Igor V. Sokolov,** *Doctor of Engineering Sciences, Director, https://orcid.org/0000-0001-7841-5319 (Institute of Mining, Ural Branch of the RAS, Yekaterinburg, Russia),* **Yuriy G. Antipin,** *Candidate of Engineering Sciences, Head of Laboratory, https://orcid.org/0000-0002-3564-0310 (Institute of Mining, Ural Branch of the RAS, Yekaterinburg, Russia),* **Artem A. Rozhkov,** *Candidate of Engineering Sciences, Senior Researcher, 69artem@bk.ru, https://orcid.org/0000-0003-3007-1099 (Institute of Mining, Ural Branch of the RAS, Yekaterinburg, Russia),* **Yuriy M. Solomein,** *Researcher, https://orcid.org/0000-0002-8226-6894 (Institute of Mining, Ural Branch of the RAS, Yekaterinburg, Russia).*

The authors declare no conflict of interests.

ISSN 2411-3336; e-ISSN 2541-9404

JOURNAL OF MINING INSTITUTE

Zapiski Gornogo instituta

Journal homepage: pmi.spmi.ru

Review article

Microbiological remediation of oil-contaminated soils

Irina D. SOZINA[1,2]✉, **Aleksandr S. DANILOV**[2]

[1] *AO Novaya Aviatsiya, Saint Petersburg, Russia*

[2] *Saint Petersburg Mining University, Saint Petersburg, Russia*

How to cite this article: Sozina I.D., Danilov A.S. Microbiological remediation of oil-contaminated soils. Journal of Mining Institute. 2023. Vol 260, p. 297-312. DOI: 10.31897/PMI.2023.8

Abstract. Microbiological remediation is a promising technology for the elimination of environmental contamination by oil and petroleum products, based on the use of the metabolic potential of microorganisms. The issue of environmental contamination by crude oil and its refined products is relevant in the Russian Federation since the oil industry is one of the leading sectors of the country. Mechanical and physico-chemical methods of treatment are widely used to clean oil-contaminated soils. However, the methods belonging to these groups have a number of significant drawbacks, which actualizes the development of new methods (mainly biological), since they are more environmentally friendly, cost-effective, less labor-intensive, and do not require the use of technical capacities. Various bio-based products based on strains and consortia of microorganisms have been developed that have proven effectiveness. They include certain genera of bacteria, microscopic fungi, and microalgae, substances or materials acting as sorbents of biological agents and designed to retain them in the soil and increase the efficiency of bioremediation, as well as some nutrients. Statistical data, the most effective methods, and technologies, as well as cases of using microorganisms to restore oil-contaminated soils in various climatic conditions are presented.

Keywords: bioremediation; oil-contaminated soils; oil; environmental contamination; reclamation; bio-based product; hydrocarbon-oxidizing microorganisms

Received: 12.05.2022 ***Accepted: 17.11.2022*** ***Online: 14.02.2023*** ***Published: 25.04.2023***

Introduction. The oil-producing and refining industries can be attributed to one of the leading industries in terms of the amount of waste generated [1]. According to Rosstat[1], in 2020 in Russia, the mass of waste after the extraction of crude oil and natural gas, as well as after the production of coke and petroleum products amounted to 8127.1 and 928.6 thousand tons, respectively. Most of the waste generated falls on oil-producing companies (more than 1 million tons of oil sludge and oil-contaminated soils), oil refineries (0.7 million tons), oil depots (0.3 million tons), railways, airports, and seaports (0.5 million tons) [2].

Oil is a valuable energy resource, providing, according to various estimates, 30-35 % of global energy consumption [3, 4].

According to the Federal Classificatory Catalogue of Wastes, oil-containing waste belongs to the third (moderately hazardous waste, oil content of 15 % or more) or fourth hazard class (low-hazard substances, oil content less than 15 %). Oil in its pure form, depending on the fractional composition and impurities, is classified as a second or third-hazard-class substance in accordance with the current regulatory documentation (GOST R 51858-2020). The presence of volatile aromatic hydrocarbons, naphthalene, and sometimes sulfur compounds and other impurities in the composition of oil causes its high environmental hazard as a waste of human activity.

---

[1] Key indicators of environmental protection. Statistical bulletin. Moscow: Federal State Statistics Service, 2021, p. 41.

Environmental contamination occurs during the construction and operation of oil-producing wells, transportation and processing of hydrocarbon raw materials, and other processes associated with an increase in oil production and transportation [5]. According to some data, more than a third of the total number of oil contamination cases is associated with transportation [6]. Due to the low solubility and nonpolar and hydrophobic nature of the oil components, the physical and chemical removal of contaminants is difficult [7]. The solubility of certain hydrocarbon fractions in water depends on their structure, molecular weight, and ambient temperature. At a temperature of 25 °C and an atmospheric pressure of 0.1 MPa, the lower hydrocarbons have the greatest solubility (Table 1). Solubility among hydrocarbons with the same number of carbon atoms declines in a row: arenes, naphthenes, and alkanes [8].

Table 1

Solubility of petroleum hydrocarbons in water at 25 °C and an atmospheric pressure of 0.1 MPa

Compound	Solubility, mg/ml	Compound	Solubility, mg/ml
Alkanes			
Methane	24.4	2-Methylpentane	13.8
Ethane	60.4	2,2-Dimethylpentane	18.4
Propane	62.4	2,4-Dimethylpentane	4.06
n-Butane	61.4	*n*-Heptane	2.93
Isobutane	48.9	*n*-Octane	0.66
n-Pentane	38.5	*n*-Nonan	0.122
Isopentane	47.8	*n*-Decane	0.022
n-Hexane	9.5		
Cyclic compounds			
Cyclopentane	156.0	Methylcyclopentane	42.0
Cyclohexane	55.0	Methylcyclohexane	14.0
Aromatic compounds			
Benzene	1780.0	Ethylbenzene	152.0
Toluene	515.0	1,2,4-Trimethylbenzene	57.0
o-Xylene	175.0	Isopropylbenzene	50.0
Polycyclic aromatic compounds			
Indane	109.1	Phenantrene	1.29
Naphthalene	31.7	Pyrene	0.135 (2.4)
Diphenyl	7.0	Anthracene	0.073 (3.2)
Fluorene	1.98	Chrysen	0.002

As a result of contamination, irreversible changes occur: disruption of natural biocenoses, changes in their species diversity; decrease in the respiratory and productive capacity of organisms; changes in the enzymatic activity of soils; deterioration of the quality of life and human health [9]. In world history, there have been many accidental oil spills, many of which have caused environmental disasters. Thus, when the Maltese tanker Erika broke up and sank in 1999 in the Bay of Biscay (about 20 thousand tons of fuel oil), about 400 km of the coast was flooded with an oil-water mixture. On the coast, 65 thousand oil-contaminated seabirds were collected, of which 50 thousand were already dead. Important coastal marine fisheries, areas of mariculture, and tourist areas in the provinces of Brittany and Vendée were affected [10].

On April 20, 2010, an explosion occurred on the Deepwater Horizon offshore drilling rig, 80 km off the coast of Louisiana (USA) in the Gulf of Mexico. The oil spill was precisely the main cause of the ecological disaster – almost 1800 km of coasts were contaminated, and tens of thousands of marine animals and birds died [10].

On November 28, 2015, the oil tanker Nadezhda crashed on Sakhalin Island near the port of Nevelsk. As a result of damage to the hull, oil products sank into the waters of the Tatar Strait. Contamination occurred over the water area of more than 20 thousand m^2, the length of the contaminated coastal strip was about 7 km, and birds and fish died en masse.

There are various methods of eliminating oil contamination: mechanical, physico-chemical, and biological [11]. Mechanical methods are most widely used, but their impact often causes no less damage to the environment than oil contamination [12, 13]. Some physico-chemical methods are also used, in particular sorption [14], the disadvantage of which is the need to recycle spent sorbents. The physico-chemical method – the introduction of ameliorants [15, 16], for example, based on sewage sludge [17] – is not always applicable and effective, and also requires additional research of each specific sediment and specifics of treated territories.

Inorganic sorbents, i.e., diatomite rocks, various clays, sand, pumice, zeolites, etc., among which diatomites and clays are used most widely due to low cost and large available volumes. These inorganic sorbents as well as sand (used for filling small areas of oil and petroleum product spills), have a low sorption capacity of 70-150 % for oil and do not retain gasoline, diesel fuel, and kerosene. When eliminating the consequences of oil spills in the aquatic environment, inorganic sorbents sink together with oil, thus contributing to the contamination of reservoirs. Most often, sorbents are disposed of by burning (that emits greenhouse gases), washing by water with surfactants or extractants (which can lead to eutrophication of reservoirs where wastewater is discharged), or by storing in dumps (becoming a source of a complex of environmental problems).

Synthetic sorbents have the lowest cost and can be produced from industrial waste. They are characterized by high volume, light weight, buoyancy after oil absorption, high sorption rate, and the possibility of regeneration and reuse. Molded polyethylene with polymer fillers, polyurethane in granular or spongy form, and other types of plastics, pressed basalt or polypropylene fibers are widely used (oil absorption rates: 6.1-7.2 g/g for basalt fibers; 3.8-4.5 g/g for polypropylene fibers). The use of carbon fiber for oil sorption increases the cost of filter elements, but shows a high cleaning effect, 10.2-10.6 g/g. Synthetic sorbents are not bio-decomposable and require incineration, which entails significant environmental issues associated with the emission of greenhouse gases and toxic combustion products of synthetic materials, and additional fuel and electricity costs.

Peat, waste paper, sawdust, wool, dried cereals, etc. are more often used as organic sorbents. Such sorbents have a small sorption capacity (no more than 15 kg/kg) and a low adsorption rate, so they are used with an oil film thickness of no more than 0.1 mm [18]. For this reason, there is a need to develop new environmentally friendly, inexpensive, simple, sustainable, and effective methods for removing oil products from contaminated soils [19]. Biological methods (bioremediation and phytoremediation) have shown promising results for the restoration of soils contaminated with crude oil [20] and the products of its processing [21].

Microbiological remediation is a method based on the ability of microorganisms to destruct organic contaminants by including such substances in its metabolic cycle, is one of the most effective methods of eliminating oil and petroleum product spills at the stage of post-treatment of contaminated sites [22, 23].

A review of the existing statistical data, Russian and foreign developments, and research directions devoted to microbiological bioremediation of oil-contaminated soils is presented.

Discussion. *Basic information about oil contamination.* Crude oil is the main resource for the production of petroleum fractions, fuels, oils, and various materials. It includes mainly such petroleum hydrocarbons as aliphatic and aromatic compounds, resins, and asphaltenes [24].

According to Rosstat data for 2019 in Russia, the area of disturbed and used land due to accidents during the transportation of oil, gas, and refined products amounted to 3120 ha, and the area of reclaimed land from this category for the same period was 806 ha (Table 2).

Table 2

The area of reclaimed and used land disturbed due to oil contamination in Russia, 2015-2019[2]

Cause of land degradation	Year				
	2015	2016	2017	2018	2019
Disturbed, ha:					
Total	136232	444503	25642	119481	194225
Due to leakage during the transit of oil, gas, and oil products	821	514	995	131	3120
Used, ha:					
Due to leakage during the transit of oil, gas, and oil products	382	463	709	188	2892
Reclaimed, ha:					
Total	86552	92052	98673	59397	102225
Due to leakage during the transit of oil, gas, and oil products	492	547	639	178	806

The area of disturbed and used lands in Russia remains significant, and the growing rates of reclamation are not able to fully compensate for the damage caused to the environment due to oil spills. The main sources of soil contamination with oil are leaks during accidents on transport and pipelines, drilling, and oil production; places of storage of oil refining waste; natural disasters; household waste, etc. [25]. In 2021, about 32 accidents with oil or petroleum product spills occurred in Russia; up to 10 thousand cases of field pipeline depressurization happen annually. The biggest accident in 2021 was an oil spill at the offshore terminal of the Caspian Pipeline Consortium near Novorossiysk. The environmental damage is estimated at more than 4 billion rubles.

Microbiological remediation. The development of bioremediation technologies for the restoration of contaminated soils began in the 1970s precisely for the purification of lands adjacent to the areas of oil production. Bioremediation is mainly applied to matrices, such as soil or some types of wastewater, and can be carried out *in-situ* (on site) or *ex-situ* (in bioreactors) [26]. Soils are the second most studied object of bioremediation after water, accounting for 46 % of articles and 36 % of patents from their total number worldwide. This indicates that this problem remains relevant [27].

The advantages of microbiological bioremediation include the relative cost-effectiveness of the technology, ease of use, availability of materials, and environmental friendliness of the method. The advantages are provided by the work of enzymatic systems of microorganisms. Their metabolism allows splitting oil and using oil fractions as a source of carbon and energy [28]. Bioremediation technologies are diverse, but a number of basic methods can be distinguished (see Figure).

In-situ bioremediation and the main methods belonging to this group are the most attractive since recovery takes place without the removal and transportation of contaminants. However, *in-situ* restoration is more suitable for the elimination of surface contamination and is not always effective when the contaminant penetrates into the deep layers of the soil [29, 30]. The *ex-situ* bioremediation method consists of the removal or extraction and restoration of contaminated soil [31].

There are also combined methods, the essence of which is the simultaneous or sequential application of a combination of methods. For example, in microbiological remediation, the combined method may consist of the removal of native microorganisms from contaminated soils, followed by introduction into the contaminated site after the cultivation of microorganisms in the reactor. The essence of the methods used for microbiological bioremediation and their main advantages and disadvantages are presented in Table 3.

---

[2] Environmental Protection in Russia. Moscow: Rosstat, 2020, p. 113.

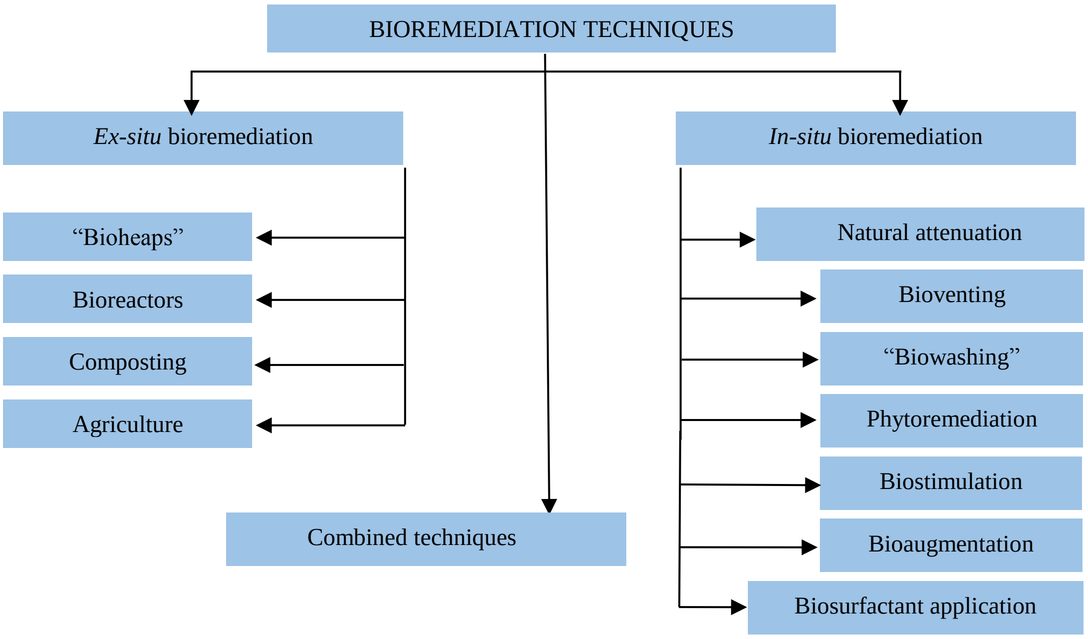

Basic techniques of bioremediation

Table 3

Basic techniques of bioremediation, their advantages and disadvantages [29, 32]

Name	The essence of the technique	Advantages	Disadvantages
Ex-situ bioremediation			
"Bioheaps"	Contaminated soil is stored above the ground in a processing area equipped with devices for aeration, temperature, and humidity control and nutrient application [32, 33]	Prevents the spread of contaminants; requires relatively small areas; economically less costly	Causes soil drying and volatilization rather than degradation of hydrocarbons; requires a continuous power supply
Bioreactors	Bioremediation technology uses a reactor to adjust the parameters of the process environment [34]	High efficiency in both aerobic and anaerobic conditions; the ability to control all parameters of the bioprocess; genetically modified microorganisms can be used	High price; laborious technique; different bioreactor designs may be required depending on the contaminant
Composting	The transformation of organic substances into humus under the action of microbial catabolic activity at elevated ambient temperatures [35]	High biological efficiency; mature compost can be used for agricultural needs; temperature rises during the process	Requires large areas and frequent mixing; the likelihood of leaching toxic intermediates in an event of a failed operation
Agriculture	Contaminated soil is evenly distributed over the surface to increase the bioavailability of contaminants [36]	Simple, less laborious, and inexpensive technique; uses a minimum amount of equipment and technologies	Requires large areas; reduced microbial activity (not suitable for toxic volatile contaminants); laborious technique; the likelihood of washing out contaminants
In-situ bioremediation			
Bioventing	A bioremediation strategy that uses controlled airflow to stimulate the destructive activity of local microorganisms against a contaminant [32, 37]	Cost-effective; enhances microbial activity	The process can be long; requires regulation of the airflow rate

End of Table 3

Name	The essence of the technique	Advantages	Disadvantages
Natural attenuation	A variety of physical, chemical, or biological processes that, under favorable conditions, operate without human intervention to reduce the mass, toxicity, mobility, volume, or concentration of contaminants in soil [38]	Inexpensive and less labor intensive	Long process; the likelihood of washing out and spreading contaminants
“Biowashing”	Similar to the bioventing technique, however, a controlled fluid flow is used to equalize the concentration of contaminants in the environment [32]	Inexpensive; fewer operational dangers	The likelihood of the spread of volatile components into the atmosphere; requires controlled water flow
Phytoremediation	An integrated technique that includes the use of plants for the extraction, accumulation, degradation, filtration, stabilization, and volatilization of contaminants from soil and water environments [39]	Less expensive; environment-friendly; used for large-scale contamination; improves soil fertility	Long process; the likelihood of spreading toxic contaminants through the food chain; not suitable for heavily contaminated soil
Biostimulation	Deliberate stimulation of native microorganisms by the addition of electron acceptors and/or donors, water, or nutrients in the form of fertilizers to accelerate the biodegradation process [40]	Increases soil nutrient content and bioavailability of contaminants; promotes the development of natural microflora	High content of nutrients (nitrogen, phosphorus) can cause algal blooms in the water; the use of surfactants can create a toxic solution in the soil
Bioaugmentation	Addition of highly concentrated and specialized populations of specific microorganisms to a contaminated site increases the biodegradation rate of the contaminant [30]	Cometabolic processes take place; high bioremediation efficiency	Environmental parameters affect microbial growth; a number of international agreements restrict the use of introduced microorganisms and genetically modified organisms; the possibility of mutual suppression of the vital activity of microorganisms of various types
Biosurfactant application	Bioaugmentation strategy that involves inoculation of a biosurfactant or biosurfactant producers into contaminated soils [29]	Increased bioavailability of contaminants; biosurfactants are environment-friendly, biodegradable, non-hazardous, and stable; have high selectivity and foaming ability; microbial surfactants are active under extreme temperature, pH, and salinity conditions [41]	High cost and low yield of substances during synthesis; a small number of microorganisms are producers of biosurfactants

The bacteria that carry out the biodegradation of oil in the soil belong mainly to the genera *Pseudomonas*, *Flavobacterium*, *Acinetobacter*, *Aeromonas*, *Arthrobacter*, and *Rhodococcus* [42, 43]. Fungi of the genera *Alternaria*, *Aspergillus*, *Candida*, *Cephalosporium*, *Cladosporium*, *Fusarium*, *Geotrichum*, *Gliocladium*, *Mucor*, *Paecilomyces*, *Penicillium*, *Rhizopus*, *Rhodotolura*, *Saccharomyces*, *Talaromyces*, *Torulopsis*, etc. [44-46], and microalgae *Chlorella vulgaris* [47, 48] also possess biodestructive ability in relation to petroleum hydrocarbons.

Bacteria are the most effective microorganisms for bioremediation due to their ability to break down almost any hydrocarbons up to the heaviest paraffins (asphalt residues) [49]. The patents describe more than 70 types of bacteria capable of metabolizing various contaminants. *Pseudomonas spp.*, *Rhodococcus spp.*, and *Acinetobacter spp.* are the most common and universal. Most of the patents belong to authors from China, the USA, Japan, the UK, India, and Korea [27]. However, bacteria are very demanding to ambient conditions, so the most favorable for the reproduction of most of them are the temperature of 30-40 °C; the presence of oxygen (aerobic conditions) and nutrients (nitrogen, phosphorus, and iron); neutral pH. The experimental data confirm that no microorganism leads to the complete decomposition of oil. Bioremediation is more effective when carried out by complex microbial consortia, in particular, developing independently in historically contaminated territories [50, 51].

Microscopic fungi are widely used for microbiological bioremediation of soils. Fungal mycelia with many branching hyphae have a large adsorption surface [52], due to which they are able to adsorb xenobiotics (phenol, phenolic compounds, and polycyclic aromatic hydrocarbons). Unlike fungi, bacteria cannot efficiently decompose polycyclic aromatic hydrocarbons with more than four aromatic rings [53, 54]. Due to the presence of hyphae, fungi can penetrate into solid particles and contribute to loosening the soil [55]. Important factors determining the effectiveness of the use of micromycetes as oil utilizers are their active enzymatic system and high viability in conditions of oil contamination [56]. Micromycetes-destructors of petroleum hydrocarbons include at least 100 species of microscopic fungi [57]. Patent documents for bioremediation techniques (most of them from China, the USA, Japan, and Taiwan [27]) mention more than 30 species of fungi. *Chrysosporium spp.*, *Phanerochaete spp.*, *Aspergillus spp.*, *Acremonium spp.*, and *Penicillium spp.* are the most common.

The total number of patents in the field of microbiological bioremediation for algae is low. More than 40 species of algae are mentioned; *Chlorella spp.*, *Scenedesmus spp.*, and *Chlamydomonas spp.* are the most frequent [58]. Almost all supported patents belong to patent holders from China and the USA [27].

Bio-based products. Microbiological composition. When developing bio-based products, special attention is paid to the following aspects: microbiological composition (active strains of bacteria, fungi, and microalgae are selected); selection of a carrier sorbent and auxiliary nutrients. Bio-based products are often developed for use in specific climatic conditions since the biodestructive activity in relation to petroleum hydrocarbons and other contaminants directly depends on the humidity and temperature characteristics when using microbiological bioremediation *in-situ*.

Native and introduced microorganisms. A number of modern studies demonstrate the high efficiency of the oil-destructive ability of microorganisms isolated from the soils of historically oil-contaminated territories [59]. Biostimulation is the key research method.

When using bio-based products for bioremediation, microorganisms are introduced into the soil. Bio-based products can have different compositions – microorganisms of the same genus, species, and strain, as well as consortia of microorganisms, can serve as active agents.

Monocultures. Bio-based products based on monocultures (*Pseudomonas putida* 36; *Acinetronacter sp*. HB-1[3]; and *Pseudomonas alcaligenes* E7[4]) were developed earlier and are significantly inferior in efficiency to bio-based products based on consortia of microorganisms.

The disadvantage of the strains is that they recycle oil at high temperatures: *Rhodococcus erythropolis* VKPM As-1668[5] (the strain is used to purify water and soil from oil contamination); *Rhodococcus globerulus* H-42[6]; *Rhodococcus spp.* [43]; *Micrococcus luteus* LER-4 [60]; and *Bacillus subtilis* [61], capable of reducing the concentration of oil to 0.48 % during the three months of the summer period.

---

[3] Zhirkova N.A., Kobelev B.C., Kholodenko V.P. Patent N RU2077579. Strain of bacterium *Acinetobacter species* used for water and soil treatment from oil and petroleum products. Publ. 20.04.1997.

[4] Ermolenko Z.M., Kholodenko V.P., Chugunov V.A. Patent N RU2134723. Strain of bacterium *Pseudomonas alcaligenes* E7 used for treatment of water and soil from oil and petroleum products. Publ. 20.08.1999.

[5] Vlasov S.A., Safarova V.I., Safarov A.M., Krasheninnikova T.K., Krasnopevtseva N.V. Patent N RU2257409. Strain *Rhodococcus erythropolis* for decomposition of petroleum and petroleum products. Publ. 27.07.2005. Bul. N 21.

[6] Vlasov S.A., Krasnopevtseva N.V., Krasheninnikova T.K., Sinitsyn A.N., Ukraintsev A.D. Patent N RU2300561. Strain *Rhodococcus globerulus* H-42 for decomposition of petroleum and petroleum products. Publ. 10.06.2007. Bul. N 16.

These strains degrade oil in the soil effectively under the conditions of a model experiment, are able to purify the environment from oil, and dispose of petroleum products (diesel fuel) in a wide temperature range of 8-37 °C.

Consortia. Bio-based products based on consortia of microorganisms have a higher proven effectiveness since different types of microorganisms have biodestructive activity against different classes of organic compounds. A large number of such bio-based products have been developed:

- “Devoroil” – five types of oil-oxidizing bacteria and yeast.
- “Ecoil” – aerobic oil-oxidizing bacteria *Mycobacterium*, *Rhodococcus*, and *Acinetobacter*; sucrose, polyethylene glycol, oil, and water [7].
- “Bak-Verad” – a bacterial product from a consortium of bacterial strains of the genera *Bacillus*, *Atherobacter*, *Rhodococcus*, and *Pseudomonas*. Research results have shown that the introduction of bio-based products significantly reduces the content of petroleum products in the soil and accelerates natural destruction by a factor of 3-4 [62].
- In the study [63] strains of *P. putida* TPHK-1, *P. aeruginosa* TPHK-4, *Acenitobacter sp*. TPHK-3, and *S. maltophilia* TPHK-2, capable of growing on petroleum hydrocarbons, were isolated from areas contaminated with oil. The introduction of these hydrocarbon-decomposing strains into samples of oil-contaminated soil led to pronounced bioaugmentation [64].
- A consortium of microorganisms composed of bacterial strains belonging to the genera *Pseudomonas* and *Microbacterium*, as well as microscopic fungi of the genus *Penicillium*, was used in [65] to evaluate the effectiveness of oil-contaminated soil purification in the Kola North. The most effective purification was achieved in experimental variants using a consortium made up of bacteria and fungi. So, the volume of petroleum products in the soil decreased by 57 % from the initial level in 30 days, by 82 % in 120 days, and by 83 % in 370 days.

Bio-based products. Sorbents-carriers. For effective bioremediation of oil-contaminated soils, it is necessary to develop mechanisms for introducing microorganisms. To this end, various sorbents have been tested and their impact on the purification of soils from petroleum products has been assessed. The introduction of sorbents into the soil during bioremediation has a positive effect on the activation of the oil-destructive ability of local or introduced microorganisms and on the growth of plants planted at the final stage of land reclamation. Due to sorbents, a decrease in soil hydrophobicity and an increase in their moisture capacity and porosity can be observed [66].

The cost of biological remediation of oil-contaminated soils using sorbents is 12-200 thousand euros/ha (as of 01.04.2022), depending on the type and amount of sorbent applied. The cost of mechanical methods of reclamation is several times higher [67].

Activated carbon. Activated carbon can serve as a sorbent for introducing microorganism-based products into the soil. This carrier type has been tested in the course of many modern studies [21, 68].

Treatment of oil-contaminated soil with the addition of 1-3 % of granular activated carbon during the experiment reduced the volume of oil hydrocarbons by 78-91 % in four months, which significantly exceeds the result of bioremediation in the control sample without additives – 55-65 % [21].

Activated carbon is a fairly cheap, effective, environmentally friendly sorbent that prevents the leaching of hydrocarbons, heavy metals, and other toxic mobile products into groundwater and surface water bodies [5].

Sapropel. In [69], the ability of six bacterial strains to destroy a number of petroleum products and oil on a solid mineral medium was studied: *Pseudomonas sp*., *Pseudomonas oryzihabitans*, *Rhodococcus erythropolis*, *Pseudomonas sp*., *Acinetobacter guillouiae* 1, and *Acinetobacter guillouiae* 2. Various modifications of sapropel have been selected to introduce bacterial cultures into the soil as a sorbent. It has been established that bacteria are able to attach, effectively retain

---

[7] Rogozina E.A., Andreeva O.A., Zharkova S.I. et. al. Comparative characteristics of domestic biological products offered for cleaning soils and soils from contamination by oil and oil products. *Oil and Gas Geology. Theory and Practice*. 2010. Vol. 5. N 3, p.10-28.

on sapropel substrates, and persist during drying. According to the research results, the destruction of oil occurred more efficiently in the variant with the addition of crushed sapropel to the contaminated soil – in seven days the oil content in the soil decreased by 65 %, which significantly exceeds the purification rates when adding pure bacterial strains. The advantage of such a carrier is its organic nature and ecological purity.

Glauconite. It is a mineral that is an aqueous aluminosilicate of iron, silica, and potassium oxide unstable. The ion-exchange properties of the mineral and the layered structure determine its high sorption activity against petroleum products. Since glauconite, when applied to the soil as part of a bio-based product, can serve not only as a sorbent carrier but also as a mineral fertilizer, its extraction and disposal are not required. As a glauconite-containing carrier, both pure glauconite and glauconite rock containing 30-80 % of glauconite can be used.

A bio-based product for biodegradation of petroleum products has been developed on the basis of glauconite [70]. It includes the association of bacteria *Bacillus megaterium* VKM B-396, *Bacillus subtilis* VKPM B-5328, *Pseudomonas putida* VKM B-1301, *Pseudomonas putida* VKPM B-5624, and *Rhodococcus erythropolis* VKPM AS-1269, immobilized on a glauconite-containing carrier in the amount of 10^8-10^{10} cells/g.

Zeolites. Zeolites are another group of minerals that can be used as sorbents. The fixation of microorganisms inside zeolite crystals allows them to safely tolerate exposure to direct sunlight and sudden changes in ambient temperatures, and the sorption and ion-exchange properties of the mineral provide microorganisms with additional sources of nutrition (petroleum hydrocarbons and mineral nutrition elements sorbed from the soil) necessary for the metabolism of microbial cells. This ensures high efficiency and an increase in the duration of the process of destruction of petroleum products.

The bio-based product for bioremediation of oil-contaminated soils for the climatic conditions of the Far North [71] in its composition contains a solid carrier substrate – crushed zeolitized tuff with a fraction of 1-3 mm with a zeolite content of 60-95 % and a consortium of hydrocarbon-oxidizing microorganisms immobilized on its surface, including strains of *Bacillus vallismoris* VKPM B-11017, *Exguobacterium mexicanum* VKPM B-11011, *Serratia plymuthica* VKM B-2819D, and *Rhodococcus sp*. VKM As-2626D. The advantage of the invention is a high degree of purification of soils and soils from oil and petroleum products (87-88 %) in the cold climate of the Far North in a short period of 60 days.

Other types of carriers. Synthetic materials can be used as sorbents-carriers. Thus, polyurethane foam is a high-quality carrier for cell immobilization thanks to its chemical and physical resistance and stability [72, 73]. However, it is necessary to extract and dispose of such sorbents after the end of bioremediation.

A patented Russian invention is a composition[8] that contains a porous carrier – foamed glassy metaphosphates and strains of microorganisms-destructors *Serratia marcescens* PL-1, *Pseudomonas fluorescens biovar* II10-1, and *Acidovorax delafieldii* 3-1 at a concentration of 10^{12} cells/g, immobilized in the pores of the carrier.

In order to optimize the removal of oil, a biological carrier has been developed for the immobilization of native hydrocarbon-destroying bacteria using peanut shell powder. Biodegradation rates after powder application increased from 26 to 61 % after 12 weeks of treatment. The use of peanut husk powder accelerated the mass transfer of water, oxygen, nutrients, and hydrocarbons and provided nutrition for microorganisms [74]. The introduction of wood chips (sawdust) into the soil with oil-destructing microorganisms significantly reduced the concentration of contaminants in the soil [75]. Studies have also been conducted with chitin or chitosan, vermiculite, etc. used as sorbents.

---

[8] Limbakh I.Yu., Karapetyan G.O., Karapetyan K.G., Novikova I.I., Boikova I.V., Pisarev I.N., Lednev V.A. Patent N RU2181701. Biological preparation “Avalon” for cleaning environmental objects to remove petroleum and petroleum derivatives, and method of preparation thereof. Publ. 27.04.2002. Bul. N 12.

Bio-based products. Nutrients. There is another aspect that needs to be taken into account when using bioremediation methods to achieve the most successful result [30]. In order to stimulate the development and support of microorganisms in the soil in concentrations sufficient for bioremediation, the presence of nutrients – nitrogen, phosphorus, potassium, and sulfur – is necessary. The biostimulation method is based on the artificial introduction of these substances into the natural environment, in which nutrients are introduced into the soil and provide aeration, which allows local microorganisms to multiply[9]. The biostimulation method is based on the artificial introduction of these substances into the natural environment, in which nutrients are introduced into the soil and provide aeration, which allows local microorganisms to multiply. Microorganisms also use these substances to produce enzymes that break down petroleum hydrocarbons and other contaminants [76].

Complexes of mineral fertilizers are used as a source of nutrients to stimulate the vital processes of microorganisms: "Azofoska" [21], urea[10], etc. Bioremediation using fertilizers to increase the concentration of nutrients – nitrogen and phosphorus, necessary for the growth of microorganisms and decomposing hydrocarbons – was used to clean the coastline from oil after the Exxon Valdez spill [77].

Bio-based products. Temperature regime. Temperature is one of the main factors influencing the intensity of biochemical transformations of organic substances under the action of the processes of vital activity of microorganisms [78]. For this reason, when selecting strains for microbiological bioremediation of soils in certain climatic conditions, it is worth considering their belonging to a group depending on the temperature optimum: psychrophiles (*Pseudomonas spp*., *Microbacterium spp*., *Rhodococcus spp*., *Arthrobacter spp*., *Brevibacterium spp*., and *Bacillus spp*.) are used most often, even in northern latitudes (t_{opt} = 10-20 °C) [65, 71, 79]; psychrotrophs (*Acinetobacter spp*., *Pseudomonas spp*., and *Rhodococcus spp*., t_{opt} = 20-28 °C); mesophylls (*Staphylococcus spp*., and *Acinetobacter spp*.) are used in mid-latitudes with other microorganisms in laboratory and field experiments (t_{opt} = 37 °C) [59]; thermophiles (some representatives of *Bacillus spp*., *Methanobacterium spp*., and *Chlamydomonas spp*.) are rarely used, mainly in model or laboratory experiments (t_{opt} = 42 °C).

The study of the effectiveness of the use of psychrophilic microorganisms for cleaning soils from oil contamination in conditions of low ambient temperatures is given in the materials of many scientific studies and dissertations [80].

The results of the work [81] show the ability to utilize oil and petroleum products with a mixed culture of psychrophilic and psychrotolerant strains that actively oxidize petroleum hydrocarbons (*Rhodococcus sp*. As-2626D + *Serratia plymuthica* As-2819D + *Bacillus vallismortis* B-11017 + + *Exiguobacterium mexicanum* B-l 1011), at low positive temperatures (4-10 °C). It was found that these strains, when introduced into permafrost soil at –45...–50 °C, retained viability and after thawing retained UV-oxidizing activity, which showed the possibility of their use for cleaning soils from oil contamination not only within the growing season. The use of the obtained bio-based product in winter before and after the formation of snow cover ensured the 44-62 % degree of soil purification at a 1 % level of oil contamination and 34-46 % at 5 % of contamination.

According to the results of the study [80], on the basis of a consortium of bacteria of the genera *Rhodococcus* and *Pseudomonas*, the "MicroBak" bio-based product was developed and patented for bioremediation of soils with an oil content of up to 15 % at low and moderate temperatures of 4-32 °C in the presence of up to 5 % of salt at pH of 6-8. A microbial association "ViO" was created, consisting of strains-destructors of the genera *Rhodococcus*, *Pseudomonas*, and *Acinetobacter*. Consortium bacteria are capable of degradation of petroleum hydrocarbons at concentrations up to 30 % in the temperature range of 4-42 °C in the presence of up to 5 % of salt at pH 4-10. The effectiveness of the prototype of the "ViO" bio-based product in field tests for cleaning the soil from oil on the territory of the Pogranichnoye field of Yamalo-Nenets Autonomous Okrug was 80 %.

---

[9] Moorthy K., Lavanya V., Malarvizhi A. et al. Isolation of soil bacteria for bioremediation of hydrocarbon contamination. *Biosciences, Biotechnology Research Asia*. 2010. Vol. 7 (2), p. 901-906.

[10] Maamar R.M., Mogadami F.S. Bioremediation of Libyan Crude Oil-Contaminated Soil under Mesophilic and Thermophilic Conditions. *APCBEE Procedia*. 2013. Vol. 5, p. 82-87. DOI: 10.1016/j.apcbee.2013.05.015

The study [82] proved the high efficiency of biotechnological techniques based on the use of the psychrotolerant consortium IB ND 1 for the remediation of contaminated objects. Table 4 provides basic information about the results of a number of studies of the oil-destructive ability of strains and consortia of microorganisms.

Table 4

Results of studies of the oil-degrading ability of strains and consortia of microorganisms

Microbiological agent	Ambient conditions, duration of an experiment	Initial concentration of oil or oil products in the soil, g/kg	Concentration of oil or oil products in the soil at the end of the experiment
Pseudomonas putida 36 [20]	20-28 °C, 5 days	–	20 °C: oil – decrease in concentration by 22.0 %; fuel oil M-40 – 10.2 %; kerosene – 75.0 % 28 °C: oil – decrease in concentration by 28.0 %; fuel oil M-40 – 9.0 %; kerosene – 93.0 %
Pseudomonas alcaligenes E7 [21]	20-28 °C, 5 days	–	20 °C: oil – decrease in concentration by 63.8 %; fuel oil M-40 – by 34.2 %; kerosene – by 81.0 % 28 °C: oil – decrease in concentration by 69.0 %; fuel oil M-40 – by 41.0 %; kerosene – by 85.0 %
Rhodococcus erythropolis VKPM As-1668 [22]	28-30 °C, 1 month (laboratory experiment) 28-30 °C, 15-30 days (long-standing oil contamination of the soil)	18.8 178.2	In 1 month – 6.5 g/kg (degree of purification – 65.4 %) In 15 days – 65.9 g/kg (degree of purification – 63.5 %) In 30 days – 52.5 g/kg (degree of purification – 70.7 %)
Micrococcus luteus LER-4 [60]	10; 20; 30; 37 °C, 3 days	Oil – 0.91 Diesel fuel – 0.91 Engine oil – 0.91	10 °C – 0.86 g/kg (5.6 %); 20 °C – 0.402 g/kg (55.8 %); 30 °C – 0.28 g/kg (68.9 %); 37 °C – 0.24 g/kg (73.8 %) 10 °C – 0.866 g/kg (4.78 %); 20 °C – 0.366 g/kg (59.76 %); 30 °C – 0.292 g/kg (67.9 %); 37 °C – 0.277 g/kg (74.98 %) 10 °C – 0.879 g/kg (3.34 %); 20 °C – 0.41 g/kg (54.98 %); 30 °C – 0.275 g/kg (69.76 %); 37 °C – 0.262 g/kg (71.16 %)
Bacillus subtilis Kolyma 7/2k [61]	Yakutsk city, three-months field experiment (summer period)	135.14	0.645 g/kg (residual oil content of 0.48 %)
Biological product based on the "Devoroil" consortium of microorganisms [23]	28-30 °C, 1 month (laboratory experiment) 28-30 °C, 15-30 days (long-standing oil contamination of the soil)	18.8 178.2	1 month – 9.6 g/kg (degree of purification – 51.1 %) In 15 days – 131.2 g/kg (degree of purification – 26 %) In 30 days – 88.3 g/kg (degree of purification – 53 %)
P. putida TPHK-1, *P. aeruginosa* TPHK-4, *Acenitobacter sp*. TPHK-3, *S. maltophilia* TPHK-2 [63]	25 °C, 10 days	0.073-0.365 (1-5 % of diesel fuel)	Initial diesel fuel concentration of 1 %: *P. putida* TPHK-1 decomposition degree of 93 %; *P. aeruginosa* TPHK-4 – 90 %; *S. maltophilia* TPHK-2 – 78 %; *Acenitobacter sp*. TPHK-3 – 73 % Initial diesel fuel concentration of 5 %: *P. putida* TPHK-1 – 87 %; *P. aeruginosa* TPHK-4 – 65 %; *S. maltophilia* TPHK-2 or *Acenitobacter sp*. TPHK-3 – 40 %
Rhodococcus erythropolis + sapropel [69]	7 days	–	Soil + *Rhodococcus erythropolis* – degree of oil decomposition – 32 % Soil + *Rhodococcus erythropolis* + substrate based on medium size sapropel – 65 %

End of Table 4

Microbiological agent	Ambient conditions, duration of an experiment	Initial concentration of oil or oil products in the soil, g/kg	Concentration of oil or oil products in the soil at the end of the experiment
"Bioionit" biological product for biodegradation of oil products (*Bacillus megaterium* VKM B-396, *Bacillus subtilis* VKPM B-5328, *Pseudomonas putida* VKM B-1301, *Pseudomonas putida* VKPM B-5624, and *Rhodococcus erythropolis* VKPM AS-1269, immobilized on a glauconite-containing carrier) [70]	100 ml of distilled water pH 4-12, 3 % of oil, 1 g of the product, 18-20 °C, 4 days	30	Decrease in oil concentration at different pH values: 3 – 0 %; 4 – 0.49 %; 4.5 – 17.4 %; 5 – 49.3 %; 6 – 79 %; 7 – 80 %; 8 – 79 %; 9 – 79 %; 10 – 66.7 %; 11 – 43.7 %; 12 – 0 %
Consortium of hydrocarbon-oxidizing microorganisms, including strains of *Bacillus vallismoris* VKPM B-11017, *Exguobacterium mexicanum* VKPM B-11011, *Serratia plymuthica* VKM B-2819D, *Rhodococcus sp*. VKM As-2626D, and zeolite tuff crushed to a 1-3 mm fraction [71]	18-22 °C, 60 days	Cryogenic bog soil – 108.34 Cryogenic taiga soil – 16.26 Cryogenic peat soil – 13.59	12.3 g/kg – 88.64 % 2.045 mg/kg – 87.42 % 7.39 mg/kg – 88.64 % The research results advise that the product cannot be used at 4-8°C
"AVALON" biological product (foamed glassy metaphosphates and strains of microorganisms-destructors *Serratia marcescens* PL-1, *Pseudomonas fluorescens biovar* II10-1, and *Acidovorax delafieldii* 3-1 at a concentration of 1012 cells/g) [24]	28 days, fuel oil and oil	–	Biodestruction degree of 86.5-88.2 %
Sorbent for immobilization of microorganisms: 0.5-1.5 mm peanut shell powder, microorganisms – native bacterial consortium [74]	Soil contaminated with crude oil from Liaohe Oilfield, Liaoning Province, China, 28 °C, 12 weeks	–	After 12 weeks of biodegradation, the concentration of oil products in the soil was 21800; 21500; 18300; and 11400 mg/kg, with removal efficiency of 26; 27; 38; and 61% respectively (for the peanut shell powder experiment)
Rhodococcus sp. As-2626D, *Serratia plymuthica* As-2819D, *Bacillus vallismortis* B-1101, and *Exiguobacterium mexicanum* B-l 1011 [81]	4-10 °C	10 5	Biodegradation degree of 44-62 and 34-46 %
"MikroBak" biological product (a consortium of bacteria of the genera *Rhodococcus* and *Pseudomonas*) [80]	June-August, oil-contaminated soils on the territory of the Pogranichnoye field of Yamalo-Nenets Autonomous Okrug	–	Purification degree of 80 %

Conclusion. Contamination by crude oil and petroleum products is a global environmental problem. Various methods have been developed aimed at restoring contaminated environments. Biological ones (bioremediation) are the most promising but they are used rarely and mainly for post-treatment processes.

The main methods of bioremediation, most often used, include *ex-situ* methods (use of bioreactors, composting, etc.), *in-situ* (biostimulation, bioaugmentation, bioventing, phytoremediation, etc.). When working with oil-destructing microorganisms (microbiological remediation), combinations of these methods are most often used.

During *in-situ* bioremediation, various types of sorbent materials, both natural and synthetic, are used to introduce strains of microorganisms to contaminated areas: wood chips (sawdust), husks, activated carbon, sapropel, glauconite, and zeolite. The greatest efficiency is shown in works using activated carbon. Natural carriers are also promising, since, in addition to performing the main function (sorption of microorganisms), they improve the physico-mechanical and physico-chemical properties of the soil.

An increase in the efficiency of microbiological remediation of contaminated soils is also achieved by introducing nutrients (nitrogen, phosphorus, sulfur, and oxygen) into the soil as part of a combined bio-based product or separately. Complex mineral fertilizers are applied to stimulate the vital processes of native soil microorganisms.

The strains of microorganisms used in microbiological remediation of oil-contaminated soils can be divided into three groups depending on the ambient temperature optimal for their vital activity: psychrophiles (t_{opt} = 10-20 °C); psychrotrophs (t_{opt} = 20-28 °C); mesophiles (t_{opt} = 37 °C); and thermophiles (t_{opt} = 42 °C). This feature of the strains must be taken into account, since highly effective thermophilic microorganisms may be unsuitable for bioremediation in the conditions of the Far North.

A number of bio-based products have been developed for the restoration of oil-contaminated soils with proven effectiveness (“Putidoil”, “Ecoil”, “Valentis”, “AVALON”, etc.). They include consortia of oil-destructing microorganisms and auxiliary substances (nitrogen, phosphorus, etc.). Strains can be placed on a sorbing material (substrates, granules, and chips). More than 70 species of bacteria (*Pseudomonas spp*., *Rhodococcus spp*., *Acinetobacter spp*., *Microbacterium spp*., etc.), at least 100 species of microscopic fungi (*Chrysosporium spp*., *Phanerochaete spp*., *Aspergillus spp*., *Acremonium spp*., *Penicillium spp*., etc.), and some types of microscopic algae (*Chlorella spp*., *Scenedesmus spp*., *Chlamydomonas spp*., etc.) are capable of oil destruction. Modern research is devoted to the study of the prospects for the use of individual strains, genera, and types of microorganisms in various conditions with different concentrations of petroleum products in the soil. Strains isolated from historically contaminated territories and prospects for their use are also being investigated. Particular attention is paid to the problem of cleaning oil-contaminated soils in the Far North, where climatic conditions limit the use of bioremediation methods. However, strains have been found capable of performing their functions with sufficient efficiency under these conditions.

A detailed study, improvement of the technology of microbiological bioremediation and the search for effective natural strains or the creation using genetic methods of new, more efficient, and less demanding to ambient conditions, strains of hydrocarbon-oxidizing microorganisms will fully realize the potential of this technology.

REFERENCES

1. Nikonov A.N., Potapova S.O. The Oil Industry is one of the Major Environmental Contaminants. *Pozharnaya bezopasnost: problemy i perspektivy*. 2018. Vol. 1. N 9, p. 666-673 (in Russian).

2. Korshunova T.Yu., Loginov O.N. Oil Sludge: Conditions of the Problem in the Russian Federation and Methods to Reduce Their Negative Influence on the Environment. *Ecobiotech*. 2019. Vol. 2. N 1, p. 75-85 (in Russian). DOI: 10.31163/2618-964X-2019-2-1-75-85

3. Pashkevich M.A., Bykova M.V. Methodology for thermal desorption treatment of local soil pollution by oil products at the facilities of the mineral resource industry. *Journal of Mining Institute*. 2022. Vol. 253, p. 49-60. DOI: 10.31897/PMI.2022.6

4. Tumanyan A.F., Tyutyuma N.V., Bondarenko A.N., Shcherbakova N.A. Influence of oil pollution on various types of soil. *Chemistry and Technology of fuels and oils*. 2017. Vol. 53. N 3, p. 369-376. DOI: 10.1007/s10553-017-0813-7

5. Vasilyeva G., Kondrashina V., Ortega-Calvo J.-J. Adsorptive bioremediation of soil highly contaminated with crude oil. *Science of the Total Environment*. 2020. Vol. 706. N 135739. DOI: 10.1016/j.scitotenv.2019.135739

6. Ushakov I.E. Detection of floods of oil products in the sea radar-tracking means. *Journal of Mining Institute*. 2016. Vol. 219, p. 421-427. DOI: 10.18454/PMI.2016.3.421

7. Lianwen Liu, Wei Li, Weiping Song, Mingxin Guo. Remediation techniques for heavy metalcontaminated soils: principles and applicability. *Science of the Total Environment*. 2018. Vol. 633, p. 206-219. DOI: 10.1016/j.scitotenv.2018.03.161

8. Khaustov A.P., Redina M.M. Transformations of Oil Damages in Geological Environment under the Effect of Liquid Substance. *Neft. Gaz. Novatsii*. 2013. N 10, p. 22-30 (in Russian).

9. Lamichhane S., Krishna K.C.B., Sarukkalige R. Surfactant-enhanced remediation of polycyclic aromatic hydrocarbons: a review. *Journal of Environ. Manag*. 2017. Vol. 199, p. 46-61. DOI: 10.1016/j.jenvman.2017.05.037

10. Sarkova O.M., Krasnopolskii V.G. Practical guide for oil spill response volunteers. URL: https://wwf.ru/resources/ publications/booklets/prakticheskoe-posobie-dlya-dobrovoltsev-po-likvidatsii-razlivov-nefti/ (accessed 01.04.2022) (in Russian).

11. Sagitov R.F., Shabanova S.V., Vasilewskaya S.P. et al. Lassification of Methods Localization and Liquidation of Oil-Contaminated Soil and Oil Products. *Nauka i Sovremennost*. 2016. N 1, p. 202-207 (in Russian). DOI: 10.17117/ns.2016.01.202

12. Shamak D.N. Methods for eliminating oil contamination. Tezisy dokladov IV Mezhdunarodnoi nauchno-prakticheskoi konferentsii "Ekologiya i zashchita okruzhayushchei sredy", 16-17 maya 2018, Minsk, Belarus. Belorusskii gosudarstvennyi universitet, 2018, p. 226-228 (in Russian).

13. Gaur N., Flora G., Yadav M., Tiwari A. A review with recent advancements on bioremediation-based abolition of heavy metals. *Environmental Science: Processes & Impacts*. 2014. Vol. 16. Iss. 2, p. 180-193. DOI: 10.1039/C3EM00491K

14. Kogan V.E. Inorganic and organic vitreous foam materials and prospect of environmental cleaning from oil and oil products pollutions. *Journal of Mining Institute*. 2016. Vol. 218, p. 331-338 (in Russian).

15. Petrova T.A., Rudzish E. Types of Soil Improvers for Reclamation of Mining-Disturbed Lands. *Mining Informational and Analytical Bulletin*. 2021. N 4, p. 100-112. DOI: 10.25018/0236_1493_2021_4_0_100

16. Petrova T.A., Rudzisha E., Alekseenko A.V. et al. Rehabilitation of Disturbed Lands with Industrial Wastewater Sludge. *Minerals*. 2022. Vol. 12. Iss. 3. N 376. DOI: 10.3390/ min12030376

17. Petrova T.A., Rudzisha E. Utilization of sewage sludge as an ameliorant for reclamation of technogenically disturbed lands. *Journal of Mining Institute*. 2021. Vol. 251, p. 767-776. DOI: 10.31897/PMI.2021.5.16

18. Sobgayda N. Sorption materials for waste and natural waters clearing from oil products. *Bulletin of the Kharkiv National Automobile and Road University*. 2011. N 52, p. 120-124 (in Russian).

19. Lekan Taofeek Popoola, Adeyinka Sikiru Yusuff. Optimization and characterization of crude oil contaminated soil bioremediation using bacteria isolates: Plant growth effect. *South African Journal of Chemical Engineering*. 2021. Vol. 37, p. 206-213. DOI: 10.1016/j.sajce.2021.06.004

20. Farag S., Soliman N.A., Abdel-Fattah Y.R. Statistical optimization of crude oil biodegradation by a local marine bacterium isolate Pseudomonas sp. sp48. *Journal of Genetic Engineering and Biotechnology*. 2018. Vol. 16. Iss. 2, p. 409-420. DOI: 10.1016/j.jgeb.2018.01.001

21. Myazin V.A., Isakova E.A., Vasilyeva G.K. The Effect of Activated Carbon on the Bioremediation Rate of the Soils Historically Contaminated With Oil Products in the Murmansk Region. *Regional Environmental Issues*. 2020. N 2, p. 20-26 (in Russian). DOI: 10.24411/1728-323X-2020-12020

22. Finley S.D., Broadbelt L.J., Hatzimanikatis V. In silico feasibility of novel biodegradation pathways for 1, 2, 4-trichlorobenzene. *BMC Systems Biology*. 2010. Vol. 4. N 7. DOI: 10.1186/1752-0509-4-7

23. Kumar R., Kaur A. Oil spill removal by mycoremediation. *Microbial Action on Hydrocarbons*. 2018, p. 505-526. DOI: 10.1007/978-981-13-1840-5_20

24. Steliga T. Role of fungi in biodegradation of petroleum hydrocarbons in drill waste. *Polish Journal of Environmental Studies*. 2012. Vol. 2. Iss. 2, p. 471-479.

25. Bulatov V., Igenbaeva N., Nanishvili O. Oil and Gas Complex Waste Products as Technological Indicator of Geoecological Condition of Russia Regions. *Bulletin of Science and Practice*. 2021. Vol. 7. N 8, p. 46-55 (in Russian). DOI: 10.33619/2414-2948/69/05

26. Zhang S., Gedalanga P.B., Mahendra S. Advances in bioremediation of 1,4-dioxane-contaminated waters. *Journal of Environmental Management*. 2017. Vol. 204. Part 2, p. 765-774. DOI: 10.1016/j.jenvman.2017.05.033

27. Quintella C.M., Mata A.M.T., Lima L.C.P. Overview of bioremediation with technology assessment and emphasis on fungal bioremediation of oil contaminated soils. *Journal of Environmental Management*. Vol. 241, p. 156-166. DOI: 10.1016/j.jenvman.2019.04.019

28. Taki G., Islam M.N., Park Seong-Jae, Park Jeong-Hun. Optimization of operating parameters to remove and recover crude oil from contaminated soil using subcritical water extraction process. *Environmental Engineering Research*. 2018. Vol. 23. Iss. 2, p. 175-180. DOI: 10.4491/eer.2017.145

29. Dhiraj Kumar Chaudhary, Jaisoo Kim. New insights into bioremediation strategies for oil-contaminated soil in cold environments. *International Biodeterioration & Biodegradation*. 2019. Vol. 142, p. 58-72. DOI: 10.1016/j.ibiod.2019.05.001

30. Ajona M., Vasanthi P. Bioremediation of petroleum contaminated soils – A review. *Materials Today: Proceedings*. 2021. Vol. 45. Part 7, p. 7117-7122. DOI: 10.1016/j.matpr.2021.01.949

31. Sivaraman C., Ganguly A., Nikolausz M., Mutnuri S. Isolation of hydrocarbonoclastic bacteria from bilge oil contaminated water. *International Journal of Environmental Science & Technology*. 2011. Vol. 8, p. 461-470. DOI: 10.1007/BF03326232

32. Azubuike C.C., Chikere C.B., Okpokwasili G.C. Bioremediation techniques-classification based on site of application: principles, advantages, limitations and prospects. *International Biodeterioration & Biodegradation*. 2016. Vol. 32, p. 58-72. DOI: 10.1007/s11274-016-2137-x

33. Dias R.L., Ruberto L., Calabró A. et al. Hydrocarbon removal and bacterial community structure in on-site biostimulated biopile systems designed for bioremediation of diesel-contaminated Antarctic soil. *Polar Biology*. 2014. Vol. 38, p. 677-687. DOI: 10.1007/s00300-014-1630-7

34. Firmino P.I.M., Farias R.S., Barros A.N. et al. Understanding the anaerobic BTEX removal in continuous-flow bioreactors for ex situ bioremediation purposes. *Chemical Engineering Journal*. 2015. Vol. 281, p. 272-280. DOI: 10.1016/j.cej.2015.06.106

35. Saum L., Jiménez M.B., Crowley D. Influence of biochar and compost on phytoremediation of oil-contaminated soil. *International Journal of Phytoremediation*. 2017. Vol. 20. Iss. 1, p. 54-60. DOI: 10.1080/15226514.2017.1337063

36. Seung-Woo Jeong, Jongshin Jeong, Jaisoo Kim. Simple surface foam application enhances bioremediation of oil-contaminated soil in cold conditions. *Journal of Hazardous Materials*. 2015. Vol. 286, p. 164-170. DOI: 10.1016/j.jhazmat.2014.12.058

37. Höhener P., Ponsin V. In situ vadose zone bioremediation. *Current opinion in biotechnology*. 2014. Vol. 27, p. 1-7. DOI: 10.1016/j.copbio.2013.08.018

38. Guarino C., Spada V., Sciarrillo R. Assessment of three approaches of bioremediation (Natural Attenuation, Landfarming and Bioagumentation – Assistited Landfarming) for a petroleum hydrocarbons contaminated soil. *Chemosphere*. 2017. Vol. 170, p. 10-16. DOI: 10.1016/j.chemosphere.2016.11

39. Ikeura H., Kawasaki Y., Kaimi E. et al. Screening of plants for phytoremediation of oil-contaminated soil. *International Journal of Phytoremediation*. 2015. Vol. 18. Iss. 5, p. 460-466. DOI: 10.1080/15226514.2015.1115957

40. Adams G.O., Tawari-Fufeyin P., Okoro S.E. et al. Bioremediation, biostimulation and bioaugmentation: a review. *International Journal of Environmental Bioremediation & Biodegradation*. 2015. Vol. 3. N 1, p. 28-39. DOI: 10.12691/ijebb-3-1-5

41. Malavenda R., Rizzo C., Michaud L. et al. Biosurfactant production by Arctic and Antarctic bacteria growing on hydrocarbons. *Polar Biology*. 2015. Vol. 38, p. 1565-1574. DOI: 10.1007/s00300-015-1717-9

42. Xingjian Xu, Wenming Liu, Shuhua Tian et al. Petroleum hydrocarbon-degrading bacteria for the remediation of oil pollution under aerobic conditions: a perspective analysis. *Frontiers in microbiology*. 2018. Vol. 9. N 2885. DOI: 10.3389/fmicb.2018.02885

43. Kuyukina M.S., Ivshina I.B. Bioremediation of contaminated environments using *Rhodococcus*. Biology of *Rhodococcus*. Cham: Springer, 2019, p. 231-270. DOI: 10.1007/978-3-030-11461-9_9

44. Al-Nasrawi H. Biodegradation of crude oil by fungi isolated from Gulf of Mexico. *Journal of Bioremediation and Biodegradation*. 2012. Vol. 3. Iss. 4. N 1000147. DOI: 10.4172/2155-6199.1000147

45. Chaporgina A.A., Korneykova M.V., Fokina N.V. The Destructive Activity of Hydrocarbon-Oxidizing Micromycetes Isolatedfrom Soils of the Kola Peninsula. *Mycology and Phytopathology*. 2019. Vol. 53. N 1, p. 36-45 (in Russian). DOI: 10.1134/s0026364819010057

46. Isakova E.A., Korneikova M.V. Destructive activity of hydrocarbon-oxidizing micromycetes isolated from substrates of the coastal territories of the Barents and White Seas. *Vestnik Murmanskogo gosudarstvennogo tekhnicheskogo universiteta*. 2021. Vol. 24. N 2, p. 178-189 (in Russian). DOI: 10.21443/1560-9278-2021-24-2-178-189

47. Korchagina Yu.S., Shchemelinina T.N. Patent N RU2764305. Method for purifying soils from petroleum contamination by the method of hydroseeding a biological mixture using microalgae *Chlorella vulgaris globosa* IPPAS C-2024. Publ. 17.01.2022. Bul. N 2 (in Russian).

48. Shchemelinina T.N., Anchugova E.M. Patent N RU2703500. Oil-oxidizing biopreparation, biosorbent based on it and method for its preparation. Publ.17.10.2019. Bul. N 29 (in Russian).

49. Hwanhwi Lee, Seo Yeong Yun, Seokyoon Jang et al. Bioremediation of polycyclic aromatic hydrocarbons in creosote-contaminated soil by *Peniophora incarnata* KUC8836. *Bioremediation Journal*. 2015. Vol. 19. Iss. 1, p. 1-8. DOI: 10.1080/10889868.2014.939136

50. Hesnawi R.M., Adbeib M.M. Effect of nutrient source on indigenous biodegradation of diesel fuel contaminated soil. *APCBEE Procedia*. 2013. Vol. 5, p. 557-561. DOI: 10.1016/j.apcbee.2013.05.093

51. Santos H.F., Carmo F.L., Paes J.E.S. et al. Bioremediation of mangroves impacted by petroleum. *Water Air Soil Pollut*. 2011. Vol. 216, p. 329-350. DOI: 10.1007/s11270-010-0536-4

52. Doneryan L.G., Vodyanova M.A., Tarasova Zh.E. Microscopic Soil Fungi – Bioindicators Organisms Contaminated Soil. *Hygiene and Sanitation, Russian Journal*. 2016. Vol. 95. N 9, p. 891-894 (in Russian). DOI: 10.1882/0016-9900-2016-9-891-894

53. Leitão A.L. Potential of Penicillium species in the bioremediation field. *International Journal of Environmental Research and Public Health*. 2009. Vol. 6. Iss. 4, p. 1393-1417. DOI: 10.3390/ijerph6041393

54. Maamar A., Lucchesi M.-E., Debaets S., Nguyen van Long N. et al. Highlighting the crude oil bioremediation potential of marine fungi isolated from the port of Oran (Algeria). *Diversity*. 2020. Vol. 12. Iss. 5. N 196. DOI: 10.3390/d12050196

55. Raghukumar S. Fungi in coastal and oceanic marine ecosystems. Cham: Springer, 2017, p. 378. DOI: 10.1007/978-3-319-54304-8

56. Zvolinskii V.P., Batovskaya E.K., Tumanyan A.F. The influence of oil contamination on the microbiological activity of soils. *Teoreticheskie i prikladnye problemy agropromyshlennogo kompleksa*. 2010. N 4, p. 39-44 (in Russian).

57. Shapiro T.N., Dolnikova G.A., Nemtseva N.V. Identification and Physiological Characterization of a Consortium of Hydrocarbon-Oxidizing Bacteria of Oil and Oil Products. *Journal of microbiology, epidemiology and immunobiology*. 2018. N 4, p. 107-113. DOI: 10.36233/0372-9311-2018-4-107-113

58. Bukharin O.V., Gogoleva O.A., Nemtseva N.V. Patent N RU2396340. *Gordona terrae* VKPM As-1741 strain for decomposing petroleum and petroleum products. Publ. 27.02.2009 (in Russian).

59. Frank Yu.A., Nikitchuk K.L., Sapega A.A. et al. Improvement of the Efficiency of Oil-Contamined Soils Remediation in the Natural Conditions of the North Tomsk Region and the Nearby Regions by Indigenous Microorganisms Application. *Bulletin of the Tomsk polytechnic university. Geo assets engineering*. 2020. Vol. 331. N 9, p. 130-139 (in Russian). DOI: 10.18799/24131830/2020/9/2815

60. Erofeevskaya L.A. Patent N RU2687131. Strain of the *Micrococcus luteus* VKM As-2627d bacteria – oil and oil products decomposer. Publ. 07.05.2019. Bul. N 13 (in Russian).

61. Neustroev M.P., Tarabukina N.P., Neustroev M.M. et al. Patent N RU2446900. Method of cleaning out of frozen soil from crude oil by spore-forming bacteria *Bacillus subtilis*. Publ. 10.04.2012 (in Russian).

62. Gamzaeva R.S. Application of the Bak-Verad biodestructor on soddy-podzolic soil contaminated with oil products. *Izvestiya Sankt-Peterburgskogo gosudarstvennogo agrarnogo universiteta*. 2019. N 55, p. 38-45 (in Russian). DOI: 10.24411/2078-1318-2019-12038

63. Ramadass K., Megharaj M., Venkateswarlu K., Naidu R. Soil bacterial strains with heavy metal resistance and high potential in degrading diesel oil and n-alkanes. *International Journal of Environmental Science and Technology*. 2016. Vol. 13, p. 2863-2874. DOI: 10.1007/s13762-016-1113-1

64. Ramadass K., Megharaj M., Venkateswarlu K., Naidu R. Bioavailability of weathered hydrocarbons in engine oil-contaminated soil: Impact of bioaugmentation mediated by *Pseudomonas spp*. on bioremediation. *Science of the Total Environment*. 2018. Vol. 636, p. 968-974. DOI: 10.1016/j.scitotenv.2018.04.379

65. Chaporgina A.A., Korneykova M.V. Evaluation of the Microorganisms Consortium Efficiency to Cleaning Soils Contaminated by Oil Products in the Kola North Conditions. *Theoretical and Applied Ecology*. 2020. N 2, p. 136-142 (in Russian). DOI: 10.25750/1995-4301-2020-2-136-142

66. Zinnatshina L.V., Strizhakova E.R., Danshina A.V., Vasileva G.K. Influence of sorbents on the rate of bioremediation and properties of soil contaminated with a mixture of petroleum products. *Natural and Engineering Sciences*. 2018. N 9 (123), p. 24-30 (in Russian).

67. Slyusarevskiy A.V., Zinnatshina L.V., Vasilyeva G.K. Comparative environmental and economic analysis of methods for the remediation of oil-contaminated soils by in situ bioremediation and mechanical soil replacement. *Ecology and Industry of Russia*. 2018. Vol. 22. N 11, p. 40-45 (in Russian). DOI: 10.18412/1816-0395-2018-11-40-45

68. Igun O.T., Meynet P., Davenport R.J., Werner D. Impacts of activated carbon amendments, added from the start or after five months, on the microbiology and outcomes of crude oil bioremediation in soil. *International Biodeterioration & Biodegradation*. 2019. Vol. 142, p. 1-10. DOI: 10.1016/j.ibiod.2019.04.008

69. Nikulina A.R. Research of the Ability of Oil Destructive Bacteria to Recover Oil-Polluted Soil. *Nauka bez granits*. 2019. N 7 (35), p. 125-128.

70. Volkov M.Yu., Ilin A.A., Kalilets A.A. Patent N RU2571219. Preparation for biodegradation of petroleum products “Bioionit” and method of obtaining thereof. Publ. 20.12.2015. Bul. N 35 (in Russian).

71. Erofeevskaya L.A., Glyaznetsova Yu.S. Patent N RU2565549. Biopreparation for bioremediation of oil-contaminated soils for climatic conditions of Far North. Publ. 20.10.2015. Bul. N 29 (in Russian).

72. Partovinia A., Rasekh B. Review of the immobilized microbial cell systems for bioremediation of petroleum hydrocarbons polluted environments. *Critical Reviews in Environmental Science and Technology*. 2018. Vol. 48. Iss. 7-9, p. 723-771. DOI: 10.1080/10643389.2018.1439652

73. Majul L., Wirth S., Levin L. High dye removal capacity of *Peniophora laxitexta* immobilized in a combined support based on polyurethane foam and lignocellulosic substrates. *Environmental Technology*. 2022. Vol. 43. Iss. 5, p. 684-695. DOI: 10.1080/09593330.2020.1801851

74. Yaohui Xu, Mang Lu. Bioremediation of crude oil-contaminated soil: Comparison of different biostimulation and bioaugmentation treatments. *Journal of Hazardous Materials*. 2010. Vol. 183. Iss. 1-3, p. 395-401. DOI: 10.1016/j.jhazmat.2010.07.038

75. Alvim G.M., Pontes P.P. Aeration and sawdust application effects as structural material in the bioremediation of clayey acid soils contaminated with diesel oil. *International Soil and Water Conservation Research*. 2018. Vol. 6. Iss. 3, p. 253-260. DOI: 10.1016/j.iswcr.2018.04.002

76. Das N., Chandran P. Microbial Degradation of Petroleum Hydrocarbon Contaminants: An Overview. *Biotechnology Research International*. 2011. Vol. 2011. N 941810. DOI: 10.4061/2011/941810

77. Ivshina I.B., Kuyukina M.S., Krivoruchko A.V. et al. Oil spill problems and sustainable response strategies through new technologies. *Environmental Science: Processes & Impacts*. 2015. Vol. 17. Iss. 7, p. 1201-1219. DOI: 10.1039/c5em00070j

78. Alkorta I., Epelde L., Garbisu C. Environmental parameters altered by climate change affect the activity of soil microorganisms involved in bioremediation. *FEMS microbiology letters*. 2017. Vol. 364. Iss. 19. DOI: 10.1093/femsle/fnx200

79. Sivtsev S.I., Erofeevskaya L.A. Sanation and reclamation of oil-contaminated lands in the soil and climatic conditions of the Republic of Sakha (Yakutia). Vysshaya shkola: nauchnye issledovaniya. Part 2. Ufa: Infinity, 2019, p. 125-131 (in Russian).

80. Filonov A.E. Microbial biopreparations for cleaning the environment from oil contamination in temperate and cold climates: Avtoref. dis. … d-ra biol. nauk. Pushchino: Institut biokhimii i fiziologii mikroorganizmov im. G.K.Skryabina RAN, 2016, p.46 (in Russian).

81. Erofeevskaya L.A. Development of a method for cleaning permafrost soils and soils from oil contamination in the natural climatic conditions of Yakutia: Avtoref. dis. … kand. biol. nauk. Yakutsk: Institut problem nefti i gaza Yakutskogo nauchnogo tsentra Sibirskogo otdeleniya RAN, 2018, p. 28 (in Russian).

82. Smolova O.S. Bioremediation of soils contaminated with hydrocarbons using psychrotolerant microorganisms with mycostatic activity: Avtoref. dis. … kand. biol. nauk. Ufa: Vserossiiskii nauchno-issledovatel'skii i tekhnologicheskii institut biologicheskoi promyshlennosti, 2015, p. 24 (in Russian).

***Authors*: Irina D. Sozina,** *Environmental Engineer*, *sozina.id@gmail.com*, *https://orcid.org/0000-0001-5521-862X* (*AO Novaya Aviatsiya*, *Saint Petersburg*, *Russia*; *Saint Petersburg Mining University*, *Saint Petersburg*, *Russia*), **Aleksandr S. Danilov,** *Candidate of Engineering Sciences*, *Associate Professor*, *https://orcid.org/0000-0003-2108-2781* (*Saint Petersburg Mining University*, *Saint Petersburg*, *Russia*).

The authors declare no conflict of interests.

ISSN 2411-3336; e-ISSN 2541-9404

JOURNAL OF MINING INSTITUTE

Zapiski Gornogo instituta

Journal homepage: pmi.spmi.ru

Research article

Use of clay-containing waste as pozzolanic additives

Andrei M. GERASIMOV[1] ✉, **Ivan D. USTINOV**[2], **Olga V. ZYRYANOVA**[1]
[1] *Saint Petersburg Mining University, Saint Petersburg, Russia*
[2] *NPK "Mekhanobr-tekhnika" (AO), Saint Petersburg, Russia*

***How to cite this article*:** Gerasimov A.M., Ustinov I.D., Zyryanova O.V. Use of clay-containing waste as pozzolanic additives. Journal of Mining Institute. 2023. Vol. 260, p. 313-320. DOI: 10.31897/PMI.2023.33

Abstract. Growing productivity of mining and processing enterprises entails an increase in the volumes of liquid tailings impoundments and upstream impoundments of ore processing waste. Enterprises face the challenge of minimizing the environmental impact of waste and guaranteeing the sanitary and epidemiological safety of population. The article presents a possibility of recycling one type of such waste (clay-containing concentration tailings of apatite-nepheline and sylvinite ores, coal beneficiation tailings) by using them after preliminary thermochemical treatment as pozzolanic additives to cements and concretes, including concrete mixtures used for soil stabilization, development of territories, reclamation of mine workings, as a component of the insulating layer of landfills for the disposal of municipal solid waste. An analysis of the phase changes of kaolinite, one of the main minerals that make up clay-containing waste, in the temperature range of 200-1,000 °C showed that a change in its mineral form during heat treatment is the main factor in changing its pozzolanic activity. The effect of heat treatment of clay minerals at temperature of 700-800 °C on their pozzolanic activity, estimated by the ability to absorb calcium hydroxide (0.7 g $Ca(OH)_2$ per 1 g of modified kaolinite), is considered. It is shown that the addition of heat-treated samples (20 % by weight) improves the quality of cement increasing its activity by 15 %, in comparison with the use of unmodified clay minerals. It was proved experimentally that partial replacement of Portland cement with thermally modified kaolinite increases the strength of consolidating stowing mixture by up to 15 %. This approach to processing of ores containing layered silicates, which provides for thermochemical modification of run-of-mine ore, intensifies the processes of tailings thickening and filtering.

***Keywords*:** clay-containing waste; pozzolanic additives; pozzolanic activity; heat treatment; kaolinite; metakaolin; stowing mixtures

Received: 24.10.2022 ***Accepted: 02.03.2023*** ***Online: 10.04.2023*** ***Published: 25.04.2023***

Introduction. A significant part of all minerals extracted from the Earth (coal, oil, salts, iron, manganese and aluminium ores, gold and platinum placers, phosphorites, non-metallic building materials, etc.) is enclosed in sedimentary rocks. Clay minerals (clays, mudstones, etc.) predominate among sedimentary rocks, the content of which is up to 50 %.

Many mineral deposits are associated with the presence (as waste rock in them) of clays, mudstones, clay shales composed of layered silicates, highly hydrophilic mineral varieties, which can swell in water. This ability to self-disperse causes great difficulties both in the extraction and processing of such ores. Concentration tailings of ores and coals containing clay minerals create serious problems during storage and disposal, which are exacerbated by process water rotation, since swelling layered silicates (clay minerals) significantly complicate the compaction and dehydration of tailings suspensions.

Water became the scarcest resource at beneficiation plants, and a ubiquitous implementation of intra-factory process water rotation became a necessity. To organize it, it is necessary to achieve the maximum separation of the liquid phase from the solid phase of tailings, for which thickening and filtration operations are used. After these process operations, the mineral part is obtained with a minimum amount of water. Further, from the dehydrated mineral part, valuable products can be obtained that are used in different industries: construction, production of sorbents and refractory materials.

Presence of clay minerals that can retain water reduces the efficiency of these operations, which leads to a decrease in the volume of process water entering the water rotation system. Ways to reduce water content are considered in [1, 2]. In this article, the use of dried ore tailings containing clay minerals is considered.

Among the trends of recycling tailings containing clay minerals, their use as pozzolanic additives to cements (a mineral additive with the ability to bind $Ca(OH)_2$ into stable hydrated forms) [3-5], and as a raw material to produce geopolymers is obvious [6-9]. Production of zeolites is one of the trends for recycling the concentration tailings [10].

Given the large formation volume of the ore concentration tailings containing layered silicates, their recycling is possible only in industries that also have a significant volume [11, 12]. In this regard, the cement industry and production of cement concretes are of greatest interest [13-15].

In the production of cement clinker a lot of fuel is consumed and a significant amount of carbon dioxide is released. Reduction of the share of clinker component and as a consequence minimization of these negative factors is possible due to the use of active mineral additives of natural and artificial origin [16-18].

Thermally activated clays are artificial pozzolans and are regulated by the European standard EN 197-1-2000 and the interstate standard GOST 24211-2008. From ancient times to the present, both natural and technogenic clay minerals were used as additives to cement materials. Pozzolanic activity of thermally activated clays in cement-lime composites depends on the degree of dehydration and chemical transformation of individual minerals during heat treatment [19-21].

In the course of heat treatment of clay minerals, new characteristics are acquired. After thermal activation of kaolinite its pozzolanic activity is much higher in comparison with other clay minerals, which is determined by the structure of kaolinite, in which the elementary package consists of two layers: silicon-oxygen tetrahedral and aluminium-oxygen octahedral having oxygen atoms [22-24].

Kaolinite is not a pozzolanic active additive; its activation (thermal) is required. It can be used as microfiller in Portland cement (in small quantities) due to its high dispersion. Kaolinite can accelerate the hydration of cement, increase compressive and flexural strength, reduce permeability, increase frost resistance, and reduce porosity.

During heat treatment of kaolinite in the range of 400-600 °C, dehydroxylation of the structure, amorphization, and the appearance of aluminium ions in coordination 5 after oxygen occur; this is what causes a high pozzolanic activity of the forming product, metakaolin [25].

In the process of dehydration of clay minerals in the range of 300-900 °C, crystallization water is removed from clay minerals (depending on the mineral variety) until the crystals are completely destroyed and the first eutectics and crystalline neoformations begin to form from the mixture of their oxides. At a temperature of 200 °C, clay activation can start before sintering begins. Different clay minerals have different temperature ranges characteristic of endothermic peaks. Polymineral clays, due to this, have much wider ranges than the monomineral form [26-28].

Methodology. In the previous studies, the authors [29] investigated the effect of different types of heating on silicate minerals: montmorillonite, illite, kaolinite, talc, as well as framework silicate – quartz, as an essential mineral of sedimentary clay rocks characterized by the minimal effect of water on its structural changes.

In this article, kaolinite obtained by beneficiation of kaolin ore from the Troshkovsky deposit is considered, which at heat treatment (convective; hydrothermal; in high-frequency currents; and combined) can change the mineral composition. To compare the thermal effect on clay minerals, montmorillonite was chosen, in which only dehydration occurs during heat treatment. Chemical composition of the materials used is given in Table 1.

Table 1

Chemical composition of silicate minerals, %

Material	SiO_2	Al_2O_3	Fe_2O_3	TiO_2	CaO	Na_2O	K_2O	MgO	H_2O	LOI
Kaolinite	56.9	27.4	2.1	0.5	0.5	0.3	0.2	0.4	–	11.7
Montmorillonite	48.7	14.1	3.2	0.2	4.2	0.9	0.4	4.3	16.2	7.8
Kaolin tailings	78.9	13.3	0.5	0.2	0.4	0.3	0.2	0.6	–	5.6

In the study of samples conventional methods of analysis were applied. To determine the mass fraction of elements in the samples, an X-ray fluorescence spectrometer with a built-in diffractometer Thermo Fisher Scientific ARL 9900 WorkStation (SC Ecosystema) was used. Pozzolanic activity was determined by the Chapel method [30] from the absorption of $Ca(OH)_2$. Changes in specific surface area of the materials were monitored using a "PSKh-10a" device. Analysis of the structural phase transformations of the studied materials was accomplished by X-ray diffraction (XRD) using a Bruker D8 focus X-ray diffractometer with a Siemens 7000 diffractometer (USA) with Cu-Kα radiation (40 kV, 30 mA, $\lambda = 1.5406$ Å). Strength was determined according to GOST 22690-2015. As a secondary tool for determining changes in the structure of minerals, a "Thermoscan-2" device was used, which makes it possible to carry out thermal gravimetric analysis (TGA) and differential thermal analysis (DTA). The material was exposed to temperatures in the range of 25-1,000 °C at atmospheric air pressure. Heating rate was 10 °C/min.

There are several ways to determine pozzolanic activity of minerals. The article [30] considers two methods: determination of the activity index based on strength and measurement of the amount of calcium hydroxide absorbed by the pozzolanic additive (French standard NF P18-513: 2010). These two methods are compared on a sample of metakaolin, and the methods for determining pozzolanic activity give comparable results [31-34].

The experiment according to the Chapel method was as follows [30]: 1 g of metakaolin/kaolinite and 2 g of freshly calcined CaO are placed in a 500 ml clean dry Erlenmeyer flask, and 200 ml of distilled water are added. The flask is hermetically sealed, a Liebig refrigerator is inserted and placed on a laboratory electrically heated magnetic stirrer. The experiment runs for 16 hours at a temperature of 85 °C with constant stirring of the flask contents with a magnetic stirrer. After stirring, the flask is cooled to room temperature. Next, 250 ml of freshly prepared sucrose solution (60 g of sucrose is dissolved in 250 ml of water) is added and stirred with a magnetic stirrer for 15 min. The content of the flask is then filtered through an ashless filter. A similar (blank) experiment is carried out without metakaolin/kaolinite. An aliquot (25 ml) is taken from the stock solution with a calibrated pipette and titrated with a 0.1N HCl burette using phenolphthalein (2-3 drops) as an indicator. The volume of 0.1N HCl used for titration of 25 ml solution of an empty (blank) sample V_1 and the volume of 0.1N HCl used for titration of 25 ml of a solution obtained by reaction with metakaolin V_2 are determined. Next, the amount of $Ca(OH)_2$ absorbed by 1 g of metakaolin additive is calculated,

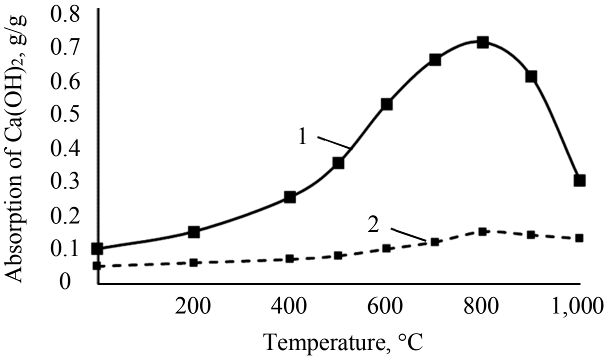

Fig.1. Effect of heat treatment on pozzolanic activity of kaolinite and montmorillonite
1 – kaolinite; 2 – montmorillonite

$$Q = 2\frac{V_1 - V_2}{V_1}\frac{74}{56}\cdot 1,000.$$

Discussion of results. A change in mineral form of kaolinite under thermal exposure affects its pozzolanic activity, which is estimated by the ability to absorb calcium hydroxide [35].

According to Fig.1, the growth of pozzolanic activity begins already at a material processing temperature of above 200 °C and reaches a maximum at a temperature of 800 °C; further, with increasing temperature, the pozzolanic activity of kaolinite decreases, which is associated with transition of metakaolin to mullite [36]. The process of calcium hydroxide absorption by heat-treated kaolinite requires a much longer time (from two hours). A comparative assessment of the effect of heat treatment of two minerals on the change in their activity showed that in the temperature range of 400-800 °C, an increase in pozzolanic activity is recorded only in kaolinite, while thermal effect on montmorillonite does not lead to any changes.

The results show that the change in the mineral form of kaolinite is the main factor of the change in its pozzolanic activity, and not the dehydration of clay, as reported in [37, 38].

During heat treatment of clays, the specific surface area (on the “PSKh-10a” device) of montmorillonite decreases due to its dehydration, while no changes are observed in kaolinite (Fig.2, *a*).

Analysis of weight loss of these minerals (Fig.2, *b*) suggests that phase composition of kaolinite changes in the temperature range of 400-600 °C, which correlates well with the data on differential thermal analysis (Fig.3).

For this analysis, two samples of kaolinite were used: initial (without heat treatment) and after convective heating at 550 °C. The choice of temperatures and type of heating are described in detail in the research [29], which states that the types of heating (convective; hydrothermal; in high-frequency currents; and combined) have the same effect on the change in phase composition of the mineral and differ only in the rate at which this effect is achieved. According to this indicator, preference was given to convective heating.

The original sample of mineral raw material (Fig.3, *a*) has an endothermic effect, the peak of which falls at 140 °C. This effect is associated with removal of physically bound water from

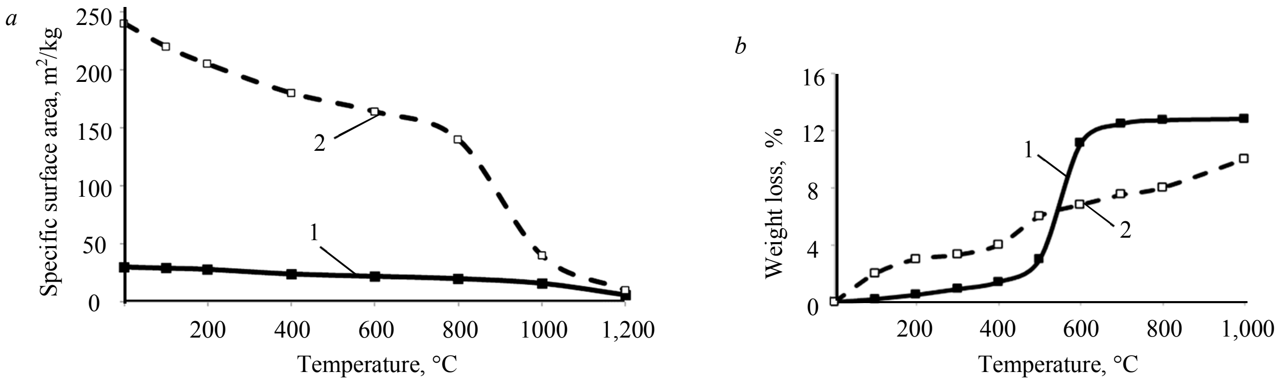

Fig.2. Effect of heat treatment on specific surface area (*a*) and dehydration (*b*) of kaolinite and montmorillonite
1 – kaolinite; 2 – montmorillonite

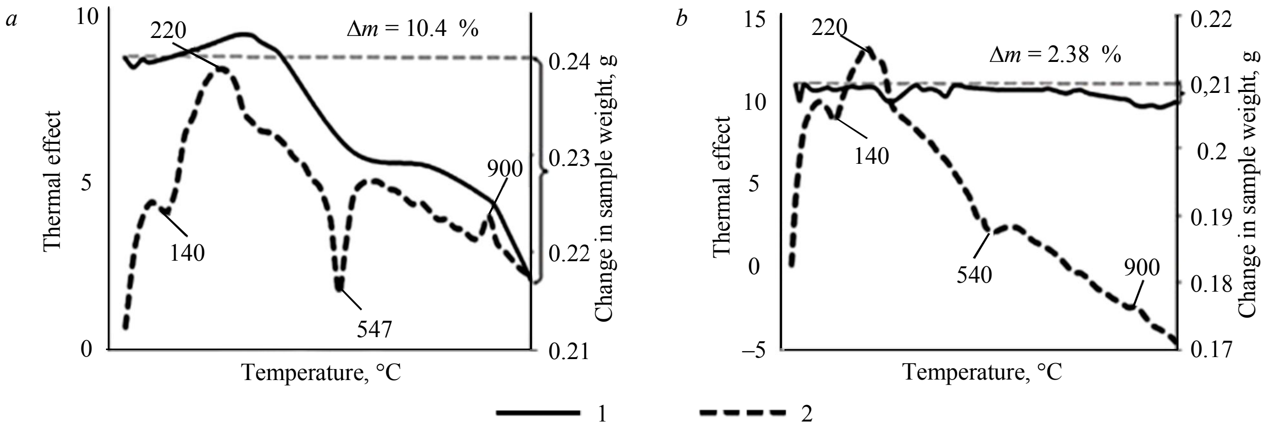

Fig.3. Differential thermal analysis of kaolinite samples: *a* – original sample; *b* – sample after heating (550 °C)
1 – weight loss; 2 – thermal impact

the channels and pores of the raw material with preservation of microstructure. The next endothermic effect peaks at 547 °C. This is the key effect, as it indicates a change in microstructure of the material and formation of metakaolin. The second endothermic peak of heat-treated material at 540 °C (Fig.3, *b*) is less intense than that of the original kaolinite. This indicates that kaolinite almost completely passed into another phase.

Data on the change in phase composition were determined by the X-ray diffraction method. During heat treatment kaolinite first transforms into metakaolin, which usually cannot be detected by the X-ray method [39]. XRD analysis showed that the height of kaolinite peak decreases after heat treatment (from 834 to 262 °C), and a new phase forms – dehydrated halloysite. Kaolinite and halloysite have a similar structure, but the latter has a certain amount of interlayer water (d = 9.5-10.2 Å). In the process of dehydration, the interplanar distance of halloysite decreases and becomes close to the value of kaolinite (d = 7.2 Å).

An increase in pozzolanic activity of kaolinite during heat treatment ensures its effect on the activity of Portland cement. It was shown in [38] that the maximum positive effect of the addition of thermally modified kaolinite is observed when its share in the binder is 20 %. Based on this, determination of the activity of the composite binder was performed on a mixture of kaolinite 20 % and cement of grade TsEM II/A-Sh 32.5N 80 %, with normal solution consistency. Kaolinite processed at different temperatures was added to the mixture. The best indicators of the activity of this binder were recorded after addition of kaolinite modified at 700 °C; the strength increased by 15 %.

In connection with a broader use of concentration tailings for backfilling the worked-out areas in mines and open pits, a possibility of using thermally modified kaolinite to replace part of Portland cement in stowing mixtures was tested. For this, the initial stowing mixture was prepared which contained 80 % of finely dispersed quartz (fineness modulus 1.5) and 20 % of binder – Portland cement. Thermally modified kaolinite was added to Portland cement, thus, the mixture contained 80 % quartz, 16 % Portland cement, 4 % kaolinite.

Studies have shown that partial replacement of Portland cement with thermally modified kaolinite increases the strength of the hardening stowing mixture by 20 % of initial compressive strength of 3.5 MPa. Partial replacement of the stowing mixture with heat-treated kaolinite gives another positive effect – disjoining pressure of the stowing mixture decreases, thus reducing the likelihood of its self-destruction when the mixture solidifies in the worked-out area. These results are confirmed by papers [35, 38] and are given in Table 2.

Table 2

Disjoining actions of stowing mixture of different composition [37]

Time, days	Disjoining pressure of mixtures, MPa		Time, days	Disjoining pressure of mixtures, MPa	
	Portland cement 100 %	Added kaolinite 20 %		Portland cement 100 %	Added kaolinite 20 %
25	0.00	0.00	200	3.50	2.30
50	1.50	1.10	250	3.60	2.40
100	2.70	1.85	350	3.60	2.50
150	3.25	2.10			

Coal tailings containing kaolinite are also of interest for use in stowing mixtures [40, 41]. For further research, beneficiation tailings of high-ash Vorkuta coals were used. The data on the effect of heat treatment of coal tailings containing 20 % kaolinite on the strength of Portland cement concrete after 28 days are presented (Table 3). Similar to other products based on kaolinite the maximum strength of concrete is recorded at a material processing temperature of 700 °C; the strength increases by 10 %.

The influence of heat treatment time of coal tailings on the modification degree was studied. It is shown that with an increase in processing time to 90 min, the strength of the mixture increases by 10-12 MPa.

Table 3

Effect of heat treatment time of coal tailings containing 20 % kaolinite on the strength of Portland cement concrete (tailings:cement 1:3) after 28 days

Time of heat treatment, min	Strength at heat treatment, MPa			Time of heat treatment, min	Strength at heat treatment, MPa		
	500 °C	600 °C	700 °C		500 °C	600 °C	700 °C
0	30.0	30.0	30.0	40	39.8	42.5	43.9
20	35.7	38.5	40.0	60	41.0	43.0	44.5
30	38.2	41.5	42.8	90	40.0	44.0	42.5

Thus, it can be concluded that preliminary thermal treatment of concentration tailings of various ores containing clay minerals makes it possible to use this type of raw material, for example, in the construction industry as an additive to cements, and to create conditions for their disposal as part of stowing mixtures.

Conclusion. As a result of studying the effect of thermal modification of clay-containing ores and coals before their beneficiation on the processes of dehydration and disposal of tailings, the following was ascertained:

- during heat treatment of kaolinite, the growth of pozzolanic activity begins already at a temperature above 200 °C and reaches a maximum at a temperature of 800 °C; further, with increasing temperature, pozzolanic activity of kaolinite decreases, which is associated with transition of metakaolin to mullite;
- change in mineral form of kaolinite is the main factor in changing its pozzolanic activity (rather than dehydration of clay, as previously presumed);
- heat treatment does not lead to a change in specific surface area of kaolinite;
- an increase in pozzolanic activity of kaolinite during heat treatment shows up in its effect on the strength of Portland cement concrete – the addition of heat-treated samples (20 % by weight) improves the quality of cement increasing its strength by 15 %;
- partial replacement of Portland cement with thermally modified kaolinite increases the strength of the hardening stowing mixture by 20 %; thermally activated kaolinite contained in tailings has a higher pozzolanic activity than kaolinite without activation, which allows to use the concentration tailings of thermally modified ores and coals (at 700-800 °C) as pozzolanic additives to cements and concretes.

The obtained results indicate that such an approach to the processing of ores containing layered silicates, which provides for thermochemical modification of run-of-mine ore, creates favourable prerequisites for using the concentration tailings of these ores as pozzolanic additives to cements and concretes. For example, they can be added to concrete mixtures used in soil stabilization; territory improvement; mine workings reclamation; and also as a component of insulating layer of municipal solid waste landfills.

The authors express their gratitude for the assistance in preparation of the material to the Chairman of the Board of Directors of NPK "Mekhanobr-tekhnika" (AO) Doctor of Engineering Sciences, Chief Researcher V.A.Arsentiev.

REFERENCES

1. Ehsani S.M., Unesi M., Tamartash R. Clay sedimentation and consolidation behavior in tailing storage facilities over mine lifetime. *Journal of Mining and Environment*. 2019. Vol. 10. N 1, p. 113-124. DOI: 10.22044/jme.2018.7165.1569
2. Islam S., Williams D.J., Liano-Serna M., Chenming Zhang. Settling, consolidation and shear strength behavior of coal tailings slurry. *International Journal of Mining Science and Technology*. 2020. Vol. 30. Iss. 6, p. 849-857. DOI: 10.1016/j.ijmst.2020.03.013
3. Javrujan H.S., Gaishun E.S., Mirina V.A. Innovative additives in the production of wall ceramics. *Engineering Journal of Don*. 2016. N 4, p. 2007-2016 (in Russian).
4. Kulikova M.A. Justification of the necessity of forming a protective screen for dumping waste dumps in the development fields. *Journal of Mining Institute*. 2013. Vol. 203, p. 185-189 (in Russian).
5. Arsentev V.A., Gerasimov A.M. Use of Clay-Containing Tailings in Geopolymer Production. *Tsvetnye metally*. 2021. N 11, p. 58-62 (in Russian). DOI: 10.17580/tsm.2021.11.08
6. Mifeng Gou, Longfei Zhou, Nathalene Wei Ying Then. Utilization of tailings in cement and concrete: A review. *Science and Engineering of Composite Materials*. 2019. Vol. 26. Iss. 1, p. 449-464. DOI: 10.1515/secm-2019-0029
7. Obenaus-Emler R., Illikainen M., Falah M. Geopolymers from mining tailings for more sustainable raw material supply. *MATEC Web of Conferences*. 2019. Vol. 274. N 05001. DOI: 10.1051/matecconf/201927405001
8. Paiva H., Yliniemi J., Illikainen M. Mine tailings geopolymers as a waste management solution for a more sustainable habitat. *Sustainability*. 2019. Vol. 11. Iss. 4. N 995. DOI: 10.3390/su11040995
9. Feng Rao, Qi Liu. Geopolymerization and its potential application in mine tailings consolidation: A review. *Mineral Processing and Extractive Metallurgy Review*. 2015. Vol. 36. Iss. 6, p. 399-409. DOI: 10.1080/08827508.2015.1055625
10. Hartati, Prasetyoko D., Santoso M. et al. A review on synthesis of kaolin-based zeolite and the effect of impurities. *Journal of the Chinese Chemical Society*. 2020. Vol. 67. Iss. 6, p. 911-936. DOI: 10.1002/jccs.201900047
11. Ermilova E.Yu., Kamalova Z.A., Rakhimov R.Z. The clay of Koschakovsky field of Tatarstan Republic as a component of hybrid additive to blended portland cement. *News of the Kazan State University of Architecture and Engineering*. 2015. N 4 (34), p. 259-263 (in Russian).
12. Rakhimov R.Z., Rakhimova N.R., Gaifullin A.R., Morozov V.P. Dehydration of clays of different mineral composition during calcination. *News of the Kazan State University of Architecture and Engineering*. 2016. N 4 (38), p. 388-394 (in Russian).
13. Shishakina O.A., Palamarchuk A.A. Technology Overview of Technology Waste Disposal in the Manufacture of Construction Materials. *International Journal of Applied and Fundamental Research*. 2019. N 4, p. 198-203 (in Russian).
14. Chukaeva M.A., Matveeva V.A., Sverchkov I.P. Complex processing of high-carbon ash and slag waste. *Journal of Mining Institute*. 2022. Vol. 253, p. 97-104. DOI: 10.31897/PMI.2022.5
15. Arsentev V.A., Marmandyan V.Z., Samukov A.D., Kabirov A.M. Innovate technologies in waste of extraction and nonmetallic raw materials processing. *Journal of Mining Institute*. 2012. Vol. 198, p. 219-222 (in Russian).
16. Lalomov D.A., Glazunov V.V. Collaborative interpretation of the data obtained by resistivity and ground penetrating radar methods for assessing the permeability of sandy clay soils. *Journal of Mining Institute*. 2018. Vol. 229, p. 3-12. DOI: 10.25515/PMI.2018.1.3
17. Litvinova T.E., Suchkov D.V. Comprehensive approach to the utilisation of technogenic waste from the mineral resource complex. *Mining informational and analytical bulletin*. 2022. Iss. 6-1, p. 331-348 (in Russian). DOI: 10.25018/0236_1493_2022_61_0_331
18. Danilov A.S., Matveeva V.A., Korelskiy D.S., Horttanainen M. Backfill of a Mined-Out Gold Ore Deposit with the Cemented Rubber-Cord and Waste Rock Paste: Environmental Changes in Aqueous Media. *Journal of Ecological Engineering*. 2021. Vol. 22. N 7, p. 190-203. DOI: 10.12911/22998993/138870
19. Klyuev S., Sevostyanov V., Sevostyanov M. et al. Improvement of technical means for recycling of technogenic waste to construction fiber. *Case Studies in Construction Materials*. 2022. Vol. 16. N e01071. DOI: 10.1016/j.cscm.2022.e01071
20. Zubkova O., Alexeev A., Polyanskiy A. et al. Complex Processing of Saponite Waste from a Diamond-Mining Enterprise. *Applied Sciences*. 2021. Vol. 11. Iss. 14. N 6615. DOI: 10.3390/app11146615
21. Kutepov Yu.I., Kutepova N.A., Vasileva A.D., Mukhina A.S. Engineering-geological and eco-logical concerns in operation and reclamation of high slope dumps at open-pit mines in Kuzbass. *Mining informational and analytical bulletin*. 2021. Iss. 8, p. 164-178 (in Russian). DOI: 10.25018/0236_1493_2021_8_0_164

22. Dubovikov O.A., Brichkin V.N. Directions and prospects of using low grade process fuel to produce alumina. *Journal of Mining Institute*. 2016. Vol. 220, p. 587-594.

23. Dubovikov O.A., Brichkin V.N., Ris A.D., Sundurov A.V. Thermochemical activation of hydrated aluminosilicates and its importance for alumina production. *Non-ferrous Metals*. 2018. N 2, p. 10-15. DOI: 10.17580/nfm.2018.02.02

24. Kotova O.B., Ustyugov V.A., Shiyong Sun, Ponaryadov A.V. Mullite production: phase trans-formations of kaolinite, thermodynamics of the process. *Journal of Mining Institute*. 2022. Vol. 254, p. 129-135. DOI: 10.31897/PMI.2022.43

25. Erasmus E. The influence of thermal treatment on properties of kaolin. *Hemijska industrija*. 2016. Vol. 70. Iss. 5, p. 595-601. DOI: 10.2298/HEMIND150720066E

26. Pashkevich M.A., Petrova T.A. Recyclability of Ore Beneficiation Wastes at the Lomonosov Deposit. *Journal of Ecological Engineering*. 2019. Vol. 20. Iss. 2, p. 27-33. DOI: 10.12911/22998993/94919

27. Kuznetsov V.S., Suprun I.K. Reduction of an Adverse Impact During Well Drilling by Means of Drilling Waste Usage. *Journal of Ecological Engineering*. 2017. Vol. 18. Iss. 2, p. 12-15. DOI: 10.12911/22998993/68211

28. Dashko R.E., Lokhmatikov G.A. The Upper Kotlin clays of the Saint Petersburg region as a foundation and medium for unique facilities: an engineering-geological and geotechnical analysis. *Journal of Mining Institute*. 2022. Vol. 254, p. 180-190. DOI: 10.31897/PMI.2022.13

29. Gerasimov A.M., Eremina O.V. Application Microwave Radiation for Directional Changes of Layered Silicates Properties. *Eurasian Mining*. 2021. N 1, p. 55-60. DOI: 10.17580/em.2021.01.11

30. Zyryanov M.S., Ahmetzhanov A.M., Manushina A.S., Potapova E.N. Determination of puzzolanic activity of metakaolins abstract. *Advances in Chemistry and Chemical Technology*. 2016. Vol. 30. N 7, p. 44-46 (in Russian).

31. Rakhimov R.Z., Rakhimova N.R., Stoyanov O.V. Clay pozzolans. Part 1. Review. *Bulletin of the Technological University*. 2016. Vol. 19. N 1, p. 5-13 (in Russian).

32. Salau M.A., Osemeke O.J. Effects of Temperature on the Pozzolanic Characteristics of Metakaolin-Concrete. *Physical Science International Journal*. 2015. Vol. 6. N 3, p. 131-143. DOI: 10.9734/psij/2015/13146

33. Juanrong Zheng, Lijie Guo, Zhenbo Zhao. Effect of calcined hard kaolin dosage on strength development of CPB of fine tailings with sulphide. *Advances in Materials Science and Engineering*. Vol. 2017. N 8631074. DOI: 10.1155/2017/8631074

34. Ferraz E., Slávka A., Walid H. et al. Pozzolanic activity of metakaolins by the French Standard of the modified Chapelle Test: A direct methodology. *Acta Geodynamica et Geomaterialia*. 2015. Vol. 12. N 3, p. 289-298. DOI: 10.13168/AGG.2015.0026

35. Zhao Cao, Yongdan Cao, Hongjuan Dong et al. Effect of calcination condition on the microstructure and pozzolanic activity of calcined coal gangue. *International Journal of Mineral Processing*. 2016. Vol. 146, p. 23-28. DOI: 10.1016/j.minpro.2015.11.008

36. Sivkov S.P., Potapova E.N., Zakharov S.A., Nazarov D.V. Hydration and Hardening of Cement in the Presence of Metakaolin. *ALITinform: Cement. Concrete. Dry Mixtures*. 2015. N 1, p. 80-89 (in Russian).

37. Amran M., Fediuk R., Klyuev S., Qader D.N. Sustainable development of basalt fiber-reinforced high-strength eco-friendly concrete with a modified composite binder. *Case Studies in Construction Materials*. 2022. Vol. 17. N e01550. DOI: 10.1016/j.cscm.2022.e01550

38. Qiao X.C., Si P., Yu J.G. A Systematic Investigation into the Extraction of Aluminum from Coal Spoil through Kaolinite. *Environmental Science & Technology*. 2008. Vol. 42. Iss. 22, p. 8541-8546. DOI: 10.1021/es801798u

39. Pashkevich M.A., Alekseenko A.V. Reutilization Prospects of Diamond Clay Tailings at the Lomonosov Mine, Northwestern Russia. *Minerals*. 2020. N 10. N 517. DOI: 10.3390/min10060517

40. Nazarenko M.Yu., Kondrasheva N.K., Saltykova S.N. The characteristic of waste of oil shale processing for use as filtering materials. *Water and Ecology*. 2018. Vol. 23. Iss. 1, p. 9-16 (in Russian). DOI: 10.23968/2305-3488.2018.23.1.9-16

41. Ivkin A.S., Vasiliev V.V., Salamatova E.V. et al. Adhesion of Bitumen to Minerals. *Coke and Chemistry*. 2022. Vol. 65, p. 24-32. DOI: 10.3103/S1068364X22010033

Authors**: Andrei M. Gerasimov,** *Candidate of Engineering Sciences*, *Associate Professor*, *Gerasimov_AM@pers.spmi.ru*, *https://orcid.org/0000-0002-2197-6200* (*Saint Petersburg Mining University, Saint Petersburg*, *Russia*), **Ivan D. Ustinov,** *Doctor of Chemical Sciences*, *Chief Researcher*, *https://orcid.org/0000-0003-3328-8621* (*NPK* "*Mekhanobr-tekhnika*" (*AO*), *Saint Petersburg*, *Russia*), **Olga V. Zyryanova,** *Candidate of Engineering Sciences*, *Associate Professor*, *https://orcid.org/0000-0001-7866-8543* (*Saint Petersburg Mining University*, *Saint Petersburg*, *Russia*).

The authors declare no conflict of interests.